
Environmental

Studies

Research

Funds

016

Assessment of Airborne Imaging Radars for the Detection of Icebergs

ENVIRONMENTAL STUDIES REVOLVING FUNDS
Report Series, No. 016

September 1985

BERGSEARCH '84

ASSESSMENT OF AIRBORNE IMAGING RADARS
FOR THE DETECTION OF ICEBERGS

James R. Rossiter, CANPOLAR Consultants Ltd.
Lyn D. Arsenault, Cold Regions Remote Sensing
Eugene V. Guy, CANPOLAR Consultants Ltd.
David J. Lapp, Norland Science and Engineering Ltd.
Edward Wedler, Associate of CANPOLAR Consultants Ltd.
Brian Mercer, INTERA Technologies Ltd.
J. Dempsey, Dobrocky Seatech Ltd.
E. McLaren, F.G. Bercha and Associates Ltd.

Scientific Adviser: J. Benoit

The correct citation for this report is:
Rossiter, J.R., L. D. Arsenault, E.V. Guy, D.J. Lapp, E. Wedler,
B. Mercer, E. McLaren, J. Dempsey, 1985. Assessment of
Airborne Imaging Radars for the Detection of Icebergs.
Environmental Studies Revolving Funds. Report No. 016.
Ottawa, xvii + 321 p.

Published under auspices
of the Environmental Studies
Revolving Funds
ISBN - 0-920783-15-5
©1985 - Canpolar Consultants Ltd.
Intera Technologies Ltd.
F.G. Bercha and Associates Limited

FOREWORD

This comprehensive final report was prepared by CANPOLAR Consultants Ltd. at the request of the funding agency, the Environmental Studies Revolving Funds, to bring together the individual reports prepared by several contractors. Therefore, some degree of stylistic consistency has been exchanged for completeness.

Several other documents relate to this study. First, a non-technical summary is submitted by CANPOLAR under separate cover. Secondly, a preliminary report on the experiment was prepared in August 1984, and is included in the Proceedings of the Ninth Canadian Symposium on Remote Sensing, St. John's, published by the Canadian Remote Sensing Society, under the title "Detection of Icebergs by Airborne Imaging Radars." Thirdly, data from the experiment are archived at the National Air Photo Laboratory, Ottawa; original imagery has been returned to the agencies which collected it. Finally, it is intended that a formal scientific paper containing the results of this project will be submitted to a refereed journal in the near future.

TABLE OF CONTENTS

| | PAGE |
|----------------------------|------|
| FORWARD | iii |
| ACKNOWLEDGEMENTS | xvii |
| SUMMARY | 1 |
| RESUME | 3 |

SECTION I REVIEW OF PREVIOUS WORK

| | |
|---|----|
| I.1 INTRODUCTION | 9 |
| I.2 SLAR ICEBERG DATA | 10 |
| I.2.1 Availability | 10 |
| I.2.2 Data Set 1 | 10 |
| I.2.3 Data Set 2 | 12 |
| I.2.4 Observations | 12 |
| I.3 SAR ICEBERG DATA | 15 |
| I.3.1 Availability | 15 |
| I.3.2 Observations | 15 |
| I.4 ANNOTATED BIBLIOGRAPHY OF ICEBERG DETECTION | 18 |
| I.4.1 SLAR Sources | 19 |
| I.4.2 SAR Sources | 30 |
| I.5 REFERENCES | 47 |

SECTION II DATA COLLECTION

| | |
|---|-----|
| II.1 SURFACE INFORMATION | 53 |
| II.1.1 Introduction | 53 |
| II.1.2 Planning Meetings | 53 |
| II.1.3 Document Preparation | 54 |
| II.1.4 Chronology of Data Collection | 54 |
| II.1.5 Post-Operation Events | 56 |
| APPENDICES | |
| Appendix A Master Data Log | 57 |
| Appendix B Data Received | 61 |
| Appendix C Surface Observation Report | 65 |
| II.2 STAR-1 DATA COLLECTION | 107 |
| II.2.1 Introduction | 107 |
| II.2.2 Phase 1: Planning and mobilization (Interim Report) | 110 |
| II.2.3 Phase 2: Data Collection (Interim Report) | 112 |
| II.2.4 Phase 3: Reporting | 114 |
| II.2.5 Summary | 132 |

| | |
|--|-----|
| II.3 WAVES RECORDED IN THE FLEMISH PASS. | 134 |
| II.3.1 Introduction. | 134 |
| II.3.2 Summary of Data Collection and Processing. | 134 |
| II.3.3 Spectrum Diagram: A Short Description. . . | 135 |

SECTION III DATA ANALYSIS AND INTERPRETATION

| | |
|--|-----|
| III.1 INTRODUCTION. | 155 |
| III.1.1 Background | 155 |
| III.1.2 Objectives | 156 |
| III.1.3 Experiment Operations. | 156 |
| III.1.4 Iceberg Nomenclature in BERGSEARCH '84 . | 162 |
| III.2 ANALYSIS OF APRIL 2 IMAGERY | 163 |
| III.2.1 Available Surface Information. | 163 |
| III.2.2 STAR-1 SAR | 174 |
| III.2.3 AES SLAR | 182 |
| III.2.4 IIP SLAR | 188 |
| III.2.5 MARS SLAR. | 195 |
| III.3 ANALYSIS OF APRIL 3 IMAGERY | 201 |
| III.3.1 Available Surface Information. | 201 |
| III.3.2 STAR-1 SAR | 213 |
| III.3.3 AES SLAR | 220 |
| III.3.4 IIP SLAR | 222 |
| III.3.5 MARS SLAR. | 229 |
| III.4 ANALYSIS OF APRIL 5 IMAGERY | 233 |
| III.4.1 Available Surface Information. | 233 |
| III.4.2 STAR-1 SAR | 239 |
| III.4.3 AES SLAR | 242 |
| III.4.4 IIP SLAR | 243 |
| III.4.5 MARS SLAR. | 247 |
| III.4.6 Evaluation of Post-Flight Maps | 247 |
| III.4.7 Target Movement. | 252 |
| III.4.8 Summary. | 252 |
| III.5 ANALYSIS OF APRIL 6 IMAGERY | 254 |
| III.5.1 Available Surface Information. | 254 |
| III.5.2 STAR-1 SAR | 254 |
| III.5.3 IIP SLAR | 257 |
| III.6 ANALYSIS OF APRIL 7 IMAGERY | 260 |
| III.6.1 Available Surface Information. | 260 |
| III.6.2 Target Detectability | 266 |
| III.6.3 Target Movement. | 266 |
| III.6.4 Target Detectability | 269 |
| III.6.5 "Mystery" Target | 275 |

| | | |
|----------|--|-----|
| III.7 | ANALYSIS OF STAR-1 DIGITAL DATA, 7 APRIL. | 279 |
| III.7.1 | Data | 279 |
| III.7.2 | Techniques and Procedures. | 279 |
| III.7.3 | Radar Image and Target Characteristics. | 281 |
| III.8 | CCRS PRELIMINARY ANALYSIS, 1 APRIL. | 285 |
| III.8.1 | Available Surface Information. | 285 |
| III.8.2 | CV-580 SAR Data. | 285 |
| III.9 | CONSIDERATIONS OF DEPRESSION ANGLE. | 291 |
| III.10 | RESULTS. | 296 |
| III.10.1 | Target Detectability by Iceberg Size. | 296 |
| III.10.2 | Target Detectability by Sea State | 296 |
| III.10.3 | Target Detectability by Aspect Angle | 302 |
| III.10.4 | Target Detectability by Radar | 302 |
| III.10.5 | Target Detectability by Altitude. | 302 |
| III.10.6 | Target Detectability vs Radar Resolution. | 302 |
| III.10.7 | Target Repeatability. | 310 |
| III.10.8 | Precipitation Effects | 310 |
| III.10.9 | Plotter Resolution. | 310 |
| III.11 | CONCLUSIONS. | 314 |
| III.11.1 | Detectability | 315 |
| III.11.2 | Aspect Angle | 316 |
| III.11.3 | Resolution. | 316 |
| III.11.4 | Imagery Interpretation. | 316 |
| III.12 | RECOMMENDATIONS. | 318 |
| III.12.1 | Operating Procedures. | 318 |
| III.12.2 | Further Analysis of Data Set. | 319 |
| III.12.3 | Further Experimental Work | 319 |
| III.13 | REFERENCES | 321 |

LIST OF TABLES

| TABLE | | PAGE |
|---|--|------|
| <u>SECTION I REVIEW OF PREVIOUS WORK</u> | | |
| I-1 | COMPARISON OF ICEBERG MEASUREMENTS FROM AIR PHOTOS AND SLAR, 1981. | 11 |
| I-2 | COMPARISON OF ICEBERG MEASUREMENTS FROM AIR PHOTOS AND SLAR, 1983. | 14 |
| I-3 | AVAILABILITY OF SAR-580 ICEBERG IMAGERY PRIOR TO BERGSEARCH '84. | 17 |
| I-4 | EXAMPLES OF DEPRESSION ANGLE RANGES VS FRACTION OF SWATH WIDTH. | 26 |
| I-5 | FACTORS AFFECTING ICEBERG DETECTION IN SEA ICE. | 27 |
| I-6 | AZIMUTHAL RESOLUTION VS SWATH WIDTH. | 28 |
| I-7 | ICEBERG DETECTABILITY FROM THE DANISH N/S LINE, 032401 | 43 |
| <u>SECTION II DATA COLLECTION</u> | | |
| II-1 | SPECIFICATIONS OF STAR-1 SYSTEM. | 108 |
| II-2 | IMAGERY SCALES FOR STAR-1 LINES. | 117 |
| II-3 | WAVERIDER DEPLOYMENT INFORMATION, 1984 | 137 |
| II-4 | ROOT MEAN SQUARE WAVE HEIGHT (METRES) TABULATED BY WAVE PERIOD | 138 |
| <u>SECTION III DATA INTERPRETATION AND ANALYSIS</u> | | |
| III-1 | WMO ICEBERG SIZE CLASSIFICATION. | 155 |
| III-2 | INFORMATION OBTAINED BY THE M.V. <u>POLARIS V</u> DURING BERGSEARCH '84. | 157 |
| III-3 | CHARACTERISTICS OF RADARS PARTICIPATING IN BERGSEARCH '84. | 159 |
| III-4 | ESRF BERGSEARCH '84 NUMBER OF PASSES FOR EACH AIRCRAFT NOT INCLUDING TRANSITS AND RADAR REFLECTOR PASSES | 160 |
| III-5 | ENVIRONMENTAL CONDITIONS DURING BERGSEARCH '84 | 161 |

| TABLE(continued) | PAGE |
|---|------|
| III-6 DATA ACQUISITION TIMES FOR ICEBERG GROUND DATA AND RADAR IMAGERY | 169 |
| III-7 GROWLER RANGE AND BEARING FROM A-1-2 1728 GMT, 2 APRIL 1984 | 172 |
| III-8 POLARIS V ENVIRONMENTAL DATA, 2 APRIL 1984 | 173 |
| III-9 STAR-1 FLIGHT LINE PARTICULARS OF FLIGHT 1, 2 APRIL 1984 | 175 |
| III-10 STAR-1 FLIGHT LINE PARTICULARS OF FLIGHT 2, 2 APRIL 1984 | 176 |
| III-11 SIGNATURE SHAPE VS PASS ON STAR-1 IMAGERY, 2 APRIL 1984 | 178 |
| III-12 FLIGHT 1 REPEATABILITY SMALL TARGET ANALYSIS STAR-1, 2 APRIL 1984 | 180 |
| III-13 AES SLAR FLIGHT LINE PARTICULARS, 2 APRIL 1984 | 183 |
| III-14 AES SLAR, 2 APRIL 1984 | 186 |
| III-15 LARGE TARGET SIGNATURE VS FLIGHT LINE AES SLAR, 2 APRIL 1984 | 187 |
| III-16 IIP SLAR FLIGHT LINE PARTICULARS, 2 APRIL 1984 | 191 |
| III-17 IIP SLAR, 2 APRIL 1984 | 194 |
| III-18 MARS SLAR FLIGHT LINE PARTICULARS 2 APRIL 1984 | 196 |
| III-19 MARS SLAR, 2 APRIL 1984. | 199 |
| III-20 DATA ACQUISITION TIMES FOR ICEBERG SURFACE DATA AND RADAR IMAGERY | 202 |
| III-21 CHARACTERISTICS OF SURFACE VERIFIED AND AIR PHOTOGRAPHED ICEBERGS AND GROWLERS, 2-4 APRIL 1984 | 205 |
| III-22 SYNOPSIS OF EVENTS RELATING TO ICEBERG A-3, 3 APRIL 1984. | 208 |
| III-23 HOURLY WEATHER AND ENVIRONMENTAL DATA, 3 APRIL 1984 | 214 |

| TABLE(continued) | PAGE |
|---|------|
| III-24 STAR-1 FLIGHT LINE PARTICULARS, FLIGHT 1, 3 APRIL 1984 | 215 |
| III-25 TARGET IDENTIFICATION STAR-1, 3 APRIL 1984 | 216 |
| III-26 STAR-1 SAR TARGET ANALYSIS, FLIGHT 1 . . . | 219 |
| III-27 AES SLAR FLIGHT LINE PARTICULARS, 3 APRIL 1984 | 221 |
| III-28 DEPRESSION ANGLE AND AZIMUTH CELL SIZE FOR DETECTED <u>POLARIS V</u> AND A-3 ON AES SLAR, 3 APRIL 1984 | 223 |
| III-29 DEPRESSION ANGLE AND AZIMUTH CELL SIZE FOR DETECTED BO08 AND ICE STRING, AES SLAR, 3 APRIL 1984 | 223 |
| III-30 AES SLAR TARGET ANALYSIS, 3 APRIL 1984 . . | 224 |
| III-31 IIP FLIGHT PARTICULARS, 3 APRIL 1984 . . . | 225 |
| III-32 DEPRESSION ANGLE AND CELL SIZE FOR <u>POLARIS V</u> , A-3, AND BO08 ON IIP SLAR . . . | 227 |
| III-33 IIP SLAR TARGET ANALYSIS, 3 APRIL 1984 . . | 228 |
| III-34 MARS FLIGHT LINE PARTICULARS, 3 APRIL 1984 | 230 |
| III-35 DEPRESSION ANGLE AND CELL SIZE FOR <u>POLARIS V</u> AND A-3 ON MARS SLAR, 3 APRIL 1984 | 231 |
| III-36 IMAGERY FOR 5 APRIL 1984 | 234 |
| III-37 TARGETS PHOTOGRAPHED AND VISITED ON 5 APRIL 1984 | 236 |
| III-38 HOURLY WEATHER AND ENVIRONMENTAL DATA, 5 APRIL 1984 | 238 |
| III-39 STAR-1 TARGET ANALYSIS FOR 5 APRIL 1984. . | 240 |
| III-40 TARGET SIZE ESTIMATE FROM STAR-1 PASS 4. . | 242 |
| III-41 AES TARGET ANALYSIS FOR 5 APRIL 1984 . . . | 244 |
| III-42 IIP TARGET ANALYSIS FOR 5 APRIL 1984 . . . | 245 |
| III-43 MARS TARGET ANALYSIS FOR 5 APRIL 1984. . . | 248 |

| TABLE(continued) | PAGE |
|--|------|
| III-44 COMPARISON OF NUMBER OF TARGETS GIVEN ON POST-OPERATION FLIGHT MAPS, 5 APRIL 1984 | 251 |
| III-45 DETECTABILITY OF SMALL TARGETS IN THE NORTHERN CLUSTER ON 5 APRIL 1984 | 251 |
| III-46 HOURLY WEATHER AND ENVIRONMENTAL DATA, 6 APRIL 1984 | 256 |
| III-47 ICEBERGS DETECTED ON PASS 4 OF STAR-1 IMAGERY. | 254 |
| III-48 IIP IMAGERY, 6 APRIL 1984. | 258 |
| III-49 IIP 100-KM SWATH IMAGERY ON 6 APRIL 1984 . | 259 |
| III-50 IMAGERY FOR 7 APRIL 1984 | 261 |
| III-51 HOURLY WEATHER AND ENVIRONMENTAL DATA FROM <u>POLARIS V</u> , 7 APRIL 1984. | 264 |
| III-52 TARGETS SEEN FROM <u>POLARIS V</u> ON 7 APRIL 1984 | 265 |
| III-53 DETECTION OF VERY SMALL TARGETS ON 7 APRIL 1984 | 267 |
| III-54 REPEATABILITY OF TARGETS BY LOOK DIRECTION | 274 |
| III-55 GROSS TARGET COUNTS FOR COMMON 140 KM ² AREA | 276 |
| III-56 OCCURRENCES OF "MYSTERY" TARGET. | 277 |
| III-57 RATIO OF TARGETS PRESENT TO TOTAL TARGETS BY RADAR AND SIZE CLASS. | 298 |
| III-58 SUMMARY OF TARGETS PRESENT VS TOTAL TARGET POPULATION | 299 |
| III-59 ASPECT ANGLE COMPARISON FOR DETECTABILITY. | 304 |
| III-60 RATIO OF TARGETS PRESENT TO TOTAL TARGETS. | 306 |
| III-61 DETECTABILITY AS A FUNCTION OF ALTITUDE AND TARGET SIZE CLASS. | 308 |
| III-62 NUMBER OF TARGETS OUT OF 17 SEEN ON REPEATED PASSES, 3 APRIL 1984 | 311 |

| | | |
|--------|--|-----|
| III-63 | PRECIPITATION DETECTED | 312 |
| III-64 | PLOTTER AND RADAR RESOLUTION (a) MOTOROLA SLAR, (b) STAR-1 SAR. | 313 |

LIST OF FIGURES

| FIGURE | | PAGE |
|--------|--|------|
|--------|--|------|

SECTION I REVIEW OF PREVIOUS WORK

| | | |
|-----|--|----|
| I-1 | DISTRIBUTION OF AVERAGE TARGET REFLECTIVITIES FOR CGC EVERGREEN AND ICEBERG DURING 1977 SLAR TESTS | 23 |
| I-2 | PREFERRED PORTION OF SWATH WIDTH ON SLAR IMAGERY FOR ICEBERG DETECTION IN SEA ICE . | 29 |
| I-3 | TYPICAL PROBABILITY OF DETECTION GIVEN AS A FUNCTION OF SIGNAL-TO-NOISE RATIO. | 32 |
| I-4 | (a) AND (b) DETERMINING ICEBERG HEIGHT FROM RADAR SHADOW | 38 |
| I-5 | RADAR CONTRAST BETWEEN ICEBERGS AND SMOOTH FIRST-YEAR ICE | 44 |

SECTION II DATA COLLECTION

| | | |
|----------------------|---|-----|
| II-1 | EXAMPLE OF STAR-1 IMAGERY. | 119 |
| II-2 | MISSIONS PROFILES, 2 APRIL 1984, FLIGHT 1. | 121 |
| II-3 | MISSIONS PROFILES, 2 APRIL 1984, FLIGHT 2. | 122 |
| II-4 | MISSIONS PROFILES, 3 APRIL 1984, FLIGHT 1. | 123 |
| II-5 | MISSIONS PROFILES, 3 APRIL 1984, FLIGHT 2. | 124 |
| II-6 | MISSIONS PROFILES, 4 AND 5 APRIL 1984. . . | 125 |
| II-7 | MISSIONS PROFILES, 6 APRIL 1984. | 126 |
| II-8 | MISSIONS PROFILES, 7 APRIL 1984. | 127 |
| II-9 | MISSIONS PROFILES, 7 APRIL 1984 (CONTINUED). | 128 |
| II-10 | IDENTIFICATION OF TARGETS, 7 APRIL 1984, LINE 9 | 130 |
| II-11 | WAVERIDER BUOY LOCATIONS AND WATER DEPTHS FOR ESRF ICEBERG DETECTION TRIALS. | 136 |
| II-12 TO II-21 | GRAPHS OF SPECTRAL DENSITY OF WAVES IN M ² /Hz VERSUS FREQUENCY IN Hz FOR ALL FOUR STATIONS. | 139 |

| FIGURE(continued) | PAGE |
|-------------------|---|
| II-22 | GRAPH OF WAVE CHARACTERISTIC HEIGHT VERSUS TIME IN DAYS FOR ALL FOUR RECORDS. 149 |
| II-23 | PERCENTAGE EXCEEDANCE PLOT OF SIGNIFICANT AND MAXIMUM WAVE HEIGHT FOR FOUR STATIONS TOGETHER 150 |
| II-24 | PERCENTAGE OCCURRENCE HISTOGRAM OF WAVE PEAK PERIOD IN SECONDS FOR FOUR STATIONS TAKEN TOGETHER 151 |
| II-25 | PLOT OF SIGNIFICANT WAVE HEIGHT IN METRES VERSUS PEAK PERIOD IN SECONDS. 152 |

SECTION III DATA INTERPRETATION AND ANALYSIS

| | |
|--------|---|
| III-1 | MARS FLIGHT LINE CONFIGURATION, 2 APRIL 1984 164 |
| III-2 | <u>POLARIS V AND A-1-2 MOVEMENTS,</u> <u>1-2 APRIL 1984</u> 165 |
| III-3 | ICEBERG A-1-2 GROUND VERIFICATION PHOTOS . 166 |
| III-4 | GROWLER B-1 NEAR A-1-2 167 |
| III-5 | GROWLER C-1 NEAR A-1-2 167 |
| III-6 | KING AIR PHOTOGRAPH OF A-1-2 170 |
| III-7 | GROWLER DISTRIBUTION AROUND A-1-2. 171 |
| III-8 | STAR-1 SAR FLIGHT 1, PASS 6, 2 APRIL 1984. 177 |
| III-9 | GROWLER COMPARISON, STAR-1 IMAGERY, FLIGHT 1 LINES 5-9, 2 APRIL 1984 181 |
| III-10 | <u>POLARIS V AND A-1-2 POSITIONS BASED</u> <u>ON AES SLAR, 2 APRIL 1984.</u> 185 |
| III-11 | AES SLAR, PASS 7, 2 APRIL 1984 189 |
| III-12 | OTHER TARGETS ON AES SLAR. 190 |
| III-13 | <u>POLARIS V AND A-1-2 MOVEMENT DURING IIP</u> <u>ACQUISITION, 2 APRIL 1984.</u> 193 |
| III-14 | MARS SLAR, PASS 2, 2 APRIL 1984. 197 |
| III-15 | COMPARISON OF MARS LINES 1-4, 2 APRIL 1984 198 |

| FIGURE(continued) | PAGE |
|--|------|
| III-16 POLARIS V AND ICEBERG POSITIONS, 2-4 APRIL 1984 | 203 |
| III-17 ICEBERG A-3, LOOKING NORTH, 3 APRIL 1984 | 206 |
| III-18 ICEBERG A-3, LOOKING SOUTHWEST, 3 APRIL 1984 | 206 |
| III-19 GROWLER D-3, 3 APRIL 1984. | 207 |
| III-20 WAVERIDER DEPLOYMENT, 3 APRIL 1984 | 207 |
| III-21 AIR PHOTO OF ICEBERG B008, 2 APRIL 1984 | 210 |
| III-22 B008 AND ICE STRING, LOOKING SOUTH AT 1414 GMT | 211 |
| III-23 B008 AND ICE STRING, LOOKING NORTHWEST AT 1423 GMT | 211 |
| III-24 SKETCH AND NOMENCLATURE FOR B008, ICE STRING, AND 17 TARGETS | 212 |
| III-25 STAR-1 SAR, FLIGHT 1, PASS 5, 3 APRIL 1984 | 218 |
| III-26 LOCATION OF SURFACE TARGETS ON 5 APRIL 1984 | 235 |
| III-27 TARGET MOVEMENT ON 5 APRIL 1984. | 253 |
| III-28 CONFIRMED TARGETS ON 6 APRIL 1984. | 255 |
| III-29 TYPICAL CONFIGURATION OF TARGETS DURING MISSIONS OF STAR-1, IIP AND AES NEAR 470'N, 470'W, 7 APRIL 1984 | 263 |
| III-30 TARGET MOVEMENT FROM STAR-1 IMAGERY, 7 APRIL 1984 | 268 |
| III-31 STAR-1, PASS 2, 7 APRIL 1984 | 270 |
| III-32 IIP, PASS 3, 8 APRIL 1984. | 271 |
| III-33 MARS, PASS 1, 7 APRIL 1984 | 272 |
| III-34 AES, PASS 2, 7 APRIL 1984. | 273 |
| III-35 DIGITAL "WINDOWS" EXTRACTED FROM CCT ESRF 12 AND CCT ESRF 12A, FOR DETAILED STUDY. | 280 |

| FIGURE(continued) | PAGE |
|--|------|
| III-36 GREY-TONE CHANGE IN BOTH ALONG-TRACK AND AZIMUTH DIRECTIONS | 282 |
| III-37 DISTRIBUTION OF SUBSCENE GREY LEVELS . . . | 282 |
| III-38 CROSS-SECTION PROFILES FOR DISCRETE TARGETS. | 284 |
| III-39 SAMPLE PROBABILITY DISTRIBUTION FOR GREY LEVELS OVER OPEN OCEAN AND DISCRETE TARGETS. | 284 |
| III-40 CV-580 IMAGERY, PASS 2, X-BAND, 1 APRIL 1984 | 286 |
| III-41 CV-580 IMAGERY, PASS 2, C-BAND, 1 APRIL 1984 | 287 |
| III-42 CV-580 IMAGERY, PASS 3, X-BAND, 1 APRIL 1984 | 288 |
| III-43 CV-580 IMAGERY, PASS 3, C-BAND, 1 APRIL 1984 | 289 |
| III-44 TWO MODELS FOR OCEAN RADAR CROSS-SECTION . | 292 |
| III-45 SLAR CLUTTER | 293 |
| III-46 SLAR CLUTTER | 293 |
| III-47 SLAR CLUTTER | 294 |
| III-48 SLAR CLUTTER | 294 |
| III-49 TARGETS DETECTED BY CLASS. | 297 |
| III-50 DETECTABILITY VS SEA STATE (BERGY BIT SIZE CLASS). | 300 |
| III-51 DETECTABILITY VS SEA STATE (GROWLER SIZE CLASS) | 301 |
| III-52 DETECTABILITY BY ASPECT ANGLE; APRIL 7 . . | 303 |
| III-53 DETECTABILITY: ALL DAYS | 305 |
| III-54 DETECTABILITY AS A FUNCTION OF ALTITUDE (a) FOR IIP SLAR, (b) FOR AES SLAR | 307 |
| III-55 DETECTABILITY VS RESOLUTION. | 309 |

ACKNOWLEDGEMENTS

This study was funded by the Environmental Studies Revolving Funds (ESRF) through contracts with F.G. Bercha and Associates Limited for experiment organization and collection of shipboard information, with INTERA Technologies Ltd. for STAR-1 data, and with a team led by CANPOLAR Consultants Ltd. for experiment planning, data analysis, and interpretation.

Shipboard data were collected from the M.V. Polaris V under charter to the Hibernia Group. Additional surface data were provided by Dobrocky Seatech Ltd. personnel on the vessel, including waverider buoy data provided by Marine Environmental Data Service. Aerial photography was provided by Atlantic Airways under contract to Mobil Oil Canada Limited.

Additional radar data were provided to the experiment by International Ice Patrol Atmospheric Environment Service, Husky-Bow Valley, to which the MARS aircraft was under contract, and the Canada Centre for Remote Sensing. The co-operation and assistance provided by all these groups both during and after the experiment are greatly appreciated.

Special thanks are due to Mr. J. Benoit who as Scientific Adviser provided very useful comments and guidance during the project.

SUMMARY

Icebergs pose potential hazards both to oil development and to shipping off Canada's East coast. Whereas in the past, detection has been largely by visual or photographic means, more recently, imaging radar has been used. Because of the generally poor visibility in the region and the potentially large swath coverage of radar, radar is expected to become a prime detection sensor for regional coverage. Two major types of radar are in use: real aperture side-looking airborne radar (SLAR) and synthetic aperture radar (SAR).

This experiment, named **BERGSEARCH '84**, was conducted over the Grand Banks of Newfoundland in April 1984, to assess the capabilities of modern, airborne, imaging radars in the detection of icebergs in open water. Of particular interest were smaller pieces of ice, namely growlers and bergy bits. Of the five radars assessed, three were SLARs and two were SARs.

Ten major conclusions were reached in this study.

1. From the experiment the following estimates of average detectability for icebergs of various sizes were determined, both in significant wave heights below 2.9 m, and with comparison to available surface and air-photo information:

| | |
|---|---------|
| Growlers (<100 m ² area) | 10-50% |
| Bergy bits (100-300 m ² area) | 60-80% |
| Small icebergs (300-2500 m ² area) | 85-100% |
| Medium and large icebergs | 100% |

These results are from all radars and at all aspect angles combined. Therefore, optimum results would be expected to be better than these averages.

2. The repeatability of detecting confirmed targets from pass to pass showed that target detectability (especially for growlers) increased with repeated passes. Two factors can affect single-pass detectability:

- Small icebergs were observed by surface observers to have significant vertical bobbing motion so that it is possible for a bergy bit or growler to be substantially submerged or obscured by waves at any particular point in time; and,
- targets in close proximity to one another have signatures that blend together.

3. Iceberg detectability decreased with increasing sea state, particularly for smaller targets. However, this experiment did not encounter conditions above 4-m wave height, and thus it is impossible to confirm how detectability might change for higher sea states. Higher resolution systems appeared to be more successful for the detection of small targets as sea state increased, which is in agreement with theory.
4. Ships, icebergs, and small floes of sea ice generally do not display different radar target signatures on either SAR or SLAR analog imagery. Occasionally larger icebergs exhibited distinctive shape information on SLAR which was sufficient to make a positive and correct identification. On SAR all targets were smeared in azimuth. No attempt was made in this study to distinguish targets on the basis of radiometric information.
5. Smaller targets appeared to be more visible and to be more easily interpreted for lower-altitude SLAR passes.
6. Smaller icebergs, bergy bits, and growlers are slightly more likely to be detected looking in the crosswave direction.
7. Typical errors in positioning the aircraft of up to 5 km were found, which is probably inadequate for many offshore applications and for reidentification of targets. Updating to known position references is important so that imagery can be used for target verification, re-identification, and iceberg motion. The availability of the satellite Global Positioning System (GPS) by the late 1980s should alleviate this problem and will make possible registration of multiple passes of data.
8. The smallest iceberg targets are less than a single resolution cell in size for all the radars used. Hence, output resolution of the plotter needs to be matched carefully to the radar resolution.
9. Precipitation echoes were noted in 10-20% of the SLAR passes, but in few of the SAR passes. The doppler shift of rain itself appears to allow a SAR processor to filter out rain echoes.
10. The dynamic range of scenes imaged is relatively high. Therefore benefits are to be expected through operational use of digital data to overcome deficiencies of the limited grey level available on film. Limited digital analysis carried out in this project showed that iceberg targets could be separated from ocean clutter on the basis of signal intensity 88% of the time with a 5% false alarm in sea states of 2-4 m.

ESLIE

es ic be s rej és nt nt un da ge p ur la na ig tti
 et la re he ch d y no ar ar s u ar e e a ô t E t
 Ca ad le i pe , es ra ar i ag ir se so t jc té a c
 mo en h i e c c te ti i, e r r or ai sa ce v su l s
 et ph to ra hi ue . La fa ol v si il té da s es té o s
 ha tu iè s t a ra de pc té d s id s ai se t ré ag
 un ô l om n it p ir c t ac nc o ie d is d s
 re on i i ar es à 'é ie le ré or le au p nc pa x yp s
 de ra ai s t am lo és e ra ar aè op ri or e tu s
 sy th ti e b la ag l té l at év at on in a es (LA)
 et le ca ar i c v t re y ch ti ie al é a to ai il is
 SA).

es é e e u no ié " (a se u g ic s 4" (d s
 no a gl is " ER SE RC "8 ") se é ou a i r l 38 s
 le G an : no c l rr -N av il e is it a ie l
 po si l é : de r da s r or és no r s ou l d te ti
 de i eb rg e e ux li re , t n ar ic l er e mi s
 ol s e it s o ie le ou gu gi n e l s r gn n
 d' e r g ro s LA e de x AR fu en co pa és

l x or lu io s i r t i r es de ce se tte e:
 L. i m p ré a x os v ti is i ie e e p l t c ra hi ie
 i c pa it m ve ie e et ct on le r i ar s c lf ra
 om e ui ou l s ia se c la e e pr ss ui
 i fi re te , in ui n r on l v g u s ig lf ca v
 i c pa sa en p s 9r

l ur ui no s su fa e 10 i² 10 10
 i ag en s i b e g 10 < i r ce < 0n) 30 10
 i ti s ce er s 30 < i r ic < 0(2) 35 10
 i et rg n ye e g os 10

L. l e ns bi it a g m nt it se on le no or d b a ge
 s cc ss fs s nt it ar c s es b e rg ig on ier
 i ct ur p iv it ni ue ce l s ia es de ré ér ie or
 c un ba ay ge

- l p l e n e i s e t n s s u p c r r it le
 s b m r g r r v ne t u e c c h r le i e le
 v g u s ; e

- l p ox ni i p us eu s i b es u p c r r it it e
 d g a du o o o : pa at ur du ra in.

L. en ib li é ra ia t n r m it av c a h c le
 s rt ut o s il es p s et te l l fa ; é se
 c e e v g u s r se ce l r d s ss is n' nt pa
 c pa se 4 n e at et ; i e t or ip ss ol c
 c n r r e ap or p éc s nt e en it l é t au et

des vagues dans une mer plus agitée. Notons toutefois que les appareils à résolution plus élevée repéraient mieux les petites cibles dans la plus forte houle observée, ce qui confirme la théorie.

4. En général, les SLAR et SAR ne départagent pas les signaux analogiques correspondant aux navires, icebergs et petites banquises. Les gros icebergs présentent parfois des profils SLAR assez distincts pour permettre une identification correcte. Toutes les images SAR étaient déformées sur leur axe d'azimut. Nous n'avons pas tenté de distinguer les cibles par des mesures radiométriques.
5. Les vols de reconnaissance avec SLAR repéraient mieux les petites cibles lorsqu'ils se déroulaient à basse altitude.
6. Les balayages radar perpendiculaires au train des vagues repéraient mieux les petits icebergs, les fragments et les bourguignons.
7. L'erreur habituelle de 5 km dans les relevés de position de l'avion empêche probablement de confirmer l'identité des cibles lors de survols répétés. En effet, on ne peut reconnaître chaque cible et dériver sa trajectoire sans se référer régulièrement à des points de repère connus. Le système de positionnement par satellite GPS ("Global Positioning System") qui sera disponible vers la fin de cette décennie résoudra le problème.
8. Il faudra relier à chaque récepteur radar une unité de dessin de résolution identique parce que les signaux renvoyés par les plus petites masses de glace engendrent des variations inférieures à l'unité de résolution du détecteur.
9. Entre 10 et 20% des survols SLAR ont capté des échos provenant des précipitations atmosphériques. Les SAR en ont capté très peu car il se pourrait que l'effet Doppler causé par les gouttes de pluie transmette des signaux que le détecteur SAR puisse filtrer.
10. La gradation des signaux captés est relativement fine. Par conséquent, nous voyons des avantages à traiter les intensités numériquement pour pallier à la gamme limitée de tons de gris disponibles analogiquement sur pellicule photographique. Un essai de traitement numérique sur quelques images a permis de distinguer les icebergs des autres cibles dans 88% des cas, avec un taux d'erreur de 5% dans des vagues entre 2 et 4 m de hauteur.

BERGSEARCH '84

SECTION I

REVIEW OF PREVIOUS WORK

James R. Rossiter, CANPOLAR Consultants Ltd.
Lyn D. Arsenault, Cold Regions Remote Sensing
Eugene V. Guy, CANPOLAR Consultants Ltd.
David J. Lapp, Norland Science and Engineering Ltd.
Jeff Sutton, INTERA Technologies Ltd.

I.1 INTRODUCTION

Prior to **BERGSEARCH '84**, a review of literature and existing data sets was made. Although it may be incomplete, it probably lists the major data sets that contain airborne radar imagery of icebergs along with any kind of confirming information. A number of agencies were contacted, including: Atmospheric Environment Service (AES), International Ice Patrol (IIP), Canada Centre for Remote Sensing (CCRS), Mobil Oil Canada, Petro-Canada, as well as SURSAT and SAR'77 project files, CCRS, and CISTI publication files.

This report summarizes literature and data sets available in early 1984 regarding the detection of icebergs using airborne imaging radar systems. Observations and results obtained from major experiments are discussed. An annotated bibliography is presented, detailing the published results of various authors who have conducted relevant research using radar systems. The geographic location of each experiment as well as the surface conditions are considered. The present location and formats of archived data sets are also given where known.

Previous experiments regarding the imaging of icebergs by airborne radar have usually been confined to the use of one or two systems. Two major types of radar are in use: real aperture side-looking airborne radar (SLAR) and synthetic aperture radar (SAR). The latter uses a coherent source and the motion of the platform to obtain, with significant data processing, uniform resolution across a swath. Both routine and special airborne reconnaissance flights are used to detect icebergs and to monitor their movement. Usually, only a few icebergs have been imaged in each case. Where the icebergs have been imaged in open water conditions, there has usually been an absence of surface information; where verification exists, it often deals with icebergs in a sea-ice background. Much of this work has been done in the Arctic and in the Labrador Sea. Research on the Grand Banks has been confined mainly to AES and IIP SLARs. Relatively few iceberg imaging missions are documented for SAR.

I.2 SLAR ICEBERG DATA

I.2.1 AVAILABILITY

Two AES SLAR data sets from 1981 and 1983 were matched with air photos and measurements in Mobil Oil Canada's possession. While of interest, these data sets have a few failings in that, of all the icebergs found in any given area on the SLAR, only a few of the icebergs were actually photographed. Although the photos and SLAR imagery correspond as to dates and sometimes to time of imaging, in several cases photographed icebergs of interest did not appear because they were located either:

- beyond the radar; or
- underneath the aircraft in the area not covered by the radar swath; or
- in an area obscured on the imagery because of a turn.

I.2.2 DATA SET 1

This data set consists of black-and-white air-photos obtained in 1981 on 9 April and 8 May in the Strait of Belle Isle area and along the Labrador Coast south of Hopedale. Although more than 20 icebergs of various sizes and shapes were photographed, only 5 of those could be found on AES flight Z625 on the same date. This discrepancy results solely from the radar coverage area differing from that of the photo reconnaissance flight. All of the photographed icebergs in the area of SLAR coverage were found and were measured.

Table I-1 compares iceberg measurements made from the air-photo and from the original SLAR negative (APS-94D). The radar imagery scale for each of the flights in the two data sets was 1:1,000,000. At this scale a swath 100 km wide was covered on each side of the aircraft. Most of the icebergs imaged were found in the more favourable centre portion of the swath. The closest iceberg imaged was at a depression angle of about 9° at 28 km from nadir, whereas the farthest iceberg imaged was at 3.9° at 62.5 km from nadir. All of these icebergs were large and, from the photographs, appeared to be good reflectors from almost any angle because they consisted of a number of facets with steep slopes (dry-dock icebergs to >50 m in height, some with pinnacles). The icebergs were located in open water and although poor quality of the film prevented an evaluation of sea state, a number of waves were visible. All of the iceberg returns were quite "solid" and were readily visible on the imagery.

It is interesting to note that two of the icebergs (nos. 1 and 2) were imaged twice at slightly different depression

TABLE I-1

Comparison of Iceberg Measurements from Air Photos and SLAR, 1981

| Date | Berg # ^a | Photo Length/Width (m) | SLAR Length/Width (m) | Distance from Nadir Azimuth Resolution (km) (A) (B) | Depression Angle | Shape |
|--------|---------------------|------------------------------|-----------------------------|--|---------------------|---------------|
| 9/4/81 | .01.02 | 165/146 | 300/30 | 28 (224) | 9° | Dry-dock (WP) |
| | .03.04 | 230/192 | 400/30 | 29.5 (236) | 8° | Dry-dock (WP) |
| | .05.06 | 183/152 | 500/60 | 36 (288) | 7° | Dry-dock (WP) |
| | .07.08 | 144/129 | 800/60 | 57 (456) | 4.2° | Pinnacle |
| | .09.10 | 320/186 | 1000/60 | 62.5 (500) | 3.9° | Dry-dock |
| | .01.02 | 165/146 | 500/60 | 37.2 (300) | 6.5° | Dry-dock (WP) |
| | .03.04 | 230/192 | 500/60 | 31.8 (255) | 7.5° | Dry-dock (WP) |
| 5/5/81 | .01.02 | N.A. ^d | 800/60 | 72 (576) | 3.3° | N.A. |
| | .09.10 | 186/159 | 800/60 | 48 (384) | 5° | Dry-dock (WP) |
| | .24.25 | 182/153 | 300/90 | 50 (400) | 4.9° | Dry-dock (WP) |
| | .30.31 | 238/178 | 300/60 | 90 (720) | 2.7° | Pinnacle |

^a NW29481 is the prefix for iceberg #'s on 9/4/81, NW20581 is the prefix for rolls iceberg #'s on 5/5/81.

^b A=Azimuth resolution at that distance from nadir (m)

^c (WP)=With pinnacle(s)

^d N.A.=Not available

angles and distances from nadir. The slight changes in depression angle and aspect angle seem to have little difference on target identification; however, the iceberg signatures are larger because of increased azimuthal cell size resolution.

1.2.3 DATA SET 2

This data set consists of black-and-white and colour air photos obtained in 1983 along the east coast of Newfoundland around the Hibernia area on 11, 17, 19, and 31 March; 1, 12, and 19 April and 8 May (11 to 31 March and 1 April photos have not yet been analyzed). Of the 43 icebergs photographed on 12 and 29 April and on 8 May, only 17 were found on the corresponding AES SLAR flights. This again is mainly due to differences in areal coverages between the photo reconnaissance flight and the radar flight. There were a large number of icebergs which were photographed but were not imaged by the radar due to aircraft turns. Table I-2 contains air photo and SLAR iceberg measurements for 12 and 29 April, and 8 May.

1.2.4 OBSERVATIONS

Based on an examination of the following data sources;

- * Cape York, Greenland, February 1978 (X-band)
- * Melville Bay, Cape York, Greenland, 1980-1981 (X-band)
- * Grand Banks pre-1972 IIP data (K-band)
- * Grand Banks pre-1975 IIP data (K-band, X-band)
- * Grand Banks pre-1978 IIP data (X-band)
- * Newfoundland/Labrador Coast, April/May 1981 AES data (X-band)
- * Newfoundland Coast and Hibernia, March-May 1983 AES data (X-band)

the following observations are made:

- SLAR systems (AN/APS-94D; various agencies) typically use film with a low dynamic range;
- SLAR imagery has fairly shallow ($<20^{\circ}$) depression angles over much of the imagery;
- SLAR imagery (AN/APS-94D) is available on both sides of the aircraft at three different scales and coverages; (a) 1:250,000/25 km, (b) 1:500,000/50 km, (c) 1:1,000,000/100 km. The swath width/scale were found to have a profound effect on the number of icebergs detected: a 40-50% drop in detected icebergs possible between 25-km and 50-km swaths covering the same area. The 100-km imagery, which was used most often, does not seem to be of great use beyond a range of 60 or 70 km;

- iceberg size and type are not possible to discern and iceberg measurements from the imagery must take into account the increasing cell size with range;
- icebergs do exhibit characteristic point target AR imagery; in the far range an elliptical, or cigar-shaped, return is produced in azimuth; for the near range, the shape of the return is more rounded;
- aspect angle is especially important when icebergs are clustered. As range increases, many closely-spaced icebergs will give fewer individual returns because a greater number of the icebergs will be taken up in filling a single resolution cell;
- detectability of icebergs appears to drop when the depression angle is less than 30° ;
- iceberg shadows and wakes can be of assistance in iceberg identification;
- some features associated with the SLAR display, such as range marks, yaw correction, and time marks are helpful during iceberg analysis;
- the area underneath the aircraft not imaged by radar should be covered by overlapping flight lines; and
- atmospheric effects at X-band were noted.

TABLE I-2

Comparison of Iceberg Measurements from Air Photos and SLAR, 1983

| Date | Berg # | Photo Length/Width (m) | SLAR Length/Width (m) | Azimuth Resolution (km) | Distance from Nadir (A) ^a (km) | Depression Angle | Shape |
|---------|--------|------------------------------|-----------------------------|----------------------------|--|---------------------|---------------|
| 12/4/83 | 5 | 154/146 | 200/30 | 6 | | 39° | Dry-dock (WP) |
| | 6 | 120/92 | 100/30 | 9 | (72) | 24° | Dry-dock (WP) |
| | 7 | 144/122 | 200/30 | 19 | (152) | 12° | Dry-dock (WP) |
| | 8 | 84/74 | 400/30 | 31 | (248) | 8° | Pinnacle |
| | 9 | 102/78 | 400/30 | 28.5 | (228) | 8.5° | Pinnacle |
| | 10 | 90/76 | 400/60 | 27 | (216) | 9° | Pinnacle |
| | 11 | 94/58 | 500/60 | 40.5 | (324) | 6° | Pinnacle |
| | 12 | 70/54 | 500/60 | 41 | (328) | 6° | Dome |
| | 2 | 220/164 | 500/60 | 27 | (216) | 9° | Dry-dock (WP) |
| | 3 | 194/188 | 500/90 | 19 | (152) | 12° | Tabular |
| | 4 | 134/82 | 300/45 | 29 | (232) | 8° | Dry-dock (WP) |
| | 8 | 108/48 | 400/60 | 25 | (200) | 9.7 | Pinnacle |
| 29/4/83 | 7 | 222/142 | 300/60 | 12 | (96) | 19° | Dry-dock |
| | 6 | 182/182 | 300/60 | 8 | (64) | 32° | Tabular |
| | 9 | 160/130 | 300/30 | 21 | (169) | 12° | Pinnacle |
| | 7 | 266/188 | 1000/60 | 74 | (592) | 3.26° | Dry-dock |
| | 8 | 172/88 | 500/30 | 65 | (520) | 3.76° | |
| | | | | | | | |
| | | | | | | | |
| | | | | | | | |
| | | | | | | | |
| | | | | | | | |
| 8/5/83 | 7 | 266/188 | 1000/60 | 74 | (592) | 3.26° | Dry-dock |
| | 8 | 172/88 | 500/30 | 65 | (520) | 3.76° | |

^a A = Azimuth resolution at that distance from nadir (m)^b (WP) = With pinnacles(s)

I.3 SAR ICEBERG DATA

I.3.1 AVAILABILITY

A review of the CV-580 SAR data sets showed that relatively few missions had imaged icebergs. Those available are summarized in Table I-3.

I.3.2 OBSERVATIONS

- X-band provided better iceberg detection and definition than L-band;
- HV polarization appeared superior to HH polarization for iceberg detection because of its greater contrast, against pack ice. This finding may be less important for detection of icebergs in open water;
- the detection of an iceberg depends on its contrast with the surrounding ice or water and although the iceberg may not always be visible, other indicators such as shadows, iceberg wakes, ice in the lee of icebergs, bob rings in the ice around icebergs, and floe break-up around large or grounded icebergs may be of help in identifying iceberg presence;
- lower depression angles (less than 8°) appear to be more favourable for iceberg detection, because the ratio of signal clutter increases significantly;
- icebergs can be hard to discriminate in pack ice when surrounded by broken floes, floe edges, and ridges;
- icebergs can also be difficult to find in high sea states increased sea clutter;
- iceberg shape and aspect angle are important for iceberg detection because icebergs with steeper sides (tabular, dry-dock and pinnacle) are usually easier to detect than those with smoother, less angled sides (domed icebergs);
- iceberg movement, such as yawing and rolling, can defocus an iceberg's image;
- icebergs can, in some cases, be reidentified over several days using the higher resolution of the SAR system which provides more detailed images than SLAR;
- despite its higher resolution, SAR is not always able to identify all icebergs without corroborating data;
- iceberg sizes obtained from SAR imagery might be more reliable than SLAR because of the low azimuthal resolution in the latter;

- digital recording of SAR imagery is possible, which allows computer-aided analysis and greater dynamic range;
- discrimination between ships and icebergs might be possible by using reflectivity and shape information;
- a ship in motion often has a wake which makes identification easier; and
- fishing ships are usually found in clusters in areas known for fishing activity, which can make their identification a little easier.

TABLE I-3

Availability of SAR-580 Iceberg Imagery prior to BERGSEARCH '84

| Project Name | Date | Location | SAR Frequency (Swath) | Data Set | No. of Icebergs |
|--------------|------------|-----------------|-----------------------|--|-----------------|
| - | May 1975 | Kennedy Channel | X | photo | 1 |
| SAR'77 | Mar. 1977 | Labrador Sea | X,L | air photo | 2 |
| SURSAT | Sept. 1978 | Baffin Bay | X,L | side-looking photo | 8 |
| SURSAT | Apr. 1979 | West Greenland | X,L | vertical photo, scatterometer, radiometer | several |
| SURSAT | Apr. 1979 | Melville Bay | X,L | vertical photo, scatterometer, radiometer | numerous |
| BERGMAP | Oct. 1979 | Baffin Bay | X(wide) | air photo | numerous |
| - | Mar. 1982 | Labrador Sea | X,L,C | vertical photo, scatterometer, radiometer, surface information | several |
| - | Apr. 1983 | Hibernia | X(wide) | colour and black-and-white vertical photo, side-looking 35 mm, surface information | numerous |
| RADARSAT | June 1983 | Hibernia | X,C | vertical photo, surface information | several |

I.4 ANNOTATED BIBLIOGRAPHY OF ICEBERG DETECTION

The following reports which are relevant to SLAR and SAR systems have been reviewed.

| Reference | Publication date | Geographic locations(s) | Year(s) |
|-------------------------|------------------|---|----------------------|
| SLAR SOURCES | | | |
| Super and Osmer | (1975) | Grand Banks | various |
| Farmer | (1972) | Grand Banks | various |
| Marthaler and Heighway | (1978) | Grand Banks | 1976-78 |
| Polar Research and Eng. | (1982) | Melville Bay | 1980-81 |
| SAR SOURCES | | | |
| Ketchum | (1977) | Kennedy Channel | 1975 |
| Larson et al. | (1978) | Labrador | 1977 |
| Parashar et al. | (1980) | Labrador | 1977 |
| Ketchum and Farmer | (1980) | Baffin Bay | 1979 |
| Gray et al. | (1980) | West Greenland | 1979 |
| Gray | (1980) | Scott Inlet Eastern Arctic | 1978 1979 |
| INTERTECH | (1980) | Lancaster Sound/ Davis Strait | 1979 |
| Kirby and Lowry | (1980) | Melville Bay Scott Inlet Cape York (SLAR) | 1979 1978 1978 |
| Lowry and Miller | (1983) | Lancaster Sound | 1979 |
| Livingstone et al. | (1983) | Eastern Arctic | 1979 |
| Pearson et al | (1980) | Eastern Arctic | 1979 |

I.4.1 SLAR SOURCES

Report: Super, A.D. and Osmer, S.R. (1975). "Remote Sensing as it Applies to the International Ice Patrol." Report by U.S. Coast Guard International Ice Patrol, Governors Island, New York.

Area: Grand Banks

Sensor(s): AN/APQ55 K-band SLAR, AN/DPD-2 Ku-band SLAR, AN/APS-94C X-band SLAR

Sea State/Iceberg Coverage: Various sea states and ice coverages

Iceberg Information: No imagery

Data Availability: USCG/IIP

Authors' Findings:

Maximum range of radar contact is proportional to the 4th root of the physical cross-sectional area of icebergs. A statistical relation derived from 152 observations shows that growlers (above-water area less than 1 x 6 m) usually cannot be detected by radar at ranges greater than 4 naut. mi.

Grand Banks and contiguous areas of the North Atlantic exhibit conditions of sub-normal radar propagation during the spring months when fog and ice hazards are most prevalent.

Waves greater than 1 m in height might obscure a dangerous growler, even with expert use of anti-clutter devices. If an ice target is not picked up beyond the sea return, it will not be detected at all.

Ice is not frequency-sensitive. The response to S- and X-bands is the same for ice and sea water.

Ice typical of that in icebergs on the Grand Banks has a reflection coefficient of approximately 0.33 and reflects radar waves 60 x less than a steel ship of equivalent cross-section.

In 1957 an AN/APQ55 (XA-1), K-band, real aperture radar was tried but with limited scope as a result of poor electric reliability.

In 1969 a modified AN/DPD-2, Ku-band, real-aperture SLAR was used on regular patrols and in 1970/71 to formulate a system of target discrimination between icebergs and other objects. This system was also used in 1972-73, however it was fairly old and was terminated because of problems with and with imagery handling.

An AN/APS-94C was used for project Icewarn 1975. It used Edo-Western dry silver negative film. The system imaged many targets including icebergs, whales, and debris. The system penetrated all weather except heavy rain. Small icebergs were consistently detected out to 48 km with a S/N ratio of at least 2.

IIP switched to AN/APS 94-D in 1976.

Report: Farmer, L.D. (1972). "Iceberg Classification Using Side Looking Airborne Radar." Report by United States Coast Guard, Office of Research and Development, Applied Sciences Division, U.S. Coast Guard Headquarters, Washington, D.C. 20591. 38 p.

Area(s) and Date(s) of Study: Grand Banks/various years

Sensor(s): AN/DPD-2 Ku-band SAR (information applicable to K- and X-band SLARs)

Sea State/Iceberg Coverage: Various

Iceberg Information: Detection information - Imagery samples in report

Data Availability: Unknown

Author's Findings:

Various clues such as size, shape, shadow (when present), tone, texture, pattern, edge sharpness, and wake presence can be used to determine the identity of targets (icebergs/ships) imaged by SLAR.

Size - although overall size may vary considerably with each target, if the length-to-width ratio exceeds 5:1 the object is usually a ship;
- if the height (calculated from a shadow, if present) exceeds 80 ft (24.4 m) the object will usually be an iceberg;
- measured dimensions of the target must be greater than the resolution at the range to the target to be significant.

Shape - the shape of targets on SLAR imagery often indicates actual shape. The shape of icebergs on SLAR imagery is repetitive and several basic shapes are seen regularly (i.e., small icebergs and growlers are usually either circular or oval whereas medium-to-large icebergs usually have

- ships and boats usually have more uniformly shaped returns.

Shadows - sometimes cast by icebergs when surrounded by ice but not seen in open water conditions.

Tone - affected by the target material, incidence angle and amount of time imaged. In relative terms metal ships are generally brighter than wooden ships, which in turn, are brighter than icebergs.

Texture - icebergs usually have more texture resulting from their generally multi-faceted surface (this is not usually true for weathered dome-like bergs);

- ships are usually more uniformly shaped and contoured.

Search Procedures

- areas of high and low target probability can be determined from past records and previous flights, hence narrowing search procedures (more applicable to IIP, but worth checking IIP records for other radar flights). Although this narrows the area to be searched, the whole area imaged should be quickly scanned.

System malfunctions and image distortions are generally caused by two main sources: aircraft/system and film handling/processing (i.e., aircraft turns cause gaps in the imagery away from the turn and overlapping in the direction of the turn). Other aircraft/system problems are altitude changes and equipment or antenna problems. Leakage of light during loading and improper or misadjusted settings can cause film problems.

Report: Marthaler, J.G. and Heighway, J.E. (1978). "Radar Image Processing of Real Aperature SLAR Data for the Detection and Identification of Iceberg and Ship Targets." Proceedings of the Fifth Canadian Symposium on Remote Sensing, Empress Hotel, Victoria, B.C. August 28-31, 1978. Edited by A. MacEwan. pp.482-505.

Area(s) and Dates of Study: Grand Banks of Newfoundland, 1976/1977/1978

Sensors: 1976/77 APS-94D SLAR with Icewarn specifications (Standard APS-94D) and modified APS-94D (includes Radar Image Processor [RIP]) in 1978.

Sea State/Iceberg Coverage: Not mentioned

Iceberg Information: Consists of author's analysis. No SLAR/photo imagery is presented although many of the author's data were verified either on the surface by ship or from aircraft visual observations or photos.

Data Availability: Unknown. Inquiries as to data location with the International Ice Patrol (IIP) were unsuccessful.

Authors' Findings:

Test indicated that adequate reliability in distinguishing iceberg and ship targets could not be achieved solely by visual examination of the standard SLAR imagery.

Ship returns are expected to be greater than those of icebergs.

A 1977 study imaging a Coast Guard ship (56 m long) stationed beside an iceberg of comparable size (60 m long by 30 m wide) at various incidence angles and target aspect angles showed that total target reflectivity should be one of the major inputs in the criteria used for target classification. The results of the study showed that whereas a considerable amount of variability can be expected from any given target, significant population differences still exist to provide target differentiation in a majority of cases (see Figure I-1).

A 1975 study for iceberg detection using the APS-94D showed that small icebergs could be consistently detected at ranges of up to 50 km (no actual dimensions of sea state conditions were mentioned). All targets detected during the study were verified visually from a reconnaissance plane. No false alarms or misses were found on 12 flights. No calibration was done to account for radar transmitter and receiver gain fluctuations or the effects of aircraft roll on the pattern of antenna gain.

Authors' Conclusions:

SLAR has the capability consistently to detect small iceberg targets (sea state and iceberg size were not mentioned. Altitude was mentioned as a maximum of 10,500 ft (3200 m) but this could vary between flights and years so depression angles could also be variable for the data presented).

Target reflectivities can be used as a means of target discrimination.

Automatic target detection, location, and tracking are possible with the SLAR/RIP system (previous to 1983, targets had to be observed visually to be verified as icebergs. In 1983 the IIP made the decision to classify probable targets

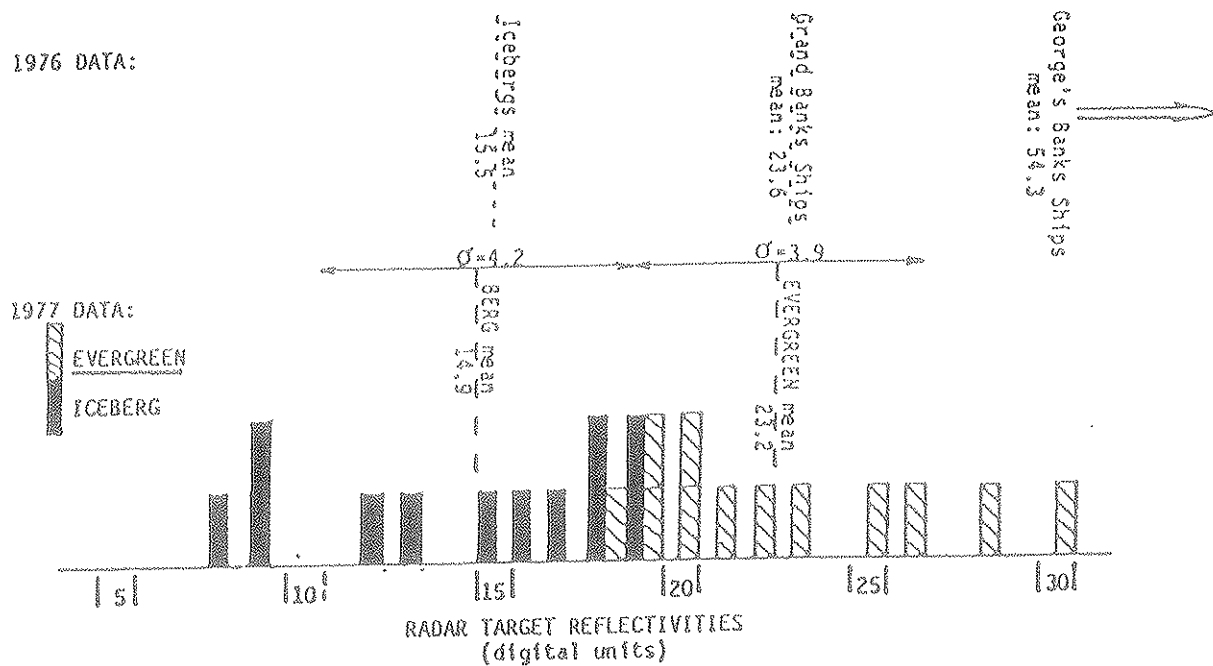


Figure I-1. Distribution of average target reflectivities for CGC Evergreen and iceberg during 1977 SLAR tests. NONIA and 1976 mean values are shown for comparison. (From Marthaler and Heighway 1978.)

as icebergs without the visual observations previously required, although targets are identified visually when possible.¹

Report: Polar Research and Engineering (1982). "Analysis of AES SLAR Imagery For the Detection of Icebergs and Other Ice Features." Report by D. Lapp for Dr. R.O. Ramseier, Senior Research Scientist, Atmospheric Environment Service, 365 Laurier Avenue West. D.S.S. Contract No. 01SE.KM605-0-0615, March 31.

Area(s) and Date(s) of Study: Melville Bay, February 1980, February 1981, Cape York, Greenland (box patterns flown)

Sensor(s): APS-94D (AES SLAR) X-band only, no photography (25- and 50-km scales)

Sea State/Iceberg Coverage: Ice-covered

Iceberg Information: Depression Angle, Scale/Swath Mode, Aspect Angle and other information on icebergs in ice

Data Availability: Original negatives (SLAR) at Ice Climatology (AES), Ottawa

Authors' Findings:

Analysis of the same piece of SLAR imagery by three individuals resulted in a variation in count of more than 100 icebergs out of a sample of about 600 (no surface verification was available but the point about variability between analysts is useful).

Iceberg signature (size and shape) was found to vary with range from the aircraft and the aspect angle at which it is viewed. The latter is important because of the difference between azimuth and range resolution.

Icebergs in the size range close to the sensor resolution or smaller had signatures which filled the resolution cell, giving an elliptical-shaped return, especially at far range.

Radar shadow was a function of location in the swath and on icebergs related to low or no-return areas.

At far ranges the radar shadow was not evident and could not be relied upon as an interpretive key.

¹CMDR N. Edwards, International Ice Patrol, pers. comm.

There was a drop in detectability for depression angles less than 3° (23% of the swath width).

More than 90% of the icebergs were found at depression angles less than 20° (20° covers 92.5% of the swath).

Aspect angle was found to be an essential parameter in resolving clusters of icebergs and icebergs in proximity to other surface features. This resulted from the combining of multiple icebergs into one signature as well as variations in clutter return and differences in azimuth and range resolution.

Swath width and scale had a profound effect on iceberg detectability. On average only 45% of the icebergs (not verified on the surface) observed on the 25-km swath width were found on the 50-km swath for the same area between two images.

Back-scatter for sea ice drops off significantly at low depression angles.

Additional information is given Tables I-4, I-5, I-6, and Figure I-2.

TABLE I-4

Examples of Depression Angle Ranges vs Fraction of Swath Width

| Depression Angle Range | Fraction of Swath Width |
|------------------------|-------------------------|
| 2.4 - 3.0 | 0.228 |
| 2.4 - 3.5 | 0.344 |
| 2.4 - 4.0 | 0.432 |
| 2.4 - 5.0 | 0.555 |
| 2.4 - 8.0 | 0.739 |
| 2.4 - 10.0 | 0.801 |
| 2.4 - 20.0 | 0.925 |

Source: After Polar Research and Engineering (1982)

TABLE I-5

Factors Affecting Iceberg Detection in Sea Ice

| Parameter | Dependent Considerations |
|---------------------------|---|
| System characteristics | Depression angle Resolution Frequency Polarization Aspect angle Scale of imagery |
| Target characteristics | Iceberg size and shape Numbers of bergs Ridge orientation and proximity to bergs Rubble proximity to bergs Proximity of bergs to each other Microwave properties of surrounding sea ice Location and proximity of shorelines, islands, shoals Location with respect to range |
| Operating characteristics | SLAR operator and image interpreter Altitude Bias and gain control levels Sensitivity - time controls SLAR film Geographic location SLAR reproduction processes Equipment malfunction Length of the flight |

Source: After Polar Research and Engineering (1982)

TABLE I-6

Azimuthal Resolution vs Swath Width

| Range (km) | Azimuthal Resolution (m) | Depression Angle |
|---------------|--------------------------|------------------|
| <u>100 km</u> | | |
| 5 | 49.3 | 40.48 |
| 10 | 81.5 | 23.11 |
| 15 | 117.0 | 15.88 |
| 20 | 153.4 | 12.04 |
| 25 | 190.2 | 9.69 |
| 30 | 227.3 | 8.10 |
| 35 | 264.4 | 6.95 |
| 40 | 301.7 | 6.09 |
| 45 | 339.0 | 5.42 |
| 50 | 376.4 | 4.88 |
| 55 | 413.7 | 4.44 |
| 60 | 451.1 | 4.07 |
| 65 | 488.5 | 3.76 |
| 70 | 526.0 | 3.49 |
| 75 | 563.4 | 3.26 |
| 80 | 600.9 | 3.05 |
| 85 | 638.3 | 2.87 |
| 90 | 675.8 | 2.71 |
| <u>50 km</u> | | |
| 5 | 40.7 | 23.11 |
| 10 | 76.7 | 12.04 |
| 15 | 113.6 | 8.10 |
| 20 | 150.9 | 6.09 |
| 25 | 188.2 | 4.88 |
| 30 | 225.6 | 4.07 |
| 35 | 263.0 | 3.49 |
| 40 | 300.4 | 3.05 |
| 45 | 337.9 | 2.71 |
| 50 | 375.3 | 2.44 |
| <u>25 km</u> | | |
| 5 | 38.3 | 12.04 |
| 10 | 75.4 | 6.09 |
| 12 | 90.4 | 5.08 |
| 15 | 112.8 | 4.07 |
| 17 | 127.8 | 3.59 |
| 20 | 150.2 | 3.05 |
| 25 | 187.7 | 2.44 |

Source: After Polar Research and Engineering (1982)

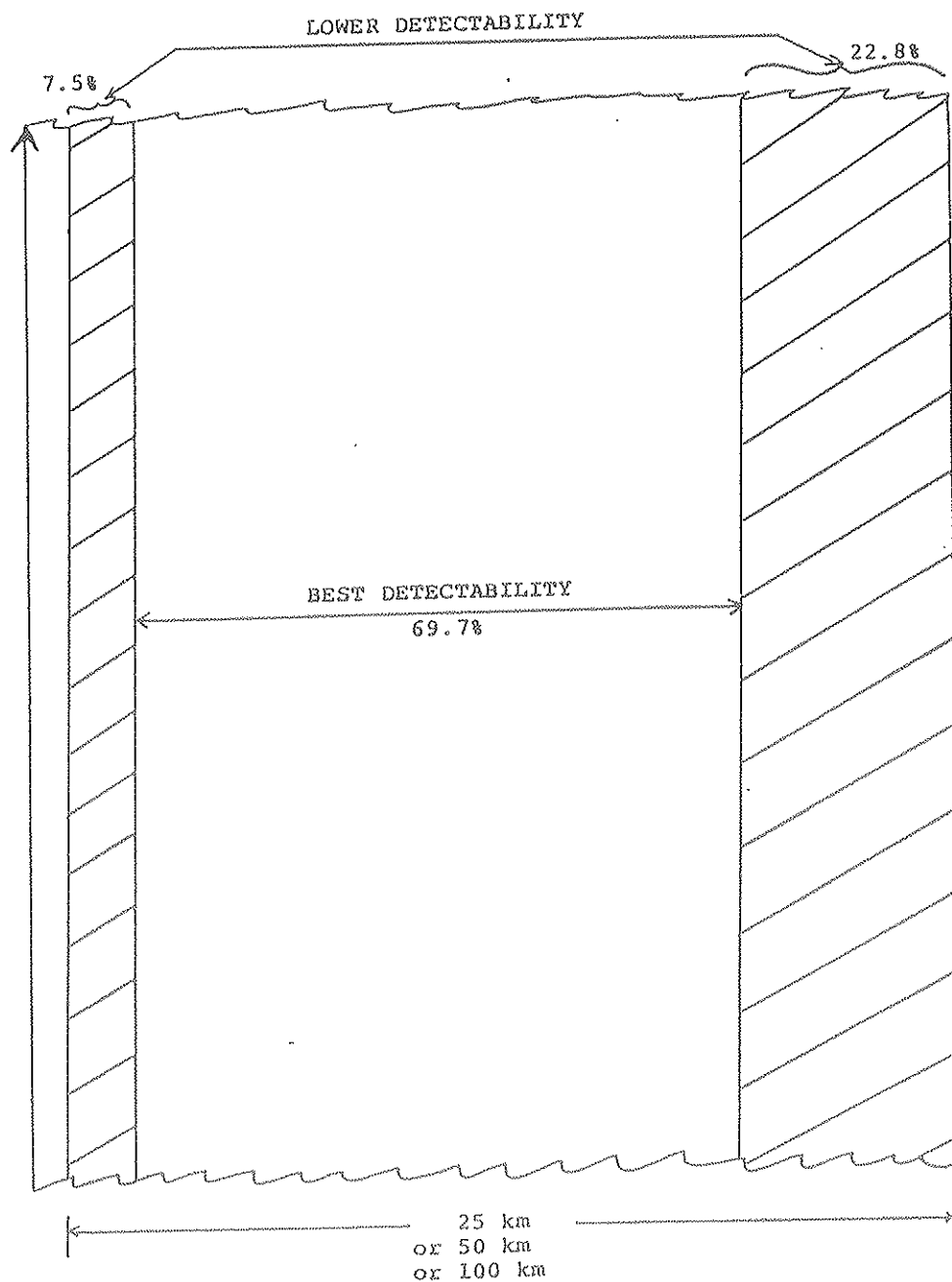


Figure I-2. Preferred portion of swath width on SLAR imagery for iceberg detection in sea ice (from Polar Research and Engineering 1982).

I.4.2 SAR SOURCES

Report: Ketchum, Jr., R.D. (1977). "An Evaluation of Side Looking Radar Imagery of Sea Ice Features and Conditions in the Lincoln Sea, Nares Strait, and Baffin Bay." Oceanography Division, Naval Oceanographic Laboratory, Naval Ocean Research and Development Activity (NORDA), NSTL Station, Mississippi, 39529, NORDA Technical Note 7.

Area(s) and Date of Study: Kennedy Channel, 7 May 1975

Sensors: Synthetic Aperture X-band radar, 5 naut mi swath width (type/designation not mentioned) and Aerial Photography (B&W)

Sea State/Iceberg Coverage: No open water present, iceberg surrounded by thick first-year ice exhibiting some deformation

Iceberg Information: One iceberg 150 m by 75 m

Data Availability: Radar Image/Air-photo in report

Authors' Findings:

Most icebergs found on the imagery were nondescript. One in particular could not readily be identified on the image even though the radar shadow and ridged ice bordering the iceberg were visible.

Signals received from the iceberg in question were a result of volume scattering from within the iceberg.

The iceberg radar signature can be less bright than that of small multi-year floes.

High resolution alone will not achieve iceberg detection.

(NOTE: L. Gray has commented that the SAR imagery was probably obtained from a relatively high altitude and that the depression angles were not less than 10° [Gray 1980].)

Report: Larson, R.W., Shuchman, R.A., Rawson, R.F., and Worsfold, R.D., (1978). "The use of SAR Systems for Iceberg Detection and Characterization." Proceedings of the Twelfth International Symposium on Remote Sensing of Environment V. 2, 20-26 April 1978. Center for Remote Sensing Information and Analysis, Environmental Research Institute of Michigan, Ann Arbor, Michigan, pp. 1127-1148.

Area and Date of Study: Labrador Sea, March 1978

Sensor: ERIM 4-channel, X-L band radar (later known as SAR-580)

Sea State/Iceberg Coverage: Ice and some small open-water areas; swell visible in ice

Iceberg Information: Detection Information and Imagery examples

Data Availability: C-CORE

Authors' Findings:

Most of the work was done on one iceberg in loose, unconsolidated, first-year pack ice. Calculated size 260 m long x 175 m wide x 70 m high, with a shadow present. Ocean swell was also present. X-band gave more information than L-band (3 dry-dock portions of the iceberg were visible). A second iceberg was identified but with more difficulty as the backscatter from the sea ice was greater.

Secondary methods to aid in iceberg detection in ridged and rafted ice are:

- high reflectivity ice to the lee of the iceberg. If grounded, the iceberg could cause the deformation of floes passing around it.
- presence of leads around an iceberg.

Ship/iceberg differentiation can be a problem. On occasion, sufficient iceberg or ship detail is present in an image. Linear ship motions result in shift of position or of focal position. Non-linear motions such as roll, pitch, or yaw resulting in unfocussed images are possible if the icebergs are rolling or pitching.

To maximize signal-to-clutter ratio, the radar should be operated at a low angle of depression. Digital records are useful to allow the storage of a high dynamic range (much greater than film). Detection probability can be found by comparing the effective signal-to-noise ratio on the X-axis to the detection probability value on the Y-axis (Figure I-3).

Authors' Conclusions:

Using SAR it is possible to:

- detect icebergs in a variety of sea ice clutter conditions;
- identify icebergs by shape characteristics;
- estimate size by using shadow information.

Secondary information is also of value in the detection and identification process.

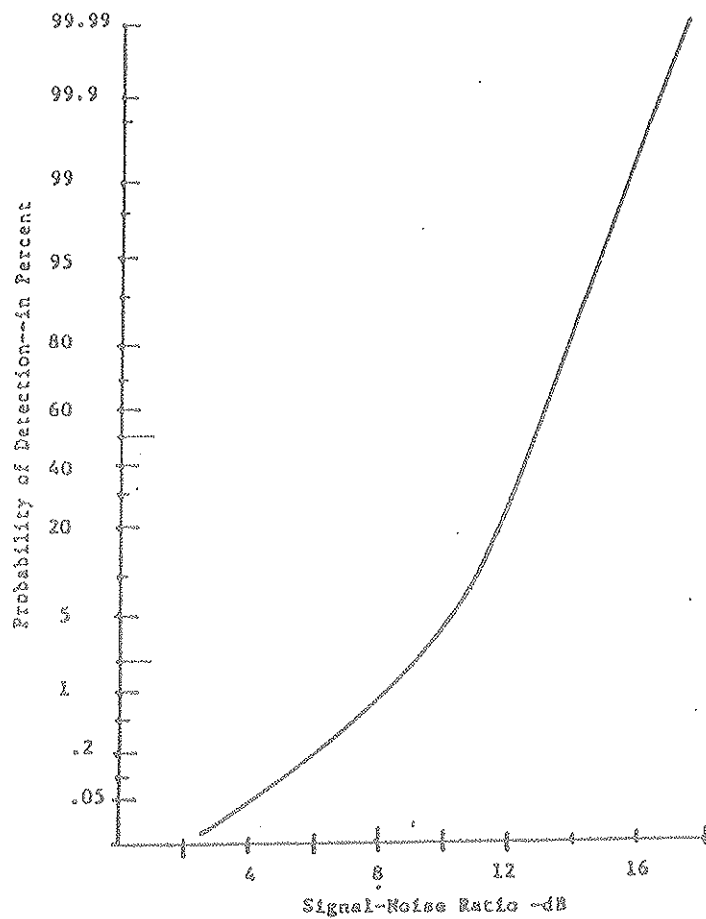


Figure I-3. Typical probability of detection given as a function of signal-to-noise ratio, assuming a false alarm of 10^{-6} and Gaussian statistics (from Larson et al. 1978).

Report" Parashar, S., Stapleton, G., Worsfold, R., and O'Neil, R. (1980). "Potential of SAR in Detecting and Monitoring Icebergs. Proceedings of the Iceberg Dynamics Symposium, 4 and 5 June 1979, St. John's, Newfoundland. Cold Regions Science and Technology, Vol. 1, Nos. 3 and 4, February, pp. 195-210.

Area and Date of Study: Labrador Sea, March 1977

Sensor: ERIM SAR, X-L band (4 channel)

Sea State/ Iceberg Coverage: Ice covered

Iceberg Information: 1 iceberg, SAR images/ air photo

Data Availability: C-CORE

Authors' Finding:

Past studies have shown icebergs to be inconsistent targets and relatively poor reflectors of electromagnetic energy. The detection of icebergs on radar imagery is dependent on the contrast between it and its surroundings of open water or sea ice. Sea clutter increases with increasing wind speed and is a function of incidence angle, etc. Sea ice clutter has a large dynamic range of 30-35 dB and is dependent on ice type, salinity, surface roughness, and temperature.

The SAR data were collected from an altitude of 3000 m with a depression angle of 30°. The iceberg imaged was surrounded by ice floes ranging from partially consolidated to consolidated. The estimated size of the iceberg, from the radar imagery, was 260 m long, 175 m wide, and 70 m high.

The detection of icebergs in open water is largely dependent on prevailing wind conditions which determine the "open water" clutter and angle of incidence. Icebergs may be difficult to detect at depression angles greater than 50° at moderate (15 m/s) wind speeds. The radar return from ships is generally higher than from icebergs and is more of a clue than shape.

Authors' Conclusions:

Cross-polarized (HV) imagery tends to present better contrast between the iceberg and its surroundings than parallel-polarized (HH) imagery.

Parallel polarization (HH) should provide better discrimination against water because of smaller clutter values.

The range of depression angles should definitely be smaller than 50° so as to make use of shadow effects to and minimize clutter.

The large dynamic range of iceberg returns (30 dB) is greater than that of present recording films (20 dB) and digital radar data appears to be more desirable.

Report: Ketchum, Jr., R.D. and Farmer, D.L. (1980). "Eastern Arctic SURSAT SAR Ice Experiment, Radar Signatures of Sea Ice Features." Section 5.2 in Proceedings of the Final SURSAT Ice Workshop, Atmospheric Environment Service, Toronto, 23-27 June 1980. Edited by R.O. Ramseier and D.C. Lapp, February 1981, 38 p.

Area and Date of Study: Baffin Bay, April 1979

Sensor(s): SAR 580 Synthetic Aperture Radar, X-L bands (Steep mode) 4 channels

Sea State/Iceberg Coverage: First-year ice cover

Iceberg Information: SAR imagery and air photos of several icebergs

Data Availability: Original SAR images at NAPL Ottawa, air photos with authors and CCRS

Author's Findings:

A number of icebergs were identified tentatively because of their bright returns and shapes. All icebergs were not identified on all three available channels (XHH, XHV, LHH).

Internal scattering on L-band produces a false image, making one iceberg in particular seem either longer or appear as two icebergs. The same iceberg is visible as only one on X-band. (Note: depression angles were not mentioned).

Figures in the report show icebergs on corresponding air photo/SAR images.

Report: Gray, L., Gudmansen, P., Overgaard, S., Skou, N., and S ndergaard Pedersen, F., (1980). "West Greenland Sea Ice Experiment, SURSAT Report No. 1." Section 5.6 in Proceedings of the Final SURSAT Ice Workshop, Atmospheric Environment Service, Toronto, 23-27 June 1980. Edited by R.O. Ramseier and D.C. Lapp, February 1981.

Area and Date of Study: West Greenland, March 1979

Sensor: SAR-580 synthetic aperture Radar, X-L band, steep mode

Sea State/Iceberg Coverage: Icebergs in sea ice

Iceberg Information: No particular icebergs/examples mentioned/given

Data Availability: SAR imagery originals at NAPL, Ottawa

Authors' Findings:

It has been shown that the SLAR can detect icebergs in sea ice better with smaller depression angles (less than about 8°) than at larger values. Inspection of the SAR imagery shows that the detection of icebergs is possible at larger depression angles, however, there is often a small contrast between the iceberg and the surrounding ice.

Other work has shown that icebergs in the size range from 10 to 100 m are much more difficult to detect reliably from high resolution, steep mode SAR imagery. The detection of the larger icebergs depended on the ability of the interpreter to see and recognize the target outline as being characteristic of an iceberg rather than the presence of back-scatter contrast between the iceberg and the sea ice.

From a simple consideration of the shape and size of icebergs, and the fact that the back-scatter from the surrounding sea ice will fall off with decreasing depression angle, one would expect the signal-to-clutter ratio to increase with decreasing depression angle for angles less than 10° (Rawson et al. 1977; Gray et al 1979). The inverse $\sin \theta$ angular dependence of the Rayleigh roughness criterion reinforces the belief that at small depression angles ($\theta < 5^\circ$) the bright regions in a SAR or SLAR image will correspond more with the larger features (e.g., ridges, icebergs, bergy bits) than would be the case at larger depression angles ($\theta > 10^\circ$).

Report: Gray, L. (1980). "Depression Angle Study, SURSAT Report No. 2" Section 5.7 in Proceedings of the Final SURSAT Ice Workshop, Atmospheric Environment Service, Toronto, 23-27 June 1980. Edited by R.O. Ramseier and D.C. Lapp, February 1981, 19 p.

Areas and Dates of Study: Scott Inlet, Baffin Island, September 1978 and the Eastern Arctic, April 1979

Sensors: SAR-580 X-L bands with some reference to the AES AS/APS-94D SLAR

Sea State/Iceberg Coverage: Calm open water and ice covered

Iceberg Information: No figures or imagery showing icebergs were presented

Data Availability: SAR-580 imagery at NAPL, Ottawa: Other data at CCRS

Authors' Findings:

Detection of Icebergs in Open Water: Using SAR-580 X-L imagery of icebergs on successive days (Scott Inlet), it was demonstrated that low depression angles and HH polarization appear to offer the best signal-to-clutter ratio (SCR) for SAR aircraft operation.

Detection of Icebergs in Sea Ice: The average contrast or SCR between icebergs and the surrounding sea ice can often be quite small when relatively large depression angles are used.

Using the Technical University of Denmark SLAR (X-band) imagery it is shown that SCR increases significantly for depression angles less than about 80°.

Discrimination of Ships and Icebergs: By using a high resolution imaging system it may be possible to discriminate on the basis of the shape of the pattern of bright returns and shape and size of the radar shadows (if they are visible).

On average, it appears that ship returns are larger than iceberg returns. Consequently, if one had a high-resolution system (to estimate size), the strength of the returns per pixel may aid in the discrimination process.

Ships in motion in open water have characteristic wakes (which icebergs do not) which are often visible on radar images. Ship wakes have been observed on SEASAT imagery even when the ship return was not significantly above the average sea clutter background.

If the radar (i.e., search radar) views the target for some time, then the fluctuations in the intensity of the back-scattered returns (target fading or scintillation) may differ characteristically for ships and icebergs.

Report: INTERTECH (1980). "Project-Bergmap." Report prepared for Petro-Canada Inc.

Areas and Date of Study: Lancaster Sound, Davis Strait area, October 1979

Sensor: SAR-580 synthetic aperture radar, X-band (wide swath mode)

Sea State/Iceberg Coverage: Pack ice and open water, some waves breaking on icebergs present

Iceberg Information: Iceberg sightings from SAR imagery, SAR images, no other sensors

Availability: Original SAR imagery locations unknown (Petro-Canada)

Authors' Findings:

Icebergs larger than 20 m can be detected and identified. Smaller icebergs may be detected but correct identification in presence of sea ice can be difficult. Large icebergs showing shape and detail can be identified from day-to-day. Small depression angles should be used to maximize iceberg returns and to minimize sea and ice returns. Depression angles should be kept constant over the entire swath; this will require operating aircraft at higher altitudes. Under certain conditions iceberg shadows could be used to estimate iceberg heights.

Re-identification of smaller icebergs is improved with the use of an iceberg drift model. (Note: the International Ice Patrol uses an iceberg drift model which it finds useful.)

Authors' Conclusions:

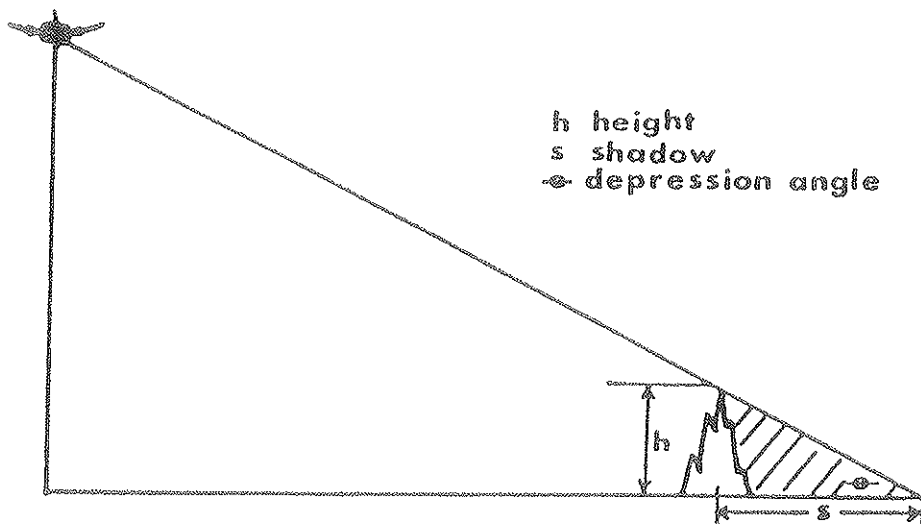
Iceberg detection and size measurement may be practical using real-time, on-board computers (Figure I-4).

The probability of detection and correct identification of large icebergs is about 100%. The probability of correct identification begins to fall for icebergs of less than 20 m and the probability of detection begins to fall for icebergs of 10 m or less. (Note: It was mentioned that the data from the study was not enough to go on by itself and surface-verified data could be of greater use.)

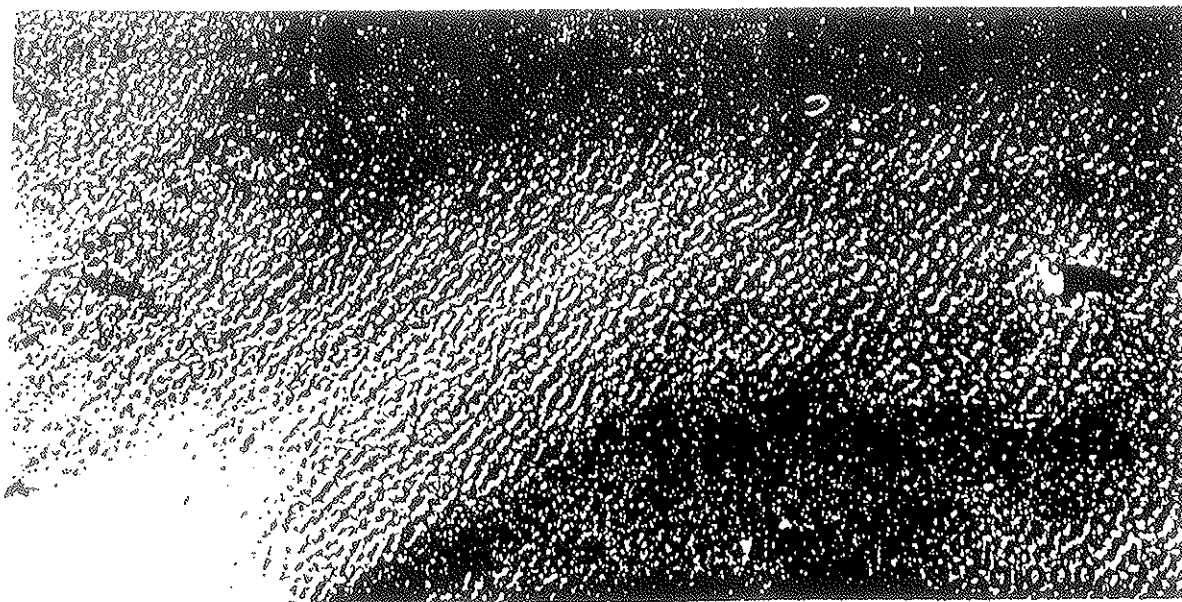
Detection performance of the radar is generally independent of environmental conditions, with the exception of sea state. Very high sea states will mask icebergs smaller than the waves, decreasing the detection of icebergs under 20 m in size. (Note: some effects can be expected on larger icebergs, such as wave smear in azimuth.)

Report: Kirby, M.E. and Lowry, R.T. (1980). "Iceberg Detectability Problems Using SAR and SLAR Systems." Section 5.13 in Proceedings of the Final SURSAT Ice Workshop, Atmospheric Environment Service, Toronto, 23-27 June 1980. Edited by R.O. Ramseier and D.C. Lapp, February, 1981. 32 p.

Areas and Dates of Study: Cape York, Greenland, March 1979; Scott Inlet, Baffin Bay, September 1978; and Cape York, Greenland, February 1978



Geometry showing how iceberg height can be calculated from radar shadow.



Iceberg in the lee of Cape Byam Martin, Bylot Island, N.W.T.
Oct 5 1979.

Figure I-4 (a)& (b). Determining iceberg height from radar shadow.

Sensors: SAR-580 synthetic aperture radar, X-L bands (steep mode) 4-channel, and 35-mm photography (oblique), and AES APS-94 SLAR imagery and 35-mm photography (oblique).

Sea State/Iceberg Coverage: Ice-covered areas in February 1978 and March 1979, mostly open water with little ice in September 1978

Iceberg Information: Numerous SLAR, SAR, and 35-mm photo examples

Data Availability: Original SAR-580 imagery negatives are at NAPL, Ottawa. Original SLAR negatives are at Ice Climatology, (AES) Ottawa, 35-mm photos with authors

Authors' Findings:

For icebergs much larger than the system resolution, tabular and blocky icebergs should be more detectable because their steep sides act as excellent corner reflectors. Dry-dock and pinnacled icebergs are generally more multi-faceted than other icebergs and should have a greater probability of detection. As their sides are more vertically oriented they would probably be better detected at shallower angles. Domed icebergs are the most difficult to detect because of their well-rounded shape and low profile. SAR-580 imagery, March 1979, collected at depression angles from 30° to 90° (steep mode) on 4-channels (XHH, XHV, LHH, and LHV), indicates:

- that X-band shows greater iceberg detail than L-band (probably due to lower L-band resolution and difference in wavelength);
- that comparison of an oblique 35-mm photo and XHH/HV SAR images shows that most of the bergy bits and of all the icebergs have been imaged (all in fast ice) although some smaller icebergs would have been difficult to identify without the photos; and
- that iceberg orientation rather than size can sometimes be the more predominant factor affecting the detectability.

SAR imagery, September 1978, collected in open water at very shallow depression angles (8°), shows:

- icebergs in pack ice fragments which have brightness levels similar to those of the icebergs. In this case spatial information allows the differentiation of the pack and icebergs;
- icebergs imaged on one flight could be identified on a flight 2 days later (most of the icebergs were probably grounded);

- the ocean quite calm for both flights, with little wave action.

SLAR imagery from Cape York, Greenland in February 1978 shows many icebergs in fast and pack ice. The surrounding ice creates problems such as:

- high returns from ridges sometimes obscuring icebergs;
- high returns from other small features such as the fast-ice edge or pieces of ice that act as corner reflectors;
- the SLAR imagery was at fairly shallow angles for many areas of the imagery;
- the SLAR film has a limited dynamic range (15 dB) so that bright targets generally saturate and bloom.

Authors' Conclusions:

Iceberg detection at depression angles less than 20° could be difficult in sea and ice backgrounds.

Greater dynamic range (i.e., 35 dB) is required for recording films.

Icebergs could not be classified according to size and type with SLAR but could be with SAR (the authors have acknowledged that their data set may be limited).

Cross-polarized, X-band imagery appeared superior to parallel-polarized imagery for iceberg detection because of larger tonal separation between icebergs and sea ice (which has also been noted by other authors).

Report: Lowry, R.T. and Miller, J. (1983). "Iceberg Mapping in Lancaster Sound with Synthetic Aperture Radar," Section 503 in the Proceedings of the 8th Canadian Symposium on Remote Sensing, Montreal, 3-6 May 1983. Edited by K.P.B. Thomson and F. Bonn.

Area and Date of Study: Lancaster Sound, October 1979

Sensor: SAR-580 synthetic aperture radar, X-band

Sea State/Iceberg Coverage: Icebergs in open water

Iceberg Information: SAR and limited air photographs

Data Availability: same as Bergmap

Authors' Conclusions:

The probability of detection and correct identification of large icebergs is about 100%. The probability of correct identification begins to decrease for icebergs of less than 20 m, and the probability of detection begins to decrease for icebergs of 10 m or less.

A quantitative assessment of how these two probabilities vary, either jointly or separately, with variation in iceberg size, cannot be made with the data currently in hand. Ideally, reliable surface-verified data are required for this task. Radar data, processed to degraded resolution, would be useful in this regard.

The detection performance of the radar is generally independent of environmental conditions, with the exception of sea state. Very high sea states will mask icebergs that are not larger than waves. Thus, the performance at less than 20 m would be reduced further by high seas.

Large icebergs can be re-identified on subsequent days by their complex shape, in spite of rotation under the conditions observed. Good surface information is required to quantify the reliability of the re-identification with SAR data, as a function of iceberg size, sea state, and radar resolution.

An analysis of the data seems to show that the largest water-line dimension of icebergs is exponentially distributed. The family of icebergs tested is not large enough to place high confidence in this hypothesis. If it can be proved valid, this theory will be useful for estimating the number of small icebergs not identified, and perhaps, for estimating the number of extreme-sized icebergs.

Report: Livingstone, C.E., Hawkins, R.K., Gray, A.L. Drapier Arsenault, L., Okamoto, K., Wilkinson, T.L., and Pearson, D. (1983). "The CCRS/SURSAT Active-Passive Experiment 1978-1980: The Microwave Signatures of Sea Ice." Data Acquisition Division, Canada Centre for Remote Sensing, Department of Energy, Mines and Resources, Ottawa, Canada, June 1983.

Areas and Dates of Study: Eastern Arctic, April 1979

Sensor: SAR-580 X-L band (4 channel)

Sea State/Iceberg Coverage: Pack ice; ice covered

Iceberg Information: Many icebergs on SAR imagery, scatterometer, radiometer, vertical and side-looking air photos

Data Availability: SAR imagery at NAPL, others at CCRS

Authors' Findings:

Of five icebergs visible in air photography of the sensor line, only two clearly showed on the SAR imagery and completely filled the scatterometer beam. Data are summarized in Table I.7. Both icebergs had dimensions of greater than 200 m in azimuth and were imaged at incidence angles near 50° . For one of the icebergs, back-scattering coefficients measured by scatterometer yielded an iceberg-to-background ice cross-polarized contrast of 10.2 dB and a like-polarized contrast of 9.5 dB, at 55° incidence angle.

A marginally detectable iceberg was also profiled by the scatterometer. The dimension in azimuth was greater than 100 m and was viewed by the SAR at a 50° incidence angle. The minimum cross-polarized iceberg-to-background contrast was 2 dB at 45° angle of incidence. HH-polarized data are unavailable.

Undetectable and marginally detectable icebergs were imaged at incidence angles of 50° to 60° ; their azimuth dimensions were 25-100 m.

Seven icebergs located in visually uniform, shore-fast, first-year ice in Melville Bay were also imaged; the presence of cracks and cemented floes was indicated by the scatterometer trace. Figure I-5 displays the iceberg-to-background contrast for these icebergs.

Overall, cross-polarized back-scattering coefficient contrasts are 2-4 dB larger than like-polarized contrasts. Variations of incidence angle in the range of 15° to 60° do not enhance contrast; iceberg back-scattering cross-sections vary with angle in the same manner as smooth first-year ice over this incidence angle range. Icebergs with lowest back-scattering coefficients were either weathered, domed, or tilted tabular icebergs imaged from the side having the smallest slope.

Report: Pearson, D., Livingstone, C.E., Hawkins, R.K., Gray, A.L., Drapier Arsenault, L., Wilkinson, T.L., and Okamoto, K., (1980). "Radar Detection of Sea Ice Ridges and Icebergs in Frozen Oceans at Incidence Angles from 0° to 90° ." Section 5.12 in Proceedings of the Final SURSAT Ice Workshop, Atmospheric Environment Service, Toronto, 23-27 June 1980. Edited by R.O. Ramseier and D.C. Lapp, February, 1981. 12 pp.

Areas and Dates of Study: Beaufort Sea, Eastern Arctic, March-April 1979

Sensors: Scatterometer (13.3 GHz) and SAR (X-band)

Iceberg Information: SAR imagery, scatterometer imagery, RC-10 photos

TABLE I-7

Iceberg Detectability from the Danish N/S Line, 032401

| RC-10 Photography Roll 1087 | | | Ku-band Scatterometer | | | Detectability of Berg in the SAR Image | | | | | |
|-----------------------------|-------|-------------------|---------------------------|------------------------------------|---------|--|------------|------------|--------------|--------------|------------|
| Berg size (type) (m) | Frame | GMT (HH:MM:SS) | Incidence angle (°) | Contrast with FY Ice HV (dB) | HH (dB) | Incidence angle (°) | HV | HH | X-Band HV | L-Band HV | HH |
| 12 x 102 (drydock) | 6687 | 15:38:14 | 45 | 2 | N/A* | 60 | marginal | marginal | undetected | undetected | undetected |
| 222 x 216 (tabular) | 6773 | 15:53:43 | off | scat | track | 60 | good | good | undetected | undetected | undetected |
| 480 x 252 (tubular) | 6781 | 15:55:04 | 55 | 10.2 | 9.5 | 51 | excellent | very good | undetected | undetected | undetected |
| 57 x 25 (pinnaculer) | 6781 | 15:55:04 | off | scat | track | 60 | undetected | marginal | undetected | undetected | undetected |
| 30 x 25 (pinnaculer) | 6781 | 15:55:04 | off | scat | track | 51 | undetected | undetected | undetected | undetected | undetected |

* N/A not available

Source: From Livingstone et al. (1983)

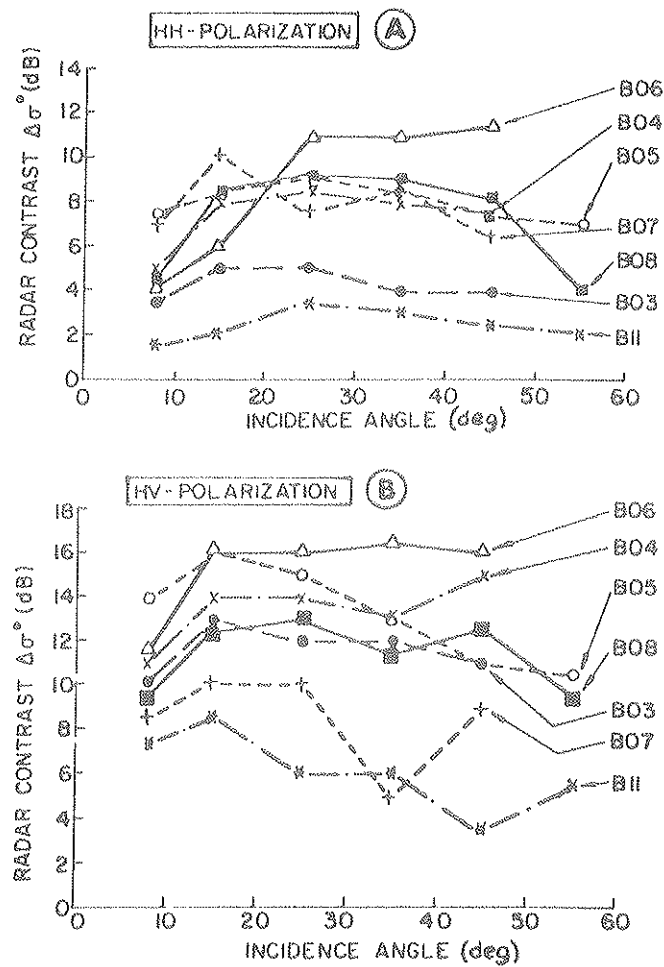


Figure I-5. Radar contrast between icebergs and smooth first-year ice (from Livingstone et al. 1983).

Data Availability:**Authors' Findings:**

Icebergs occurring in a sea-ice background were imaged by SAR and scatterometer, and were also photographed. Numerous icebergs occurred on the photos, but only five were covered by the scatterometer; of these five, the SAR identified only two owing to the steep depression angle. The others were not distinguishable from the background sea-ice. Both imaged icebergs were >200 m in along-track dimension and were imaged at incidence angles of $\sim 50^\circ$. The remaining three icebergs not visible on the imagery were also imaged at a 50° incidence angle, but had along-track dimensions of 25-125 m.

Authors' Conclusions:

Radars operating with incidence angles of $16-45^\circ$ are not suitable for iceberg detection. Incidence angles of $0-65^\circ$ give poor detectability, especially for icebergs in a background of broken first-year ice.

Icebergs which were poorly detectable or undetectable by SAR had along-track dimensions between 25 and 125 m and were viewed at an incidence angle of $\sim 50^\circ$.

Because a 10-15 dB target-to-background contrast is needed for an identification accuracy of 90%, many icebergs and bergy bits larger than the SAR resolution cell will not be detected in steep depression angles by SAR.

I.5 REFERENCES

- Farmer, L.D. 1972. Iceberg classification using side looking airborne radar. Report by United States Coast Guard, Office of Research and Development, Applied Sciences Division, U.S. Coast Guard Headquarters, Washington, D.C. 20591. 38 p.
- Gray, L. 1980. Depression angle study, SURSAT Report No. 2. Section 5.7 in Proceedings of the Final SURSAT Ice Workshop, Atmospheric Environment Service, Toronto, 23-27 June 1980. Edited by R.O. Ramseier and D.C. Lapp, February 1981. 19 p.
- Gray, L., P. Gudmansen, S. Overgaard, N. Skou, and Pedersen F. Sondergaard, 1980. West Greenland sea ice experiment, SURSAT Report No. 1. Section 5.6 in Proceedings of the Final SURSAT Ice Workshop, Atmospheric Environment Service, Toronto, 23-27 June 1980. Edited by R.O. Ramseier and D.C. Lapp, February 1981.
- INTERTECH 1980, Project-Bergmap. Report prepared for Petro-Canada Inc.
- Ketchum, Jr., R.D. 1977. An evaluation of side looking radar imagery of sea ice features and conditions in the Lincoln Sea, Nares Strait, and Baffin Bay. Oceanography Division, Naval Oceanographic Laboratory, Naval Ocean Research and Development Activity (NORDA), NSTL Station, Mississippi, 39529, NORDA Technical Note 7.
- Ketchum, Jr., R.D. and D.L. Farmer. 1980. Eastern Arctic SURSAT SAR ice experiment, radar signatures of sea ice features. Section 5.2 in Proceedings of the Final SURSAT Ice Workshop, Atmospheric Environment Service, Toronto, 23-27 June 1980. Edited by R.O. Ramseier and D.C. Lapp, February 1981, 38 p.
- Kirby, M.E. and R.T. Lowry. 1980. Iceberg detectability problems using SAR and SLAR systems. Section 5.13 in Proceedings of the Final SURSAT Ice Workshop, Atmospheric Environment Service, Toronto, 23-27 June 1980. Edited by R.O. Ramseier and D.C. Lapp, February, 1981. 32 p.
- Larson, R.W., R.A. Shuchman, R.F. Rawson, and R.D. Worsfold. 1978. The use of SAR systems for iceberg detection and characterization. Proceedings of the Twelfth International Symposium on Remote Sensing of Environment, V. 2, 20-26 April 1978. Center for Remote Sensing Information and Analysis, Environmental Research Institute of Michigan, Ann Arbor, Michigan. p. 1127-1148.

- Livingstone, C.E., R.K. Hawkins, A.L. Gray, L. Drapier Arsenault, K. Okamoto, T.L. Wilkinson, and D. Pearson. 1983. The CCRS/SURSAT active-passive experiment 1978-1980: the microwave signatures of sea ice. Data Acquisition Division, Canada Centre for Remote Sensing, Department of Energy, Mines and Resources, Ottawa, Canada, June 1983.
- Lowry, R.T. and J. Miller. 1983. Iceberg mapping in Lancaster Sound with synthetic aperture radar. Section 503 in the Proceedings of the 8th Canadian Symposium on Remote Sensing, Montreal, 3-6 May 1983. Edited by K.P.B. Thompson and F. Bonn.
- Marthaler, J.G. and J.E. Heighway, 1978. Radar image processing of real aperture SLAR data for the detection and identification of iceberg and ship targets. Proceedings of the Fifth Canadian Symposium on Remote Sensing, Empress Hotel, Victoria, B.C. 28-31 August 1978. Edited by A. MacEwan. p. 483-505.
- Parashar, S., G. Stapleton, R. Worsfold, and R. O'Neil. 1980. Potential of SAR in detecting and monitoring icebergs. Proceedings of the Iceberg Dynamics Symposium, 4-5 June 1979, St. John's, Newfoundland. Cold Regions Science and Technology 1:195-210.
- Pearson, D., C.E. Livingstone, R.K. Hawkins, A.L. Gray, L. Drapier Arsenault, T.L. Wilkinson, and K. Okamoto. 1980. Radar detection of sea ice ridges and icebergs in frozen oceans at incidence angles from 0° to 90°. Section 5.12 in Proceedings of the Final SURSAT Ice Workshop, Atmospheric Environment Service, Toronto, 23-27 June 1980. Edited by R.O. Ramseier and D.C. Lapp, February 1981. 12 p.
- Polar Research and Engineering. 1982. Analysis of AES SLAR imagery for the detection of icebergs and other ice features. Report by D. Lapp for Dr. R.O. Ramseier, Senior Research Scientist, Atmospheric Environment Service, 365 Laurier Avenue West. D.S.S. Contract No. 01SE.KM605-0-0615, March 31.
- Super, A.D. and S.R. Osmer. 1975. Remote sensing as it applies to the international ice patrol. Report by U.S. Coast Guard International Ice Patrol, Governors Island, New York.

BERGSEARCH '84

SECTION II

DATA COLLECTION

BERGSEARCH '84

SECTION II CHAPTER 1
SURFACE INFORMATION

F.G. Bercha and Associates Limited
Ottawa, Ontario

II.1 SURFACE INFORMATION

II.1.1 INTRODUCTION

In accordance with the Canadian Oil and Gas Lands Administration ESRF update, Volume I (1) dated 16 September 1983, F.G. Bercha and Associates Limited submitted a document dated 12 October 1983, outlining their proposal for participation in the study titled: Assessment of Airborne Imaging Radars for the Detection of Icebergs.

F.G. Bercha and Associates Ltd. were tasked with the conduct of the Phase II: Data Collection portion of the study, which encompassed participation in the design of the data acquisition program, co-ordination of the operational acquisition of radar data, co-ordination and participation in the acquisition of surface data; processing, initial interpretation, and distribution of data.

Phase II of the study can now be considered complete. Minutes of meetings conducted through-out the study have received wide circulation and an interim progress report was submitted with each "application for payment."

This final report provides a summary of activities carried out during the conduct of the study, presents a listing of data acquired and includes a complete surface observations report enclosed as Appendix C.

II.1.2 PLANNING MEETINGS

At a preliminary meeting in Ottawa on 1 December 1983 to define the objectives of the program and arrange a tentative schedule of events, the participants were the ESRF Program Officer, the ESRF Scientific Adviser and principals of F.G. Bercha and Associates Limited.

All participants were invited to attend an operations meeting in Ottawa on 10 January 1984. During the meeting a general overview of all phases of the study was presented and a tentative operations plan was drafted. Minutes of the meeting were prepared and forwarded to all attendees.

All participants were invited to attend another operations meeting in Ottawa on 22 February 1984. All participants were invited to attend. The meeting was briefed on all aspects of the pending data-acquisition phase of the study, including sources of ice and weather data, aircraft operations, surface information procedures, communications channels, and reporting procedures. Detailed minutes of the meeting were prepared and forwarded to all attendees.

A series of meetings were convened with a number of other agencies to ensure the provision of weather information, ice information, aircraft flying control, telecommunications equipment, office equipment and supplies, office and operations room accommodation, and accommodation for participants in Gander, Newfoundland.

II.1.3 DOCUMENT PREPARATION

Surface Truth Manual A Surface Truth Manual was prepared to assist personnel in the collection and reporting of surface data.

Surface Truth Log A Surface Truth Log was designed and circulated to various applicable agencies. On receipt of approval, the log was produced on waterproof paper, in pad form, for operational use.

Operations Manual An operations manual detailing all aspects of the operational data-acquisition phase of the project was designed and forwarded to all participants. The manual contained the names, addresses, and telephone numbers of all participants and agencies involved in the study; outlined procedures to be followed during the pre-flight, flight, and post-flight periods; and listed the required distributions of data and documents.

II.1.4 CHRONOLOGY OF DATA COLLECTION

27 March 1984

- Weather briefing requirements finalized.
- Design of weather briefing packages for the Ops room and Aircrew finalized.
- Use of Dept. of Transport Board Room for weather and ops briefing confirmed.
- Aerodrome and aircraft control procedures finalized.
- Communications procedures finalized.
- Operations room organized.

28 March 1984

- Gander airport closed due to a snow storm.

30 March 1984

- All participants notified that the program would proceed effective 1 April 1984.

1 April 1984

- All participants arrived at Gander.
- The CCRS CV-580 flew one mission.
- A full briefing was held in the Orange room of the Sinbad's Motel. The briefing included:
 - (a) Introduction of participants.
 - (b) An outline of program activities.

- (c) Communications procedures.
- (d) Air control procedures.
- (e) Flight parameters.

2 April 1984

- Weather briefing in hangar at 0730.
- Target co-ordinates were provided to crews,
- All aircraft flew.
- Operations plotted flight tracks provided by crews, compared coverage with known surface data and checked flight logs.
- De-briefing was held at 2000 in Sinbad's Motel.
- Medium sea-state flights are considered complete.

3 April 1984

- Weather briefing in the hangar at 0730.
- Target co-ordinates were provided to crews.
- All aircraft flew, but returned late in the evening.
- Operations plotted flight tracks provided by crews, compared coverage with known surface data and checked flight logs.

4 April 1984

- No flying due to the absence of the required sea-state.
- Plots of data acquired on 2 and 3 April were updated.
- De-briefing held at 2000 hrs in Sinbad's Motel.
- Ops area for Operations Flight provided to crews, to permit planning of flight lines.
- Low sea-state flights considered complete.

5 April 1984

- Weather briefing in the hangar at 0730.
- Operations flight data reviewed.
- Aircraft flew, and on landing, commenced their plot of icebergs.
- Operations assembled surface data available.
- Data received from crews at 2000 during de-briefing.
- Operations synthesized data from AES and IIP to produce an operations ice map and message for fax transmission to Mobil in St. John's.
- Fax transmitted at 0115 April 6.
- CF MAR performed an interpretation on their own data in St. John's and passed maps plus applicable data to Husky-Bow Valley.
- The Intera aircraft returned to base unserviceable, after obtaining 50% cover of the operations area. They could not perform interpretation on quick-look data available from the STAR-1 system.
- A "Target of Opportunity" area was given to crews who wished to fly on 6 April.

6 April 1984

- Official day off from program flying.
- Major de-briefing held at 2000 to discuss progress to date and to show fax resulting from operational flights.

- briefing for last research flight.

7 April 1984

- Weather briefing at 1130 at high sea-states not expected until evening.
- Individual de-briefings carried out with aircraft crews, as they arrived late from flight.
- High sea-state flights considered complete.

8 April 1984

- Final flight data received
- Operations room closed at 1200.

NOTE: 1. Data receipt master log attached as Appendix A.
2. Data received is listed in Appendix B.

II.1.5 POST-OPERATION EVENTS

16-26 April 1984

- Annotation of 35-mm surface data negatives carried out.

27 April 1984

- 35-mm negative delivered for printing.

30 April 1984

- Prints of 35-mm negative received and passed to CANPOLAR.

9 May 1984

- Annotation of 15 rolls of SLAR negative imagery was completed and passed to the National Air Photo Library Reproduction Centre (NAPL/RC) for cleaning and the production of transparencies.

1 June 1984

- Transparencies of SLAR imagery were picked up by CANPOLAR at NAPL/RC. Inspection revealed that the quality of reproduction was poor.
- CANPOLAR commenced interpretation of the inferior quality transparencies.
- Negatives were returned to NAPL/RC for further production.

26 June 1984

- STAR negatives received and forwarded to NAPL/RC for transparency production.

12 July 1984

- Transparencies of STAR data were picked up at NAPL/RC for transparency production.

1 September 1984

- Final transparencies of SLAR data were received from NAPL/RC.

| BERG SEARCH 84 MASTER DATA LOG | March | | | | April | | | | | | |
|-----------------------------------|-------|------|----|----|-------|------|------|---|---|---|------|
| | ← | 29 | 30 | 31 | 1 | 2 | 3 | 4 | 5 | 6 | 7 |
| <u>SLAR IMAGERY</u> | | | | | | | | | | | |
| - AES | - | - | - | - | - | X | X | - | X | - | X |
| - IIP | - | - | - | - | - | X | X | - | X | X | X |
| - CF MAR | - | - | - | - | - | X | X | - | X | - | X |
| - CCRS - Quick Look | - | ? | - | - | ? | ? | ? | - | - | - | - |
| - Transparency | - | ? | - | - | ? | ? | ? | - | - | - | - |
| - STAR 1 - Quick Look | - | - | - | - | - | ? | ? | - | ? | - | ? |
| - Transparency | - | - | - | - | - | ? | ? | - | ? | - | ? |
| <u>AERIAL PHOTOGRAPHS</u> | | | | | | | | | | | |
| - Atlantic | - | - | - | - | - | X | - | - | X | X | - |
| - Other | - | - | - | - | - | - | - | - | - | - | - |
| <u>GROUND TRUTH DATA</u> | | | | | | | | | | | |
| - 35 mm photographs | - | - | - | X | X | X | X | X | X | X | X |
| - Colour polaroids | - | - | - | - | X | X | X | X | X | X | X |
| - Other | - | - | - | - | - | - | - | - | - | - | - |
| <u>OTHER REMOTE SENSING DATA</u> | | | | | | | | | | | |
| - CCRS Scatterometer | - | - | - | - | - | ? | - | - | - | - | - |
| - CF MAR Video Tape | - | - | - | - | - | - | - | - | ? | - | - |
| - Other - Atlantic Radar | - | - | - | - | - | X | - | - | X | X | - |
| - CCRS SAR | - | - | - | - | - | - | - | - | - | - | - |
| - TRANSIT | - | - | - | - | - | - | - | - | - | - | - |
| - (Quick Look) | - | X(2) | - | - | X | X(3) | X(3) | - | - | - | - |
| - STAR 1 TRANSIT | - | - | - | - | - | - | - | - | - | - | - |
| - (Quick Look) | - | - | - | - | - | X | - | - | - | - | - |
| <u>FLIGHT LINE MAPS</u> | | | | | | | | | | | |
| - AES | - | - | - | - | - | X | X(2) | - | X | - | X |
| - IIP | - | - | - | - | - | X | X | - | X | △ | △ |
| - CF MAR | - | - | - | - | - | X | X | - | X | - | X |
| - CCRS | - | ? | - | - | ? | X | ? | - | - | - | - |
| - STAR 1 | - | - | - | - | - | X(3) | X | X | X | X | X(2) |

X = Data in hand
△ = Not plotted

? = Data not received

- = Data not obtained
on this day

| BERG SEARCH 84 MASTER DATA LOG | March | | | | April | | | | | | |
|---|-------|----|----|----|-------|---|---|---|---|---|---|
| | ← | 29 | 30 | 31 | 1 | 2 | 3 | 4 | 5 | 6 | 7 |
| <u>GROUND TRUTH MAPS</u> | | | | | | | | | | | |
| - Mobil Ice Recce (Atlantic Airways) | - | - | - | - | - | - | - | X | X | X | - |
| - Others | - | - | - | - | X | X | X | - | - | - | - |
| <u>OPERATIONS MAPS</u> | | | | | | | | | | | |
| - AES | - | - | - | - | - | - | - | - | X | - | - |
| - IIP | - | - | - | - | - | - | - | - | X | △ | - |
| - CF MAR | - | - | - | - | - | - | - | - | X | - | - |
| - STAR 1 | - | - | - | - | - | - | - | - | X | - | - |
| <u>MISCELLANEOUS MAPS</u> | | | | | | | | | | | |
| - Mobil Ice Recce | - | - | - | - | - | - | - | X | - | - | - |
| - Nordco Report | - | - | - | - | - | - | - | X | - | - | - |
| - IIP Theoretical Flight Lines | - | - | - | - | - | X | - | - | - | - | - |
| - Rig Location Base Map | - | - | - | - | X | - | - | - | - | - | - |
| <u>WEATHER DATA</u> | | | | | | | | | | | |
| - St. John's | X | X | X | X | X | X | X | X | X | X | X |
| - Gander | X | X | X | X | X | X | X | X | X | X | X |
| - Polaris V | - | - | - | - | ? | ? | ? | ? | ? | ? | ? |
| <u>OCEAN DATA</u> | | | | | | | | | | | |
| - St. John's | X | X | X | X | X | X | X | X | X | X | X |
| - Gander | X | X | X | X | X | X | X | X | X | X | X |
| - Polaris V | - | - | - | - | ? | ? | ? | ? | ? | ? | ? |
| <u>ICE MAPS</u> | | | | | | | | | | | |
| - St. John's | X | X | X | X | X | X | X | X | X | X | X |
| <u>SHIP REPORTS</u> | | | | | | | | | | | |
| - Fisheries | X | X | X | X | X | X | X | X | X | X | X |
| - Coast Guard | X | X | X | X | X | X | X | X | X | X | X |

X = Data in hand
△ = Not plotted

? = Data not received

- Data not obtained
on this day

| BERG SEARCH 84 MASTER DATA LOG | March | | | | April | | | | | | |
|-------------------------------------|-------|----|----|----|-------|---|---|---|---|---|---|
| | ← | 29 | 30 | 31 | 1 | 2 | 3 | 4 | 5 | 6 | 7 |
| <u>DATA LOGS</u> | | | | | | | | | | | |
| Flight Logs Plotted by OPS | | | | | | | | | | | |
| Room | | | | | | | | | | | |
| - AES | - | - | - | - | - | X | X | - | X | - | X |
| - IIP | - | - | - | - | - | X | X | - | X | X | X |
| - CF MAR | - | - | - | - | - | X | X | - | X | - | X |
| - CCRS | - | X | - | - | X | X | X | - | - | - | - |
| - STAR 1 | - | - | - | - | - | X | X | X | X | X | X |
| Aerial Photo Logs | | | | | | | | | | | |
| - Atlantic | - | - | - | - | - | - | - | - | X | X | - |
| Iceberg Position Logs | | | | | | | | | | | |
| - AES | - | - | - | - | - | X | X | - | △ | - | △ |
| - IIP | - | - | - | - | - | X | X | - | △ | △ | △ |
| - CF MAR | - | - | - | - | - | △ | △ | - | △ | - | △ |
| - CCRS | - | X | - | - | X | X | X | - | - | - | - |
| - STAR 1 | - | - | - | - | - | △ | △ | △ | △ | △ | △ |
| Flight Logs Provided by | | | | | | | | | | | |
| Aircrews | | | | | | | | | | | |
| - AES | - | - | - | - | - | X | X | - | X | - | X |
| - IIP | - | - | - | - | - | X | X | - | X | X | X |
| - CF MAR | - | - | - | - | - | X | X | - | X | - | X |
| - CCRS | - | X | - | - | X | X | X | - | - | - | - |
| - STAR 1 | - | - | - | - | - | X | X | X | X | X | X |
| Miscellaneous | | | | | | | | | | | |
| - Mobil Spector Radio | - | - | - | - | X | - | - | - | - | - | - |
| - Iceberg Ops Messages to Mobil | - | - | - | - | - | - | - | - | - | X | - |
| - Fax Transmission Rx | - | - | - | - | X | X | X | X | X | X | X |
| - Mobil Weather Forecasts | - | - | - | - | X | X | X | X | X | X | X |
| - Mobil Ice Recce Status Reports | - | - | X | X | X | X | X | X | - | - | - |

X = Data in hand
△ = Not plotted

? = Data not received

- = Data not obtained
on this day

DATA RECEIVED

SLAR IMAGERY

| | | | | |
|--------|---|--|----------|-----------------------------|
| AES | - | April 2 | Roll #A1 | ESRF Flight #1 |
| | | April 3 | Roll #A2 | ESRF Flight #2 |
| | | April 5 | Roll #A3 | ESRF Flight #3 (Ops Ft) |
| | | April 7 | Roll #A4 | ESRF Flight #4 |
| IIP | - | April 2 | Roll #1 | ESRF Flight #1 |
| | | April 3 | Roll #2 | ESRF Flight #2 |
| | | April 3 | Roll #3 | ESRF Flight #2 |
| | | April 3 | Roll #4 | ESRF Flight #2 |
| | | April 5 | Roll #5 | ESRF Flight #3 (Ops Ft) |
| | | April 6 | Roll #6 | ESRF Targets of Opportunity |
| | | April 7 | Roll #7 | ESRF Flight #4 |
| CF MAR | - | April 2 | Roll #M1 | ESRF Flight #1 |
| | | April 3 | Roll #M2 | ESRF Flight #2 |
| | | April 5 | Roll #M3 | ESRF Flight #3 (Ops Ft) |
| | | April 7 | Roll #M4 | ESRF Flight #4 |
| CCRS | - | - only transit data provided - quick look and transparency will take some time to receive - transit data may have reflectors appearing | | |
| STAR 1 | - | - only one piece of transit data - Intera would not hand over quick look data - seems it is required for processing transparencies - transparencies will not be available for some time - Intera will only turn them over to CANPOLAR | | |

AERIAL PHOTOGRAPHS

Atlantic Airways - Log Sheets

| | | |
|---------|---------------|----------------|
| April 2 | 30 Exposures | Roll #M8401-03 |
| April 5 | 144 Exposures | Roll #M8402-03 |
| April 6 | 162 Exposures | Roll #M8403-03 |

Others - No aerial imagery reported by other aircraft.

GROUND TRUTH DATA

| | |
|-------------------|--|
| 35 mm photographs | - all black and whites |
| | - taken on MV Polaris V |
| Polaroids | - mostly colour, with a few black and white images taken on MV Polaris V |

OTHER REMOTE SENSING DATA

- CCRS Scatterometer - No info presently available to determine when flown, although flight logs indicate scat data obtained April 3.
- CF MAR Video Tape - some oblique video data obtained before darkness during the Ops Flight
 - release will be necessary from Husky-Bow Valley
- Other - it is not known if other sensors were operated by participants, except for the Atlantic Radar Altimeter which can be used to:
 - 1) determine height of icebergs, and
 - 2) digitized photos which can be used to give 1 m contours of bergs.
- output of radar altimeter appears on air photographs
- digitization of photos must be requested through Monil and can only be done for those bergs with stereo pair photos.

FLIGHT LINE MAPS

- Flight maps were plotted in the field when possible.
- AES ops maps are also available.
- CCRS maps for pre-period flights and ESRF Flight #2 not available.
- IIP flight maps for Target of Opportunity and ESRF Flight #4 were not plotted.

GROUND TRUTH MAPS

- Mobil Ice Recce's (visual and photo)
- Others - miscellaneous reports

OPERATIONS MAPS

- AES and IIP were plotted immediately after flight and used to construct a master which was faxed to Mobil St. John's at 0115 hrs on April 6.
- STAR 1 data was received too late to fax. It did not have new data that warranted further operational analysis.

- CF MAR downlinked data to rigs during flights and did a plot for Husky-Bow Valley operations in St. John's.

MISCELLANEOUS MAPS

- These maps were plotted in the field to assist with day to day operations.

WEATHER DATA

- Data from St. John's and Gander is as complete as possible.

OCEAN DATA

- Data from St. John's and Gander is as complete as possible.

ICE MAPS

- Received from Coast Guard in St. John's.

SHIP REPORTS

- In folders containing weather and ocean data.

DATA LOGS

- Flight logs plotted by the Operations Room
 - These were done to translate a/c logs into a standard form to facilitate the plotting of flight line maps and the location of bergs.
- Aerial Photo Logs
 - These give positions of the photographed icebergs.
- Iceberg Position Logs
 - These are being plotted by CANPOLAR.
 - Position logs completed in the field are included.
- Flight Logs Provided by Aircrews
 - These are the flight logs as presented to Ops Room with film.

ASSESSMENT OF AIRBORNE IMAGING RADARS
FOR THE DETECTION OF ICEBERGS
PHASE II: DATA COLLECTION

SURFACE OBSERVATIONS REPORT

NOTE: Appendix "A" - 3 hour Manmar observation is not included with this report. Enquiries for this information should be directed to:

Jim Dempsey (Technical Manager)
Dobrocky Seatech (Nfld.) Ltd.
P.O. Box 2278, Station "C"
St. John's, Newfoundland
A1C 6E6

General Considerations for Interpreters

The methodology of data acquisition during the ESRF Airborne Radar Program is presented below. In addition, observations made of the ice conditions, berg characteristics and limitations of the data are outlined. Supplementary information generated by other ongoing programs is also itemized with indication as to personnel responsible listed at the end of this section. Finally, all data sheets recorded initially, are held by F.G. Bercha and Associates Limited and any query or question concerning these data will gladly be answered by S. Digby at the Ottawa office or S. Martindale in Calgary.

All measurements, observations and photographs, with the exception of icebergs "seen but not visited" and various growlers, were made from the starboard side of the ship, and either the bridge or helideck which stands 7.3 m (24') above sea level.

Contents

1. Details of equipment utilized onboard
2. Official nomenclature
3. Considerations when assessing radar reliability
4. Sources of information
5. Activity summary

1. DETAILS OF EQUIPMENT ONBOARD

a) Navigation

An integrated display system, the JLZ-50 Color SATLON was installed, providing satellite derived data, using the JLE 3800 satellite system, and shore based LORAN-C (JNA 760) and display video screen (NWU 50 A Color Plotter). The satellite system was updated only when the satellite was overhead and therefore was subject to sudden changes on update. The LORAN-C was poor - being beyond its capabilities (distance offshore). It recorded positions up to 87°S 79°E in error.

b) Cameras

Pentax MG 35 mm with Pentax Digital Data M Back.

Vivitar 70-210 mm f 4.5 Macro focusing zoom lens.

Polaroid EE-100 Special land camera b/2 FL = .112 mm.

Polaroid Sonar One step colour FL = .116 mm.

c) Laser Rangefinder Optech

The laser was found to be inoperative on icebergs as for the most part no return was received. This was possibly due to icing. Confidence in the few readings obtained from the laser was not high enough to justify employment of it. An optical rangefinder was utilized. Results also appeared to be subject to gross error possibly due to the height of the helideck from the water line or the roll of the ship. For distances > 0.1 nm the ship's radar was used to record distances, but with bergs < 0.1 nm, estimates by eye were made. All estimates were discussed with the Captain. Where the optical rangefinder was used, height, width, and length measurements are designated on the data forms as DC (Dubrocky Calculated). Where the ship's radar and measurements from photographs were made, they were designated SC (Self Calculated). Where estimates by eye are used SE (Self Estimate) is used. All SE numbers were the result of at least two people's judgement. The estimate of mass is based on the 3 dimensions of the berg and thus is subject to the above restraints, calculated thus.

$$\text{MASS } m^3 = h \times w \times l \times 3.$$

All wave and atmospheric data was taken using the MANMAR scheme.

2. OFFICIAL NOMENCLATURE

Although the MANICE document clearly outlines a scheme of classification for icebergs, several alternate systems are in use in the Grand Banks area, Newfoundland. As icebergs and associated features (berg bits and growlers) have predominantly different characteristics to those found off the coast of Labrador, some of the accepted nomenclature from the MOBIL/NORCOR Ice Management Program was incorporated into the ESRF classification to provide a more comprehensive approach. The iceberg sizing however was taken from AES MANICE.

a) Iceberg sizes

1. Growler (GG) \leq 1 m in freeboard height
2. Bergy Bit (BB) 1-5 m height
3. Small Berg (SB) 5-10 m height
4. Medium Berg (MB) 10-30 m height
5. Large Berg (LB) 30 m height

b) Iceberg type

1. Growler (GGG) as above
2. Bergy Bit (B) as above
3. Tabular (TAB) predominantly flat topped
4. Pinnacled (PNC) rises to one or more sharp peaks
5. Domed or Spherical (SPH) rounded
6. Wedge (WDG) tilted flat berg
7. Drydock (DDK) berg which had partially or wholly broken through to form a shallow 'canal' or 'dock' with two distinct above water sections
8. Weathered (WETH) berg with highly dissected and eroded surface so that a 'skeleton' remains of the more resistant or massive ice only. These gave the appearance of cauliflowers or karstic scenery at times.

c) Iceberg conditions

Iceberg conditions include the state of the ice itself, the weathering process and accretion recorded.

- i) Ice characteristics - bergs were observed to have several distinctive properties that may or may not

affect the radar return. Most ice displayed a record of its formation, and therefore events in the glacial history of the ice were evident.

Types:

- dirt bands - indicated on each surface truth log sheet, have been observed to run horizontally, vertically and to be involuted.
- blue ice bands - formed probably by refreezing of glacier ice do not form more or less resistant ice on a regular basis, but have been observed to 'etch out' on some bergs.
- cleavages - observed on most bergs when the spray etched serac patterns, were probably formed by former crevassing events.

ii) Weathering etched out the weaker ice and displayed many resulting forms. Erosion is also included in this section as the transport of H_2O in solid or liquid form is difficult to determine in some cases. Mechanical weathering is evident, in fact predominant, in the zone of max-min wave height, while spray etching is more predominant in higher areas. Cauliflower weathering - intensive weathering of cleavages which results in skeletal ice protruberences often rounded by accretion or erosion. These often extended from a distinctive wave cut platform.

Karstic formation - where the cleavages were oriented in 90° planes the ice formed dirt and gryke like ice pavements.

Knobbly ice - formed when the cleavage system was more open and erosion generated rounded balls formed one on top of another, giving the appearance of tree galls.

- iii) Accretion of ice was observed on the first few days, but atmospheric conditions for the later flights were not conducive to icing. Several ice forms were noted:
pebbled surface - where rounded clear ice formed on a glacier ice surface, with uniform overall nature icicles - many overhangs supported extensive icicle arrays.
Rime, surficial icing and frosting were also observed. The large crystals of the glacier ice were distinct from any subsequent icing.

3. CONSIDERATIONS WHEN ASSESSING RADAR RELIABILITY

It became very evident early on in the ground truth program that a simplistic approach to iceberg movement and weathering may affect the accuracy of the analysis. Therefore the following characteristics were noted when observed to provide a better concept of ground variables throughout the flights.

- a) ROLL/TIP - Many icebergs, particularly those of any areal extent were affected by swell. Large bergs, however, often showed little tendency to tilt. Rolling was observed in all sizes of bergs, and could be very subtle, yet dramatic. The berg that the ship 'stood off' on 3rd April was recorded as a dry drock, but it repeatedly rolled at least 90° around one axis on a frequent basis. The berg was observed to roll at least 16 times and presented very different surface characteristics 'on its side' (domed) as opposed to 'upright' (dry dock). In addition the berg rotated.
- b) ROTATION - Particularly with bergs that presented a very sharp face in one aspect alone, rotation is very important. Rotations both clockwise and anticlockwise were observed, of magnitudes in excess of 90° in 20 minutes. Multi-face recordings may record 3 or 5 faces of the box in such cases.
- c) BOBBING was observed in many bergs, but seemed critical to radar detection in the growler/bergie bit/small berg classes. Bergs that bobbed appeared to have a conical, rounded shape. Often a domed berg was observed to bob in the swell from 0 - twice

its average height. Many were wave washed at the low of their periodicity.

d) WAVE WASHED bergs, particularly growlers and bergy bits that were very weathered, were wave covered except for 2 or 3 protruberences. These often were extremely angular and therefore were good enough radar targets.

4. SOURCES OF INFORMATION

For each day of overflights, all sources of information are listed which includes material collected indepedently of overflights. A summary of this information and contact personnel is listed as follows:

1. TYPE: MANMAR - A selected ship's meteorological log (AES).
FORMAT: A report made every three hours. See attachement A.
CONTACT: Jim Dempsey (Technical Manager)
Dobrocky Seatech (Nfld.) Ltd.
P.O. Box 2278
Station 'C'
St. John's, Newfoundland ALC 6E6
Tel: (709) 364-2981
2. TYPE: Vessel Ice Report
FORMAT: A report made every three hours. See Attachment B.
CONTACT: Jim Dempsey, Dobrocky Seatech (address above).
See MANMAR contact address.
3. TYPE: Record of Communications
FORMAT: Notes on File.
CONTACT: Jim Dempsey (as for MANMAR).
4. TYPE: Ship's Log
FORMAT: Brief (62 sentence) statement of day's activities.
CONTACT: CARINO Company Ltd.
P.O. Box 6146, East Post Office
St. John's, Newfoundland ALC 5X8
Tel: (709) 753-5359
5. TYPE: Ship's Location at Sea
FORMAT: Every three hours the ship's location is relayed to Mobil in St. John's.

CONTACT: J. Benoit
Mobil Oil Canada Ltd.
Atlantic Place (Box 62)
215 Water Street
St. John's, Newfoundland A1C 6C9

6. TYPE: Trip reports
FORMAT: Reports will be prepared by J. Dempsey, and
D. Nazarenko (Mobil rep. from Calgary office).

CONTACT: J. Benoit (see above for address).

7. TYPE: Video tape of selected events
FORMAT: Video tape/release subject to Mobil approval.

CONTACT: H.H. Lanziner, President
1974 Spicer Road
N. Vancouver, B.C. V7H 1A2
Tel: (604) 929-7961

8. TYPE: Wave Rider
CONTACT: J. Benoit (To our understanding, analysis of
this data has been contracted out.)

5. ACTIVITY SUMMARY

| | |
|-----------------|---|
| April 1 - Sun | - Ground truthed bergs |
| | - Stood away from berg during overflights |
| April 2 - Mon | - Stood away from berg during overflights |
| April 3 - Tues | - Ground truthed bergs |
| | - Stood by tipping berg during overflights |
| April 4 - Wed | - Revisited 2 bergs of April 3 |
| | - Profiling program - Dobrocky Seatech |
| April 5 - Thurs | - Ground truthed large number of bergs |
| April 6 - Fri | - Ground truthed many bergs |
| April 7 - Sat | - Stood by bergy bit throughout day of overflights. |

Sunday

Activity Log

1 April 1984

- 1100 - As yet no instructions as to where the study area is but will ground truth bergs seen evening of 31st. Assuming Convair will fly.
- 1240-1636 - Ground truthed 2 bergs and 2 growlers.
- 1500 - Contacted Mobil base to obtain information on ESRF program.
- 1620 - Message that Convair is flying and to move back from bergs.
- 1915 - Waverider deployed for 2 hours.
- 2130 - Steaming towards 47° 00'N, 47° 00'W.
- 2400 - Call from J. Benoit - all planes will be flying commencing 0900 NST 2 April.

Sources of Information

Included

APPENDICES

- A - 3 hr Manmar weather observations
- B - Berg data sheets
- C - Berg location charted (D. Nazarenko, J. Dempsey)
- D - Ship location from M. vessel ice report

- 1.3 -

APPENDIX D

Ships location taken from Mobil ice report.

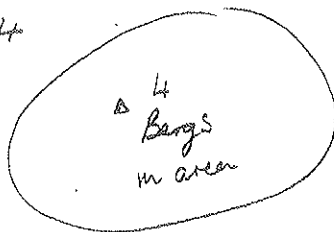
| GMT | Speed (km)/Heading | N | W |
|------|--------------------|-----------|------------|
| 0000 | --- | 47° 0.27' | 47° 13.1' |
| 0345 | 05/350 | 47° 0.49' | 47° 58.5' |
| 0545 | 06/287 | 47° 14.5' | 46° 02.2' |
| 0845 | 06/163 | 47° 15.3' | 47° 20.1' |
| 1145 | 10/097 | 47° 55.5' | 47° 11.21' |
| 1445 | 10/094 | 46° 55.0' | 47° 54.4' |
| 1745 | --- | 46° 49.4' | 46° 48.7' |
| 2045 | --- | 46° 46.7' | 46° 49.8' |

Appendix C

Copy of chart

SM / APR 4 1984

COMPOSITE FOR 1 APRIL - 2 APRIL 1984



▲ Berg

Bergy Bit

47°W

▲ BERG
BIT

46°30' W

Berg +
▲ M321
APR 1.

+ 47°N

▲ A3
▲ C-3

▲ D-1

▲ M321
APR 2

+
▲ 47°W

+ 46°30' N
46°30' W

75 #4
↓ #3

Monday

Activity Log

2 April 1984

- 1000 Z - Standing by for instructions on where to locate during overflights. Call not received.
- 1530 Z - AES Electra overhead. Personnel will relay concerns re: communication.
- Stood 9 nm N from berg during day (# 221).
- 1400-2123 - Waverider obtained data.
- 1918 - J. Benoit called with information on berg locations and instructions re positioning of ship.

Sources of Information

Included

APPENDICES

- A - 3 hr Manmar observations
- B - hourly summary of weather/environmental data
- C - Summary of ships location from M. ice reports
 - Mobil ice reports
 - Bergs location - see Appendix C for 1 April
 - Photos of sea state

APPENDIX C

Ships position from ice summary.

| Time | Speed km/Hdg | N | W |
|-------------|--------------|-----------|-----------|
| 0000-15 min | 00/xxx | 46° 45.1' | 46° 50.0' |
| 0245 | 02/330 | 46° 43.5' | 46° 54.1' |
| 0600 | 01/335 | 46° 44.2' | 46° 57.8' |
| 0900 | 05/316 | 46° 45.0' | 46° 58.1' |
| 1145 | 01/296 | 46° 45.6' | 47° 03.7' |
| 1515 | 02/330 | 46° 45.2' | 47° 08.5' |
| 1745 | 01/225 | 46° 44.8' | 47° 11.2' |
| 2045 | 01/157 | 46° 41.5' | 47° 10.9' |
| 2345 | 00/xxx | 46° 42.2' | 47° 16.2' |

↑
questionable given
waverider deployment

APPENDIX B

Hourly Weather/Environmental Data 2 April 1984

| Time GMT | Primary Waves | | Secondary Waves | | Wind | | Temp. | | Cloud | | Vis nm | Ice Cond. |
|-------------|---|------|-----------------|--------|------|-------|-------|------|-------|----------|-----------|--------------------|
| | Height | DirN | Period | Height | DirN | Speed | DirN | Air | Sea | Height | | |
| 1200 | | | | | | 19 | 180 | -0.1 | 0.5 | obscured | 4½ | 0/w |
| 1300 | 0.4 | NE | 3 sec | 2.0 | NNE | 16 | 360 | -0.5 | 1.0 | 100 m | 72 | 0/w |
| 1400 | 0.2 | NW | 2 sec | 1.2 | NNW | 18 | 310 | -0.1 | 1.0 | 150 m | 72 | 0/w |
| 1500 | 0.1 | W | 1 sec | 1.0 | NW | 19 | 164 | -0.1 | 0.7 | 150 m | 72 | 0/w |
| 1600 | 0.1 | WNW | 1 sec | 0.8 | NNW | 16 | 014 | -1.0 | -0.7 | 200 m | 72 | 0/w |
| 1700 | 0.1 | WNW | 1 sec | 0.6 | NNW | 13 | 159 | -0.8 | -0.5 | 500 m | 710 | 0/w King Air |
| 1800 | <0.1 | NW | 1 sec | 0.6 | NW | 11 | 264 | -1.2 | -0.5 | 200 m | 5 | 0/w |
| 1800a | Weather changing rapidly - wind increasing, snow and squalls in vicinity. | | | | | | | | | | | |
| 1900 | 0.1 | NNW | 2 sec | 0.5 | NNW | 17 | 090 | -1.0 | +0.5 | 200 m | 78 | 0/w |
| 2000 | 0.1 | N | 1 sec | 1.0 | N | 17 | 100 | -1.5 | +0.5 | 200 m | 78 | 0/w |

Tuesday

Activity Log

3 April 1984

- 0945 - Started ground truth on bergs specified to be in area of $47^{\circ} 00'N$, $46^{\circ} 45'W$ as indicated by J. Benoit in phone conversation of previous evening. Only 3 of 4 bergs said to be in area were found. Gave position of 1st berg visited to J. Benoit in phone patch made at that time. Ground truthed 3 bergs and group of 3 growlers.
- 1300 - On location standing by berg A-3 position $46^{\circ} 55.58'N$, $46^{\circ} 48.43'W$. Standing by 500 m from iceberg. Berg tipped through 90° to present two very different profiles at intervals throughout the day.
- 1410 - Line to waverider caught in starboard bow thruster. (Waverider deployed over starboard.)
- 1910 - Waverider taken out.

Sources of Information

Included

APPENDICES

- A - 3 hr Manmar weather observations
- B - Hourly weather/environmental data
 - Video tape of rolling berg A-3 during standby
 - Mobil ice report made every 3 hrs by J. Dempsey
- C - Summary of ships course from ice reports
- D - Notes on rolling berg
 - Berg data sheets - 3 bergs + growler group

APPENDIX B

Hourly Weather/Environmental Data April 3, 1984

| Time GMT | Primary Waves | | Secondary Waves | | Wind | | Temp. | | Cloud Height | Vis nm | Ice Cond. |
|-------------|---------------|------|-----------------|---------|------|---------|-------|------|-----------------|-----------|--------------|
| | Height | DirN | Period | Height | DirN | Speed | Air | Sea | | | |
| 1300 | 0.2 | 10° | 1 sec | 1.4 | 260° | 2 | -0.2 | +1.5 | >600 m | >25 | 0/w |
| 1400 | 0.2 | 10° | 1 sec | 1.2 | 280° | 3 | -0.1 | 1.5 | >600 m | >15 | 0/w |
| 1500 | 0.1 | 280° | 41 sec | 1.2 | 330° | 4 | 0.0 | 1.5 | >600 m | >15 | 0/w |
| 1600 | 0.2 | 310° | 1 sec | 1.1 | 350° | 4 | -0.5 | 1.5 | >600 m | >15 | 0/w |
| 1700 | 0.1 | 120° | 1 sec | 1.0 | 320° | 3 | 0.0 | 1.5 | >600 m | >15 | 0/w |
| 1800 | 0.1 | 240° | 1 sec | 1.0 | 330° | 4 | -0.2 | 1.5 | >600 m | >15 | 0/w |
| 1900 | 0.2 | 300° | 1 sec | 0.8 | 320° | 3 | -0.3 | 1.5 | >600 m | >10 | 0/w |
| 2000 | NO | DATA | | NO DATA | | NO DATA | | NO | DATA | | |
| 2100 | 0.1 | 310° | 1 sec | 1.0 | 0° | 2 | -1.0 | 1.0 | >600 m | >15 | 0/w |
| 2230 | DARK | | | 0.8 | 330° | 3 | -1.5 | 1.0 | >600 m | >15 | 0/w |

APPENDIX C

Summary of ships position from ice reports.
84-04-03

| Z | Speed (km)/Hdg | N | W |
|-------------|----------------|-----------|-----------|
| 0000-15 min | - | 46° 42.2' | 47° 16.2' |
| 0245 | 05/038 | 46° 50.1' | 47° 02.1' |
| 0545 | 05/020 | 46° 04.5' | 46° 48.9' |
| 0845 | 02/240 | 47° 58.2' | 46° 45.7' |
| 1145 | 10/005 | 46° 58.9' | 46° 49.8' |
| 1445 | 00/xxx | 46° 54.5' | 46° 50.3' |
| 1745 | 00/xxx | 46° 53.0' | 46° 51.9' |
| 2045 | 00/xxx | 46° 50.8' | 46° 50.9' |
| 2345 | 00/xxx | 46° 48.0' | 46° 51.0' |

84-04-04

| | | | |
|------|--------|-----------|-----------|
| 0245 | 00/xxx | 46° 45.9' | 46° 52.1' |
| 0545 | 00/xxx | 46° 44.5' | 46° 51.9' |

APPENDIX D

Berg A-3 - Notes

Berg A-3 which the ship stood by tipped through 90° at various intervals throughout the observation period. A record of the behaviour exists on 35 mm slides and on video tape.

Roll 2 Frame 13 - Roll 4 Frame 22 35 mm

A few events during the standby period were also noted as follows:

| | |
|------|---|
| 1336 | - Growlers broke off berg during roll |
| 1354 | - Ships radar turned off |
| 1401 | - Transponder (X-band) turned on but was possibly not working |
| 1342 | - Berg rolled |
| 1436 | - Two rolls in rapid succession |
| | - Berg appears to take 10-15 minutes to change positions |
| 1453 | - Rolled 4 times in succession |
| 1600 | - Berg movement reduced |
| 1645 | - Berg tipping again |
| | - During rolling, no ice breakup occurred |
| 1704 | - Sharp side pointing west |
| 1910 | - Waverider taken out |
| 2107 | - Berg actively rolling and turning |

Wednesday

Activity Log

4 April 1984

- 0930 Z - Revisited berg A-3 which we stood by during overflights the previous day. Searched for and found C-3 for re-documentation.
- 1315 Z - Message from J. Benoit to dedicate day to profiling. The rest of the day was spent obtaining an underwater profile of C-3.
- 2145 Z - Course set for tomorrow's overflight area as defined by conversation of this morning.
- 1130-2145 - Ship by berg C-3.

Sources of Information

Included

APPENDICES

- A - 3 hr Manmar observations
- B - Berg data reports
 - Mobil ice report - J. Dempsey
- C - Summary of ships course taken from Mobil ice reports

- 5.3 -

84-04-04

Summary of ships movements from Mobil ice report.

| GMT | Speed/Hdg | N | W |
|-------------|-----------|-----------|-----------|
| 0000-15 min | 00/xxx | 46° 48.0' | 46° 51.0' |
| 0245 | 00/xxx | 46° 45.9' | 46° 52.1' |
| 0545 | 00/xxx | 46° 44.5' | 46° 51.9' |
| 0845 | 00/xxx | 46° 43.6' | 46° 52.9' |
| 1245 | 00/xxx | 46° 52.3' | 47° 00.3' |
| 1545 | 00/xxx | 46° 49.5' | 46° 54.7' |
| 1745 | 00/xxx | 46° 47.9' | 46° 54.7' |
| 2045 | 00/xxx | 46° 47.7' | 46° 57.2' |
| 2345 | 00/xxx | 46° 49.6' | 47° 18.4' |

1005 Z - Ground truthing commenced at 1005 Z in the area specified by J. Benoit the previous day.

Area: $46^{\circ} 50'N$, $47^{\circ} 30'N$
 $48^{\circ} 00'W$, $49^{\circ} 00'W$

As requested, as many bergs as possible were ground truthed with a reduced information package. Time, position, length, width, height of bergs were requested as were hourly seastate and meteorological observations.

1336 Z - Requested by J. Benoit to alter course to northern edge of box and concentrate on small bergs, bergy bits and growlers.

1700 Z - Worked along ice edge in northern section, ground truthed bergs south of southern most streamer of pack. Ship icing up.

Total number of bergs documented - 36.

1650 Z - Streamer location at $47^{\circ} 16.31'N$, $48^{\circ} 04.03'W$.

Sources of Information

Included

APPENDICES

- A - 3 hr Manmar weather observations
- B - 1 hr reduced meteorological and oceanographic parameters
 - Video tape of Berg G-5 and ice edge (H. Lanziner)
 - Map of ice edge - Jim Dempsey (Debrocky)
 - Mobil ice report made every 3 hrs by J. Dempsey
 - Ships course is indicated by bergs visited
- C - Summary of ships course taken from ice reports
- D - Berg summary
 - Data sheets on 36 bergs

APPENDIX B

Hourly Weather/Environmental Data
5 April 1984

| Time GMT | Primary Waves | | Secondary Waves | | | Wind | | Temp. | | Cloud | | Vis nm | Ice Cond. | |
|-------------|---------------|------|-----------------|--------|------|--------|-------|-------|------|-------|--------|-----------|--------------|-----|
| | Height | DirN | Period | Height | DirN | Period | Speed | DirN | Air | Sea | Height | | | % |
| 1000 | 0.6 | 33 | 1 sec | 2.0 | 0 | 8 sec | 22 | 310 | -4.5 | -1.0 | 200 | 90% | >15 | 0/w |
| 1100 | 0.3 | 27 | 1 sec | 1.5 | 310 | 6 sec | 18 | 330 | -4.8 | -1.0 | 200 | 90% | >15 | 0/w |
| 1200 | 0.7 | 330 | 1 sec | 2.0 | 320 | 6 sec | 25 | 340 | -4.0 | -1.0 | 200 | 75% | >15 | 0/w |
| 1300 | 0.8 | 330 | 1 sec | 2.0 | 310 | 8 sec | 13 | 253 | -3.8 | -1.0 | 200 | 60% | >15 | 0/w |
| 1400 | 0.6 | 300 | 2 sec | 1.7 | 320 | 4 sec | 13 | 253 | -4.0 | -0.2 | 200 | 70% | >15 | 0/w |
| 1500 | 0.8 | 270 | 3 sec | 2.0 | 270 | 5 sec | 24 | 316 | -4.0 | -0.2 | 200 | 80% | >15 | 0/w |
| 1600 | 0.8 | 280 | 3 sec | 1.5 | 280 | 5 sec | 25 | 301 | -3.5 | -0.2 | 200 | 60% | >15 | 0/w |
| 1700 | 0.8 | 270 | 3 sec | 1.5 | 270 | 6 sec | 21 | 312 | -4.0 | -0.2 | 200 | 60% | >15 | 0/w |
| 1800 | 1.2 | 300 | 3 sec | 1.7 | 270 | 8 sec | 22 | 308 | -4.5 | -0.2 | 200 | 40% | >15 | 0/w |
| 1900 | 0.9 | 350 | 2 sec | 1.5 | 340 | 7 sec | 20 | 310 | -4.2 | -0.2 | 200 | 60% | >15 | 0/w |
| 2100 | 1.5 | - | 4 sec | 2.1 | 340 | 9 sec | 15 | 300 | -3.5 | -0.1 | dark | - | - | - |
| 0000 | 1.0 | - | 3 sec | 2.0 | 340 | 9 sec | 13 | 300 | -4.5 | -0.5 | dark | - | - | - |

APPENDIX C

Ships positions extracted from Mobil ice report.

84-04-05

| Time & 0000-15 | Speed (km)/Heading | N | W |
|-------------------|--------------------|-----------|-----------|
| min | 05/275 | 46° 49.6' | 47° 18.4' |
| 0245 | 07/005 | 46° 49.1' | 47° 38.0' |
| 0545 | 06/339 | 47° 13.7' | 47° 36.7' |
| 0845 | 08/275 | 47° 21.1' | 47° 51.9' |
| 1145 | 09/160 | 47° 16.6' | 47° 48.8' |
| 1445 | - | | |
| 1745 | - | 47° 10.8' | 48° 11.8' |
| 2045 | 07/320 | 47° 24.0' | 48° 14.5' |
| 2445 | 05/182 | 47° 19.7' | 48° 19.7' |

84-04-06

| | | | |
|------|--------|-----------|-----------|
| 0245 | 03/245 | 47° 07.2' | 48° 25.8' |
| 0545 | 03/270 | 47° 07.4' | 48° 36.9' |

APPENDIX D

Summary

5 April 1984

| | | | | | |
|---|------------|----------------|-------|-----|------|
| A | 47° 17.3' | Sph/Tab | 42 | 21 | 7 |
| | 47° 54.5' | | | | |
| B | 47° 17.3' | B bit | | | |
| | 47° 54.5' | | | | |
| C | 47° 16.7' | DDK | 108 | 60 | 35 |
| | 47° 48.1' | | | | |
| D | 47° 14.8' | Pinacle | 66 | 37 | 20 |
| | 47° 46.3' | | | | |
| E | 47° 14.4' | Wedge | 54 | 42 | 16 |
| | 47° 45.4' | | | | |
| F | 47° 08.4' | DDK | 70 | 70 | 25 |
| | 47° 40.9' | | | | |
| G | 47° 04.9' | Pinacle/Polar | 74 | 74 | 24 |
| | 47° 38.9' | Duke | | | |
| H | 47° 04.6' | B bit/towed by | | 2.5 | |
| | 47° 46.6' | W. Sealhunter | | | |
| I | 47° 12.03' | DD | 23 | 17 | 8 |
| | 48° 01.03' | | | | |
| J | 47° 12.8' | 2 growlers | 2 | 4 | .5 |
| | 47° 60.0' | | | | |
| K | 47° 13.1' | 3 growlers | { 1.5 | { 1 | { .5 |
| | 47° 58.7' | | { 3 | { 7 | { .8 |
| L | 47° 13.2' | B bit | 15 | 10 | 2 |
| | 47° 58.2' | | | | |
| M | 47° 13.0' | B bit | 20 | 30 | 3 |
| | 47° 58.1' | | | | |
| N | 47° 14.5' | B bit | 4 | 3 | .5 |
| | 48° 09.6' | | | | |
| O | 47° 18.3' | Med berg | - | - | - |
| | 48° 11.5' | | | | |
| P | 47° 16.8' | B bit | 5 | 4 | 2.5 |
| | 48° 11.9' | | | | |
| Q | 47° 17.4' | Growler | 3 | 3 | 1 |
| | 48° 12.0' | | | | |
| R | 47° 18.6' | Tab | - | - | - |
| | 48° 12.3' | | | | |
| S | 47° 18.8' | Growler | 2 | 1.5 | .75 |
| | 48° 12.3' | | | | |
| T | 47° 18.9' | B bit | 15 | 7 | 2 |
| | 48° 12.3' | | | | |
| U | 47° 19.5' | 2 B bits bum- | 10 | 11 | 2 |
| | 48° 12.0' | ping together | 8 | 6 | 2 |
| V | 47° 19.7' | Wedge | 30 | 20 | 10 |
| | 48° 12.1' | | | | |
| W | 47° 19.8' | Growler | 10 | 10 | 1 |
| | 48° 12.0' | | | | |
| X | 47° 20.0' | Small bergs | 25 | - | 1 |
| | 48° 11.3' | two? | | | |
| Y | 47° 20.2' | Sph | 18 | 10 | 5 |
| | 48° 10.5' | | | | |
| Z | 47° 20.5' | DDK | 25 | 9 | 5 |
| | 48° 06.2' | | | | |

| | | | | | |
|----|-----------|-------------|----|----|----|
| | | | | | 2 |
| AA | 47° 20.8' | B bit | 6 | 4 | 1 |
| | 48° 06.5' | | | | |
| BB | 47° 22.4' | Growler | | | |
| | 48° 12.7' | | | | |
| CC | 47° 22.9' | DDK | 33 | 29 | 10 |
| | 48° 13.3' | | | | |
| DD | 47° 23.3' | Growler | 1 | 1 | .3 |
| | 48° 13.6' | | | | |
| EE | 47° 24.0' | 2 growlers | 1 | 3 | .5 |
| | 48° 14.5' | | 1 | 2 | .5 |
| FF | 47° 24.3' | 20 growlers | | | |
| | 48° 16.8' | | | | |
| GG | 47° 24.8' | Weathered | 25 | 20 | 4 |
| | 48° 15.8' | | | | |
| HH | 47° 24.8' | DD | 40 | 30 | 20 |
| | 48° 15.8' | | | | |
| II | 47° 25.6' | Growlers | 2 | 2 | .7 |
| | 48° 16.3' | | | | |

- Instructions from J. Benoit the previous evening to limit the study area to the northern section of 5th April box as defined by $47^{\circ} 10'N$. Ground truth to concentrate on small bergs, bergy bits and growlers.
 - Made an effort not to get distracted by bergs to the north edge so as to cover as much of the box as possible. Bergs not as closely spaced as on 5th. Initially very few bergs were sighted.
- 1740 Call from J. Benoit to call off present ground truth so as to position ourselves for tomorrow's flight given impending storm and poor visibility. Storm did not materialize as predicted. Stationed initially by bergy bits at nightfall. Drifted away overnight.

Sources of Information

Included

APPENDICES

- A -- 3 hr Manmar weather observations
- B -- 1 hr summary of weather and ocean parameters
 - Video tape of bobbing berg M-6 (H. Lanzier)
 - Mobil ice report made every 3 hours -- J. Dempsey
- C -- Summary of ships course taken from M. ice report
- D -- Ships course as indicated by bergs visited
 - Berg summary
- E -- Bergs observed by ships radar at 1943Z
 - Data sheets on 20 icebergs

APPENDIX B

Hourly Weather/Environmental Data 6th April 1984

| Time GMT | Primary Waves | | | Secondary Waves | | | Wind | | Temp. | | Cloud | | Vis nm | Ice Cond. |
|-------------|---------------|------|--------|-----------------|------|--------|-------|------|-------|------|--------|-----|-----------|--------------|
| | Height | DirN | Period | Height | DirN | Period | Speed | DirN | Air | Sea | Height | % | | |
| 0900 | 0.5 | 280 | 3 sec | 1.5 | 310 | 8 sec | 13 | 127 | -1.0 | 0.5 | 200 | 10% | >15 | 0/w |
| 1000 | 0.6 | 270 | 1 sec | 1.0 | 290 | 8 sec | 14 | 260 | -0.6 | -0.1 | 200 | 0% | >15 | 0/w |
| 1100 | 0.5 | 270 | 2 sec | 1.2 | 290 | 10 sec | 14 | 260 | -0.6 | -0.1 | 200 | 0% | >15 | 0/w |
| 1200 | 0.5 | 270 | 3 sec | 1.2 | 290 | 10 sec | 15 | 272 | -0.5 | 0.0 | 200 | 0% | >15 | 0/w |
| 1300 | 0.5 | 240 | 3 sec | 1.0 | 290 | 10 sec | 12 | 258 | -0.2 | 0.0 | 200 | 0% | >15 | 0/w |
| 1400 | - | - | - | - | - | - | - | - | - | - | - | - | - | - |
| 1500 | 0.4 | 290 | 3 sec | 1.0 | 270 | 10 sec | 13 | 266 | +0.5 | 0.0 | 200 | 0% | >15 | 0/w |
| 1700 | 0.4 | 310 | 3 sec | 1.0 | 270 | 10 sec | 10 | 262 | +0.2 | 0.0 | 600 | 70% | >15 | 0/w |
| 1800 | - | - | - | 1.0 | 270 | 3 sec | 10 | 230 | +0.5 | 0.0 | 600 | 70% | >15 | 0/w |
| 2100 | - | - | - | 1.0 | 230 | 3 sec | 06 | 230 | 0.0 | 0.0 | 600 | - | >15 | 0/w |
| 0000 | - | - | - | 1.5 | 230 | 3 sec | 08 | 200 | 0.0 | 0.0 | 600 | - | >15 | 0/w |

APPENDIX C

84-04-06

| GMT | speed km/Hdg | N | W |
|---------------|--------------|------------|-----------|
| 0000 (-.0015) | 05/182 | 47° 19.7' | 48° 19.7' |
| 0245 | 03/245 | 47° 07.2' | 48° 25.8' |
| 0545 | 03/270 | 47° 07.4' | 48° 36.9' |
| 0845 | | | |
| 1145 | | 48° 08.9' | 48° 14.4' |
| 1445 | 05/180 | 47° 03.9' | 47° 54.9' |
| 1745 | 10/360 | 46° 55.1' | 48° 01.9' |
| 2045 | | 47° 05.3' | 47° 51.4' |
| 2445 | 01/180 | 47° 50.01' | 47° 55.2' |

84-04-07

| | | | |
|------|--------|-----------|-----------|
| 0245 | 00/xxx | 47° 07.2' | 47° 54.6' |
| 0545 | 00/xxx | 47° 07.9' | 47° 54.2' |

APPENDIX D

Summary

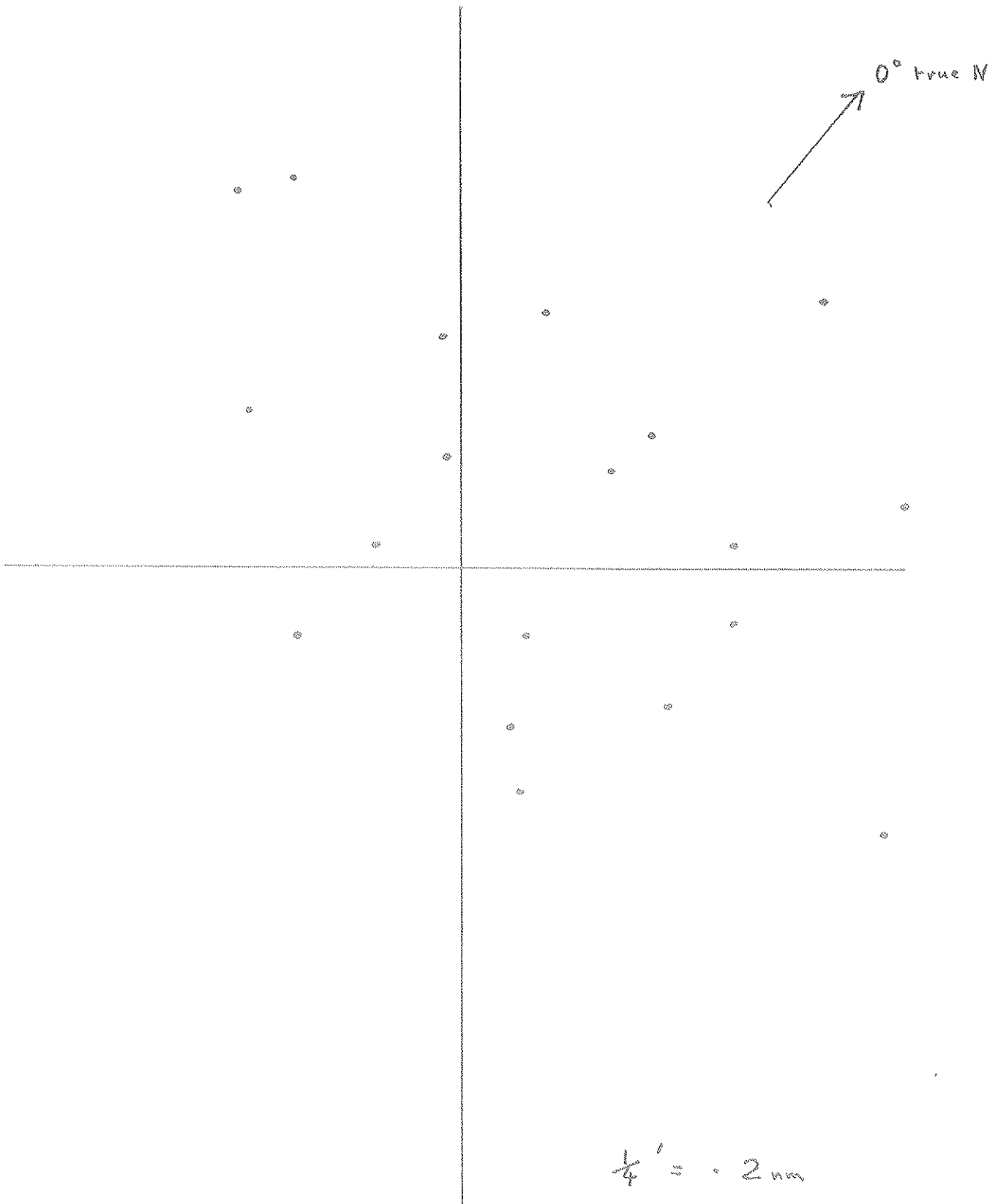
6th April 1984

| | | | C | W | H | Z |
|---|------------|--------------------|-----|-------|-----|------|
| A | 47° 08.8' | B bit | 14 | 7 | 2 | 1102 |
| | 48° 21.5' | | | | | |
| B | 47° 11.2' | DDK | 70 | 1 | 20 | 1125 |
| | 48° 17.9' | | | | | |
| C | 47° 09.01' | WEDGE | 46 | 42 | 7 | 1135 |
| | 48° 16.1' | | | | | |
| D | 47° 09.0' | B bit | 34 | 26 | 7 | 1204 |
| | 48° 11.3' | | | | | |
| E | 47° 10.5' | TAB | 75 | - | 15 | 1219 |
| | 48° 10.6' | | | | | |
| F | 47° 10.5' | 2/GROW | 1 | 1 | .3 | 1220 |
| | 48° 10.6' | | 1 | 2 | .4 | |
| G | 47° 07.6' | GROW | 2 | 1 | .5 | 1238 |
| | 48° 06.8' | | | | | |
| H | 47° 06.0' | TAB | 43 | 25 | 7 | 1256 |
| | 48° 04.0' | | | | | |
| I | 47° 05.8' | Weathered | 28 | 19 | 8 | 1320 |
| | 47° 59.5' | | | | | |
| J | 47° 06.6' | sph | 39 | 27 | 8 | 1335 |
| | 47° 58.7' | | | | | |
| K | 47° 06.5' | GROW | 3 | 2 | 1 | 1347 |
| | 47° 56.9' | | | | | |
| L | 47° 06.4' | BB | 7 | 5 | 2 | 1353 |
| | 47° 50.3' | | | | | |
| M | 47° 04.1' | sph | 12 | 5 | 3 | 1428 |
| | 47° 56.8' | (The bobbing berg) | | | | |
| N | 47° 04.4' | GROW | 2.5 | 2 | .5 | 1443 |
| | 47° 55.8' | | | | | |
| O | 47° 04.2' | B bit | 20 | 12 | 6 | 1451 |
| | 47° 55.2' | | | | | |
| P | 47° 01.0' | Wedge | 30 | 15 | 5 | 1519 |
| | 47° 51.7' | | | | | |
| Q | 47° 00.9' | Wedge | 35 | 30 | 6 | 1524 |
| | 47° 51.7' | | | | | |
| R | 47° 01.3' | sph | 30 | 20 | 7 | 1537 |
| | 47° 53.3' | | | | | |
| S | 46° 59.2' | DDK | | small | | 1628 |
| | 47° 53.7' | | | | | |
| T | 46° 57.21' | sph | 60 | 51 | 9.2 | 1653 |
| | 47° 54.19 | | | | | |

* Correction on yesterday's information.

I-5 location is 47° 12.03
48° 01.03.

2 4.13 local
1943 Z
6 April



Bengs observed from ships radar

- 1100Z - Selected location by iceberg (bergy bits).
Position $47^{\circ} 07.23'N$, $47^{\circ} 45.67'W$
As per instructions, the position referenced to the bergy bit was maintained throughout the day and the waverider was deployed. The relationship between the berg, ship and waverider varied due to the constraints of keeping the mooring rope extended.
- 1545 - Waverider deployed (Buoy # 245). Ship standing by approximately 300-500 m from bergy bit.
- 1930 - Ship at $47^{\circ} 09.81'N$, $47^{\circ} 45.0'W$.
Winds SE 30, seas 5-8 ft.
- 2300 - Waverider taken in and ship moved from bergy bit due to visibility/weather conditions and safety considerations.

Sources of Information

Included

APPENDICES

- A - 3 hour Manmar weather observations
- B - Weather and ship position at hourly information
- Mobil ice report made every 3 hours - J. Dempsey
- C - Summary of ships position from M ice report
- D - Diagrams of ships position
- E - Berg information for target (A-7)
- F - Photos of radar screen (35 mm) + locational information.

APPENDIX B

Hourly Weather/Environmental Data
7th April 1984.

| Time GMT | Primary Waves | | Secondary Waves | | Wind | | Temp. | | Cloud % | Vis nm | Position |
|-------------|---------------|------|-----------------|--------|------|--------|------------|------|------------|-----------|---|
| | Height | DirN | Period | Height | DirN | Period | Speed | DirN | Air | Sea | |
| 1230 | 0.3 | 160 | 1 sec | 1.2 | 160 | 5 sec | 20 | 135 | 0.5 | -0.5 | - |
| 1300 | 0.4 | 180 | 1 sec | 1.5 | 180 | 4 sec | 20 | 150 | 0.75 | -0.5 | 47° 07.51'N 47° 45.80'W |
| 1418 | 0.6 | 130 | 2 sec | 2.0 | 190 | 6 sec | 20 | 135 | 0.7 | +0.5 | 47° 07.71'N 47° 45.02'W |
| 1501 | 1.5 | 150 | 3 sec | 2.0 | 180 | 5 sec | 22 | 146 | 1.0 | +0.5 | 47° 07.84'N 47° 44.62'W |
| 1600 | 2.0 | 150 | 4 sec | 2.0 | 160 | 5 sec | 24 | 150 | 1.25 | +0.5 | 47° 07.44'N* |
| 1700 | 1.5 | 160 | 0.3 sec | 2.0 | 160 | 5 sec | 22 | 130 | 0.9 | +0.5 | 47° 45.39'W 47° 07.99'N |
| 1800 | 1.0 | 140 | 2 sec | 2.0 | 140 | 6 sec | 21 | 150 | 1.2 | 0.5 | 47° 47.37'W 47° 08.48'N |
| 1900 | 1.0 | 100 | 4 sec | 2.5 | 140 | 7 sec | 24 | 155 | 1.1 | 0.5 | 47° 45.26'W 47° 09.11'N |
| 2000 | 1.0 | 140 | 4 sec | 2.5 | 140 | 6 sec | 25 (30) | 155 | 1.5 | 0.5 | 47° 49.09'W 47° 10.15'N |
| 2100 | 1.0 | 140 | 3 sec | 2.7 | 140 | 5 sec | 25 (30) | 150 | 1.7 | 0.5 | 47° 45.00'W 47° 10.82'N |
| 2200 | - | - | - | - | - | - | 25 (30) | 150 | 1.5 | 0.5 | 47° 43.93'W 47° 11.31'N 47° 44.25'W |

* Possibly 47 07 44 N incorrect.
As this is duplicated in radar data
.. Inaccuracy due to navigation instrument failure.

APPENDIX C Ships position from Mobil Ice Report

84-04-07

| | | |
|------------------|------------|-----------|
| 0000-0.15 hr | 47° 50.0' | 47° 55.2' |
| 0245 | 47° 07.21' | 47° 54.6' |
| 0545 | 47° 07.9' | 47° 54.2' |
| 0845 | 47° 09.4' | 47° 51.4' |
| 1145 | 47° 07.2' | 47° 45.7' |
| 1445 | 47° 07.8' | 47° 44.9' |
| 1745 | 47° 08.2' | 47° 45.1' |
| 2045 | 47° 10.6' | 47° 44.9' |
| 2345 01/180 | 47° 10.8' | 47° 44.2' |

84-04-08

| | | |
|------------------|-----------|-----------|
| 0245 01/180 | 47° 07.3' | 47° 45.1' |
| 0545 00/xxx | 47° 04.8' | 47° 46.0' |

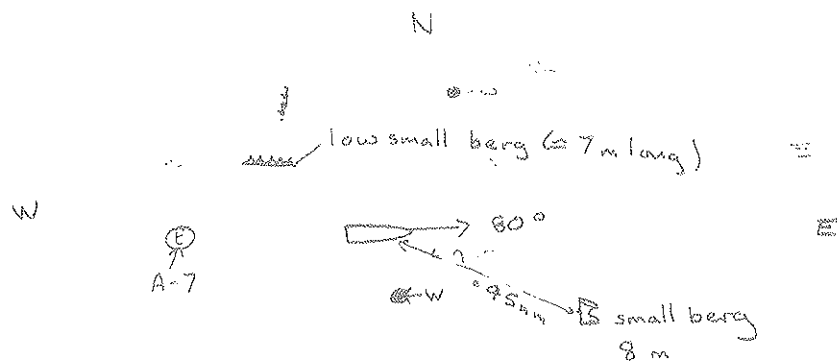
14
7 APRIL

Appendix D

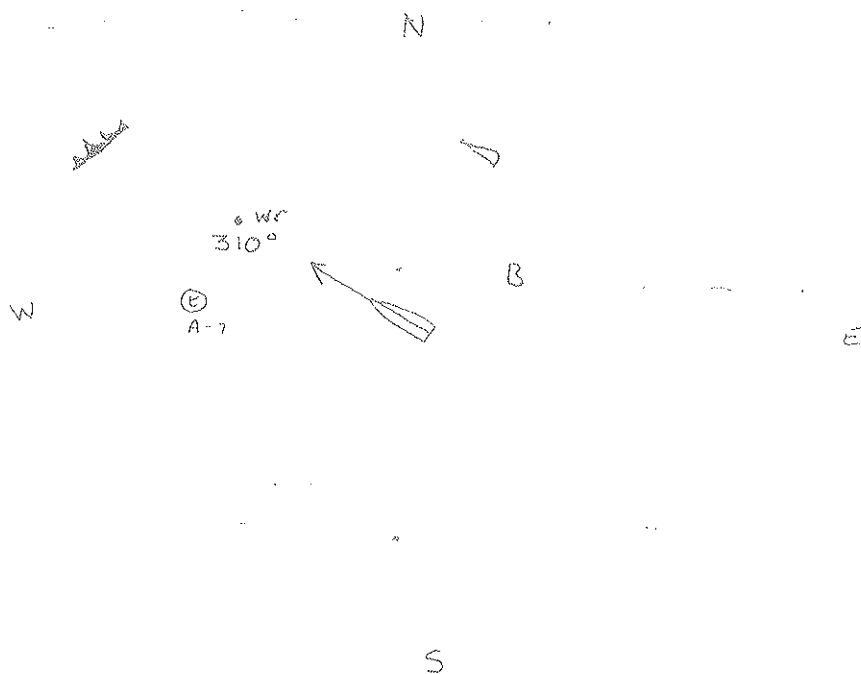
1600 Z

Diagrams showing ship in relation
to target berg A-7 and the wave rider buoy
with other nearby targets shown

⊙ A-7 — berg
• wr — wave rider



1632 Z



APPENDIX F

Photographic Log of Radar Screen for Overflight Period.
7th April 1984.

| Film Roll | Range | | Time GMT | Heading | | Location | |
|--------------|-------|------|-------------|---------|------|-------------------|----------------------|
| | 6 nm | 3 nm | | 6 nm | 3 nm | Latitude | Longitude |
| 12 | 20 | 21 | TEST | - | - | 47° 07.80' | 0° 44.90' |
| 12 | 22 | 23 | 1435 | 70 | 80 | 47° 07.87' | 47° 44.66' |
| 12 | 24 | 25 | 1500 | 35 | 37 | 47° 07.87' | 47° 44.72' |
| 12 | 26 | 27 | 1530 | 50 | 56 | 47° 07.45* | 47° 45.39' |
| | 28 | 29 | 1600 | 35 | 42 | 47° 07.66' | 47° 45.62' |
| | 32 | 33 | 1630 | 345 | 348 | 47° 07.99' | 47° 45.37' |
| | 34 | 35 | 1700 | 246 | 248 | 47° 08.39' | 47° 45.20' |
| 13 | 1 | 2 | 1730 | 311 | 311 | 47° 08.46' | 47° 45.19' |
| 13 | 3 | 4 | 1800 | 26 | 24 | 47° 08.85' | 47° 45.31' |
| 13 | 5 | 6 | 1830 | 44 | 34 | 47° 09.15' | 47° 45.05' |
| | 7 | 8 | 1900 | 240 | 232 | 47° 10.68" | 47° 45.03' |
| | 9 | 10 | 1930 | 75 | 74 | 47° 10.11' | 47° 45.08' |
| | 13 | 14 | 2000 | 263 | 273 | 47° 10.66' | 47° 44.26' |
| | 16 | 17 | 2030 | 285 | 281 | 47° 10.74' | 47° 44.03' |
| | 19 | 20 | 2100 | 5 | 9 | 47° 10.96' | 47° 44.12' |
| | 21 | 22 | 2130 | 80 | 78 | 47° 11.29' | 47° 44.12' |
| | 23 | 24 | 2200 | 52 | 52 | Lost berg at dark | to follow |
| | 26 | 25 | c2250 | - | - | 47° 11.53' | 47° 44.13' |
| | | 27 | 2300 | 45 | 30 | | Waverider taken out. |

Wave rider deployed.

Berg 315 m

Berg 500 m

Berg 500 m

Waverider buoy.

Waverider taken out.

* Questionable navigation accuracy - See Appendix B.

BERGSEARCH '84

SECTION II CHAPTER 2

STAR-1 DATA COLLECTION

INTERA Technologies Ltd.

Calgary, Alberta

II.2 STAR-1 DATA COLLECTION

II.2.1 INTRODUCTION

The primary mission for INTERA in Bergsearch '84 was to assess the capability of the STAR-1 system to detect icebergs in open water under various environmental conditions and parametric variations.

The STAR-1 system is INTERA's name for its state-of-the-art, operationally oriented, airborne SAR (synthetic aperture radar). Relevant parameters of the system are shown in Table II.1. There was particular interest in the use of STAR-1 for iceberg detection because of its high-resolution capability combined with a reasonably wide swath.

The STAR-1 data collection component of the program was comprised of three phases: planning and mobilization; data collection; and reporting. The elements of each of these are summarized below.

Planning and Mobilization Phase

- Logistical planning for STAR-1 and the field personnel.
- Interface with other members of the project, including participation in two Ottawa planning meetings.
- Assistance in developing the overall experimental plan.
- Internally funded test flights to simulate the experimental field plan.
- Assembly and test of a transcription facility to enable digital data to be transferred from on-board, high-density digital tapes to standard computer-compatible tapes.
- Preparation of interim report.

TABLE II-1

Specifications of STAR-1 System

| System Parameter | | Detailed Specification |
|----------------------------|---|---|
| Nominal operating altitude | | 10,000 m (33,000 ft) |
| Wave length | | X-band |
| Polarization | | HH |
| Viewing direction | | Left or right |
| Sensitivity | | Better than -30 dB approximately across the swath |
| Processing | | Real-time digital |
| Recording | | Full band-width recording of image data on High Density Digital Recorder at 1.4 MBPS |
| Downlink | | Full band-width downlink to ground receiver station with display and tape recorder. Range 350 km at 10,000 m altitude |
| Display | o | High resolution laser beam recorder aboard aircraft recording on heat processed paper |
| | o | High resolution wet chemically processed display on ground |
| | | <div>High Resolution</div> <div>Wide Swath</div> |
| Swath width | | 23 km 46 km |
| Range resolution | | 6 m 12 m |
| Azimuth resolution | | 6 m 6 m |
| Number of looks per pixel | | 7 7 |

Data Collection Phase

- Mobilization of STAR-1 aircraft from the Beaufort Sea to Gander Nfld., the operational headquarters of the field activities.
- Mobilization of additional personnel from Calgary to Gander.
- Daily STAR-1 data collection missions conducted from 2-7 April 1985 inclusive. These missions incorporated the following:
 - Wave detection flights as well as the primary iceberg detection mission. The former were part of another ESRF project in which INTERA was sub-contracted.
 - Both 'Research' and 'Operational' iceberg detection mission flights.
 - The four research flights involved repetitive flight patterns over a small (25 x 25 km) target area to test the effect of various radar and environmental parameters on iceberg detectability.
 - The two operational flights were flown over large areas to simulate operational surveillance missions.
 - Real-time iceberg counting exercises during the operational flights.
 - Research mission profiles that enabled the following factors affecting iceberg detectability to be studied:
 - * spatial resolution
 - * depression angle
 - * upwind, downwind and cross-wind detectability
 - * repeatability of detection
 - End of mission flights over corner reflectors at Gander for potential calibration purposes.
 - 'Quick Look' imagery in real-time plus recording onto high density digital tapes for later playback.
 - Daily briefing and debriefing sessions.
 - Demobilization of STAR-1 and personnel.
 - Preparation of interim report.

Reporting Phase:

- Provision of imagery including:
 - Transcription of data from HDDT (High Density Digital Tapes) onto high-quality negative transparencies (ie. hardcopy imagery).
 - Annotation of imagery.
 - Dissemination of flight logs and other supporting information to CANPOLAR Consultants Ltd.
 - Participation in preparatory data analysis meeting.
- Provision of selected CCTs (computer-compatible tapes) including:
 - Transcription from HDDTs onto CCTs of selected data.

- Dissemination of CCTs along with supporting information to CANPOLAR Consultants Ltd. for digital analysis.
- Limited analysis of data for purpose of contributing to the BERGSEARCH '84 workshops.
- Participation in the interim (St. John's) and final (Toronto) BERGSEARCH '84 workshops.
- Preparation of final report.

Organization of the Final Report

The prime objectives of this report are twofold:

- to produce a comprehensive description of the tasks that were undertaken by INTERA in order to accomplish its STAR-1 data collection requirements; and
- to provide supplemental information which would be useful for any follow-on analysis of the data. In particular, this will include the locating of the data, its various forms, the relationship of the particular flight lines to specific experimental objectives and other useful information.

The report follows the organization of the project as summarized in Section 1.1 above. In so doing, it will incorporate the first two interim reports dealing with phases 1 and 2. Phase 3 appears as a final report and will include a description of the tasks accomplished as part of the reporting phase, as well as the supplemental information described in paragraph (2) above.

While analysis of the data was part of the mandate of CANPOLAR Consultants, a limited analysis for purposes of quality control was performed and is reported under Phase 3.

II.2.2 PHASE 1: PLANNING AND MOBILIZATION (INTERIM REPORT)

Planning

Two trips to Ottawa were made to participate in the logistics planning meetings of 10 January and 22 February 1984. The first meeting was attended by the (temporary) project manager whereas the second was attended by the project manager, mission scientist, and principal project pilot.

A meeting and several telephone conversations were held with Dr. Rossiter of CANPOLAR for purposes of discussing an optimum experimental plan within the physical constraints of the participants. The results of these discussions were subsequently adopted for the experimental flight plans.

Discussions were also held with Dr. Rossiter concerning reflector deployment at Gander. These discussions concerned

reflector size, deployment pattern, and their effect on radiometric calibration and determination of radar resolution.

During the course of the planning exercise it became apparent that the original flight profiles planned for STAR-1 would be difficult to achieve owing to the transit distance from base to target area, coupled with the large amount of on-site flying required to achieve project objectives. The original flight plan involved STAR-1 flying the complete mission at high altitude (30,000-33,000 ft) to reduce turbulence and to conserve fuel. Look-angle variation was to be achieved through use of an offset box pattern. To reduce on-site flying time during this part of the mission, it was necessary to establish whether a combined high/medium altitude profile would be satisfactory. To this end, a special purpose flight was made at INTERA's expense over the Beaufort Sea winter ice regime to test the following:

- possible defocussing or other negative factors caused by increased turbulence encountered at lower altitude;
- the increased fuel consumption at this altitude; and
- the necessity for gain changes or antenna pointing angle changes at lower altitudes.

As a result of these tests it was determined that the high/medium altitude combination was viable, and the experiment flight profile plans were changed accordingly, with operating altitudes of 18,000-19,000 ft incorporated in addition to the altitudes of 30,000-33,000 ft altitudes already planned.

Despite the improvement in on-site flying time offered by the change in flight plan, it was considered necessary, at least during the early research flights, to plan for two flights per mission day. To accomplish this, and especially in view of the long transit flight from Inuvik to Gander that immediately preceded it, a second flight crew was planned into the schedule.

Transcription Facility

A transcription facility enabling the HDDT's (High Density Digital Tapes) which are recorded on the aircraft - typically 7 hours imagery per tape - to be transcribed onto ordinary CCT's (Computer Compatible Tapes) was assembled and successfully tested. These tapes can then be used for computer-based image analysis or other digital manipulations. The CCT's have a capacity of about 4 minutes, or 30 km, per tape.

The transcription facility includes a combination of a HDDT tape drive, a 1.4 m byte downlink bottom end, and a

RIDS-C station. High resolution images of STAR-1 imagery were successfully transcribed onto CCT and displayed on the RIDS video screen in colour and in black and white format. At present this limited MIDAS facility has the ability to scroll through imagery.

The CCT format, while suitable for RIDS, is not 'friendly' for general computer users. INTERA will be re-writing the CCTs that are to be forwarded to CANPOLAR to make them more easily used by non-software specialists.

The bulk of the deliverable to be presented to CANPOLAR will be in the form of negative transparencies. A second Edo Western hardcopy unit has recently been purchased and tested by INTERA and will smooth the logistics of preparing these products.

Calibration

Following the decision to place corner reflector patterns at the Gander site it was decided that a separate calibration test at Tuktoyaktuk would be redundant.

II.2.3 PHASE 2: DATA COLLECTION (INTERIM REPORT)

Logistics and Operations

The STAR-1 data collection program was carried out during the six-day period 2-7 April 1984. A total of 67.4 hours flight time was logged of which 40.0 hours was mission related, the remainder being spent in transit from Inuvik to Gander to Inuvit. Eight flights were made during these six mission days.

The aircraft was ferried from Inuvik to Gander by one crew (pilot + radar operator) and met there by a second crew. Two research missions were flown on each of the next two days utilizing both crews. Owing to a change in schedule over the following three days (a single 'wave' mission followed by two single operational missions), it was possible to release the second crew by mid-week. Apart from the aircraft crew, the plane was accompanied by either the mission scientist or project manager on each flight.

Throughout the period the aircraft and radar performed flawlessly with the exception of an intermittent HF radio that caused some inconvenience but no loss of flying time, and a cooling fan failure which produced a thermal shutdown of certain radar equipment, causing the first operations mission to be shortened by about one hour.

The aircraft was hangered and thus experienced no lift-off delays or expense caused by freezing rain (until the

final night prior to transit when a bad weather forecast caused us erroneously to park the aircraft outside where it collected 0.5 cm of ice).

When double missions were flown, the aircraft landed in St. John's for refuelling, permitting total flight times of 10.5 hours.

An extra flying day, beyond the terms of contract, was arranged in the field and approved by the ESRF administration authority in order to take advantage of a rising sea state condition at the end of the project. This day is included within the flying hour statistics described above.

Technical

Recording and Display. The modus operandi for STAR-1 during the project was to obtain real-time information aboard the aircraft on the VISOR system which produces a positive print on dry silver paper, while simultaneously recording the full data set on high-density digital tape (HDDT). The VISOR product is essentially used for quick look purposes, as its quality is inferior to the wet chemical transparency product that is obtained from the Edo Western system. During "normal" operations the data would be downlinked to the Edo Western ground station and the product would appear in real time. However, for this experiment the ground station was not available and the method of achieving higher quality products was to play the HDDT back through the ground station subsequent to the mission.

Thus, only VISOR quick look images were available in the field. This proved adequate and was used aboard the aircraft to confirm repeatability of detection and on one occasion when a low level visual inspection of targets was made, it served as a "map" with which specific visual sightings could be correlated.

At the time of writing this report, the HDDTs have been run through the Edo Western system once. All data is present and the quality appears excellent. Another pass will be made to correct a scale error which occurred on the first pass, and it will be the latter product that is forwarded to CANPOLAR for analysis.

Research Flight Objective. The three prime objectives were to assess, as a function of sea state:

- repeatability of target detection for constant aspect angle;
- look angle, aspect angle and wave direction impact on detection; and
- resolution and display scale detection dependence.

Flight profiles were flown to accomplish these objectives. In particular, a very good set of statistics will be available concerning repeatability from the last of the three research flights when a large number of icebergs and growlers were within the target area that was verified on the ground.

Unfortunately the sea states were not as high as desired during this period so that nature prevented all objectives from being achieved. Preliminary scrutiny suggests that sea state was not a very significant factor in the detection process during this project.

II.2.4 PHASE 3: REPORTING

Following the completion of the data collection phase of the program, the HDDTs (high-density digital tapes) on which the digital data were recorded during the STAR-1 flight were returned to INTERA's Calgary office for playback. The quick-look hardcopy obtained in the field and the flight logs were retained to aid in the image-identification and annotation process. The transcription process produced two types of product:

- hard copy images in the form of high quality negative transparencies of about 200 mm width; and
- computer-compatible tapes (CCTs) of selected scenes for digital display and analysis.

A brief summary of the salient features of each of the three data recording systems is provided in the following section.

Characteristics of the Recording Systems

The High-density Digital Recording System. The STAR-1 downlink system takes the digitized radar video, annotation, and timing data and serializes it for on-board recording and transmission. A wide-band instrumentation recorder, the SABRE III, is used to record this serial data stream in real time with sufficient capacity to require only occasional tape changes. The tapes used on this recorder are referred to as high-density digital tapes (HDDT), and have a typical capacity of around 1.3 gigabytes of imagery. Fourteen tracks are used to record the serial data on a one-inch wide tape, with each track typically holding 30 minutes worth of imagery. The imagery is recorded in the form of successive scan lines composed of 4096 eight-bit pixels per line. The same type of recorder that is used in the aircraft is used for the purposes of replaying this data on the ground, and transcribing it into a computer-compatible format.

The Computer Compatible Tape Formats. Although the HDDT format is ideally suited for real-time recording on the aircraft, it is not a format that lends itself to being easily read by a standard half-inch computer tape drive. A tape transcription facility was developed to read the data from the HDDT and to record it on a computer-compatible tape (CCT). A typical half-inch wide CCT can hold about 40 megabytes on a 2400-foot reel. The 4096 pixels per line are recorded on the CCT in blocks of four lines each, with each tape holding about 2000 blocks. This gives a imagery capacity of around 32 megabytes per CCT. For the purpose of simplifying data analysis, these data were converted from four lines per block to one line per block. An 80-byte ASCII header record was added at the start of each tape to provide information about the contents of the tape. The title 'BERGSEARCH '84', followed by the ESRF #, LINE #, HDDT #, and DATE was stored in this record.

The Hard Copy Output Device. A fibre optic plotter manufactured by EDO Corporation Western Division (Model 590 Series) is currently used to produce transparent film and dry silver paper hard-copy output. The SAR image scan lines are displayed on a cathode ray tube and transferred to photographic film via a fibre optic bundle. The size of the optical fibres and the nature of the film medium used gives a minimum across-track pixel size of 0.127 mm for the dry silver film and 0.0635 mm for the transparent film. The EDO is calibrated to produce an image which is 186 mm across, corresponding to a nominal scale of 1:125,000 for high resolution, full-width imaging. This yields an image of 1464 across-track pixels with the dry silver paper, and 2928 pixels with the transparent film. The nominal ground swath width is 24.622 km, so the across-track resolution of the dry silver paper is about 16.8 m per pixel, whereas the transparent film gives 8.4 m per pixel.

Image Geometry

Slant Range Correction. The real-time processor aboard the aircraft produces an image that is corrected for slant range distortion. That is, the image is presented in a rectilinearly correct, ground swath format. Deviations from absolute accuracy can be introduced at the film processing stage causing stretch or compression in the along-track or cross-track images. The errors for these data are less than 1% and 3% respectively, and in the case of the cross-track compression was persistent throughout the data set.

Offset. The inner edge of the image swath is offset from the aircraft radar position. The flight logs show the "Range Delay" which is programmed into the on-board computer to provide this offset. As the range delay is provided in units of slant range (km) it must be converted by the usual trigonometric method to obtain the offset in terms of ground range. That is :

$$\text{Ground Range Offset} = [(\text{Range delay})^2 - (\text{Aircraft Altitude})^2]^{1/2}.$$

For example on 7 April, the majority of the mission was flown at an altitude of 27,000 ft (8.2 km) with a range delay set as 23 km. The offset in terms of ground range was therefore 21.4 km.

The location of the swath and the targets within it can then be obtained from the aircraft co-ordinates which are recorded at beginning and end of line and at intermediate points for long lines.

Scale. The majority of the lines flown are displayed on a scale of 1:125,000 corresponding to the high-resolution mode, (full-width) display. This corresponds to nominal swath width 25 km (actual ground swath is 24.6 km). A few lines were flown in the wide swath (full-width) mode corresponding to 12-m rather than 6-m range resolution and a scale of 1:125,000.

It is also possible electronically to enlarge the displayed image by selecting for display either 1/2 or 1/4 of the swath width. Thus in high-resolution mode (1/2 width) a scale of 1:62,500 is produced whereas high resolution (1/4 width) produces a scale of 1:31,250. The latter scale was used over the corner reflectors.

A list showing dates, line numbers, and scale is shown in Table II.2.

Navigation

Positioning of the aircraft is achieved by Inertial Navigation System (INS). Such INS systems typically drift at a rate of about 1 nautical mile per hour. When flying for prolonged periods over the same target area this produced no analytical difficulty, as the target patterns could easily be registered against each other.

As part of the Wave Detection experiment, the STAR-1 was flown daily past the drill rig West Venture which appeared in the imagery. Checking against the known co-ordinates of the West Venture, confirmed an INS rate of drift of about one nautical mile per hour.

Production and Annotation of Transparencies

The HDDTs were played back through the Edo Western display system. A second pass was performed to correct a significant scaling error that had occurred on the first pass.

TABLE II-2
Imagery Scales for STAR-1 Lines

| Date | Flight | Lines | Nominal Scale |
|---------|--------|-----------|---------------|
| April 2 | 1 | 1-9 | 1:125,000 |
| April 2 | 2 | 1-6, 8-10 | 1:125,000 |
| | | 11 | 1:125,000 |
| April 3 | 1 | 2, 5-8 | 1:250,000 |
| | | 3-4 | 1:125,000 |
| April 3 | 2 | 2-11, 13 | 1:125,000 |
| April 5 | 1 | 1-3 | 1:250,000 |
| | | 4-6 | 1: 62,500 |
| April 6 | 1 | 1-5, 7, 8 | 1:125,000 |
| | | 10 | 1: 31,250 |
| April 7 | 1 | 3-16 | 1:125,000 |

Annotation. Flight logs recorded the relevant information for each "line" flown including line number, event marks recorded on the image, time, aircraft co-ordinates and other flight parameters, look direction, radar parameters, HDDT track and footage, and operator comments.

Because nearly 90 lines were flown it was necessary to perform double checking procedures to ensure that the lines were correctly labelled. This was done by checking the event marker codes against the logs and also by checking the imagery itself against the quick-look imagery which was annotated in the field.

Each line was hand annotated with date, line number, flight direction, look direction, and start and end of line markers.

These strips were cut into convenient lengths and were forwarded to CANPOLAR Consultants Ltd. for analysis. Additional annotation was added to the images by CANPOLAR at that stage.

Grey Scale. An attempt was made to optimize the gain and offset of the display system such that small targets or sea spikes would be visible above the background, while trying at the same time to prevent bright targets from saturating the film. The latter would have the effect of masking structure on bright or multiple targets.

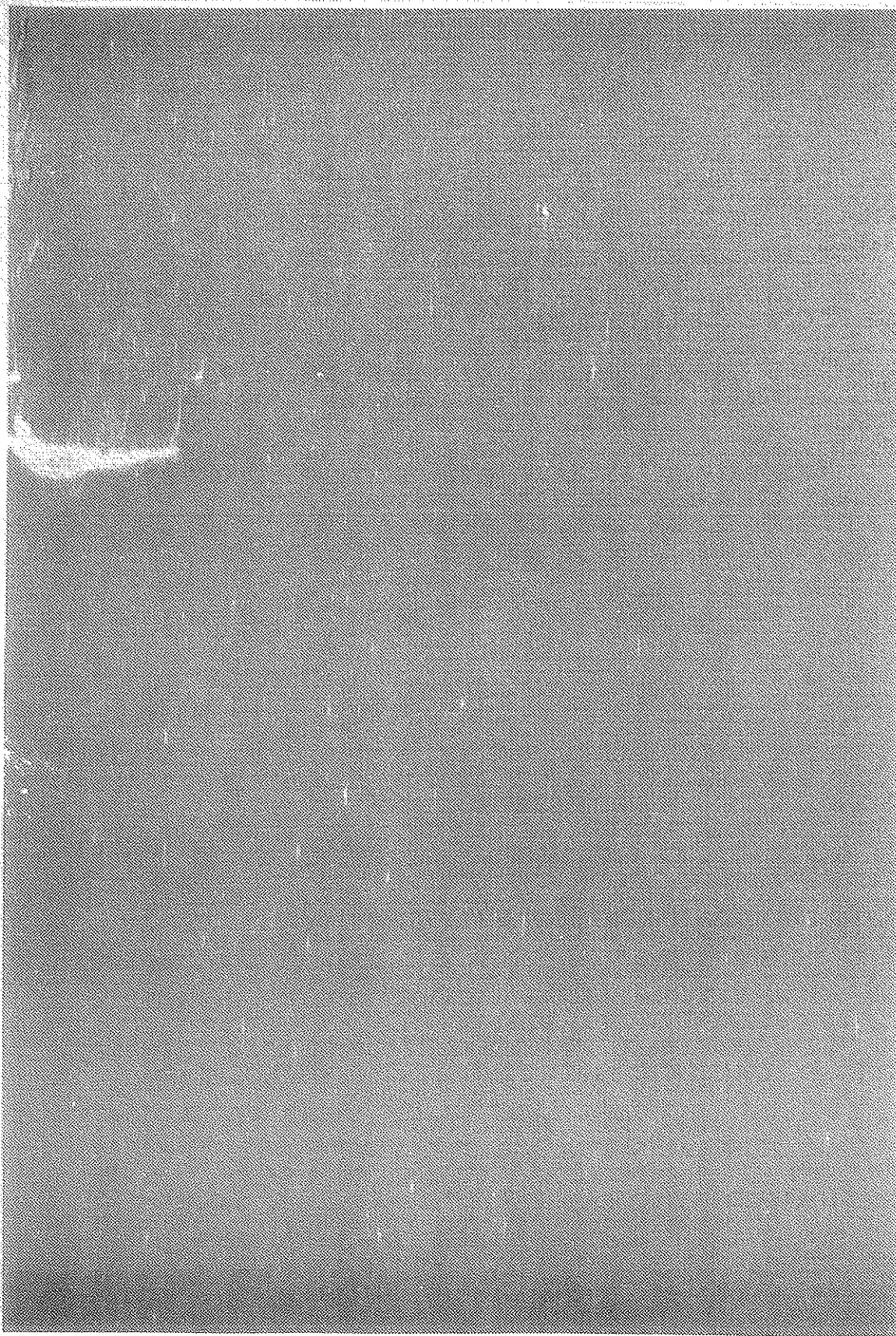
Image Quality. The resultant transparencies were of quite uniform good quality. In the analysis, it was possible with a scaled eye-piece to measure target widths of less than 10 m. This is the limitation imposed by the film when displayed at a scale of 1:125,000. The system resolution is 6 m and can be better used with digital imagery or enlargements.

An example of a typical scene (Figure II-1) is a reproduction of a contact print made from the negative transparency. The annotation referred to is not shown on this figure.

Production of Computer-Compatible Tapes

A small selection of computer-compatible tapes were produced for purposes of digital analysis. The format and related information has already been described.

The following CCT's were forwarded to CANPOLAR Consultants Ltd.:



Scale 0 1 2 3 4 5 Kilometers

SAR image of
 'Icebergs
 'Bergy Bits
 'Growlers
 'Sea Ice

Near Hibernia April 7, 1994



INTERA
 TECHNOLOGIES

Figure II-1. Example of STAR-1 imagery.

| CCT number | Line number | Date |
|---------------|----------------|---------------|
| 12 | 9 | 07 April 1984 |
| 12A | 9 | 07 April 1984 |
| 16 | 10 | 07 April 1984 |

The analysis performed on the digital data from line 9 is described in Section III, Chapter 7.

Other CCT's were produced for purposes of the wave detection experiment. These did not, however, include ice-berg targets.

Additional sets of tapes are being prepared for post-ESRF data analysis purposes. These include:

| Line number | Date |
|----------------|---------|
| 6 | April 2 |
| 5 | April 3 |
| 1 | April 5 |
| 4 | April 5 |
| 8, 13, 15 | April 7 |
| 16, 19 | |

Relationship of Lines Flown to Project Objectives

Because of the large volume of data collected by STAR-1 it is helpful to categorize the lines flown in a pictorial manner, with respect to the objectives of the project - in particular with respect to the lines flown on the 'research days'. This is done in Figures II-2 to II-9 which follow.

Each picture shows the approximate orientation of the flight line(s) with respect to the target area. Accompanying text summarizes the objectives of the set of lines flown and the relevant parameters.

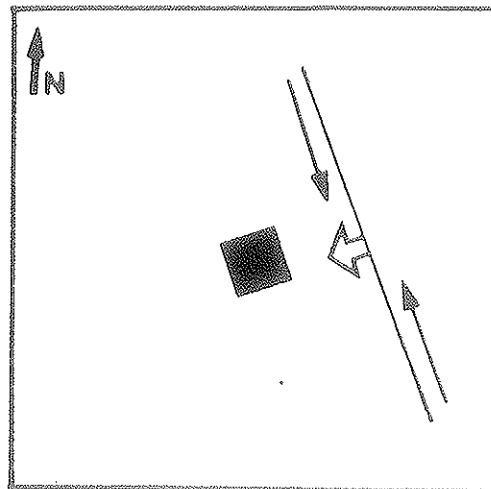
Results

As stated earlier, data collection, not analysis, was INTERA's function in this project. However, in order to contribute effectively at the BERGSEARCH '84 workshop in St. John's it was necessary to perform a small amount of

RESEARCH FLIGHT

1. Repeatability Tests
High Resolution (full width)

Lines 1, 2, 3, 4, 5, 6, 7, 8, and 9
Scale 1:125 000



2. Wave Imaging
High Resolution (full width)

Lines 10 and 11
Scale 1:125 000

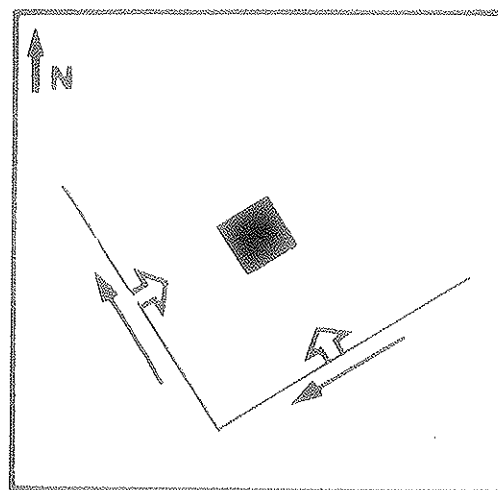


Figure II-2. Mission profiles, 2 April 1984, Flight #1.

RESEARCH FLIGHT

1. Aspect Angle Tests

Lines 1-4
High Resolution (Full Width)
High Altitude
Scale 1:125 000

2. Resolution Test

Lines 5, 6, 7 (compare with lines 1-4)
Wide Swath (Half Width) - 1st Half
High Altitude
Scale 1:125 000

Note: Box moved approximately 5 miles
toward WSW.

3. Look Angle Test (High Alt. vs. Low Alt.)

Lines 8, 9, 10 (compare with lines 5, 6, 7)
Wide Swath (Half Width) - 1st half
Low Altitude
Scale 1:125 000

Note: Box moved approximately 3 miles
toward WSW.

4. Corner Reflectors (Gander)

Line 11
High Resolution (Full Swath)
High Altitude
Scale 1:125 000

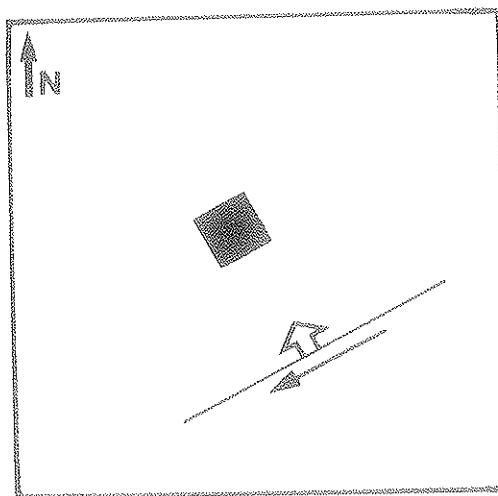
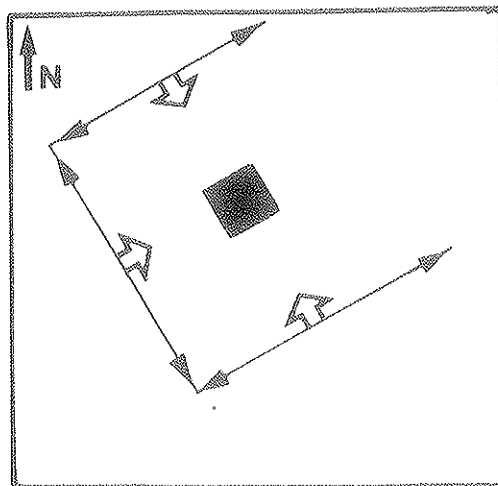
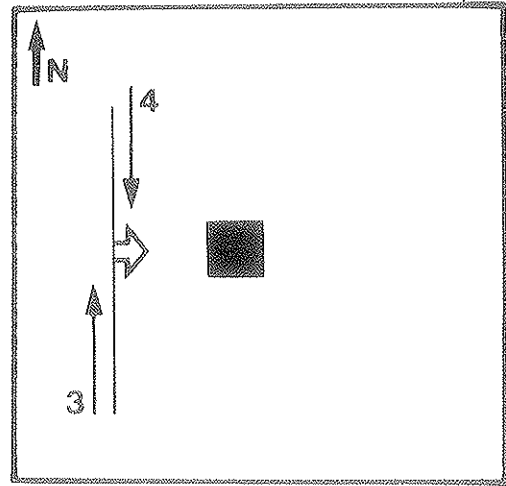


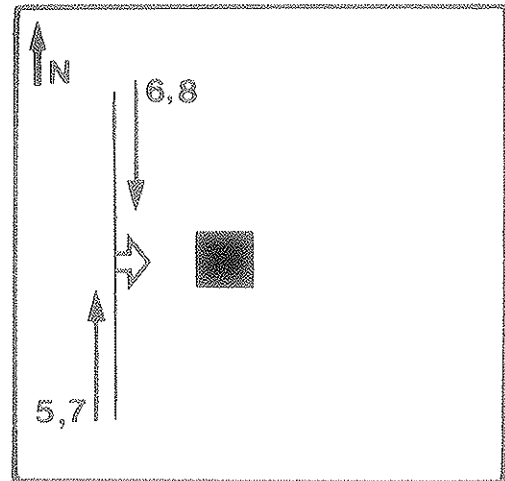
Figure II-3. Mission profiles, 2 April 1984, Flight #2.

RESEARCH FLIGHT

1. Repeatability Tests
High Resolution (Full Width)
Lines 3 and 4
Scale 1:125 000



2. Repeatability Tests
Wide Swath (Full Width)
Lines 5, 6, 7, and 8
Scale 1:125 000



3. Wave Imaging
High Resolution (Full Width)
Lines 10 and 11
Scale 1:125 000

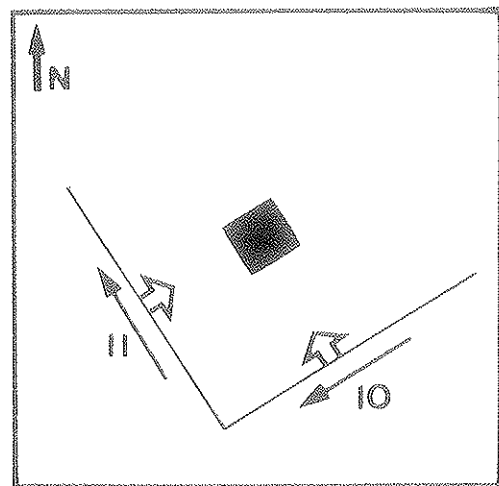


Figure II-4. Mission profiles, 3 April 1984, Flight #1.

RESEARCH FLIGHT

1. Box Turns

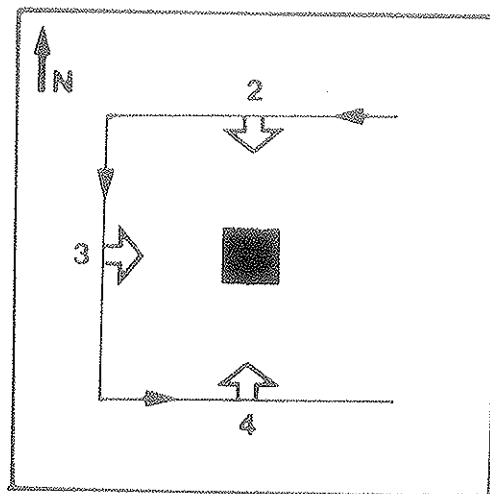
Wide swath (1/2 width) 1st 1/2

High altitude: 10 km

Lines 2, 3 and 4

Aspect angle and resolution tests

Scale 1:125 000



2. Box Turns

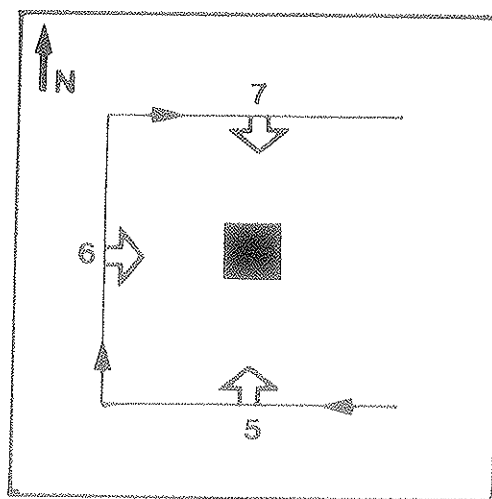
(particulars as above)

Wide swath (1/2 width) 2nd 1/2

Lines 5, 6 and 7

Aspect angle and resolution tests

Scale 1:125 000



3. Resolution Tests

High resolution (full width)

Lines 8, 9 and 10

These lines are comparable to
lines 5, 6 and 7

Scale 1:125 000

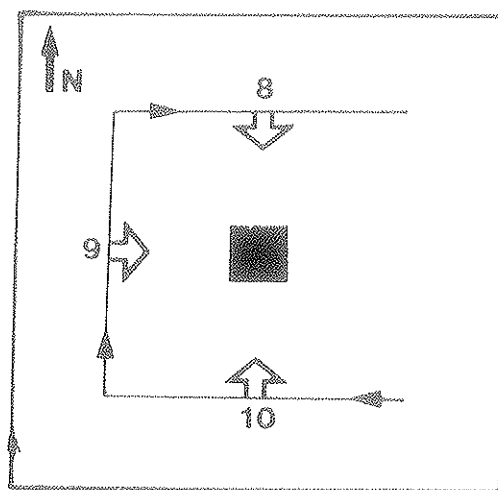


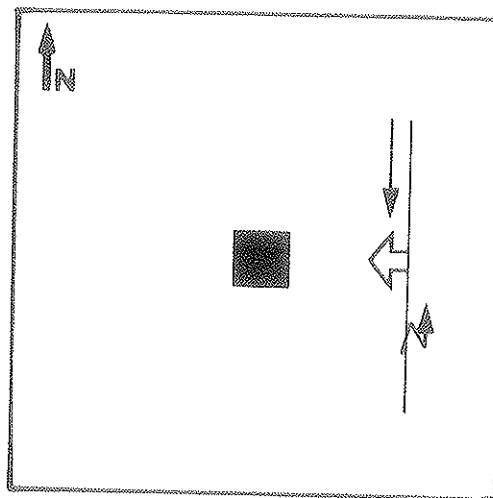
Figure II-5. Mission profiles, 3 April 1984, Flight #2.

4 April 1984

RESEARCH FLIGHT

Repeatability tests
Wide swath (full width)

Lines 1, 2, 3, 4 and 5
Scale 1:250 000

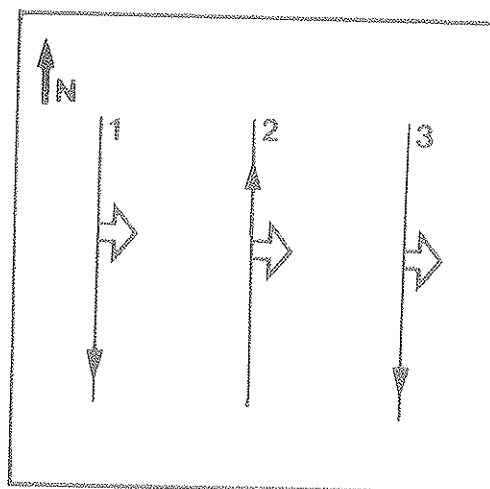


5 April 1984

OPERATIONS FLIGHT

1. Wide swath (full width) - 1st 1/2

Lines 1, 2 and 3
Scale 1:250 000



2. High Resolution (1/2 width) - 2nd 1/2

Lines 4, 5 and 6
Scale 1:62 500

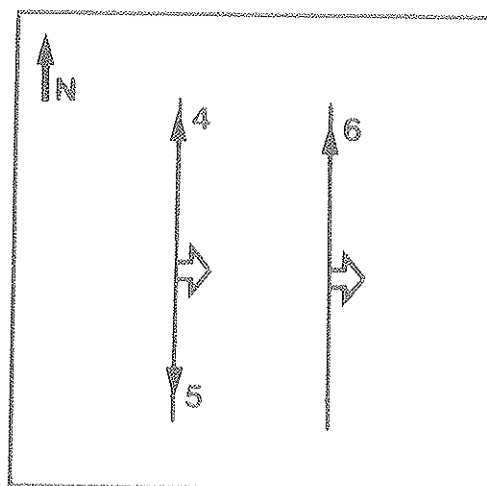
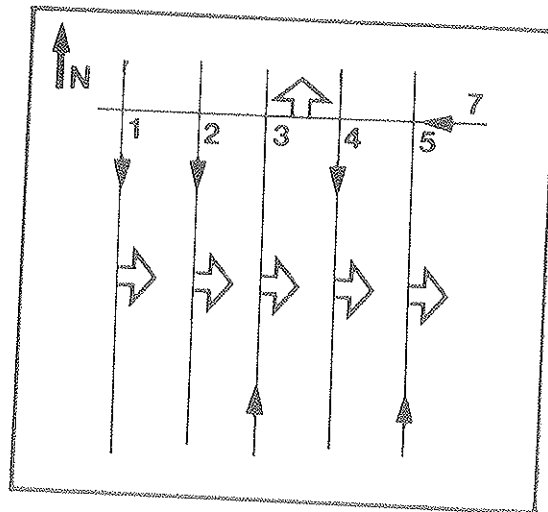


Figure II-6. Mission profiles, 4 and 5 April 1984.

OPERATIONS FLIGHT

Lines 1, 2, 3, 4, 5 and 7
(Flown 2, 3, 4, 5, 7, 1)

All lines are high resolution (full width)
except reflector pass (high resolution (1/4))



Line 10: Reflectors (3 look, high resolution,
1/4 swath width)

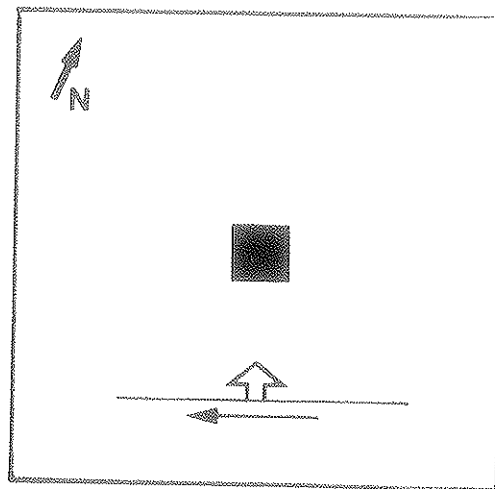


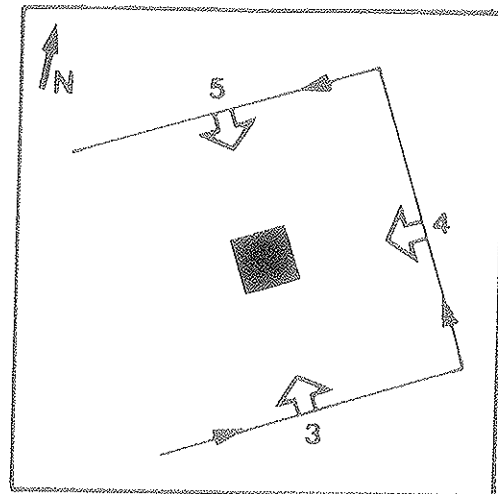
Figure II-7. Mission profiles, 6 April 1984.

RESEARCH FLIGHT

1. Aspect Angle Tests
High resolution (full width)

Lines 3, 4 and 5

Scale 1:125 000

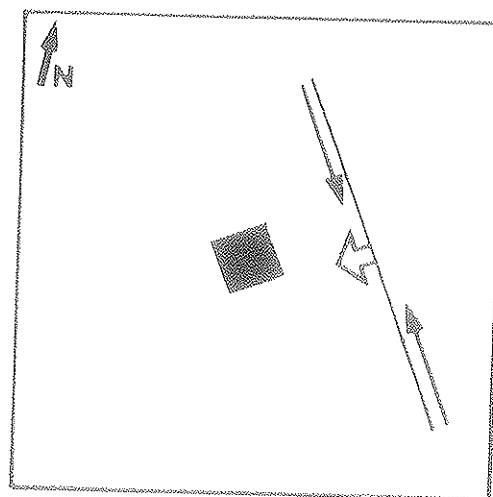


2. Repeatability Tests
High Resolution (full width)

Lines 6, 7, 8, 9, 10, 11 and 12

Scale 1:125 000

These lines are comparable to Line 4.



3. Resolution Test
Wide swath (1/2 width) 1st 1/2

Line 13

Scale 1:125 000

Look Angle: Near edge 20°
Far edge 10°

This line is comparable to Line 12.

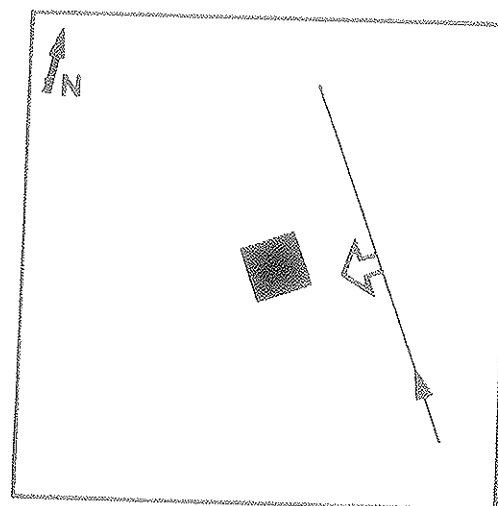


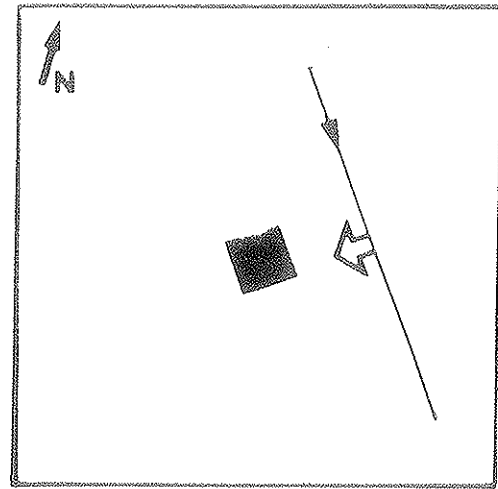
Figure II-8. Mission profiles, 7 April 1984.

4. Look Angle Tests
Wide swath (1/2 width) 2nd 1/2

Line 14
Scale 1:125 000

Look angles: Near edge 10°
Far edge 6.7°

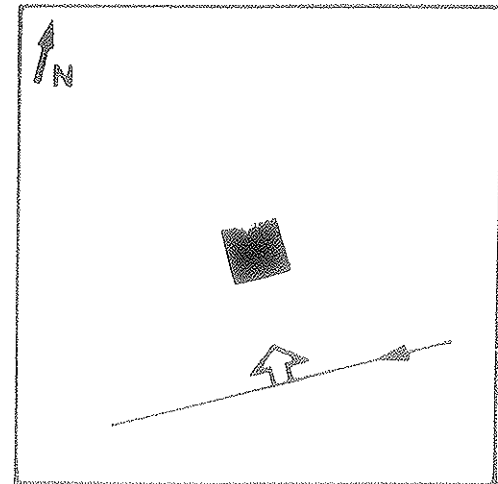
This line is comparable to Line 13.



5. Resolution Test Looking Upwind,
Aspect Angle Test and Look Angle Repeat

Line 15
Wide swath (1/2 width) - 2nd 1/2
Look Angles: Near edge 10°
Far edge 6.7°

This line is comparable to line 3
(resolution), line 14 (aspect), and
line 16 (repeat).



6. Line 16
Wide swath (1/2 width)
Repeat of line 15.

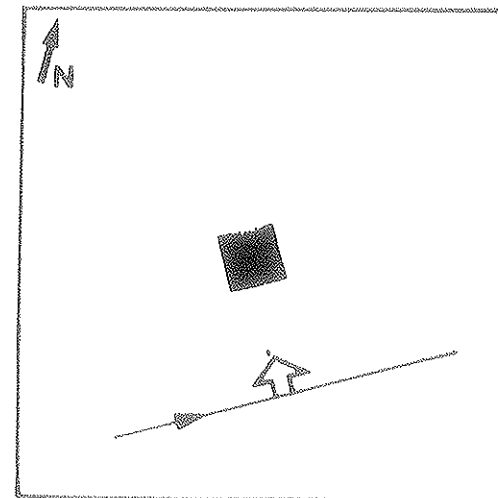


Figure II-9. Mission profiles, 7 April 1984 (continued).

analysis. The results of this analysis were presented at that workshop and at a poster session of the Canadian Remote Sensing Symposium which accompanied the workshop. An expansion of that analysis was presented at the final BERGSEARCH '84 meeting in Toronto and is summarized here.

The Problem. Perhaps the most important question to be resolved is the reliability or probability of correctly detecting iceberg targets of a given size range in given sea-state conditions. Some measure of this can be obtained by flying repetitive lines over the same target area and examining the repeatability of detection of individual targets from one line to the next. At the same time, given adequate resolution, estimates of the sizes of the targets can be directly measured from the imagery.

The mission flown on 7 April 1984 was excellent for this purpose as there were some 100 or more icebergs of size ranging from growlers to small icebergs in a target area about 25 x 25 km. Moreover, there was swell and wave action with combined amplitude of 2-4 m at the time.

The Analysis. A box was drawn on the images such as to include most of the targets in the area, but to exclude the pack ice and its adjacent areas where bits of pack ice and iceberg targets had sloughed off and were drifting together. This is shown in Figure II-10 below. Each of the targets was numbered on one of the lines and an attempt made to re-identify each of these targets on each of the other six lines.

Simple statistical counts could then be used to determine the variability of detection. In particular, by re-identifying each target from line to line (as opposed to comparing the total numbers of each sample) it ensures that both disappearing and re-appearing or newly appearing targets are accounted for. Moreover, given the time period over which the seven lines were flown (about 70 minutes) it ensures that spurious sea-spikes are not included among the 'persistent' targets.

Each of the targets was measured in the cross-track direction to provide a one-dimensional size indication. The targets were then put into three bins according to this size classification. The bin sizes were <10 m, 10-20 m, and >20 m.

Results. A total of 81 targets were identified within the box on line #9. Re-identification was achieved on the other lines as follows:

- * All 81 targets were re-identified on five of the seven lines (i.e., 100% re-identification).
- * 80 of 81 targets were re-identified on six of the seven lines (i.e., 96% re-identification).



Figure II-10. Identification of targets, 7 April 1984, line 9.

* 78 of 81 targets were re-identified on all seven of the lines (i.e., 96% re-identification).

These 81 targets were distributed in size as follows:

| Number | Type | Size | Percentage |
|--------|-----------------------------------|---------------|------------|
| 29 | Growlers | (<10 m size) | 36% |
| 39 | Bergy Bits | (10 m - 20 m) | 48% |
| 13 | Small Bergs and larger targets | (>20 m) | 16% |
| Total | 81 | | 100% |

Note: the above assignments of type are based upon measurement of the width in the range direction, with no surface verification.

Azimuthal Smear. The relatively fine resolution achieved by SAR is achieved in the range or cross-track direction by pulse compression techniques whereas in the azimuthal or along-track direction, it is achieved through processing of the Doppler spectrum of the target return. The Doppler spectrum is usually a result of the aircraft motion with respect to a stationary target. Motion of the target causes an additional Doppler component. In the case of a moving target such as an iceberg in open water with waves and swell, the motion causes the image of the target to be elongated or smeared in the azimuthal direction (see Figure II-1). The range direction is unaffected.

The same phenomenon is produced by the breaking waves which are responsible for "sea spikes." It appears however, that the smearing is relatively greater for sea spikes. This means that the energy is spread over more pixels than for the icebergs. The net result of this phenomenon is that sea spikes appear to be preferentially suppressed compared to the icebergs.

Thus the azimuthal smear appears to be a mixed blessing. On the negative side, the azimuthal smear causes:

- potential overlapping of targets in the azimuthal direction (no effect in the range direction); and
- inability to estimate target size in azimuthal direction.

On the positive side, the azimuthal smear causes:

- preferential suppression of the sea clutter spikes

- compared to iceberg returns; and
- accentuation of the target appearance on the imagery.

Archiving of Data

A copy of all imagery annotated and analysed by CANPOLAR will be archived with the National Air Photo Laboratory (NAPL) in Ottawa. Flight logs will accompany the imagery.

The originals of this imagery will be returned to INTERA and archived in-house. Additionally, all HDDTs will be retained by INTERA in-house along with the flight logs.

CCTs already presented to the CANPOLAR analysis team will be retained by Mr. E. Wedler until his analysis program is completed, at which time they will be returned to INTERA for archiving.

II.2.5 SUMMARY

The STAR-1 data collection component of the ESRF study "Assessment of Airborne Radars for the Detection of Icebergs" was successfully completed as described here. The INTERA program was conducted in three phases: Planning and Mobilization; Data Collection; and Reporting.

The highlight of the program was the six-day field portion from 2-7 April 1984 during which STAR-1 flew eight missions with 40 flying hours being over target and 27 hours flown in transit to and from the operations centre at Gander, Newfoundland. During these missions both "research" and operational flight profiles were flown. The objectives of the 'research' profiles, summarized in this document, were achieved, as were the operational profiles.

The imagery, recorded digitally on magnetic tape aboard the aircraft was subsequently replayed onto high-quality negative transparencies, controlled for quality, annotated, and forwarded to the CANPOLAR team for analysis. A limited number of flight lines were also transcribed from the high density digital tapes onto computer-compatible tapes and were forwarded to CANPOLAR for digital image analysis.

The results of brief analysis performed by INTERA on the repeatability of detection of iceberg targets are presented in this document. They indicate a very high repeatability of detection in 2-4 m waves and swell for targets of estimated size down to 10 m (i.e., growlers).

To facilitate further analysis, this document contains supporting information concerning the equipment used, data formats, quality control procedures, and archiving.

BERGSEARCH '84

SECTION II CHAPTER 3

WAVES RECORDED IN THE FLEMISH PASS

Dobrocky Seatech Ltd.
St. John's, Newfoundland

II.3 WAVES RECORDED IN THE FLEMISH PASS

II.3.1 INTRODUCTION

During April 1984, Dobrocky Seatech was involved with the collection of ground verification data for the ESRF Iceberg Detection Trials Project in the Flemish Pass area. Specifically, Dobrocky personnel were required to launch and recover a Datawell waverider and to record wave data during the ESRF over-flight. Four wave data records were recovered from four different locations in the Flemish Pass area (Figure II.11). The waverider buoy at each location was not moored to the bottom but was tethered to the survey vessel Polaris V for ease of deployment. The WAREP receiver was operated on continuous mode during buoy deployment. Information on the buoy deployments is given in Table II-3.

II.3.2 A SUMMARY OF DATA COLLECTION AND PROCESSING

The wave records recovered from each of the four locations were processed by MEDS¹ in Ottawa and the wave data are presented in this report. The waverider recording station on board the Polaris V was designated Station No. 245

Data products accompanying this report include:

1. Table of root mean square wave height (metres) tabulated by wave period in seconds for all four stations (Table II-4).
2. Ten pages of graphs of spectral density of waves in m^2/Hz versus frequency in Hz for all four stations (Figures II-12 to II-21).
3. Graph of a wave characteristic height in metres versus time in days for all four records (Figure II-22).
4. Percentage exceedance plot of significant and maximum wave height for four stations together (Figure II-23).
5. Percentage occurrence histogram of wave peak period in seconds for four stations taken together (Figure II-24).
6. Plot of significant wave height in metres versus peak period in seconds for four stations together (Figure II-25).

Note that data products 1 and 2 are tabulated by data records which include a side and tape number as recorded in the on-board WAREP. The table of root mean square wave height in metres tabulated by wave period in seconds matches data tape records to hours and days recorded.

¹ Marine Environmental Data Service, Government of Canada, Department of Fisheries and Oceans.

Data products 3 through 6 were generated by using all four wave records from all four sites of deployment.

II.3.3 SPECTRUM DIAGRAM: A SHORT DESCRIPTION

The spectrum diagram shows the variance spectral density of the water surface elevation as a function of frequency. The densities are computed at about 60 discrete values of frequency between 0.05 and 0.5 Hz using the Cooley-Tukey fast fourier transform algorithm. Each 20-minute wave record is broken up into several blocks of 1024 data points. The number of such blocks will be determined by the digital sampling frequency. The final value at each frequency is the average of the densities at the frequency over all the blocks.

If corrections were required for either instrument response or, in the case of a pressure cell, for the attenuation of the pressure fluctuations with depth they will have been applied to the spectrum.

The units of variance spectral density are feet (or metres) squared per hertz and the units of frequency are hertz. The wave record can be identified by the record-side-tape number and the station number annotated in the upper right-hand corner. The time of recording and other pertinent information must come from accompanying documentation. The abbreviations SWH and PEAK PER if they appear are followed by the significant wave height in feet and the peak period in seconds. The peak period is the inverse of the frequency at which the maximum spectral density occurred. The significant or characteristic wave height is four times the square root of the area under the spectrum.



Figure II-11. Waverider buoy locations and water depths for ESRF icebergs detection trials.

TABLE II-3

Waverider Deployment Information, 1984

| Date of Deployment | Time of Recorded Wave Data (GMT) | Position of Deployment | Charted Water Depth in Deployment Area (m) |
|-----------------------|---|---------------------------|---|
| April 1 | 1857-2037 | 46°49'24"N 46°48'42"W | 1177 |
| April 2 | 1700-2040 | 46°45'24"N 47°11'15"W | 639 |
| April 3 | 1340-1840 | 46°55'00"N 46°48'42"W | 1183 |
| April 7 | 1600-2240 | 47°07'46"N 47°45'24"W | 184 |

WAVES RECORDED OFF IMAGING RADAR (FLEWISSE PASS)

[illegible]

FIGURE II-12

GRAPHS OF SPECTRAL DENSITY OF WAVES IN M^2/HZ
VERSUS FREQUENCY IN HZ FOR ALL FOUR STATIONS

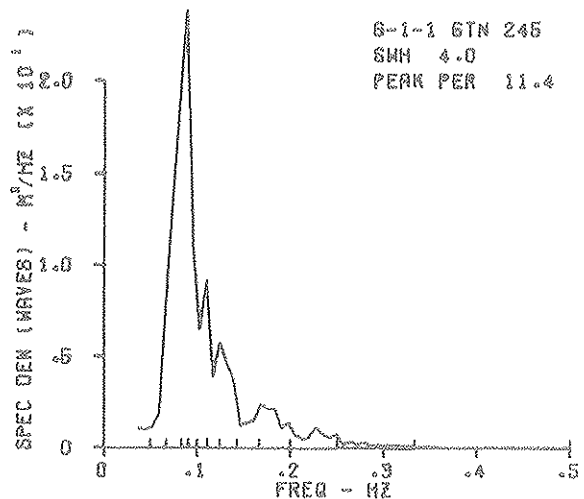
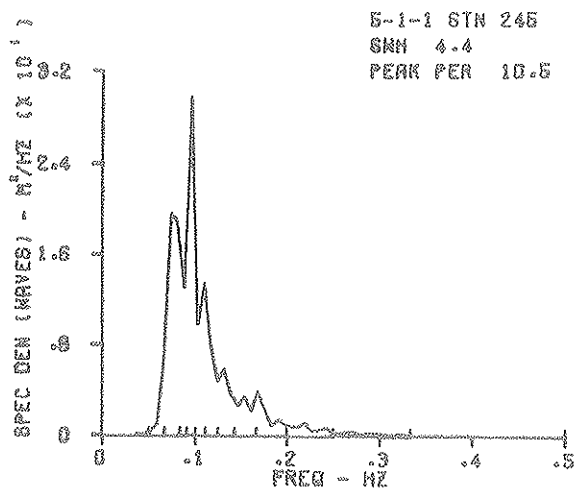
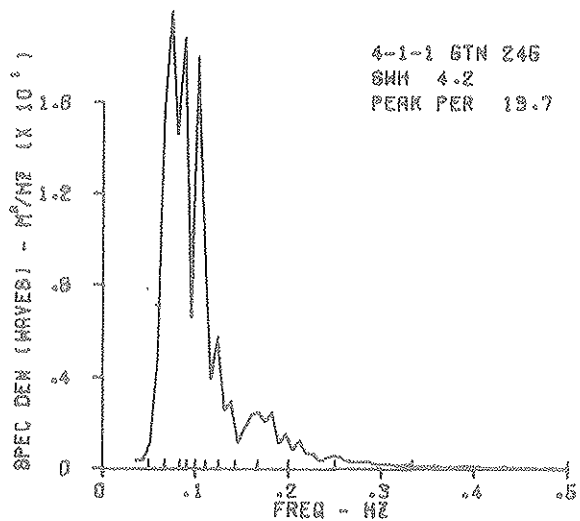
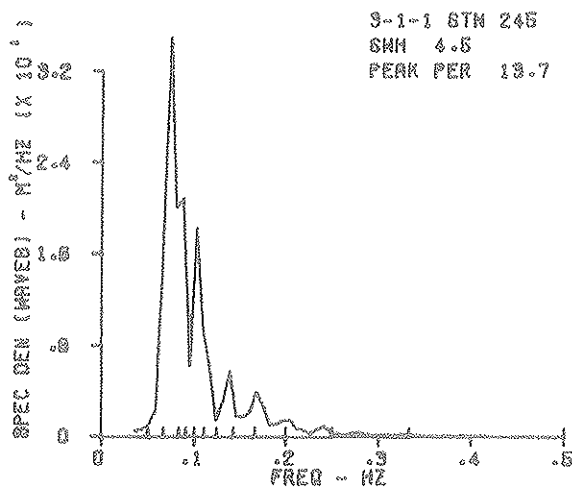
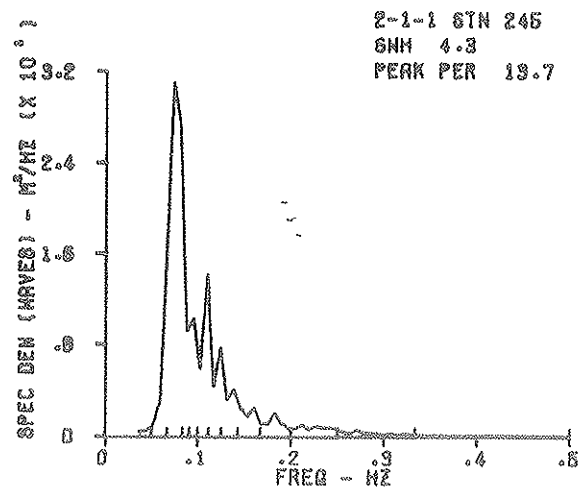
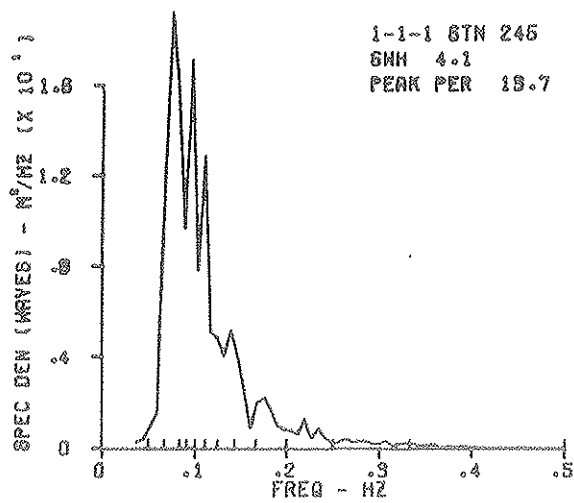


FIGURE II-13

GRAPHS OF SPECTRAL DENSITY OF WAVES IN M^2/HZ
VERSUS FREQUENCY IN HZ FOR ALL FOUR STATIONS

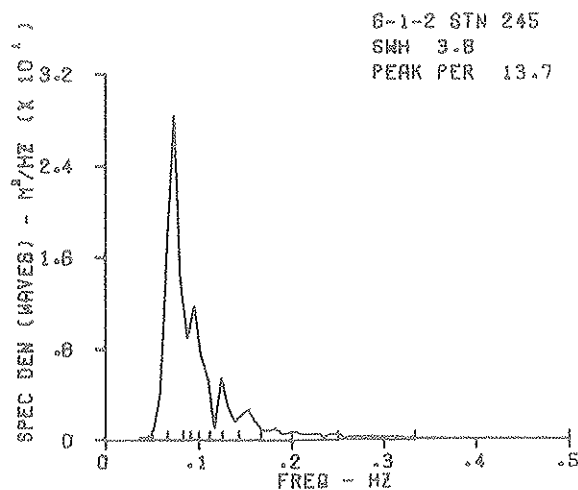
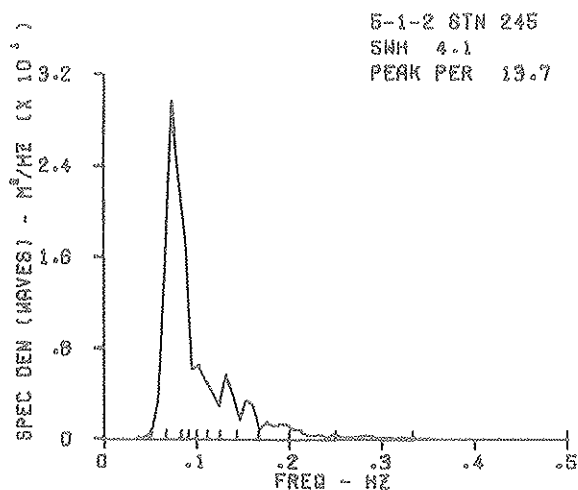
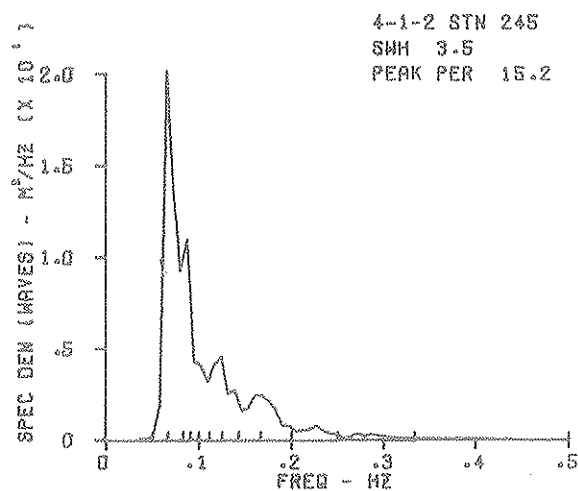
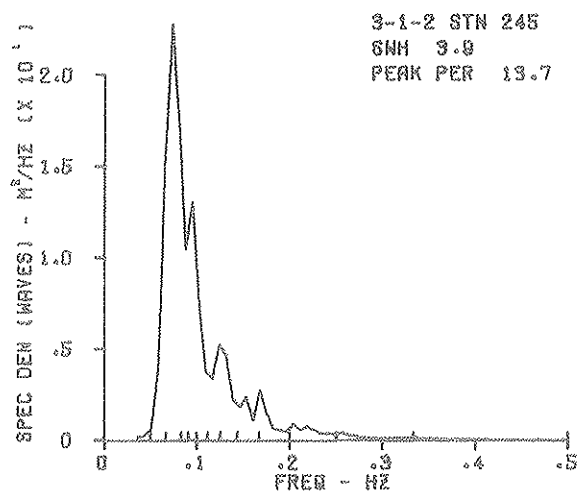
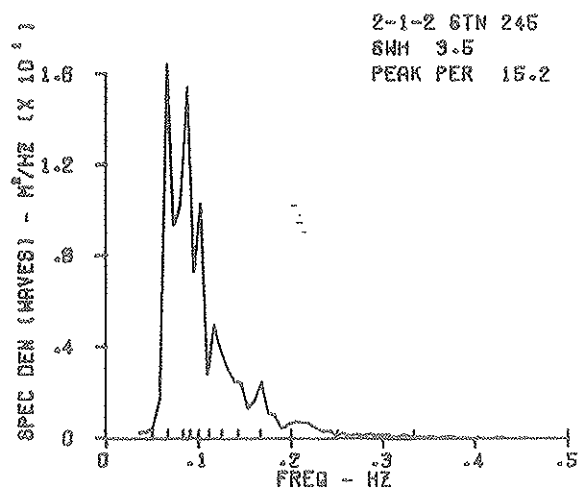
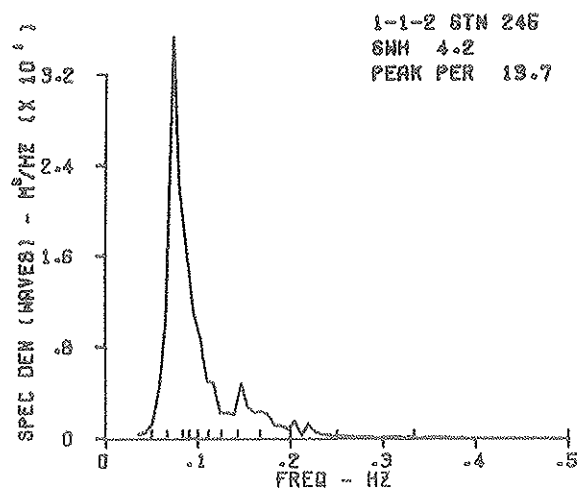


FIGURE II-14

GRAPHS OF SPECTRAL DENSITY OF WAVES IN M^2/HZ
VERSUS FREQUENCY IN HZ FOR ALL FOUR STATIONS

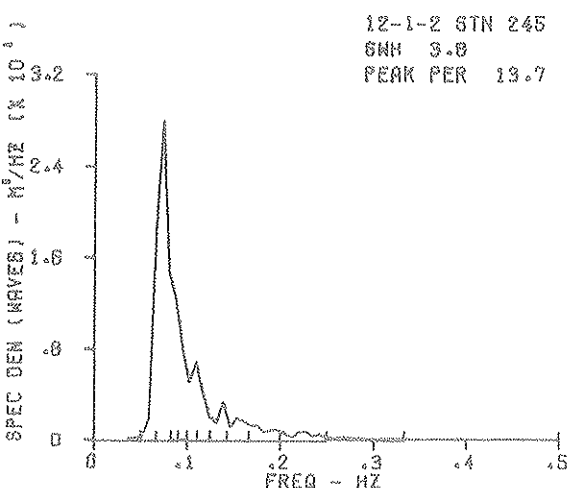
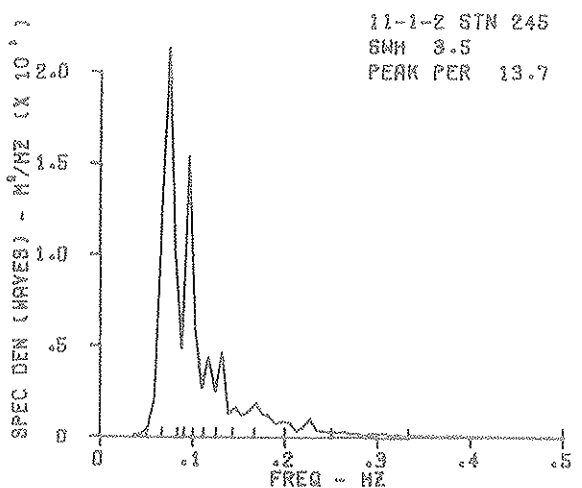
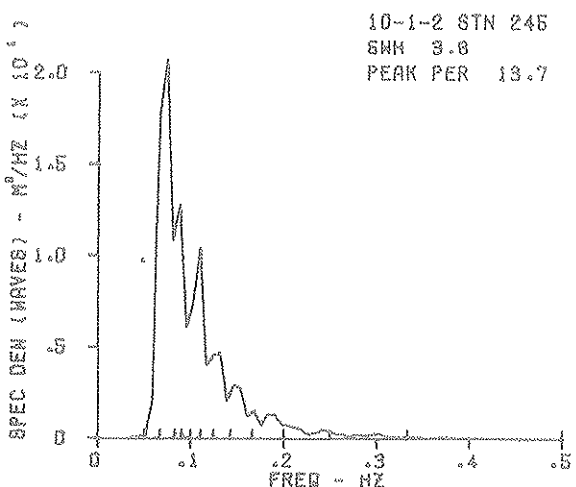
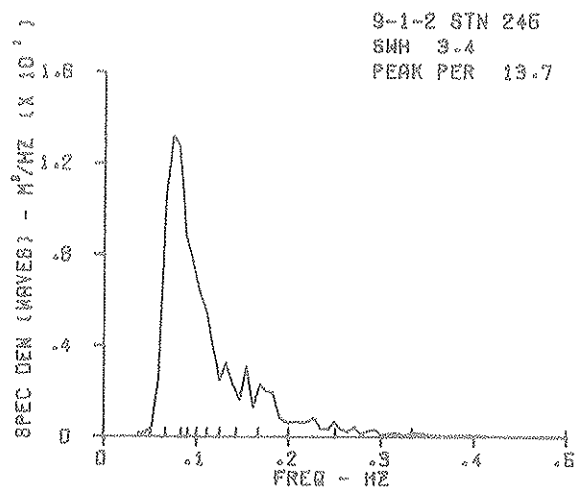
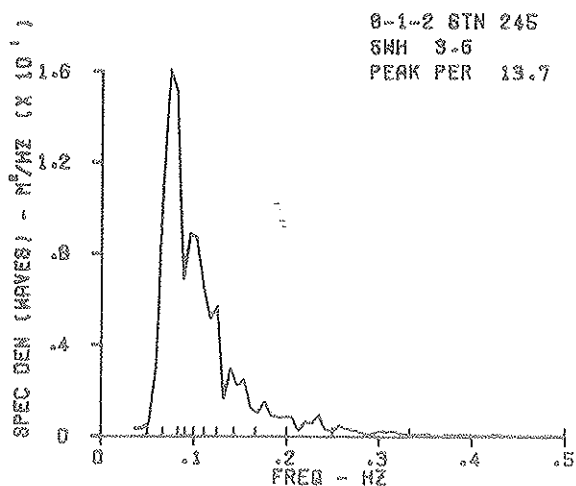
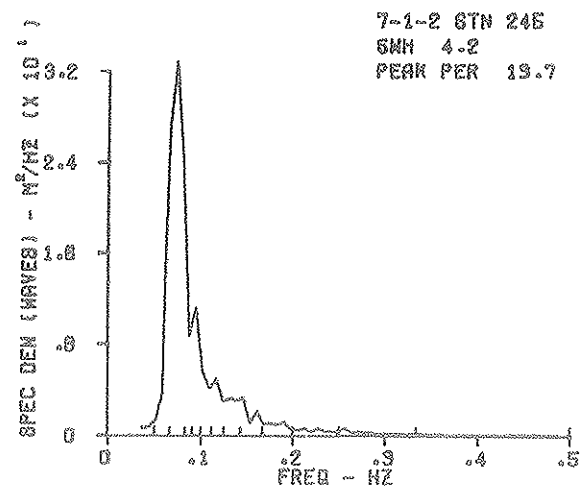


FIGURE II-15

GRAPHS OF SPECTRAL DENSITY OF WAVES IN M^2/HZ
VERSUS FREQUENCY IN HZ FOR ALL FOUR STATIONS

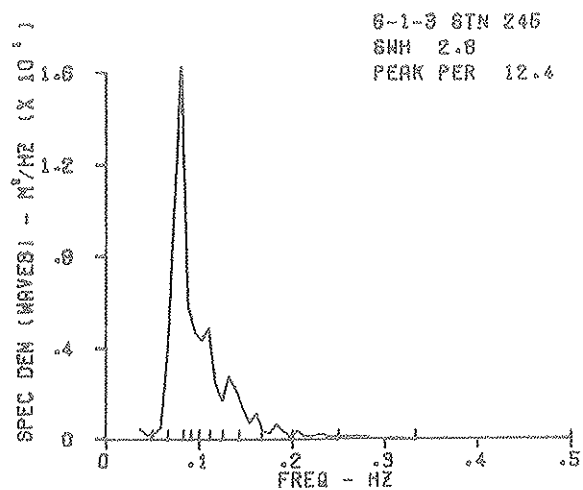
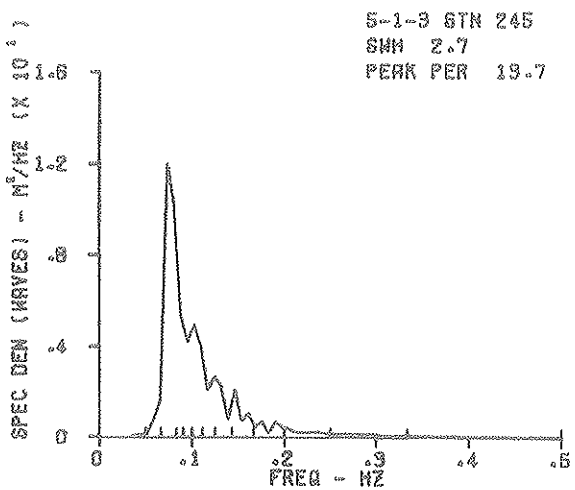
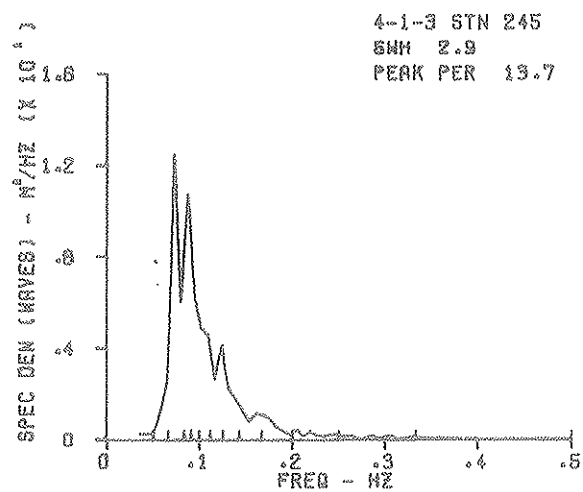
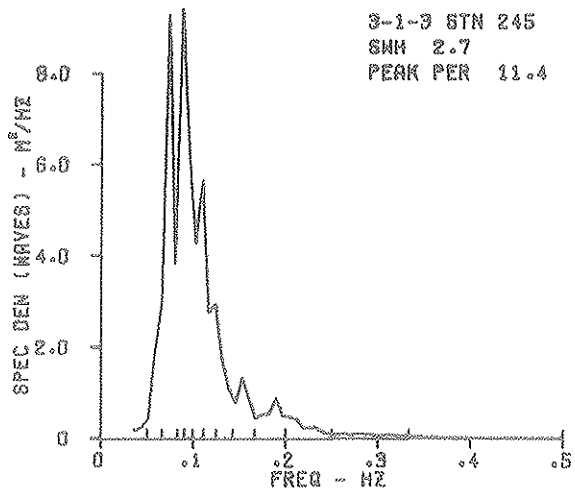
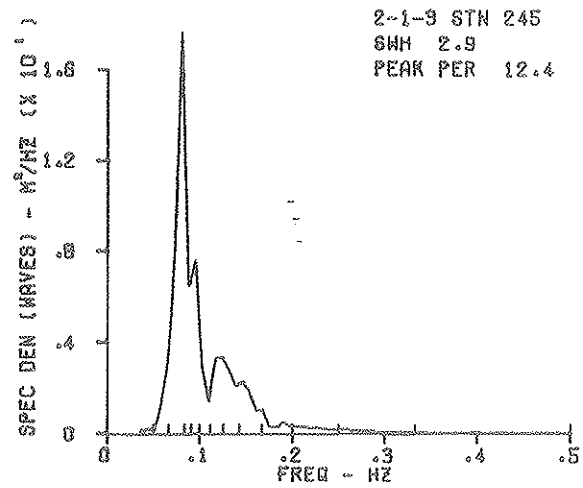
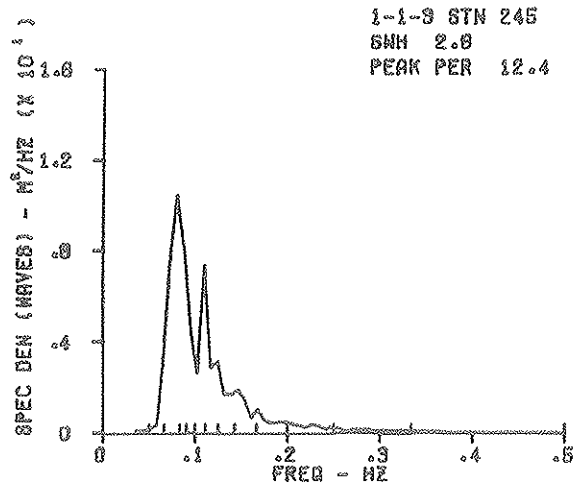


FIGURE II-16

GRAPHS OF SPECTRAL DENSITY OF WAVES IN M^2/HZ
VERSUS FREQUENCY IN HZ FOR ALL FOUR STATIONS

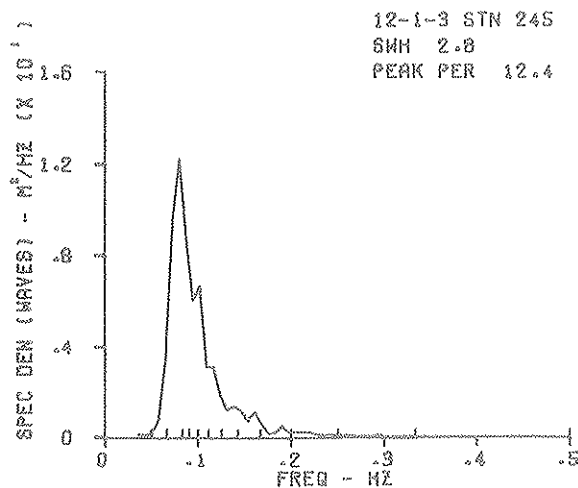
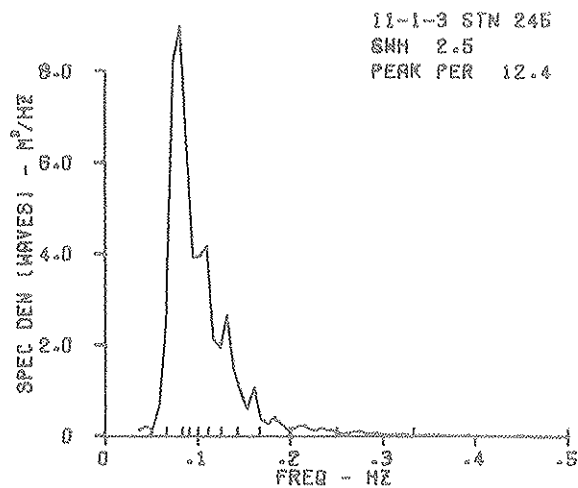
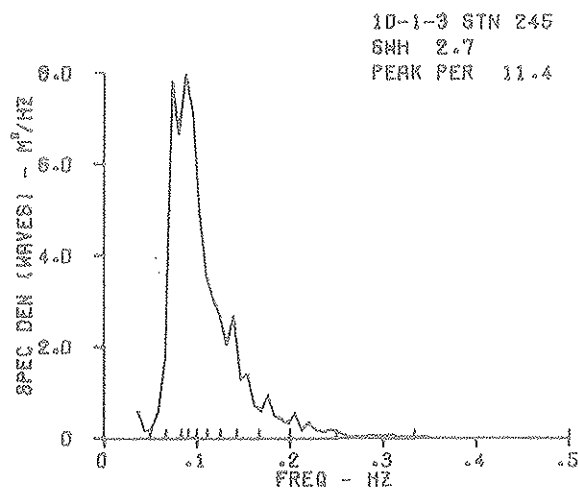
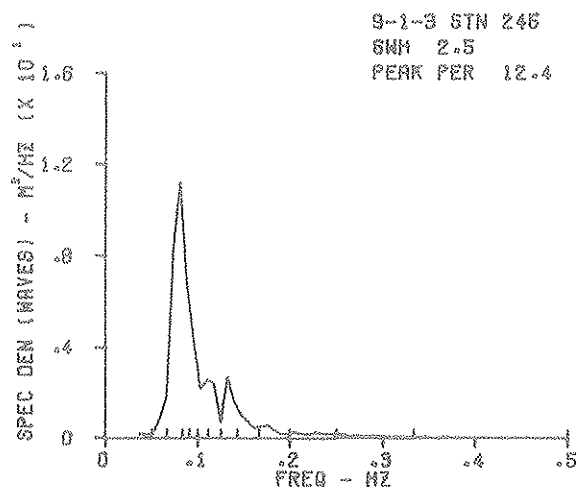
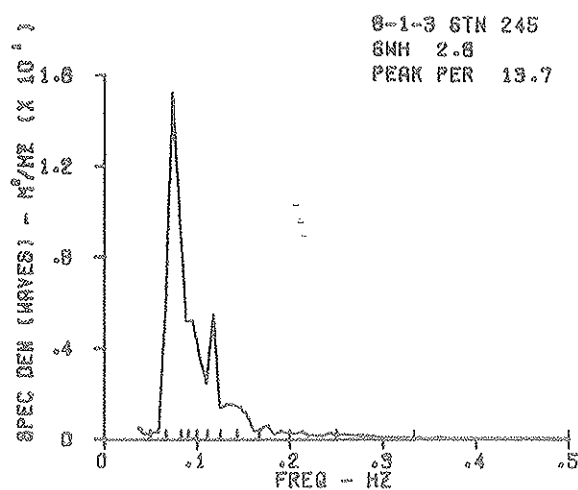
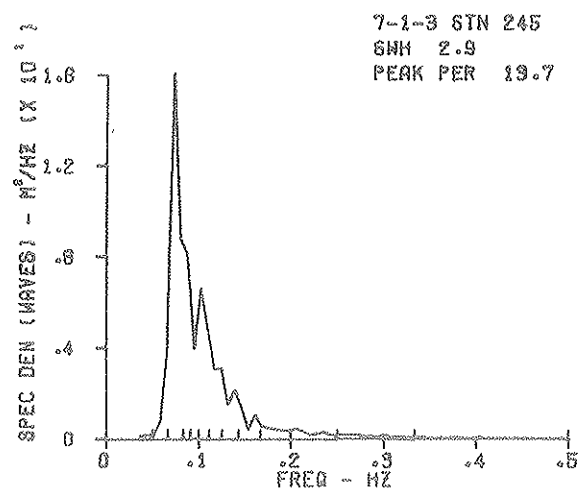


FIGURE II-17

GRAPHS OF SPECTRAL DENSITY OF WAVES IN M^2/HZ
VERSUS FREQUENCY IN HZ FOR ALL FOUR STATIONS

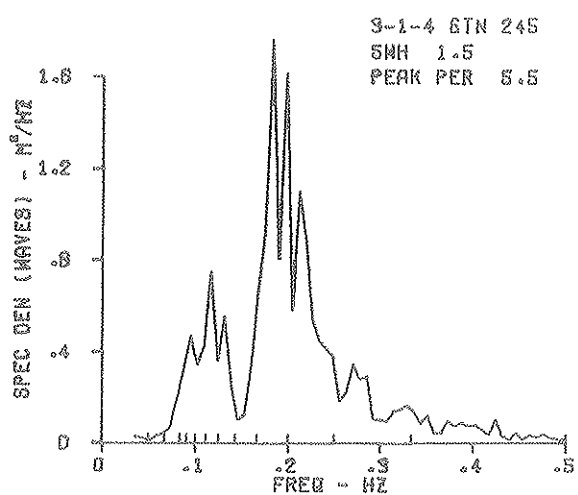
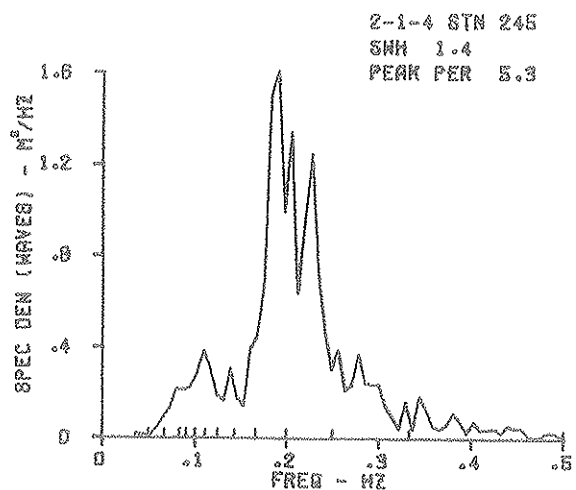
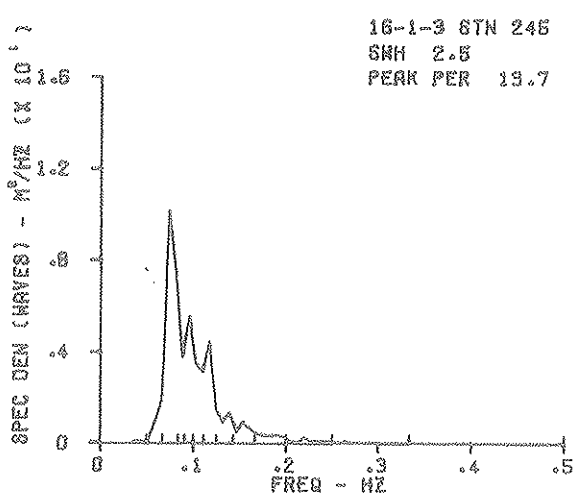
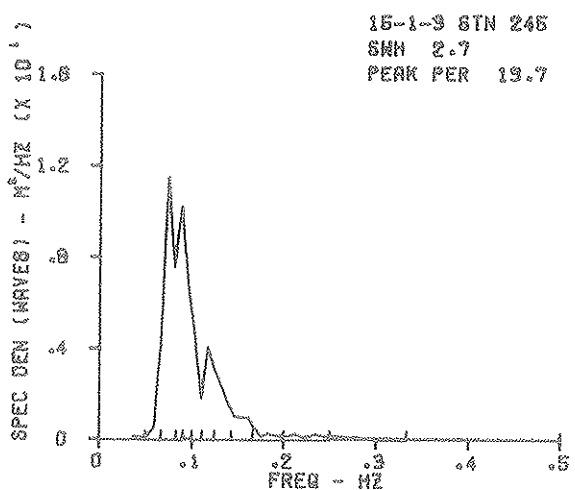
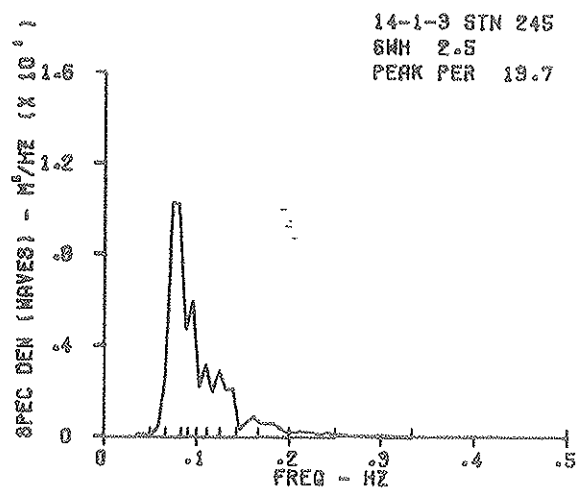
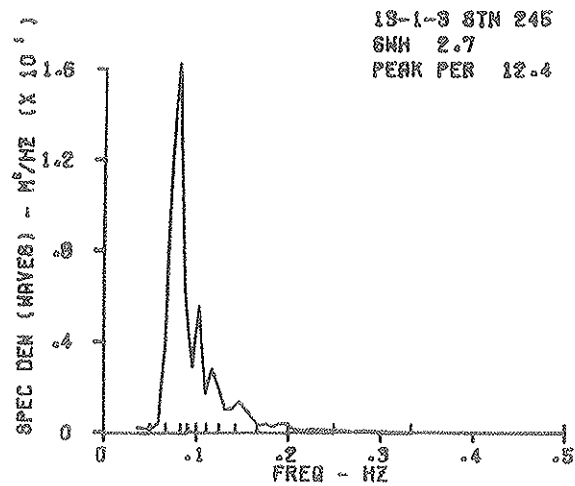


FIGURE II-18

GRAPHS OF SPECTRAL DENSITY OF WAVES IN M^2/HZ
VERSUS FREQUENCY IN HZ FOR ALL FOUR STATIONS

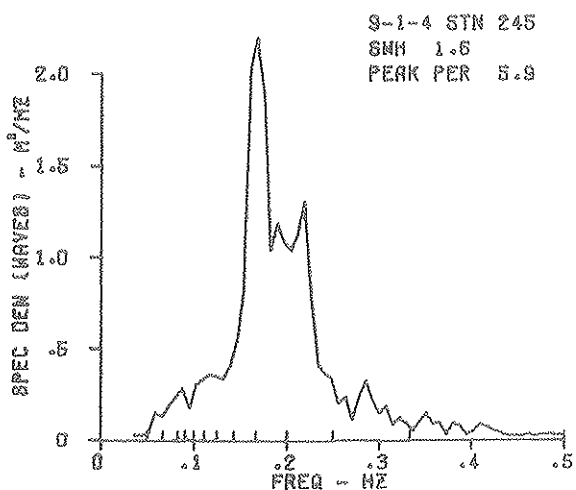
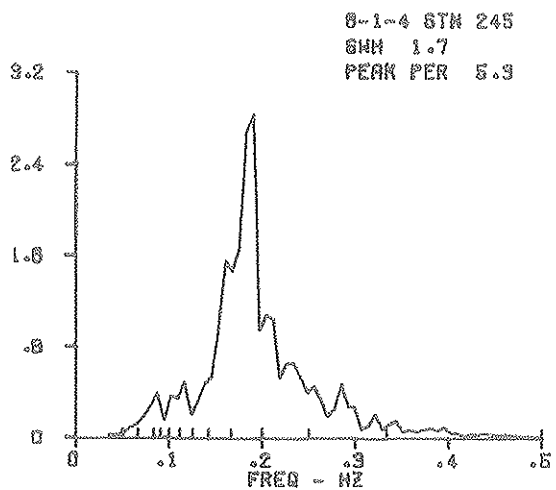
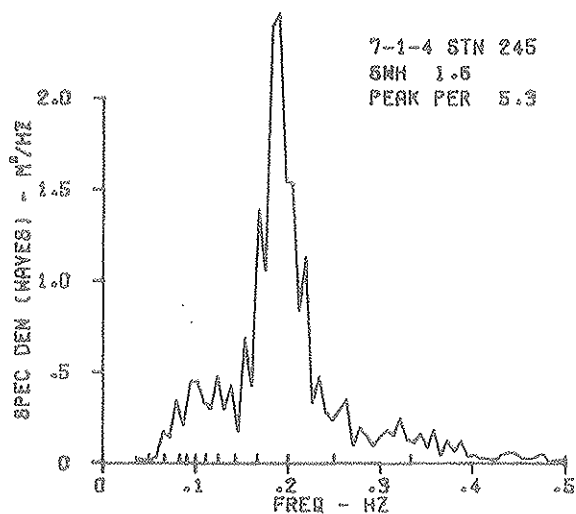
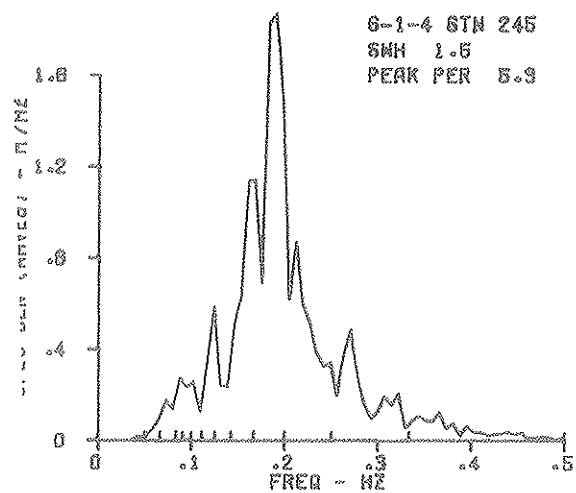
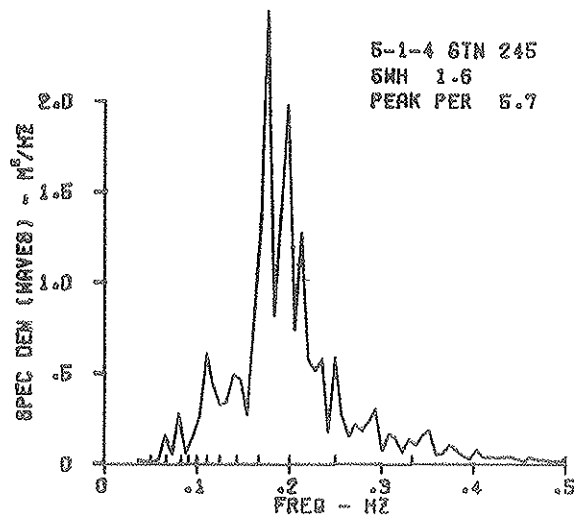
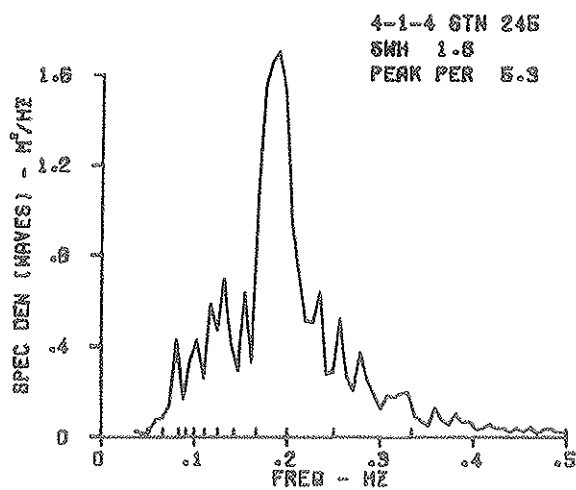


FIGURE II-19

GRAPHS OF SPECTRAL DENSITY OF WAVES IN M^2/HZ
VERSUS FREQUENCY IN HZ FOR ALL FOUR STATIONS

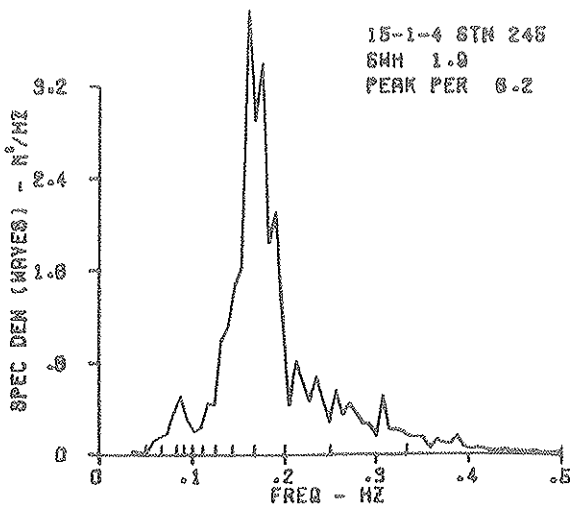
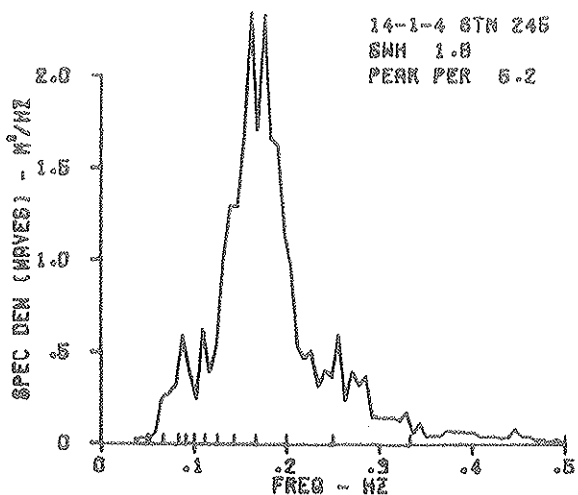
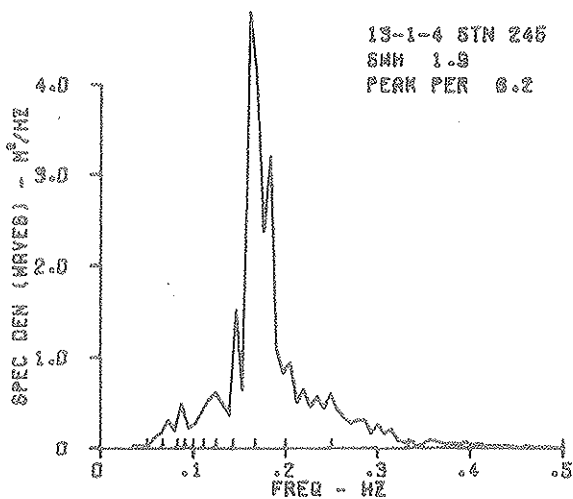
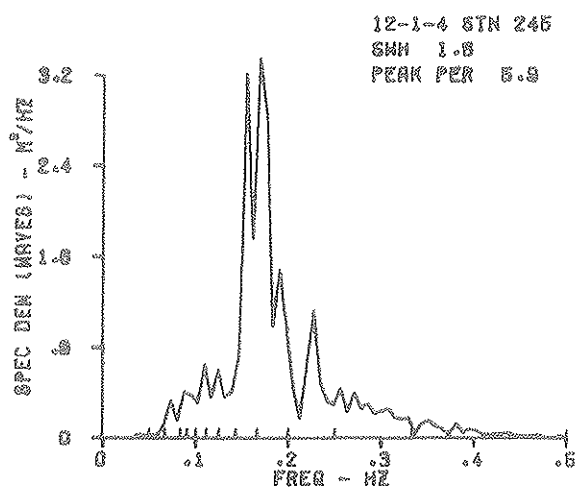
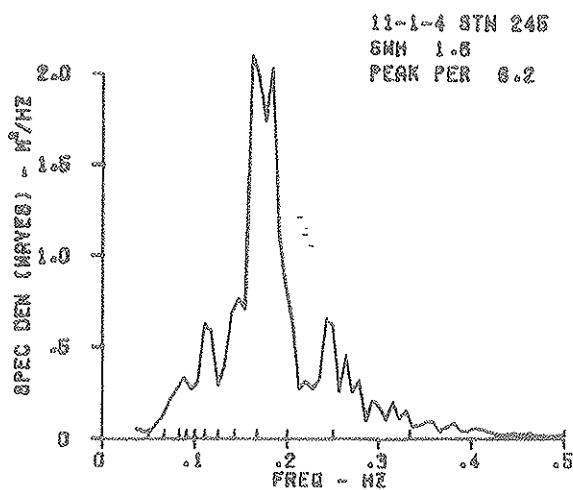
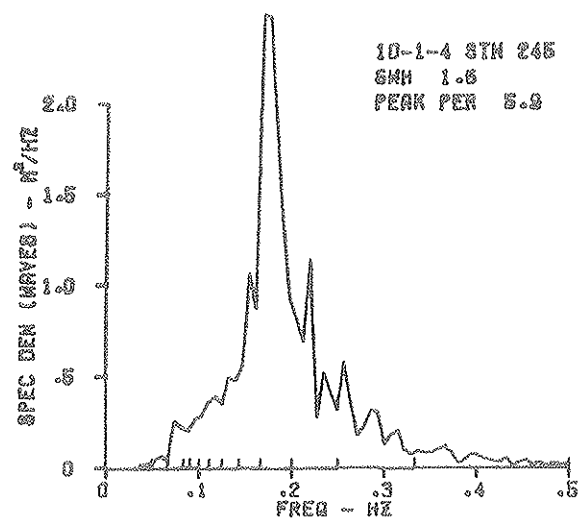


FIGURE II-20

GRAPHS OF SPECTRAL DENSITY OF WAVES IN M^2/Hz
VERSUS FREQUENCY IN HZ FOR ALL FOUR STATIONS

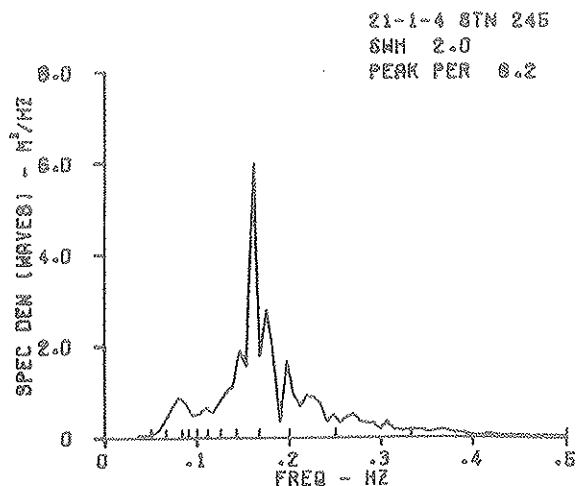
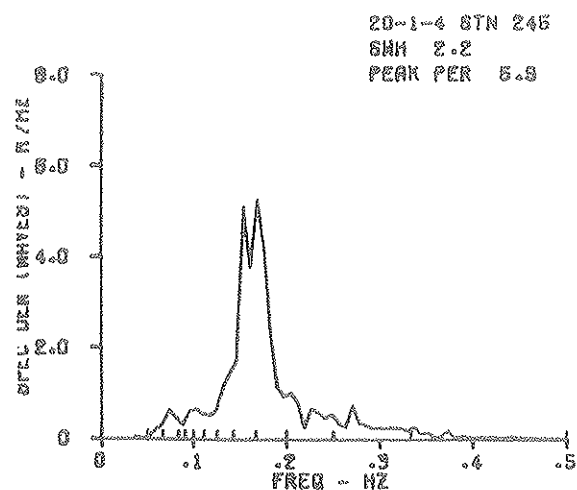
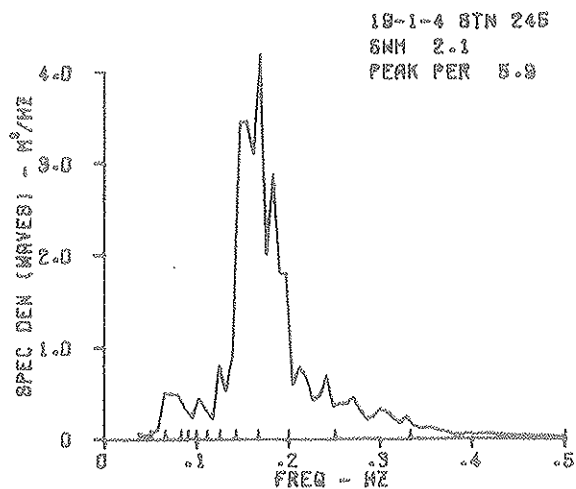
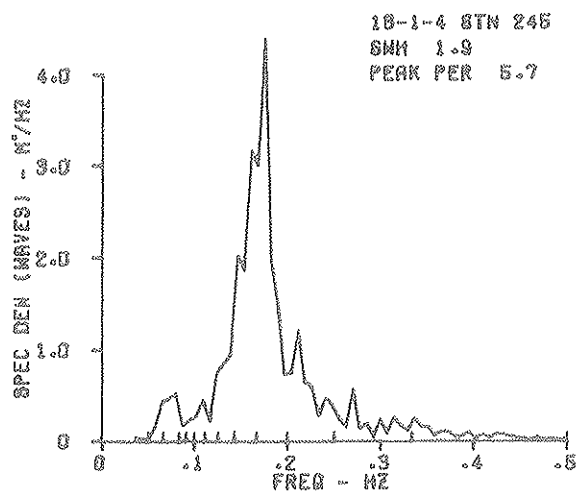
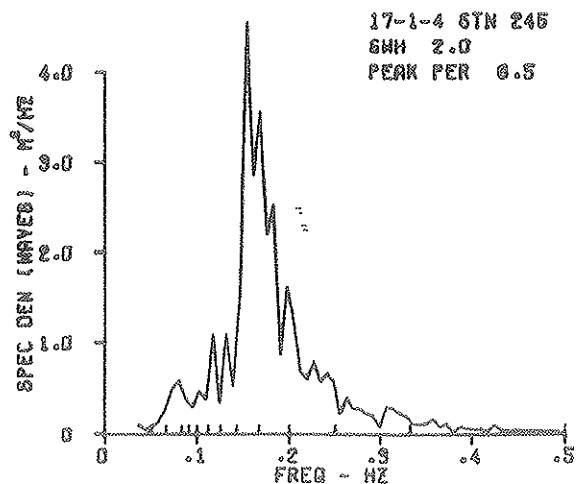
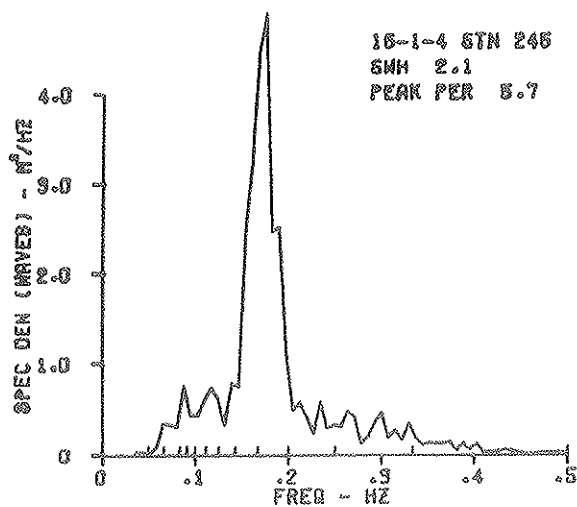
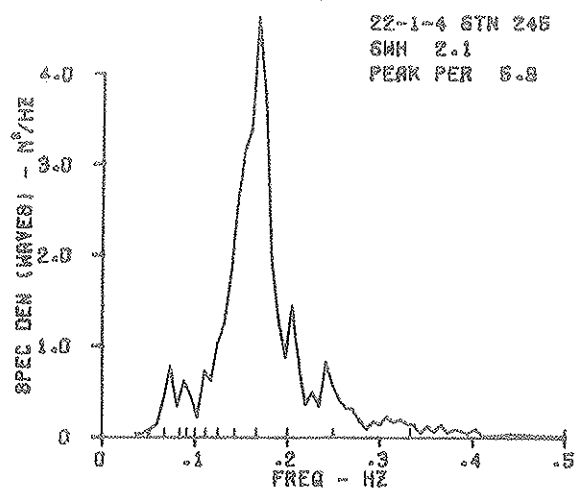


FIGURE II-21

GRAPHS OF SPECTRAL DENSITY OF WAVES IN M^2/HZ
VERSUS FREQUENCY IN HZ FOR ALL FOUR STATIONS



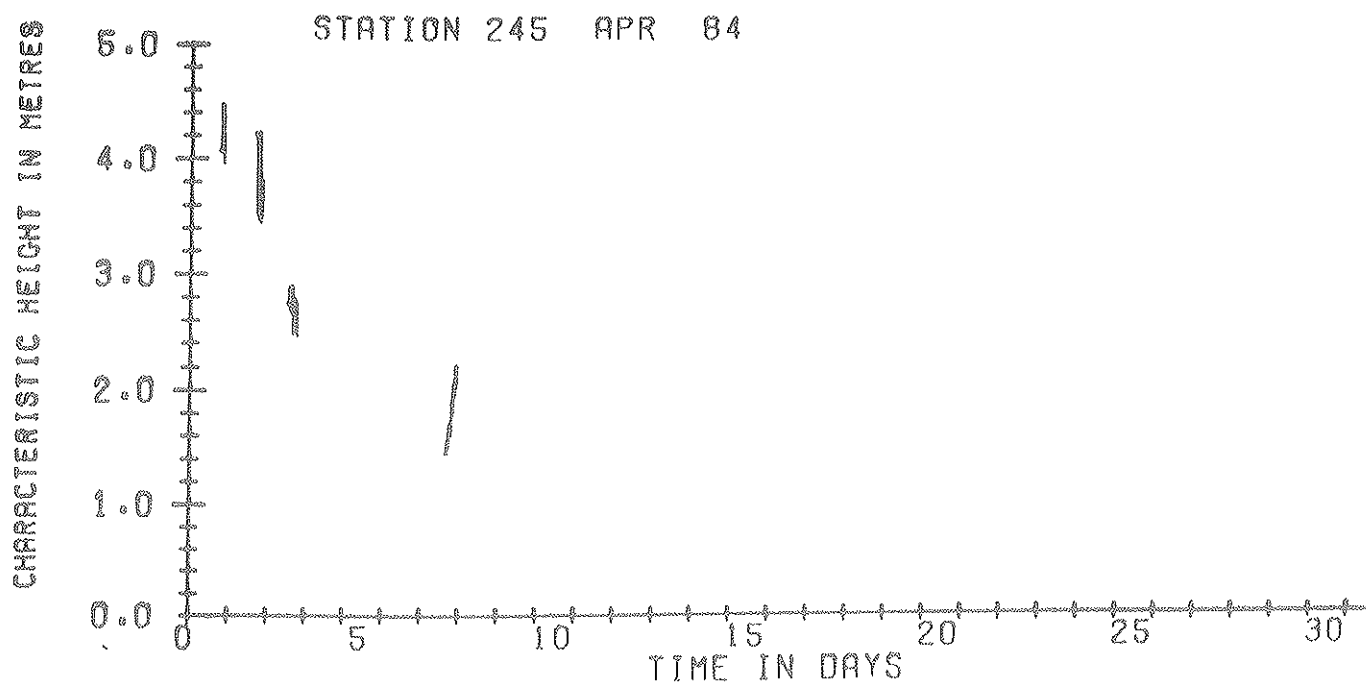


Figure II-22. Graph of wave characteristic height versus time in days for all four records.

FIGURE II-23

PERCENTAGE EXCEEDANCE PLOT OF SIGNIFICANT AND
MAXIMUM WAVE HEIGHT FOR FOUR STATIONS TOGETHER

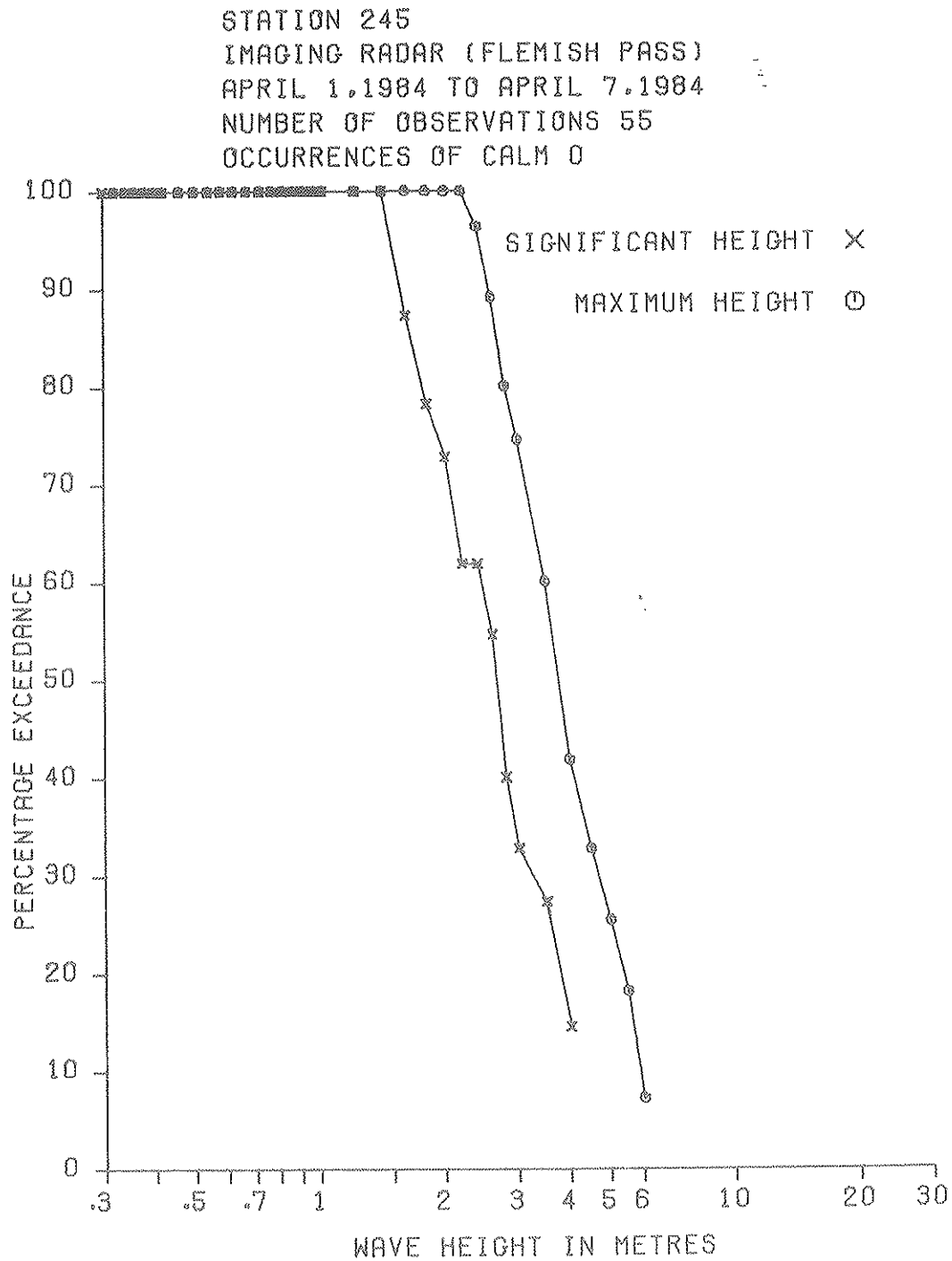


FIGURE II-24

PERCENTAGE OCCURRENCE HISTOGRAM OF WAVE PEAK
PERIOD IN SECONDS FOR FOUR STATIONS TAKEN TOGETHER

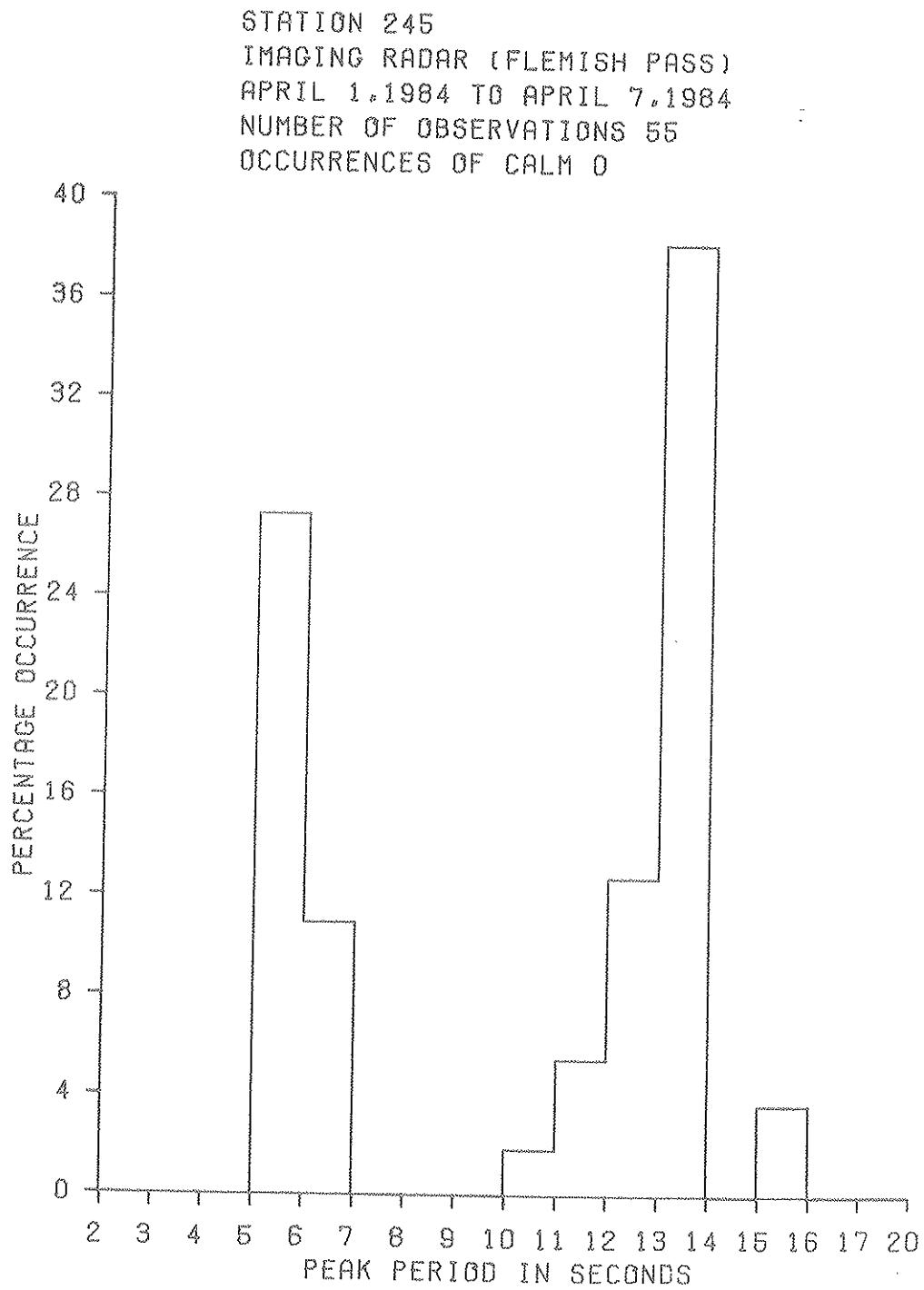
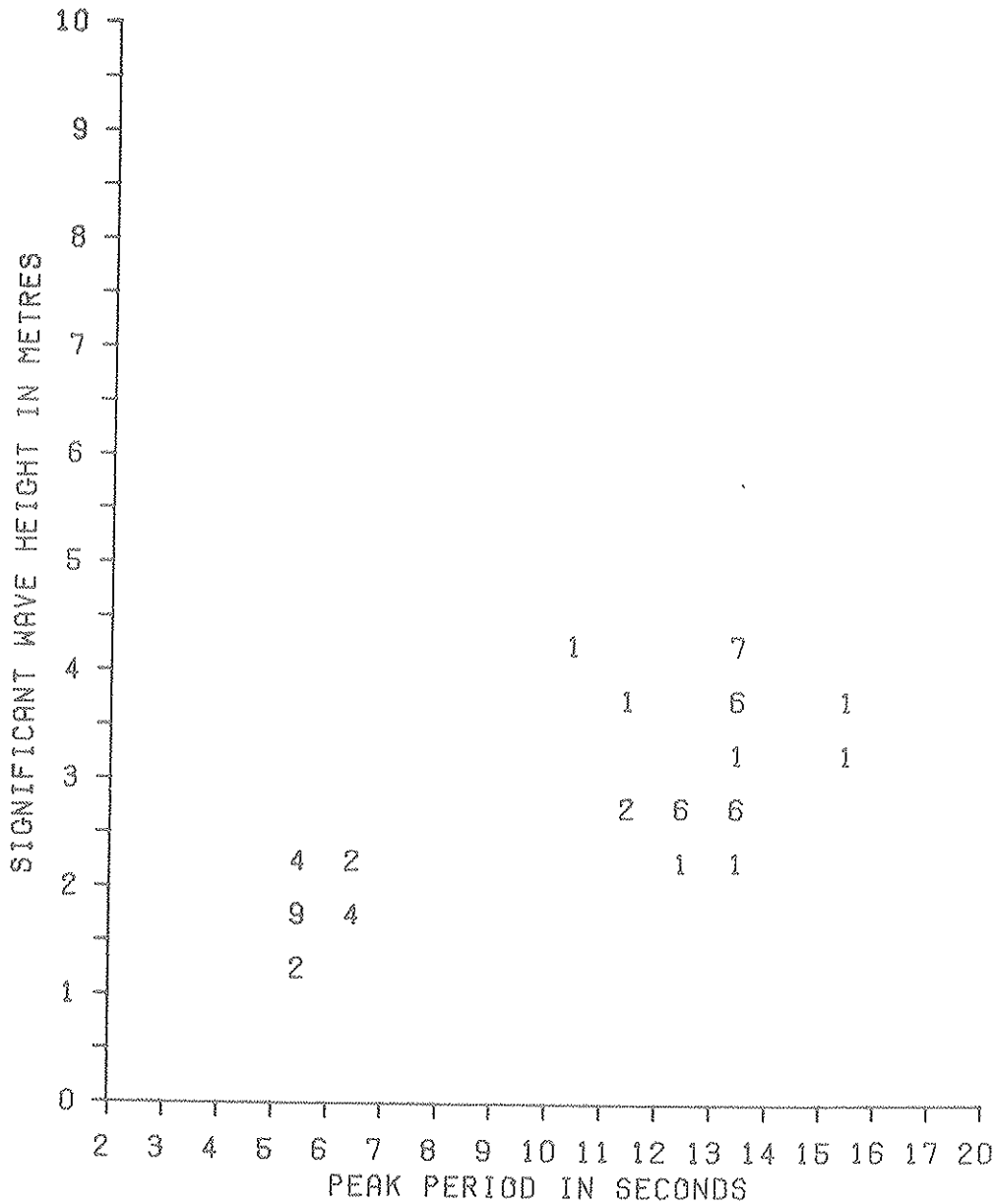


FIGURE II-25

PLOT OF SIGNIFICANT WAVE HEIGHT IN METRES VERSUS
PEAK PERIOD IN SECONDS

STATION 245
IMAGING RADAR (FLEMISH PASS)
APRIL 1, 1984 TO APRIL 7, 1984
NUMBER OF OBSERVATIONS 55
OCCURRENCES OF CALM 0



BERGSEARCH '84

SECTION III

DATA ANALYSIS AND INTERPRETATION

James R. Rossiter, CANPOLAR Consultants Ltd.
Lyn D. Arsenault, Cold Regions Remote Sensing
Eugene V. Guy, CANPOLAR Consultants Ltd.
David J. Lapp, Norland Science and Engineering Ltd.
Edward Wedler, Associate of CANPOLAR Consultants Ltd.

III.1 INTRODUCTION

III.1.1 BACKGROUND

Icebergs pose potential hazards both to oil exploration and production and to shipping off Canada's East coast. Both routine and special reconnaissance flights are used to detect icebergs and to monitor their movement. In the past, detection has been largely by visual or photographic means; more recently, imaging radar has been used. Because of the generally poor visibility in the region, and the potentially large swath coverage of radar, radar is expected to become a prime detection sensor for regional coverage. However, the effectiveness of this technique has still to be evaluated quantitatively (see Section I of this study for a review of previous work).

Two major types of radar are in use: real aperture side- looking airborne radar (SLAR) and synthetic aperture radar (SAR). The latter uses a coherent source and the motion of the platform to obtain, with significant data processing, uniform resolution across a swath.

This experiment, which has been named **BERGSEARCH '84**, was conducted in April 1984 to assess the capabilities of five modern, airborne, imaging radars in the detection of icebergs in open water. Of particular interest were smaller pieces of ice, growlers and bergy bits. The World Meteorological Organization (WMO) iceberg size classification is given in Table III-1. Of the five radars, three were SLARs and two were SARs.

TABLE III-1
WMO Iceberg Size Classification

| Name | Length (m) | Area (m ²) | Height (m) |
|--------------------|------------|------------------------|------------|
| Growler | < 10 | <100 | <1 |
| Bergy bit | 10- 20 | 100-300 | 1-5 |
| Small iceberg | 20- 50 | | |
| Medium iceberg | 50-100 | | |
| Large iceberg | 100-200 | | |
| Very large iceberg | <200 | | |

NOTE: other classifications may vary slightly.

III.1.2 OBJECTIVES

Data were collected to assess:

- target detectability as a function of:
 - . target size
 - . look angle with respect to wind, waves
 - . depression angle
 - . sea state/wind speed; and
- statistics of target fluctuations from pass to pass.

Typically each aircraft flew a box configuration around the target area with the radar looking toward the inside of the box. A ship conducting surface verification measurement was stationed within the target area. Three lines of the box were orthogonal to each other, whereas the fourth was at a 45° oblique angle, with the box oriented in a regular pattern to the prevailing wind. To separate effects of depression angle and resolution cell size, the SLAR's used two altitudes and two flight-line offsets; the SARs used two swath widths and two offsets. To calculate target fluctuations, each aircraft made several identical passes.

III.1.3 EXPERIMENT OPERATIONS

The base of operations was located in Gander, Newfoundland, with the target area over the Grand Bank. Operational logistics and offshore surface verification was coordinated by F.G. Bercha and Associates Ltd. At the end of the experiment, the collected data were passed to a team assembled by CANPOLAR Consultants Ltd., which was responsible for interpretation and evaluation of imagery.

The location of areas imaged varied from day to day, depending on iceberg occurrences. For all flights, surface data collection and target verification were provided by F.G. Bercha personnel on board M.V. Polaris V which was on charter to the Hibernia group. The data shipbased activities are summarized in Table III-2, and the following information was obtained:

Visual air photographs of verified icebergs were obtained using an Zeiss RMK A15/23 camera from a Beech Beechcraft King Air aircraft on charter to Mobil Oil (see Table III-2).

- . data sheets on icebergs
- . hourly ice reports
- . hourly weather and sea state during overflight
- . three hourly MANMAR weather and sea state on 24-hour basis
- . waverider buoy deployment at selected times
- . video coverage of two icebergs and ice edge

TABLE III-2

Information obtained by the M V Polaris V
during BERGSEARCH '84

| Date | Shipbased Activities |
|---------|---|
| April 1 | Four icebergs visited - ship stood back from icebergs during flight |
| April 2 | One iceberg visited - ship stood back from iceberg during flight |
| April 3 | Three icebergs visited - ship stood tipping iceberg |
| April 4 | Two icebergs from 3rd revisited - no overflights |
| April 5 | 38 icebergs visited - by this date, pack had released icebergs |
| April 6 | 19 icebergs visited - emphasis on growlers and bergy-bits |
| April 7 | Stood by bergy-bit during overflight and monitored surrounding icebergs - day of maximum seastate |

Radar Aircraft

Five aircraft equipped with imaging radar participated: a Convair 580 operated by the Canada Centre for Remote Sensing (CCRS), supporting a multichannel SAR; a Lockheed Electra operated by the Atmospheric Environment Service (AES), using a Motorola AN/APS 94E SLAR; a Lockheed HC-130 operated by the International Ice Patrol (IIP), using a modified Motorola AN/APS-135 SLAMMR; a Cessna Conquest operated by Intera Technologies Ltd., using the STAR-1 SAR; and a Grumman G-1 Gulfstream, operated by Marine Aerial Remote Sensing (MARS) Ltd., using a modified Motorola AN/APS-94D SLAR. Details of each radar system are summarized in Table III-3.

Data Collection

Data collection occurred mainly during the period of 2-7 April, 1984 however, the CV-580 also flew missions on March 29 and April 1. The number of passes performed by each aircraft over the target area is given in Table III-4; environmental conditions are summarized in Table III-5.

On April 5 crews flew an operational mission to simulate routine iceberg reconnaissance in support of offshore activity. During this flight, crews chose their own search parameters. At the end of its mission, each crew prepared a chart showing the plotted positions of imaged icebergs and radar targets; this chart was delivered to the Bergsearch '84 operations room whence it was transmitted by fax to Mobil for broadcast to offshore operations.

By the time of its conclusion, the experiment had yielded a total of 288 passes for all target areas. All SLAR data were recorded in negative transparency format; SAR data were recorded on positive real-time plotters and on digital tape.

Surface data consisted of detailed weather and wave logs, (see Table III-5) waverider buoy data, surface photographs, and written descriptions of all icebergs verified from the ship. Black-and-white air photographs of 23 cm format from 500-1000 ft. altitude were taken as weather permitted. Surface data were recorded by position and by time to facilitate cross-referencing of verified icebergs with their location on radar imagery. All data were copied and distributed to members of the CANPOLAR team for analysis, with the exception of CV-580 SAR data which were digitally processed and are described in Section III.8.

This report describes the analysis performed on the data sets by the CANPOLAR Team for each day of data collection. A summary of the analysis is given in Section III.10 and in a

TABLE III-3

Characteristics of Radars Participating in BERGSEARCH '84

| Aircraft Affiliation | AES Electra | IIP HC-130 | INTERA Conquest | CCRS CV-580 | MARS Ltd. G-1 |
|--------------------------|---------------------|------------------------------|------------------------------------|-----------------------------|-----------------------------|
| Name of radar | Motorola AN/APS-94E | Motorola AN/APS-135 (SLAMMR) | STAR-1 SAR | Multi-channel SAR | Motorola AN/APS-94D |
| Operating freq band | X | X | X | X+ (C or L) | X |
| Polarization | HH | VV | HH | HV, HH VH, VV | HH |
| Transmit peak power (kw) | 45 | 200 | N/A | N/A | 65 - 85 |
| Azimuth resolution | 0.5° | 0.5° | 7m | 2.1m | 0.45° |
| Range resolution | 30m | 30m | 6, 12m | 1.5m | 30m |
| Depression angle range | 2° - 45° | 1.5° - 45° | 8° - 35° | 2° - 90° | <1° - 45° |
| Swath widths | 25, 50 100 km | 25, 50 100, 150 km | 25, 50 km | 6, 22 km | 25, 50 100 km |
| Left/right looking | L + R | L + R | L or R | L or R | L + R |
| Number of looks | N/A | N/A | 7 | 1 | N/A |
| Output | Negative film | Negative film | Positive paper; (9"); digital tape | Positive paper digital tape | Negative film (wet process) |

TABLE III-4

ESRF Bergsearch '84 Number of Passes for Each Aircraft
not Including Transits and Radar Reflector Passes

| Date | CV-580 | MARS | STAR-1 | AES | IIP | Total |
|--------------------|--------|------|--------|-----|-----|-------|
| 03/29 | 7 | | | | | 7 |
| 04/01 | 8 | | | | | 8 |
| 04/02 | 9 | 12 | 22 | 16 | 17 | 76 |
| 04/03 | 16 | 17 | 16 | 14 | 25 | 88 |
| 04/04 | | | 7 | | | 7 |
| 04/05 ^a | | 8 | 6 | 6 | 9 | 29 |
| 04/06 | | | 10 | | 3 | 13 |
| 04/07 | | 8 | 20 | 15 | 17 | 60 |
| TOTALS | 40 | 45 | 81 | 51 | 71 | 288 |

^a "operational" flight

TABLE III-5

Environmental Conditions During Bergsearch '84

| Date | Significant Wave(m) ^a | Windspeed (knots) ^b | Cloud Coverage ^b (%) |
|--------|----------------------------------|--------------------------------|---------------------------------|
| Mar 29 | 3.0 - 6.5 | not available | not available |
| Apr 1 | 3.5 - 4.0 | 5 - 25 | 90 |
| Apr 2 | 3.0 - 3.5 | 11 - 19 | 90 |
| Apr 3 | 2.0 - 3.0 | 2 - 4 | 10 |
| Apr 5 | 1.5 - 2.5 | 13 - 25 | 70 |
| Apr 6 | 1.0 - 1.5 | 6 - 15 | 20 |
| Apr 7 | 2.0 - 4.0 | 20 - 30 | 95 |

^a from West Venture waverider buoy

^b from Polaris V

separate Summary Report (see Foreword).

III.1.4 ICEBERG NOMENCLATURE IN BERGSEARCH'84

The nomenclature of iceberg identification is unfortunately non-uniform:

- on radar imagery icebergs are plain-numbered sequentially;
- the King Air photo reconnaissance plane identified icebergs with a "B" prefix (for "iceberg"), followed by a sequential three digit number (e.g., B012); and
- Polaris V identification was a letter in order of observation on a particular day, followed by the date number. If the iceberg was identifiable from a previous day's observation, the next date number was just added on. For example, B-1-2 would be the second iceberg seen on April 1, seen again on April 2.

Furthermore, during data analysis, previously unlabelled or unreferenced icebergs were given arbitrary letter or number labels such as Q, 7, or T/10 to be referenced in the associated text.

III.2 ANALYSIS OF APRIL 2 IMAGERY

This was considered to be a research day for all aircraft, and it was the first formal day of data acquisition during the experiment. On this day the STAR-1, AES, IIP and MARS (and CCRS) aircraft flew a series of flight lines in a regular pattern which viewed the target area from four different aspect angles. Flight lines were flown in somewhat of a box pattern with three of the lines orthogonal to each other while the fourth one was oriented at 45° . The intention was to image the target area in a regular relationship to the prevailing wind and wave patterns so as to determine their effect on detectability. A typical series of flight lines flown by the MARS aircraft are shown in Figure III-1.

The target site for Polaris V on this day was located at $46^{\circ}46.0'N$ and $47^{\circ}01.1'W$. The planned orientations of the aircraft were 340, 070, 205 and 250 degrees to true north. This being the first day of the experiment during which all agencies were involved, some difficulties were encountered in coordinating the locations of the airborne crews with the location of the surface-truthing team. Consequently, the Polaris V was not found at the initial coordinates which the crews were given during the pre-flight briefing. This caused some problems in the positioning of flight lines.

III.2.1 AVAILABLE SURFACE INFORMATION

Two main targets were imaged on April 2, the M.V. Polaris V and a medium-sized dry-dock iceberg named A-1-2 (also called Mobil 321). A-1-2 was estimated to be about 22 m high and ranged between 60 and 90 m in above-water diameter. This iceberg was first found on April 1 and was observed between 1240 and 1335 GMT. It was revisited by the ship on April 2 around 1030 GMT. Later on in the day, at 1730 GMT, the iceberg was photographed by the King Air aircraft. The documented positions for A-1-2 and Polaris V for April 1 and 2 are plotted in Figure III-2.

Figure III-3 shows several polaroid photographs of iceberg A-1-2 taken on April 1 and 2. It consisted of two pinnacles at approximately right angles to each other and the upper surface was smooth. It was observed to be calving numerous growlers during the observation periods. Figure III-4 shows polaroids of two of the growlers created on April 1 which were about $3 \times 2 \text{ m}^2$ in plan and 0.5 m in height. More than 50 growlers were created within the half-hour observation period on April 1, and more than 30 growlers were observed around the iceberg between 1030 and 1600 GMT on April 2. It is likely that such growlers were being created occasionally throughout these days. It is also probable that many of them melted away within a few hours, although this has not been documented.

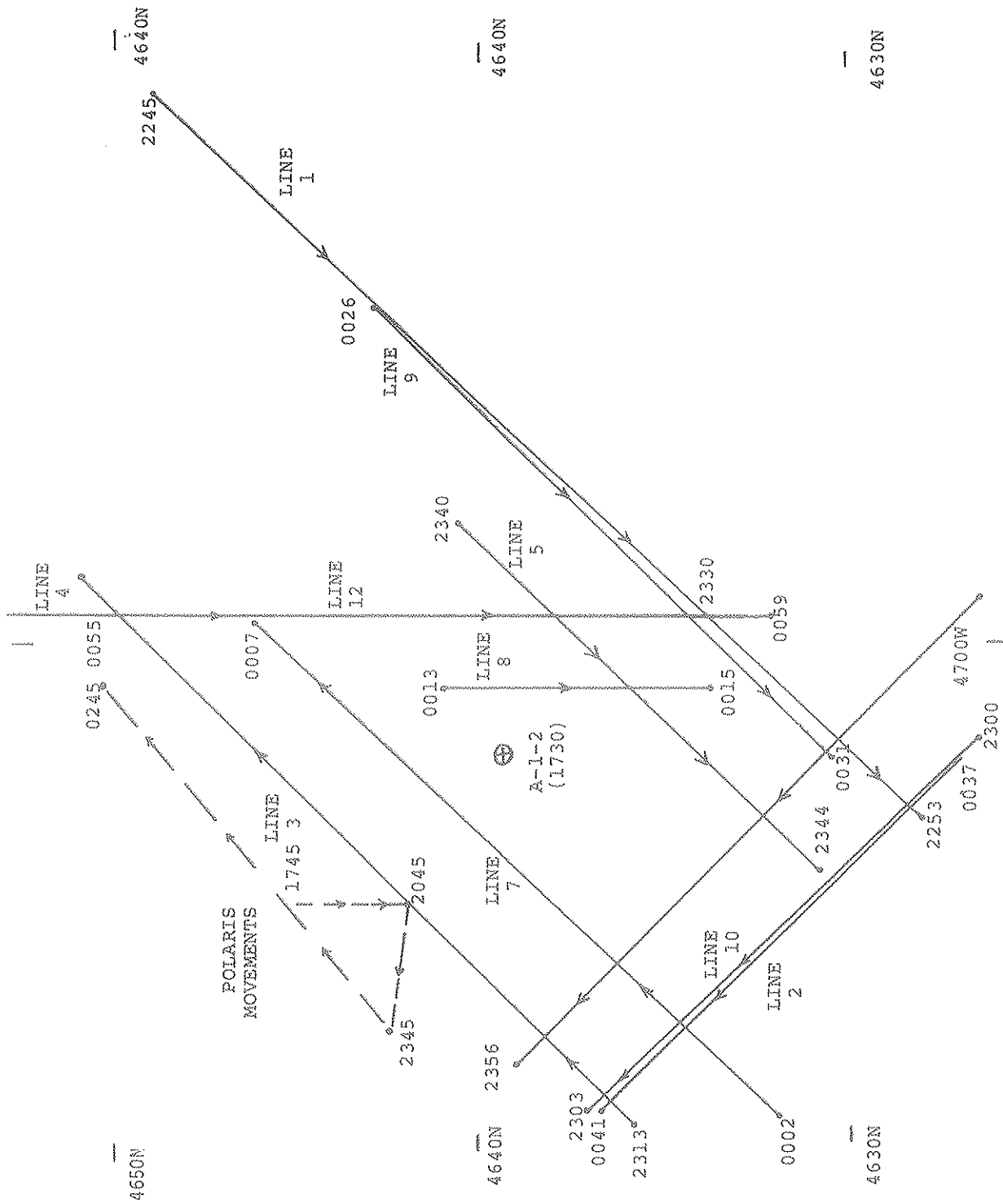
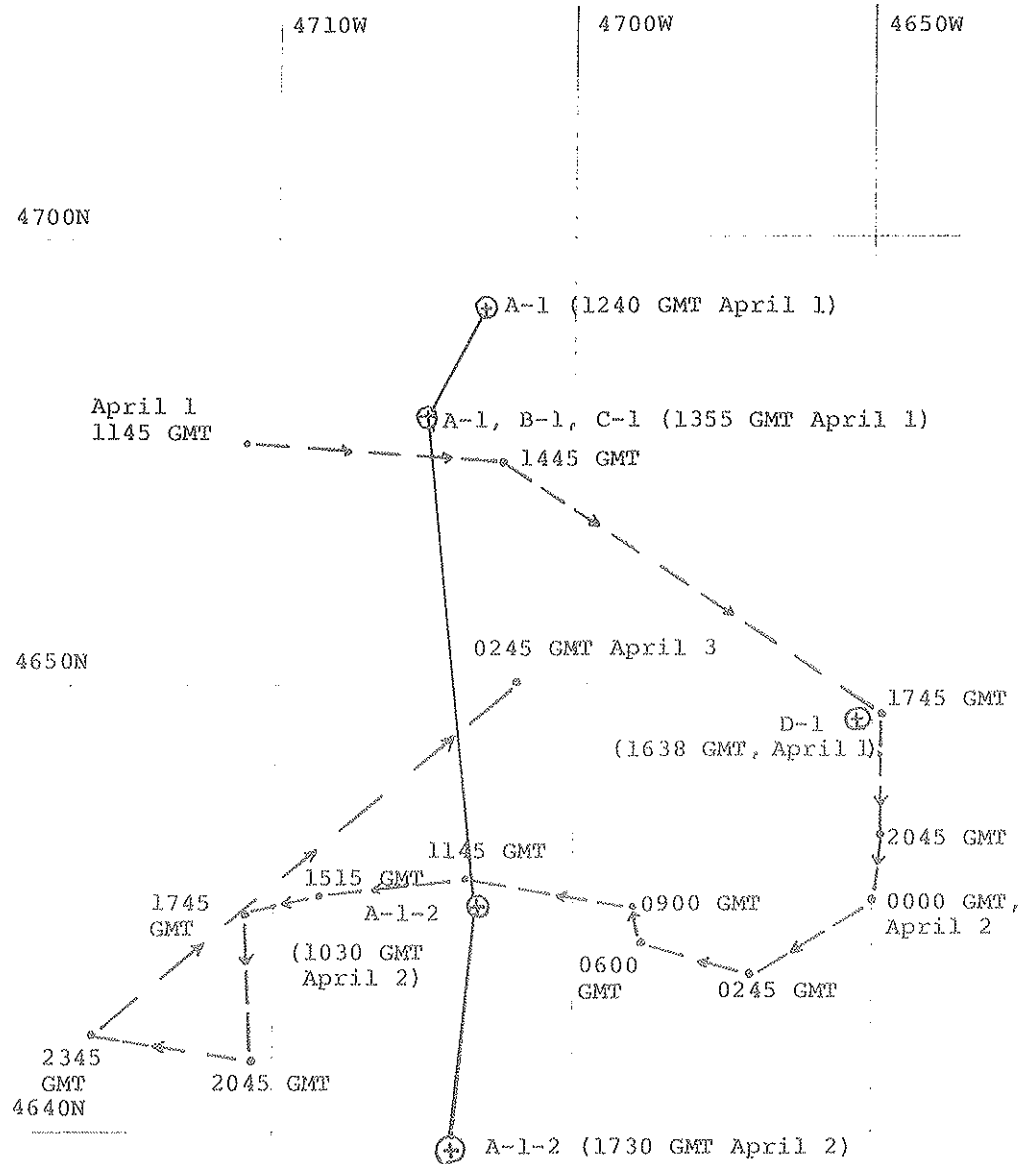


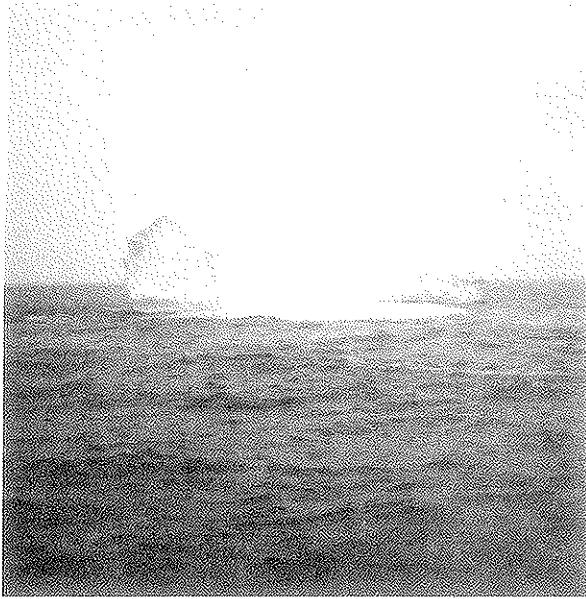
Figure III-1. MARS flight line configuration, 2 April 1984.



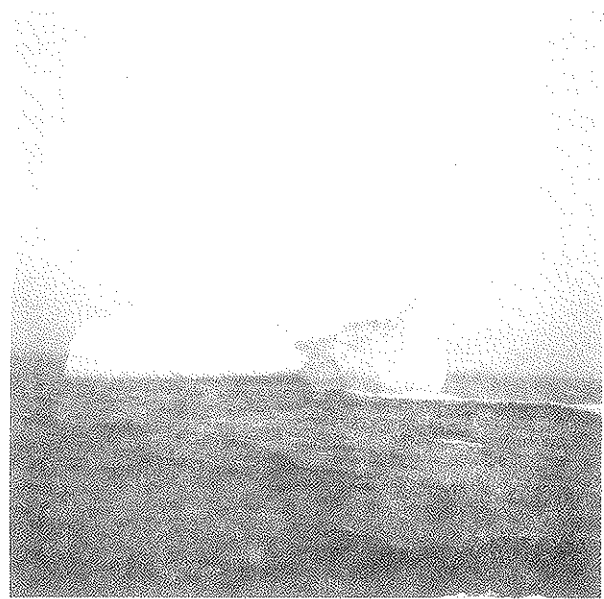
LEGEND

- A-1-2 movements
- Polaris movements

Figure III-2. Polaris V and A-1-2 movements, 1-2 April 1984.



(a)



(b)

(c)

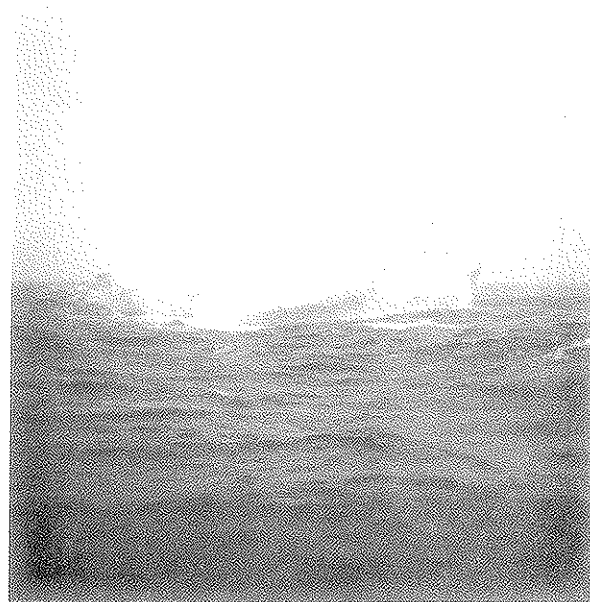


Figure III-3. Iceberg A-1-2 ground verification photos.
a) April 1 1300 GMT Look 1;
b) April 1 1300 GMT Look 3;
c) April 2 1030 GMT Looking SE 300 m from ship.

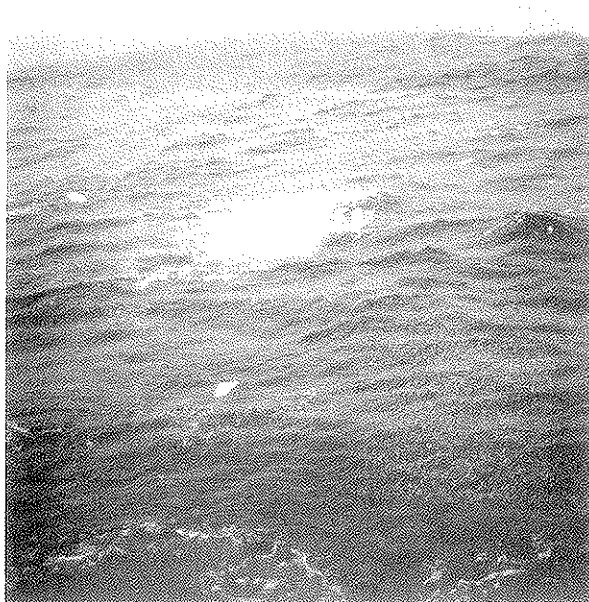


Figure III-4. Growler B-1 near A-1-2, 1 April 1984 1346 GMT.

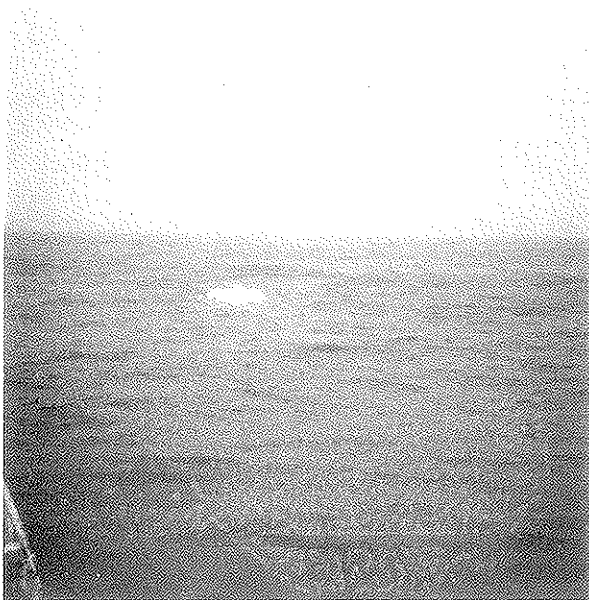


Figure III-5. Growler C-1 near A-1-2, 1 April 1984, 1355 GMT.

The air photographs of iceberg A-1-2 were taken at the time closest to when the area was being imaged by AES, IIP, and STAR-1. Table III-6 summarizes the times of ground verification activity, air photography of the area, and the imaging times for the various aircraft.

Figure III-6 shows one of the air photographs of A-1-2 taken from an altitude of 989 feet (301 m). Growlers are evident around the iceberg as indicated by the arrows. Figure III-7 shows the main iceberg and associated growlers which were identified on the photograph. A total of 24 growlers were found amongst the three images. Table III-7 summarizes the range and bearing of these growlers from the iceberg with respect to true north. It was evident that many of the growlers were being washed over by waves or were bobbing to the point where they would mainly disappear below the water surface. Their disappearance and reappearance was in the order of seconds, because the time between photos was 2-3 seconds and many of the growlers were seen on one or two of the three photographs. The significant wave height at this time was 3.5 m with a peak period of 15.17 seconds. The aerial extent of the photographs around A-1-2 is about a 300 m radius. This translates to a very small area at the normal scales of the radar images: e.g., at 1:250,000 scale (typical for SLAR) this represents only 1.2 mm on the original imagery.

There is limited size information on the growlers for April 2, although the air photographs indicate a typical size range of 3 m or less in the immediate vicinity of iceberg A-1-2. Two growlers (named B-1 and C-1) spawned from A-1-2 measured by the Polaris V team on April 1 were $3 \times 2 \text{ m}^2$ and $2 \times 2 \text{ m}^2$, respectively, and had freeboards of about 0.5 m.

Unfortunately the surface data were collected several hours before any aircraft imaged the area. If the positions of the ship and the air photography are accurate, there was considerable net drift of the iceberg between 1030 and 1730 GMT. This discrepancy is the main limitation to the surface verified data because it is not known exactly how many growlers were created and distributed around the imaged iceberg during the time data were being acquired by the four aircraft.

Wind, wave, and temperature information collected by Polaris V on April 2 are summarized in Table III-8. On this day the winds were extremely variable in direction (from 014° through 360°) on an hourly basis through the time of data acquisition. Wave direction was much less variable and the sea state was moderate.

TABLE III-6

Data Acquisition Times for Iceberg Ground Data
and Radar Imagery

| Date | Type | Time (GMT) | Targets |
|-------|--|------------|---|
| Apr 1 | <u>Polaris V - Ground Verification Team</u> | 1240-1636 | A-1-2, D-1 icebergs; B-1, C-1 growlers |
| Apr 2 | <u>Polaris V - Ground Verification Team</u> | 1030-1100 | A-1-2 |
| | King Air-Zeiss RMK A 15/23 Air Photography | 1723-1728 | <u>Polaris V</u> + A-1-2 |
| | AES SLAR | 1548-1848 | <u>Polaris V</u> + A-1-2 |
| | IIP SLAR | 1627-1846 | <u>Polaris V</u> + A-1-2 |
| | STAR-1 SAR - Flight 1 | 1614-1720 | <u>Polaris V</u> + A-1-2 |
| | - Flight 1 | 2038-2359 | <u>Polaris V</u> + A-1-2 |
| | MARS SLAR | 2245-0059 | <u>Polaris V</u> + A-1-2 |

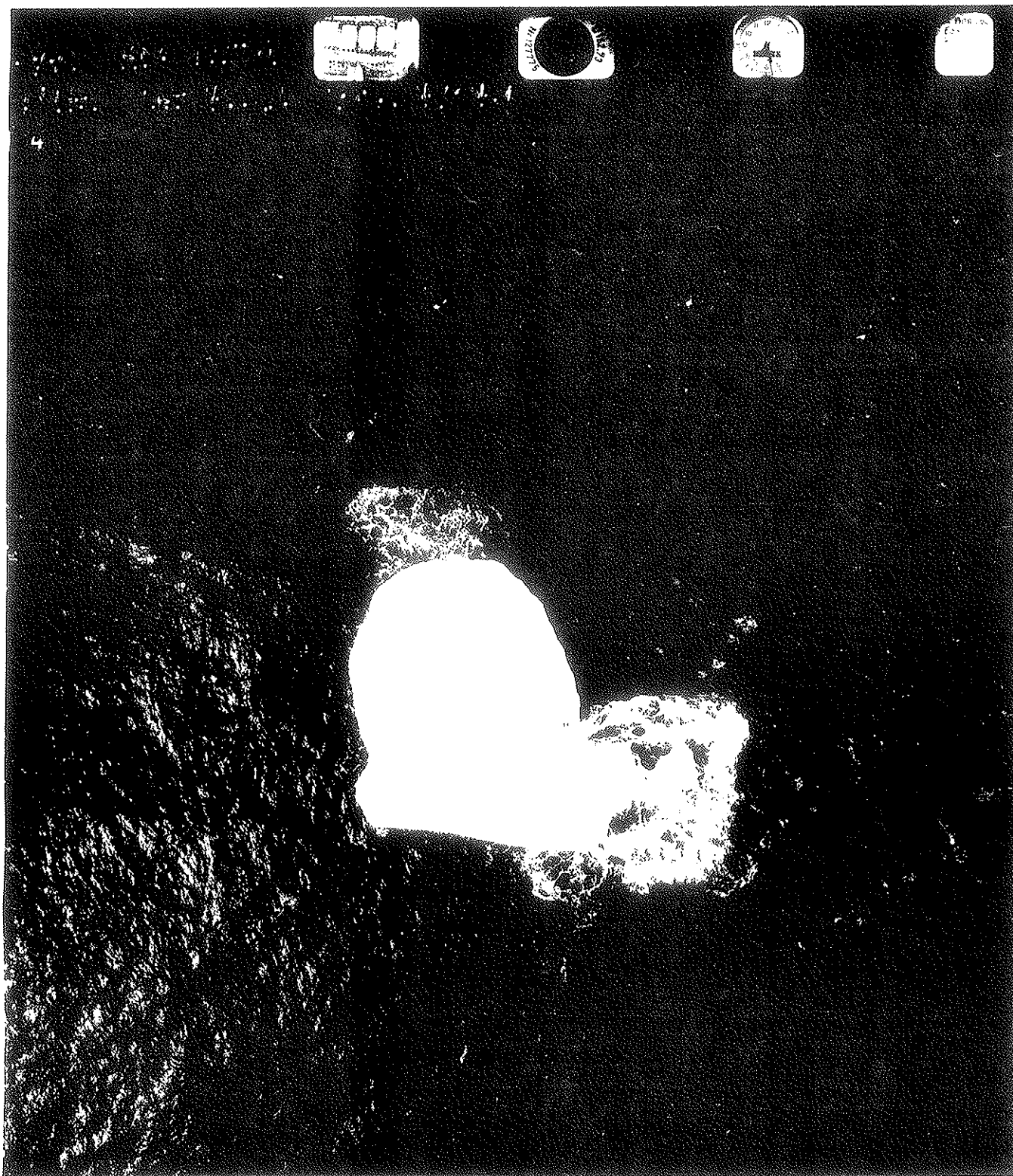


Figure III-6. King Air photograph of A-1-2, 1728 GMT, 2 April 1984.

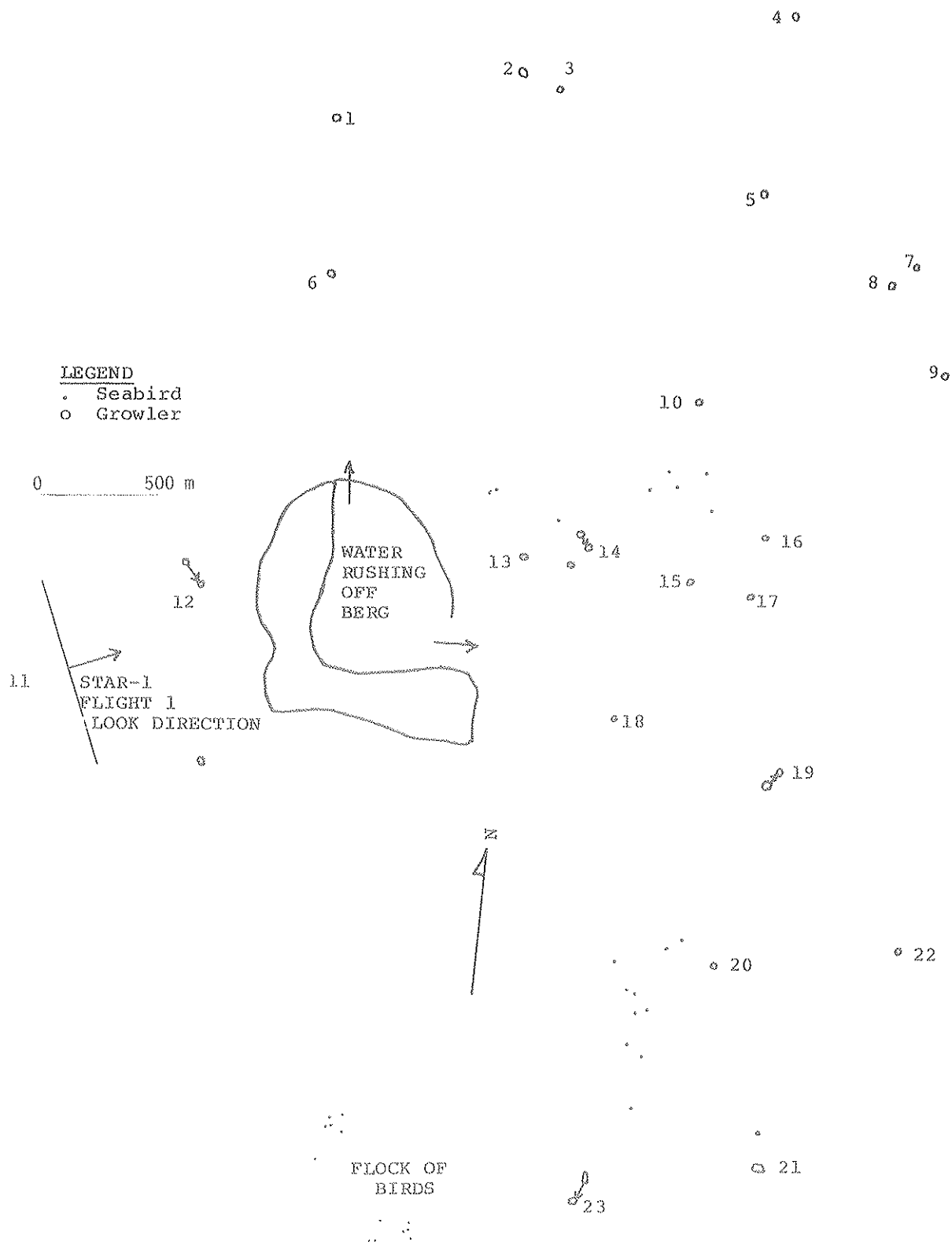


Figure III-7. Grouper distribution around A-1-2, 1728 GMT,
 2 April 1984.

TABLE III-7

Growler Range and Bearing from A-1-2
1728 GMT, 2 April 1984

| Growler No. | Range (m) | Bearing (°T) |
|-------------|-----------|--------------|
| 1 | 169 | 353 |
| 2 | 181 | 016 |
| 3 | 181 | 020 |
| 4 | 258 | 035 |
| 5 | 193 | 042 |
| 6 | 85 | 007 |
| 7 | 229 | 055 |
| 8 | 195 | 055 |
| 9 | 219 | 065 |
| 10 | 122 | 065 |
| 11 | 132 | 265 |
| 12 | 20 | 268 |
| 13 | 32 | 065 |
| 14 | 57 | 068 |
| 15 | 97 | 080 |
| 16 | 130 | 074 |
| 17 | 130 | 082 |
| 18 | 55 | 092 |
| 19 | 122 | 096 |
| 20 | 75 | 118 |
| 21 | 136 | 122 |
| 22 | 193 | 111 |
| 23 | 193 | 167 |
| 24 | 35 | 227 |

TABLE III-8

Polaris V Environmental Data, 2 April 1984

| Time GMT | Primary Waves | | | Secondary Waves | | | Wind | | Temp. | | Cloud Height (m) | Vis (naut mi.) | Ice Cond. |
|-------------|---|------------------|-----------------|-----------------|------------------|-----------------|----------------|-------------------------|-------------|-------------|------------------------|----------------------|--------------------|
| | Height (m) | Dir ^N | Period (sec) | Height (m) | Dir ^N | Period (sec) | Speed (kts) | Dir ^N (°) | Air (°C) | Sea (°C) | | | |
| 1200 | | | | | | | 19 | 180 | -0.1 | 0.5 | obscured | < ½ | 0/w |
| 1300 | 0.4 | NE | 3 | 2.0 | NNE | 9 | 16 | 360 | -0.5 | 1.0 | 100 | > 2 | 0/w |
| 1400 | 0.2 | NW | 2 | 1.2 | NNW | 8 | 18 | 310 | -0.1 | 1.0 | 150 | > 2 | 0/w |
| 1500 | 0.1 | W | 1 | 1.0 | NW | 6 | 19 | 164 | -0.1 | 0.7 | 150 | > 2 | 0/w |
| 1600 | 0.1 | WNW | 1 | 0.8 | NNW | 6 | 16 | 014 | -1.0 | -0.7 | 200 | > 2 | 0/w |
| 1700 | 0.1 | WNW | 1 | 0.6 | NNW | 6 | 13 | 159 | -0.8 | -0.5 | 500 | >10 | 0/w King Air |
| 1800 | <0.1 | NW | 1 | 0.6 | NW | 5 | 11 | 264 | -1.2 | -0.5 | 200 | 100 | 5 0/w |
| 1800a | Weather changing rapidly - wind increasing, snow and squalls in vicinity. | | | | | | | | | | | | |
| 1900 | 0.1 | NNW | 2 | 0.5 | NNW | 7 | 17 | 090 | -1.0 | +0.5 | 200 | 100 | > 8 0/w |
| 2000 | 0.1 | N | 1 | 1.0 | N | 7 | 17 | 100 | -1.5 | +0.5 | 200 | 90 | > 8 0/w |

III.2.2 STAR-1 SAR

Two sets of flights were conducted on April 2. The first flight consisted of a series of repeatability passes flown so that imaging of the target area was cross-wind and cross-wave. The second set of passes was flown in a C-shaped box pattern around Polaris V and A-1-2. Tables III-9 and III-10 summarize the flight line particulars and general comments on the imagery.

Large Target Detection

Polaris V and A-1-2 were detected and imaged from every aspect when the swath width covered the area in which the targets were located. However, their signatures differed considerably even between the repeatability lines for flight 1. The pinnacles on iceberg A-1-2 were not seen on any of the lines because of smearing of the signature in azimuth. For flight 1 lines the pinnacles of the iceberg were oriented away from the radar as shown on Figure III-7. A typical signature for both targets is seen in Figure III-8 from flight 1, line 6, which shows the iceberg to have a bell shape away from the radar look-direction whereas Polaris V is an extended cigar shape. The iceberg has white streaks extending in azimuth from the main body of the signature which probably are created from iceberg motions and the multiple number of looks used in the processing.

The shape of each target was found to vary widely between lines and also between the two targets. Table III-11 summarizes the shape information compared to the look direction. Two conclusions can be drawn from the table.

1. Considerable differences exist in signature shape between repeatability lines, for which all radar parameters had been kept constant.
2. Signature differences of Polaris V and A-1-2 permit neither to be distinguished from the other on the basis of the imagery alone. This would apply also to reidentification of the same targets.

The large target signatures also saturated the film (as a result of processing) and their edges were blurred, probably the result of wave action and bobbing.

Small Target Detection

Smaller targets were found on all the STAR-1 lines which were imaged looking cross-wave. Most of these targets were found in the vicinity of A-1-2 and were presumed to be growlers. On line 6 a total of 19 targets were classified as probable growlers and an additional four were suspected around A-1-2. Their identification was based on their

TABLE III-9

STAR-I Flight Line Particulars of Flight 1, 2 April 1984

| Line No. | Altitude (ft) | Heading (°) | Swath Width (km) | Start (GMT) | Finish (GMT) | Elongation/Shortening of Imagery | General Comments |
|----------|---------------|-------------|------------------|-------------|--------------|----------------------------------|--|
| 3 | 29,000 | 160 | 23 | 1614 | 1617 | N/A | 23 km offset so targets missed |
| 4 | 29,000 | 340 | 23 | 1623 | 1627 | N/A | A-1-2 not imaged in bad section of swath |
| 5 | 29,000 | 160 | 23 | 1634 | 1637 | N/A | Alternating lighter and darker band on imagery |
| 6 | 29,000 | 340 | 23 | 1646 | 1649 | N/A | |
| 7 | 29,000 | 160 | 23 | 1656 | 1659 | N/A | Line too far east, offset would put imagery out of target area |
| 8 | 29,000 | 340 | 23 | 1708 | 1711 | N/A | Lighter and darker bands alternating in azimuth |
| 9 | 29,000 | 160 | 23 | 1717 | 1720 | N/A | Antenna pattern on imagery in first half of swath |

TABLE III-10

STAR-1 Flight Line Particulars of Flight 2, 2 April 1984

| Line No. | Altitude (ft) | Heading (°) | Swath Width (km) | Start (GMT) | Finish (GMT) | Elongation/Shortening of Imagery | General Comments |
|----------|---------------|-------------|------------------|-------------|--------------|----------------------------------|--|
| 1 | 29,000 | 068 | 23 | 2038 | 2041 | N/A | Line too far to the east to image ground verification targets. High altitude, high resolution. |
| 2 | 29,000 | 250 | 23 | 2049 | 2054 | N/A | Waves parallel to flight track clearly evident. High altitude, high resolution. |
| 3 | 29,000 | 340 | 23 | 2101 | 2106 | N/A | Missed ground verified targets but did image growlers around A-1-2. High altitude, high resolution. |
| 4 | 29,000 | 070 | 23 | 2111 | 2114 | N/A | Antenna patterns on imagery in near range. High altitude, high resolution. |
| 5 | 29,000 | 250 | 46 | 2123 | 2128 | N/A | Waves very distinctive, nearly parallel to flight track. High altitude, wide swath. |
| 6 | 29,000 | 160 | 46 | 2134 | 2139 | N/A | Offset line 5 km. to south of line 3. Considerable streaking in azimuth. Line should be further west of plotted line. High altitude, wide swath. |
| 7 | 29,000 | 070 | 46 | 2143 | 2148 | N/A | |
| 8 | 19,000 | 250 | 46 | 2200 | 2207 | N/A | Waves parallel to flight track distinctive. Low altitude, wide swath. |
| 9 | 19,000 | 340 | 46 | 2213 | 2225 | N/A | No wave pattern. Low altitude, wide swath. |
| 10 | 19,000 | 070 | 46 | 2226 | 2232 | N/A | Waves at 45° to track. |

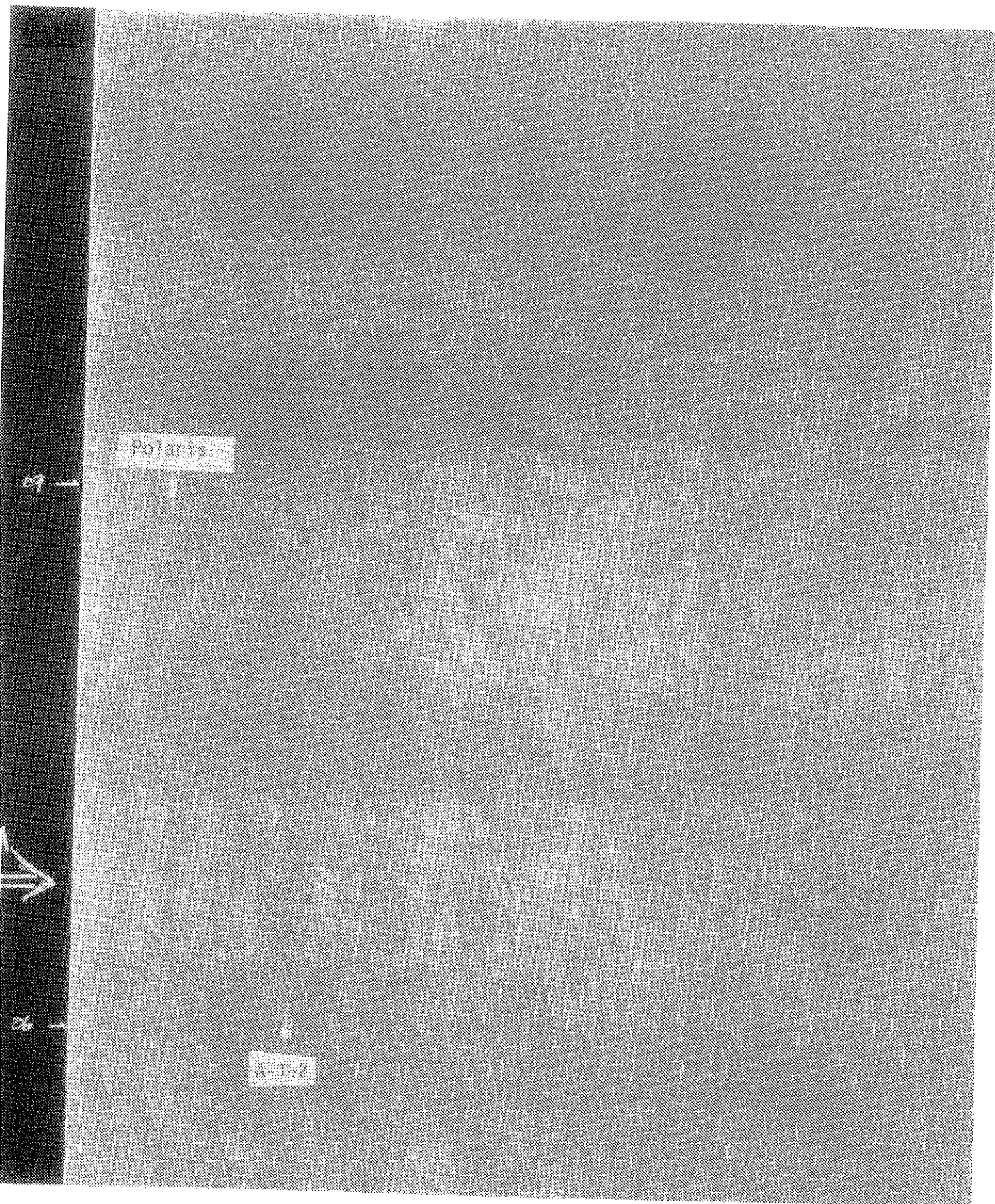


Figure III-8. STAR-1 SAR flight 1, pass 6, 2 April 1984.

TABLE III-11

Signature Shape vs Pass on STAR-1 Imagery, 2 April 1984

| Flight and Line Number | Look Direction | <u>POLARIS V</u> | A-1-2 |
|---|-------------------|--|---|
| 1-4 | 070R | Long and narrow | NI |
| 1-5 | 070L | Narrow cigarshape | Bellshape away from A/C |
| 1-6 | 070R | Cigarshape | Bellshape towards A/C |
| 1-7 | 070L | Circular with azimuth streaks | Long, cigarshape |
| 1-8 | 070R | Circular with star- shaped signature | Circular target with white streaks in azimuth |
| 1-9 | 070L | Circular with azimuth streaks | Similar to <u>Polaris V</u> except more bloomed and azimuth streaks are longer |
| 2-2 | 340R | NI | Flattened in azimuth direction |
| 2-3 | 070R | NI | NI ^a |
| 2-4 | 160R | Bellshape towards A/C | NI |
| All above lines high altitude, narrow swath. | | | |
| 2-5 | 340R | Flattened ellipse | NI |
| 2-6 | 070R | Flattened ellipse, diffuse edges | Bellshape away from A/C |
| 2-5 and 2-6 are high altitude, wide swath. | | | |
| 2-8 | 340R | NI | Fusiform shape, diffuse edges |
| 2-9 | 070R | Cigarshape, stretched in azimuth with spikes | Somewhat bellshape away from A/C |
| 2-10 | 160R | Star-shaped signature | NI |
| Lines 2-8 to 2-10 are low altitude, wide swath. | | | |

^aNI = Not imaged because not within image swath or line was ended before target was imaged.

relative brightness to the ocean background and a white streak signature in the azimuth direction.

When the area around the iceberg was imaged upwave or downwave these smaller targets were no longer visible. In these cases the wave patterns became visible, giving sea clutter with comparable returns to the growlers. Any azimuthal streaks appeared to be part of the wave pattern. In cross-wave images the wave pattern was not evident and the general background was more subdued, which allowed the smaller growler targets to be identified with more confidence.

The limited data provide some indication of the effect of resolution on the detectability of the smaller targets. Line 3 which was flown at high altitude, high resolution ($6 \times 6 \text{ m}^2$), detected 19 targets around A-1-2 which were identified with a high degree of confidence, plus an additional 4 targets elsewhere in the imagery, and 4 more suspected targets. Six targets plus two more suspected ones around A-1-2 were found on line 9, flown at $6 \times 12 \text{ m}^2$ radar resolution. Although the size and exact number of targets is not known, the increased resolution apparently resulted in a threefold increase in targets, from 6 to 19, in the closest comparison in time which could be identified with confidence.

Repeatability Lines

The repeatability lines from flight 1 were analysed for small target identification in the common imaged area around Polaris V and A-1-2. The results are summarized in Table III-12. The variability between flight lines probably results from the wave action and bobbing of the growlers which makes them "disappear" at the time of imaging.

The targets in the vicinity of A-1-2 were compared between flight lines in an effort to determine how many could be seen on most, if not all, of the lines. Figure III-9 shows the distribution of targets and number of passes that were seen out of the total of five.

A total of 36 different targets were identified in the vicinity of A-1-2 with a frequency as follows:

- . identified on all 5 passes - 4
- . identified on all 4 passes - 4
- . identified on all 3 passes - 3
- . identified on all 2 passes - 4
- . identified on 1 pass - 21.

Most of the targets identified on more than one line were identified by their position relative to A-1-2 rather than by their signature on the imagery. There was greater confidence in the interpretation when the target was seen more than once.

TABLE III-12

Flight 1 Repeatability Small Target Analysis
STAR-1, 2 April 1984

| Line | Highly Probable Targets | Suspected Targets | Total Targets |
|------|----------------------------|----------------------|------------------|
| 5 | 16 | 10 | 26 |
| 6 | 21 | 7 | 28 |
| 7 | 15 | 4 | 19 |
| 8 | 14 | 12 | 26 |
| 9 | 18 | 12 | 30 |

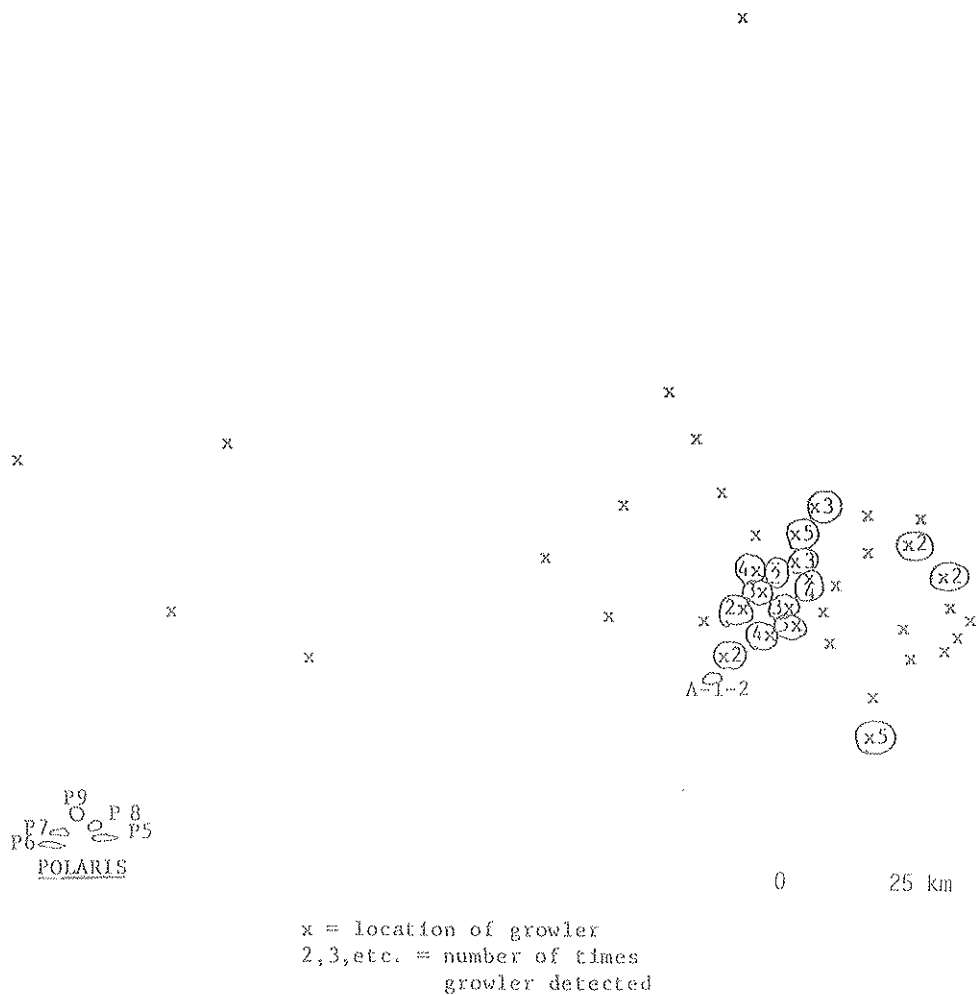


Figure III-9. Growler comparison, STAR-1 imagery, flight 1 lines 5-9, 2 April 1984.

The fact that repeating lines seem to reveal more new small targets than reconfirm old ones suggests that detection of the entire growler population is unlikely no matter how many lines are flown, in part a result of:

- . the bobbing, wave action, and movement of growlers causing them to disappear occasionally,
- . the calving and oblatting of growlers between lines,
- . the incorrect discrimination of growlers from sea clutter.

Other Findings

The imagery from flight 2 line 6 contains a bright white target near Polaris V which is of an unknown origin. The target has a diffuse signature and is located about 500 m to the NE of the ship. Discussions with the Polaris V personnel indicated there was no iceberg target or ship at that distance during the time of acquisition, nor was the waverider buoy deployed that far away. None of the other project aircraft were in the area at the time (2135 GMT) so no other imagery was available to identify this target, neither were there any ground data.

Imagery from flight 2 line 8 showed a linear ocean pattern within the swath. The two subsequent passes did not image the area in which the feature was located. This pattern was seen on many of the MARS flight lines (see Figure III-14). The linear pattern is thought to be an oceanographic feature, perhaps caused by temperature variations or upwelling.

III.2.3 AES SLAR

The flight line particulars for the AES SLAR are summarized in Table III-13. The aircraft flew at two different altitudes and generally used the 25 km swath width setting. Parts of several lines were flown at 50 km to image Polaris V and the A-1-2 iceberg. Line 9 was not analysed because the aircraft was climbing to the higher altitude, and lines 14 to 16 also were not analysed because of altimeter drift noted in the logs.

Two general observations can be made with regards to the imagery:

1. Stretching, shortening, and elongation of the imagery;
2. Discrepancy in target positions between lines and between the imagery and positions noted by the ship and the King Air aircraft.

TABLE III-13

AES SLAR Flight Line Particulars, 2 April 1984

| Line No. | Altitude (ft) | Heading (°) | Swath Width (km) | Start (GMT) | Finish (GMT) | Elongation/Shortening of Imagery | General Comments |
|----------|----------------|-------------|------------------|-------------|--------------|----------------------------------|---|
| 1 | 5,000 | 119-166 | 25 | 1548 | 1554 | E - 2 km | A/C appeared to be rotating along track a total of 45° to original heading. |
| 2 | 5,000 | 260 | 25 | 1557 | 1603 | E - 4 km | Suspect line is north of its plotted position. Magnitude unknown. |
| 3 | 5,000 | 338 | 25 | 1606 | 1612 | S - 1.8 km | Line relocated 3.5 km east because of INS drift. |
| 4 | 5,000 | 114 | 25 | 1618 | 1624 | E - 1 km | Line relocated south 3.4 km and oriented more SW than S. |
| 5 | 5,000 | 164 | 25/50 | 1632 | 1638 | NONE | Flown east of INS location. |
| 6 | 5,000 | 256 | 25 | 1642 | 1649 | E - 3 km | Line started 7 km before location indicated by INS. |
| 7 | 5,000 | 338 | 25 | 1653 | 1702 | E - 2.5 km | Flown 5 km east of INS location. |
| 8 | 5,000 | 115 | 25/50 | 1705 | 1713 | S - unknown | 50-km swath 1705-1709. Serious shortening of image along track. A/C turned during data acquisition. |
| 9 | 5,000 - 10,000 | 167 | 25 | 1722 | 1735 | - | A/C climbing, changing scale and depression angle relationships. |
| 10 | 10,000 | 256 | 25 | 1740 | 1744 | | <u>Polaris V</u> not imaged as A/C turned. |
| 11 | 10,000 | 336 | 25 | 1748 | 1754 | | |
| 12 | 10,000 | 110 | 25 | 1758 | 1805 | E - 3 km | A-1-2 outside of swath. |
| 13 | 10,000 | 161 | 25 | 1814 | 1820 | | |
| 14 | 10,000 | 333 | 25 | 1825 | 1831 | | Altimeter drift. Not reliable location. |
| 15 | 10,000 | 163 | 25 | 1836 | 1839 | | As for line 14. |
| 16 | 10,000 | 327 | 25 | 1842 | 1851 | | As for line 14. |

The shortening or elongation results in part, from INS drift, but it is suspected that the image processor may not have been advancing the film at a uniform rate. The discrepancy in target positions is illustrated in Figure III-10. The position of A-1-2 as determined by its location on the imagery between passes 6 and 8 differs by about 20 km even though the passes were flown only 15 minutes apart. Most of the other passes showed A-1-2 to be located between these two extremes. The discrepancy between target positions and flight line locations was not significant for the purposes of the April 2 analysis because there were only two large targets to be tracked and their relative positions did not change much between lines.

The appearance of clutter on the imagery was more subdued for the higher altitude lines (5,000 ft vs. 10,000 ft). This change did not seem to affect detection of larger targets because they were readily apparent on the imagery and both contrasted well to the background at both altitudes. Results for the targets versus look direction are summarized in Table III-14.

Large Target Detection

Both Polaris V and A-1-2 were evident on the imagery to the unaided eye whenever the swath covered the area in which these targets were located. On certain passes one or both targets were not detected because they were located in the blind zone underneath the aircraft, or the aircraft turned before the target was imaged.

Table III-15 summarizes the signature shape and tone by line number compared to look direction and wind direction. In general these targets were small to medium in size on the image and tones ranged from light grey to white. Both were fainter and stretched more in azimuth at the farther ranges. Both of these factors are related to the decreasing azimuthal resolution with range.

The pinnacles for iceberg A-1-2 were evident on the imagery for lines 3 and 7, which were flown at the same altitude and aspect angle (68°N look direction). The target was located in the near third of the range. The pinnacles could be seen with aid of an eyepiece as right-angle spurs, indicated by an indentation and shadow within the centre of the signature of A-1-2. No shape information for A-1-2 was evident for flight lines at the same aspect but at the higher altitude.

It was not possible to differentiate Polaris V from A-1-2 on the basis of the imagery alone, except for those lines in which the shape of the iceberg could be seen.

4640W

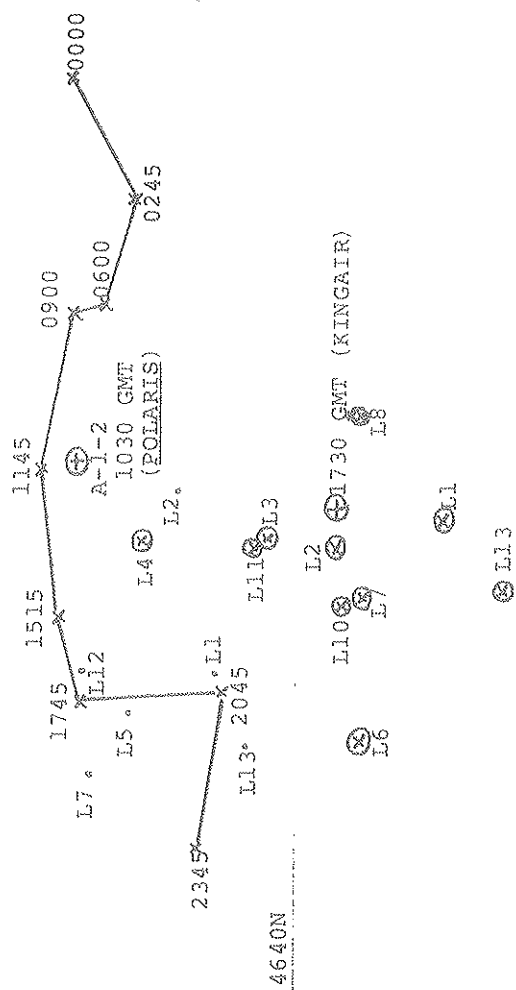
4650W

4700W

4710W

4650N

L4



0 5 km

Note: L denotes
Line Number

Figure III-10. Polaris V and A-1-2 positions based on AES SLAR, 2 April 1984.

TABLE 111-14

AES SLAR, 2 April 1984

| Look Direction | Target ID | Other ID | Line No. | Presence ^a | Size ^b | Tone ^c | Comments |
|----------------------|-----------|-----------|----------|-----------------------|-------------------|-------------------|------------------------|
| Upwind | - | Polaris V | 2 | X | - | - | |
| | 03 | A-1-2 | 2 | P | ME | W | |
| | - | Waves | 2 | P | - | G | Faint, discontinuous |
| | - | Polaris V | 6 | X | - | - | |
| | 21 | A-1-2 | 6 | P | SE | W/LG | |
| | - | Waves | 6 | Partial | - | G | Faint in farther range |
| | - | Polaris V | 11 | X | - | - | |
| | 45 | A-1-2 | 11 | P | S | W | |
| Downwind | - | Waves | 11 | A | - | - | |
| | 08 | Polaris V | 4 | P | SE | LG | |
| | 10 | A-1-2 | 4 | P | SE | LG | Fainter than Polaris V |
| Crosswind (90°) | - | Waves | 4 | P | - | DG | |
| | 25 | Polaris V | 7 | P | S | W | |
| | 24 | A-1-2 | 7 | P | S | W | Shape seen |
| | - | Waves | 7 | Partial | - | DG | |
| | - | Polaris V | 10 | X | - | - | |
| | 43 | A-1-2 | 10 | P | SE | W | |
| Crosswind (45°) | - | Waves | 10 | Partial | - | DG | |
| | - | Polaris V | 3 | X | - | - | |
| | 05 | A-1-2 | 3 | P | S | W | Shape seen |
| | - | Waves | 3 | Partial | - | DG | |
| | 27 | Polaris V | 8 | P | S | LG | Imaged at 50-km swath |
| | 29 | A-1-2 | 8 | P | S | W | |
| | - | Waves | 8 | A | - | - | |
| | 55 | Polaris V | 12 | P | S | W | |
| | - | A-1-2 | 12 | X | - | - | |
| | - | Waves | 12 | A | - | - | |
| Crosswind (variable) | 01 | Polaris V | 1 | P | SE | LG | |
| | 02 | A-1-2 | 1 | P | SE | LG | |
| | - | Waves | 1 | A | - | - | |
| | 11 | Polaris V | 5 | P | S | LG | Imaged at 50-km swath |
| | - | A-1-2 | 5 | X | - | - | |
| | - | Waves | 5 | P | - | L-DG | |
| | 58 | Polaris V | 13 | P | S | W | |
| | 60 | A-1-2 | 13 | P | S | W | |
| | - | Waves | 13 | A | - | - | |

^a P - Present
A - Absent
X - Not in swath

^b M - Medium
S - Small
E - Elliptical

^c W - White
G - Grey
LG - Light grey
DG - Dark grey

TABLE III-15

Large Target Signature vs Flight Line
AES, SLAR, 2 April 1984

| Line Number | Look Direction | Polaris V | A-1-2 |
|-------------|---|--|---|
| 1 | Variable, 209-256R (Crosswind, variable) | Cigar-shaped dash Light grey At far range | Cigarshape dash Light grey |
| 2 | 350R (Upwind) | NI | Cigarshape with some indication of pinnacles Light grey |
| 3 | 68R (Crosswind, 45°) | NI | Rounded with small protrusions resembling pinnacles White, somewhat blurred |
| 4 | 204R (Downwind) | Strong white tone elongated in azimuth | Light grey, fainter than Polaris V, elliptical shape, at far range. |
| 5 | 254R (Crosswind, variable) | Imaged at 50-km swath Very faint, circular shape, light grey | NI |
| 6 | 346R (Upwind) | NI | Disc elongated in azimuth, off white tone. |
| 7 | 68R (Crosswind, 90°) | Circular shape Not very bright and has white tone. | Spurs from pinnacles evident, white tone |
| 8 | 205R (Crosswind, 45°) | Thin dash-like appearance Weak return imaged at 50-km scale | Larger, stronger return than Polaris V. No evidence of spurs, elliptical shape, white tone |
| 9 | - | - | - |
| 10 | 346R (Crosswind, 90°) | NI | Flattened ellipse Strong white return |
| 11 | 66R (Upwind) | NI | Circular, strong white return |
| 12 | 200R (Crosswind, 45°) | Elongated in azimuth Strong, white return | NI |
| 13 | 251R (Crosswind, variable) | Flattened ellipse, strong white return | Stronger return than Polaris Larger than ship in range, same length in azimuth and same in shape |
| 14-16 | All these lines had altimeter drifting. | | |

NOTE: Lines 1-8 flown at 5,000 ft; lines 10-16 flown at 10,000 ft.
NI = not imaged

Figure III-11 shows the two targets as imaged on line 7. Target 24 was identified as A-1-2 and shows two spurs in the signature which probably are the right-angled pinnacles. Target 25 is Polaris V which has a circular shape. Based on the positions of these targets and the time the data was acquired compared to the ground truth positions, it would appear that line 7 was flown about 5 km east of its position as determined by the INS. Targets 22 and 23 were identified as an iceberg and ship respectively, but were not targets used for this analysis. Target 26 is unknown as there was no positive visual identification.

Small Target Detection

Assessing the SLAR for small targets on this day proved difficult because of the sparse surface information on the growlers around A-1-2 at the time the imagery was acquired. A comparison between the growlers from the air photography and the imagery showed that none of the targets could be seen on the latter. This is not surprising given the resolution of the SLAR, the small size (3 m and less) of these growlers, and their bobbing motion at the scale of the image. A 5x enlargement of the imagery around the iceberg failed to show any of the targets.

Later lines on the SLAR did reveal two targets which consistently appeared on the imagery and which were not identified from the Polaris V. Figure III-12 shows the position of these two targets, found on lines 10 to 12, and mapped in their locations based on the INS coordinates. These targets appeared after 1740 GMT. It is suspected that they are growlers which may have calved off A-1-2 around that time. They were not seen on earlier lines although the imagery should have covered these areas. A conflicting piece of evidence is that these targets were located from the suspected source iceberg.

These targets were not detected on IIP pass 10 which flew by the area around 1752 GMT. No other aircraft were imaging in the area at the time.

III.2.4 IIP SLAR

IIP flew the target area at nearly the same time as the AES SLAR. Details of the flight lines are contained in Table III-16. Lines were flown at two altitudes (4,000 ft and 8,000 ft) in a mostly triangular pattern around the target area.

There was no perceptible elongation or shortening of the imagery, which seemed to match the expected length based on INS coordinates and the scale. Perhaps the most beneficial feature of the imagery was the imprinted latitude/longitude grid which greatly speeded up the analysis. There was also

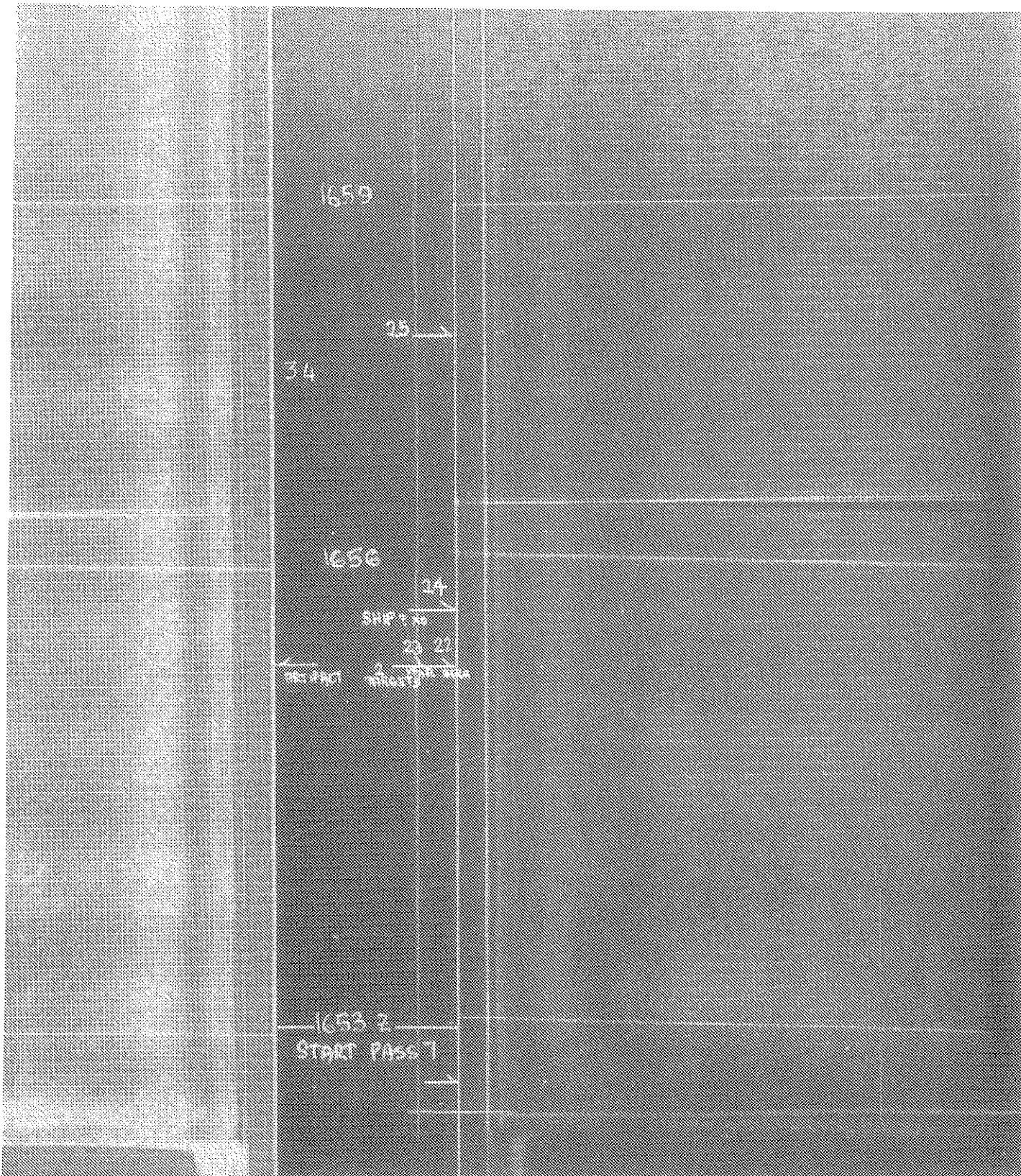


Figure III-11. AES SLAR, pass 7, 2 April 1984 (scale 1:250,000).

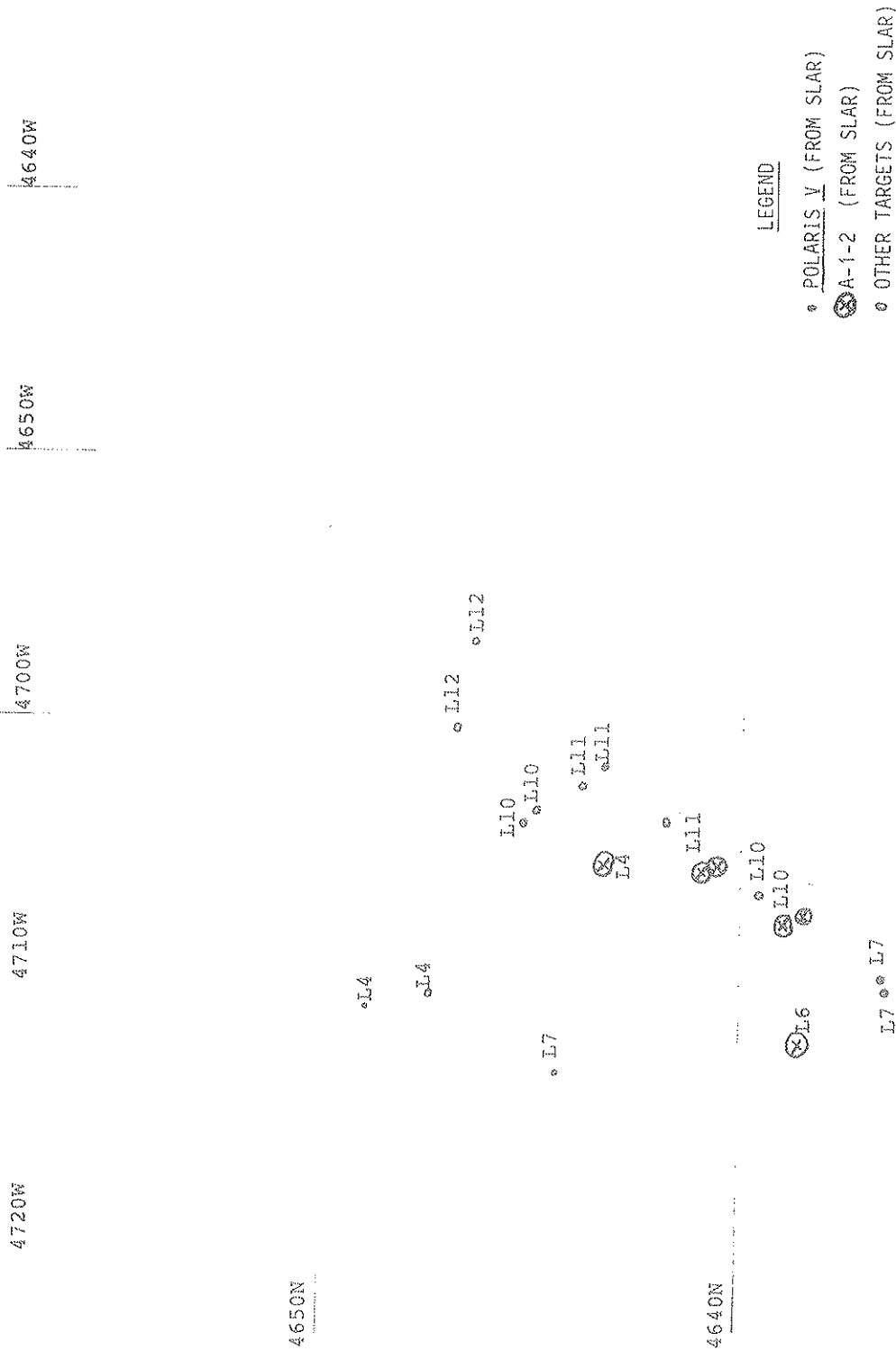


Figure III-12. Other targets on AES SLAR.

TABLE III-16

IIP SLAR Flight Line Particulars, 2 April 1984

| Line No. | Altitude (ft) | Heading (°) | Swath Width (km) | Start (GMT) | Finish (GMT) | Elongation/Shortening of Imagery | General Comments |
|----------|---------------|-------------|------------------|-------------|--------------|----------------------------------|--|
| 1 | 4,000 | 064 | 25 | 1633 | - | None | |
| 2 | 4,000 | 288 | 25 | 1642 | - | None | |
| 3 | 4,000 | 175 | 25 | 1652 | - | None | |
| 4 | 4,000 | 196 | 25 | 1657 | - | None | |
| 5 | 4,000 | 055 | 25 | 1701 | - | None | |
| 6 | 4,000 | 250 | 25 | 1714 | - | None | |
| 7 | 4,000 | 067 | 25 | 1724 | - | None | |
| 8 | 4,000 | 290 | 25 | 1733 | - | None | |
| 9 | 4,000 | 158 | 25 | 1740 | - | None | |
| 10 | 8,000 | 008 | 25 | 1741 | - | None | Imagery darker. Background more subdued. |
| 11 | 8,000 | 248 | 25 | 1807 | - | None | |
| 12 | 8,000 | 065 | 25 | 1812 | - | None | Ocean pattern found marked by lighter and darker imagery tones |
| 13 | 8,000 | 285 | 25 | 1820 | - | None | As for line 12. |
| 14 | 8,000 | 160 | 25 | 1828 | - | None | |
| 15 | 8,000 | 333 | 25 | 1836 | - | | |
| 16 | 8,000 | 165 | 25 | 1844 | - | | |

increased confidence in the identification of the targets on different lines despite varying signatures on the imagery. The lines facilitated a more accurate relative position for each target.

Figure III-13 shows the mapped positions of Polaris V and A-1-2 according to the imagery and compared to positions of ship and iceberg established by the Polaris V and air photography teams. If the locations are correct, then the large iceberg underwent a complex motion. What is more likely is that some or all of the lines should be adjusted slightly with respect to their position and orientation. The IIP personnel noted that there was drift in the INS during each of the lines. As with AES, these differences in position did not affect the April 2 analysis; however, if more targets were present this would create much more difficulty in resolving and locating them without any fixed-point reference.

Results for target identification versus look direction are summarized in Table III-17.

Large Target Detection

There was no difficulty in identifying the two large targets in the study area when the swath covered the areas in which they were located. Aspect angle and its relationship to prevailing wind and wave direction did not affect detectability. It was not possible to differentiate between the two targets on the basis of their signatures on the imagery alone. There was no consistent difference between the two in tone or size, except when one was imaged at far range where it was elongated in azimuth and faint in tone.

The shape of the Polaris V signature was consistent regardless of aspect angle, appearing as a flattened ellipse. Certain aspects did show shape information A-1-2 for; this was improved at the lower altitude.

There was a radar shadow behind the iceberg or on one pass (line 7), when there was enough sea clutter to contrast with the dead zone behind the target.

Small Target Detection

Because the number of growlers in the vicinity of A-1-2 was not known, it is difficult to assess their detectability using this radar system. However, the smaller growlers known to be around A-1-2 from the air photographs were not evident on the imagery. The sea clutter was such that fainter targets would not have sufficient contrast for easy detection and it would require an enlargement and close scrutiny to make identification certain. No growlers could be distinguished and identified on any of the passes with any confidence. The two targets found on the higher altitude AES

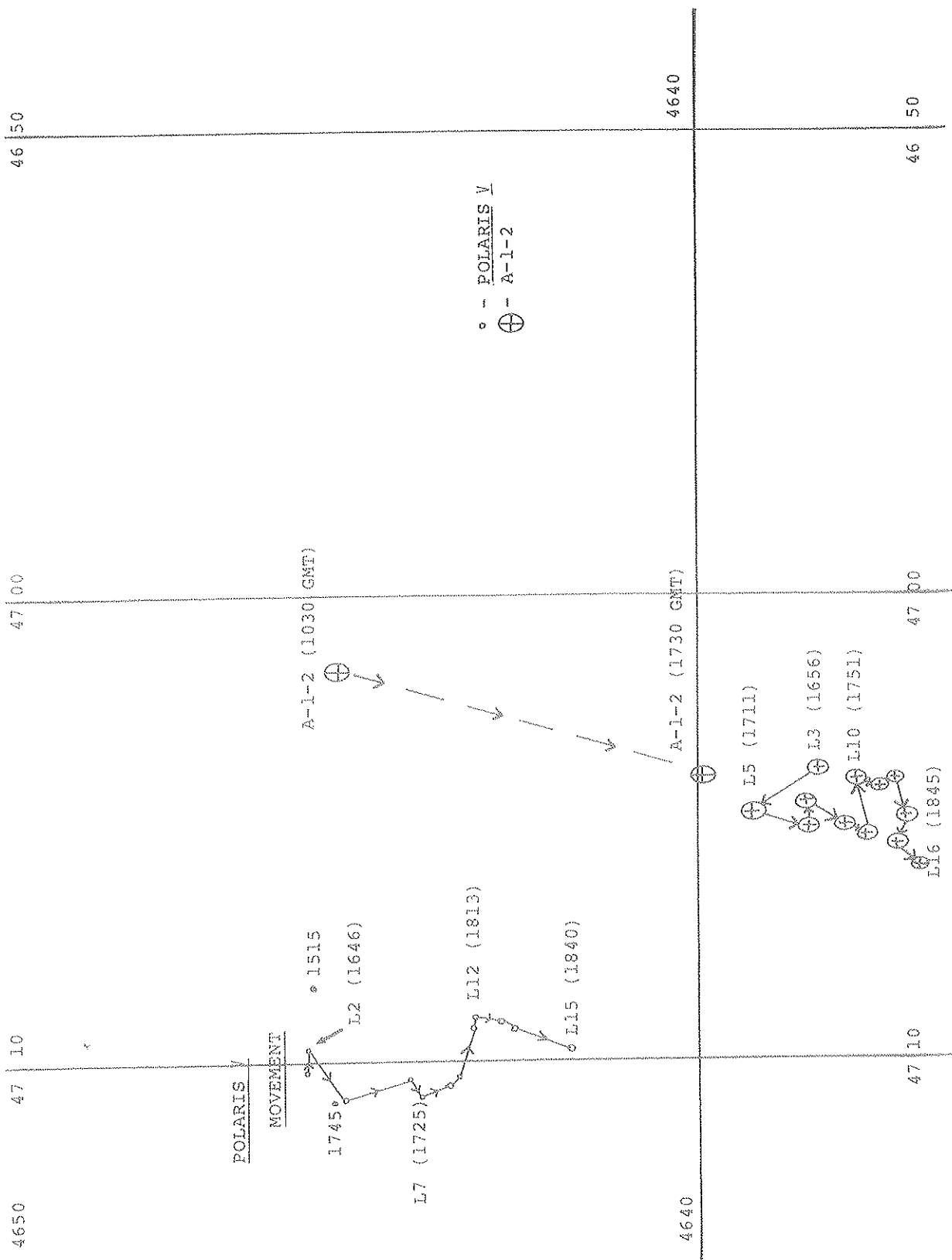


Figure III-13. Polaris V and A-1-2 movement during IIP acquisition, 2 April 1984.

TABLE III-17
IIP SLAR, 2 April 1984

| Look Direction | Target ID | Other ID | Line No | Presence ^a | Size ^b | Tone ^c | Comments |
|--------------------|-----------|-----------|---------|-----------------------|-------------------|-------------------|---|
| Upwind crosswave | 23 | Polaris V | 3 | P | S | G | |
| | 47 | A-1-2 | 3 | P | S | LG | Shape (spurs seen) 45° to flight track |
| | - | Waves | 3 | P | - | G | |
| | 33 | Polaris V | 9 | P | SE | W | |
| | 34 | A-1-2 | 9 | P | S | W | Twin signature |
| | - | Waves | 9 | P | - | L-DG | |
| | 51 | Polaris V | 14 | P | S | W | |
| | 52 | A-1-2 | 14 | P | M | LG | Extreme range |
| | - | Waves | 14 | P | - | DG | |
| | 45 | Polaris V | 16 | P | S | W | |
| Downwind crosswave | 46 | A-1-2 | 16 | P | M | W | Shape (spurs seen) |
| | - | Waves | 16 | A | - | - | |
| | 22 | Polaris V | 2 | P | S | LG | |
| | - | A-1-2 | 2 | X | - | - | |
| | - | Waves | 2 | A | - | - | |
| | 42 | Polaris V | 13 | P | S | W | |
| | - | A-1-2 | 13 | X | - | - | |
| | - | Waves | 13 | A | - | - | |
| | 44 | Polaris V | 15 | P | M | W | |
| | 43 | A-1-2 | 15 | P | M | W | Shadow inside signature |
| Crosswind upwave | - | Waves | 15 | A | - | - | |
| | 21A | Polaris V | 1 | P | M | W | |
| | - | A-1-2 | 1 | X | - | - | |
| | - | Waves | 1 | P | - | G | |
| | 26 | Polaris V | 5 | P | SE | LG | |
| | 25 | A-1-2 | 5 | P | SE | LG | |
| | - | Waves | 5 | P | - | DG | |
| | 30 | Polaris V | 7 | P | S/M | LG | |
| | 29 | A-1-2 | 7 | P | - | LG | Shape evident, radar shadow seen. |
| | - | Waves | 7 | P | - | DG | |
| Crosswind downwave | 35 | Polaris V | 10 | P | SE | LG | |
| | 50 | A-1-2 | 10 | P | S | W | |
| | - | Waves | 10 | A | - | - | |
| | 41 | Polaris V | 12 | P | S | W | |
| | 40 | A-1-2 | 12 | P | S | LG | |
| | - | Waves | 12 | A | - | - | |
| | 24 | B002 | 4 | P | S | W | |
| | - | Waves | 4 | P | - | DG | |
| | 27 | Polaris V | 6 | P | S | LG | Twinning |
| | 28 | A-1-2 | 6 | P | S | LG | |
| | - | Waves | 6 | P | - | DG | |
| | 37 | Polaris V | 11 | P | S | W | |
| Crosswind upwave | 36 | A-1-2 | 11 | P | M | W | |
| | - | Waves | 11 | P | - | L-DG | |

^a P - Present
A - Absent
X - Not in swath

^b M - Medium
S - Small
E - Elliptical

^c W - White
G - Grey
LG - Light Grey
DG - Dark Grey

SLAR, lines 10 to 12, after 1740 could not be found on the corresponding IIP flight lines flown at higher altitude.

III.2.5 MARS SLAR

The flight line particulars for the MARS SLAR are summarized in Table III-18. The aircraft flew much later in the day, which resulted in a greater elapsed time since any surface information had been collected. The sortie began shortly before the end of the second flight of STAR-1.

Minor shortening and elongation of the resulting imagery was found for most of the lines. Any perceived difference was within the error estimates of the aircraft navigation system.

Two general observations were found from the analysis:

1. The imagery was noticeably darker than that of the other SLARs, with the background passes having a "salt-and-pepper" texture.
2. The presence of a linear ocean feature on most of the lines.

This latter feature appeared as a line extending over 17 km and could have been caused by currents or temperature differences in the water, resulting in upwelling. This feature is shown in Figure III-14, which also shows Polaris V and iceberg A-1-2. This feature was a useful reference point for determining the relative positions of flight lines and targets.

Using this feature and line 1 as references, flight lines were relocated as shown in Figure III-15. This assumed the linear feature did not move with time. It can be seen that the errors are within those typical for INS-based positions. The position of A-1-2 seems to be close to that found by the other aircraft several hours earlier. It appears the iceberg was oscillating somewhat which was found by the other aircraft. There is a discrepancy between the positions of the ship as reported by Polaris V and the positions estimated from the imagery. Probably both are in error but it is impossible to reconcile the differences.

Table III-19 summarizes the analysis of verified targets versus look direction. There were several other targets on the imagery which were not found on data from earlier flights. The identity of these targets is unknown.

TABLE III-18

MARS SLAR Flight Line Particulars, 2 April 1984

| LINE NO. | ALTITUDE (ft) | HEADING (°) | SWATH WIDTH (km) | START (GMT) | FINISH (GMT) | ELONGATION/SHORTENING OF IMAGERY | GENERAL COMMENTS |
|----------|---------------|-------------|------------------|-------------|--------------|----------------------------------|---|
| 1 | 6,000 | 230 | 25 | 2245 | 2253 | E* | Left side of imagery very dark in near range. Right side lighter. Dark background contrasts well. |
| 2 | 6,000 | 312 | 25 | 2300 | 2303 | E* | Right side of imagery much darker than left. |
| 3 | 6,000 | 042 | 25 | 2313 | 2318 | S* | Right side darker than left - good contrast with targets. Large number of small specular returns. |
| 4 | 6,000 | 186 | 25 | 2325 | 2330 | None | Left side of image much darker than right. |
| 5 | 6,000 | 230 | 25 | 2340 | 2344 | S* | Left side dark. |
| 6 | 6,000 | 311 | 25 | 2351 | 2356 | E* | Right side dark especially in near range. |
| 7 | 6,000 | 041 | 25 | 0002 | 0007 | E* | Right side very dark. Left side dark in first 1/3 of range. |
| 8 | 6,000 | 186 | 25 | 0013 | 0015 | S* | Left side of imagery much darker than right. A few specular targets on right side. |
| 9 | 12,000 | 230 | 25 | 0026 | 0031 | E* | Imagery as a whole much darker than previous passes. Little background detail. |
| 10 | 12,000 | 310 | 25 | 0037 | 0041 | E* | As for 9. |
| 11 | 12,000 | 042 | 25 | 0051 | 0052 | E* | As for 9. |
| 12 | 12,000 | 187 | 25 | 0055 | 0059 | E* | As for 9. |

* minor, within position error estimates.

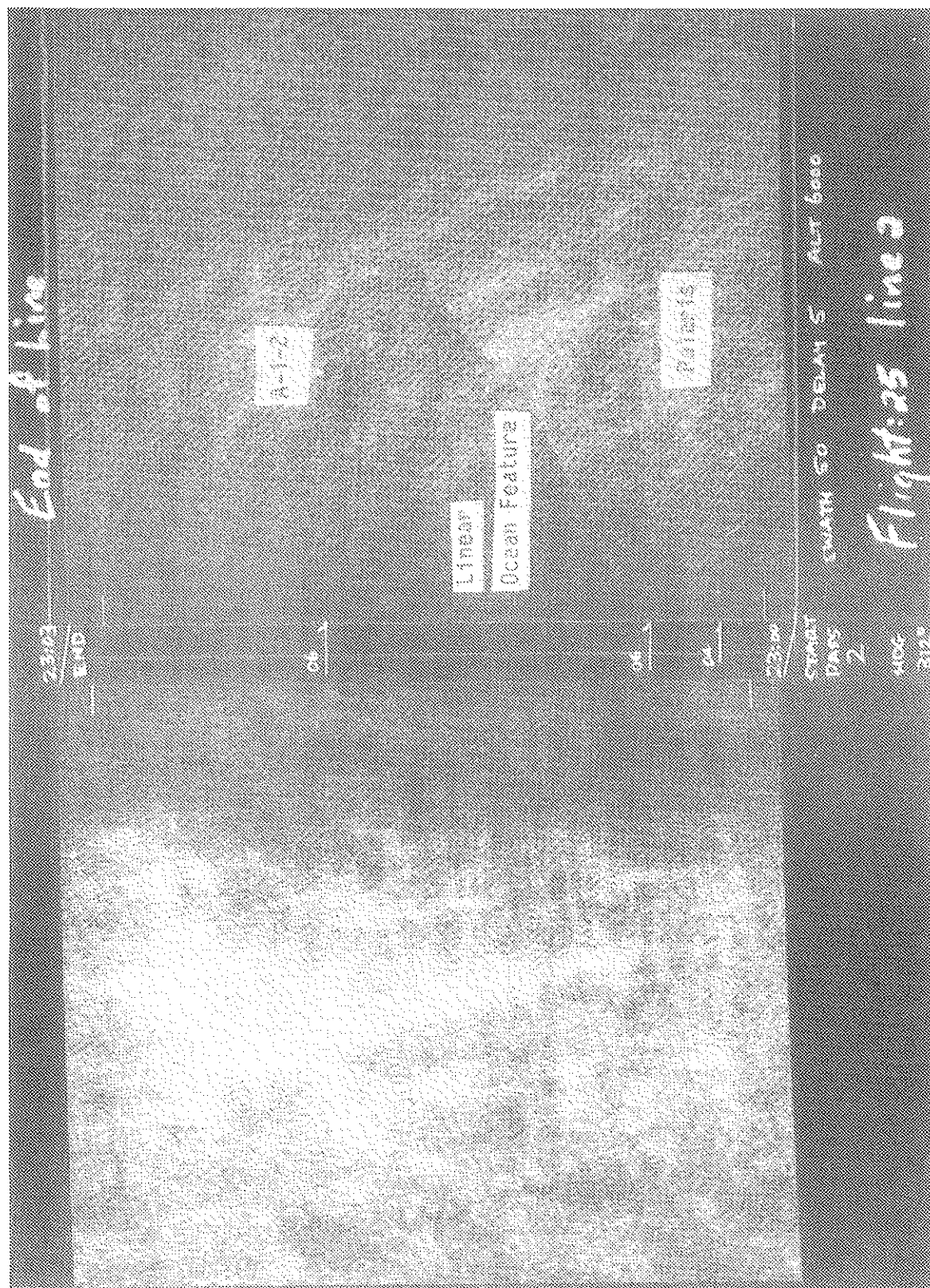


Figure III-14. MARS SLAR, pass 2, 2 April 1984 (scale 1:250,000).

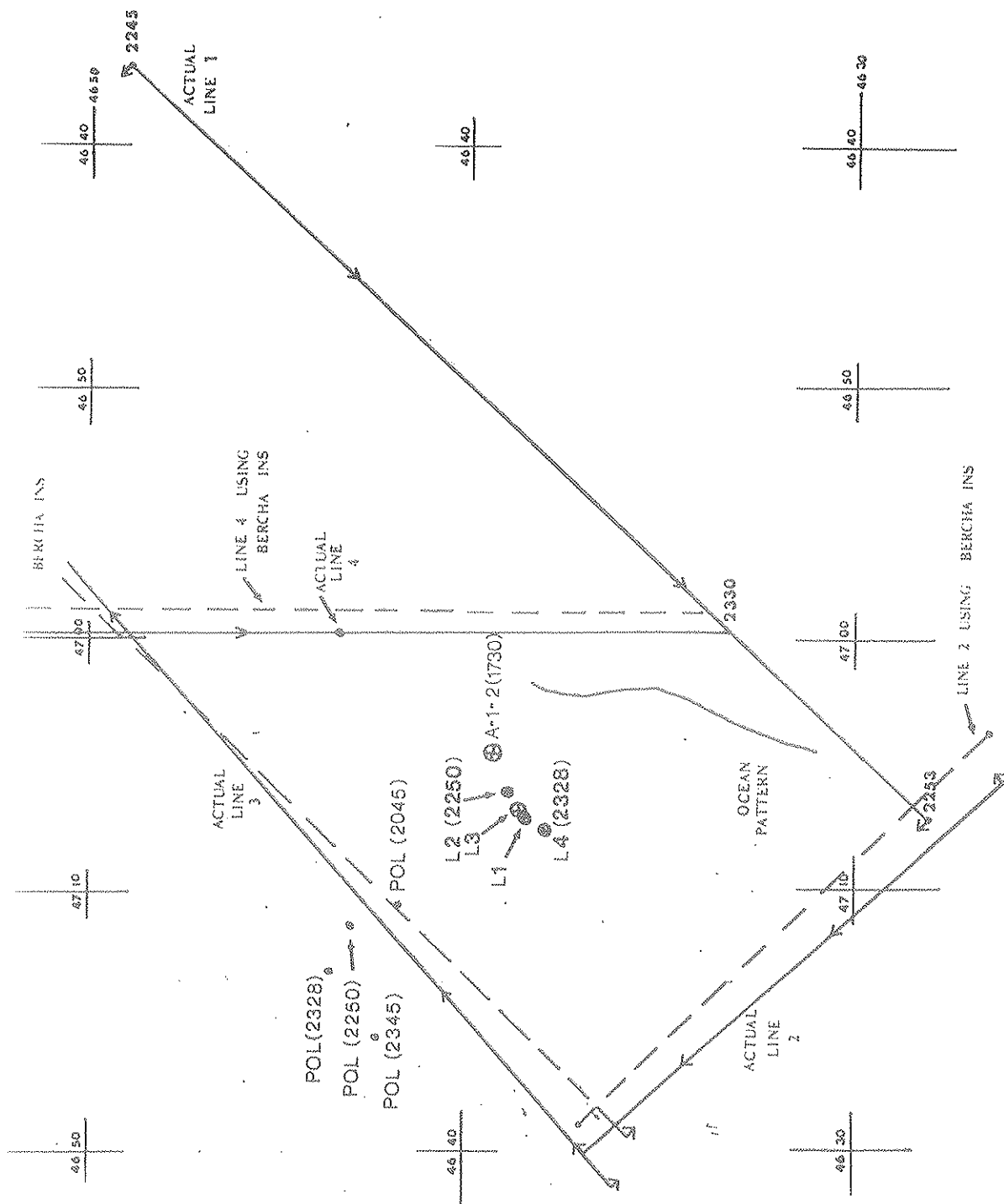


Figure III-15. Comparison of MARS lines 1-4, 2 April 1984.

TABLE III-19
MARS SLAR, 2 April 1984

| LOOK DIRECTION | TARGET ID | OTHER ID | LINE NO | PRESENCE ^a | SIZE ^b | TOPE ^c | COMMENTS |
|------------------|-----------|-------------|---------|-----------------------|-------------------|-------------------|---|
| Upwind | 02 | Polaris | 1 | P | M | W | Waves from N, wind varying 280 to 310 |
| Upwave at 40° | 03 | A-1-2 | 1 | P | ME | W | |
| | - | Waves | 1 | P | - | DG | |
| | 14 | Polaris | 5 | P | M | W | Evidence of shape from spurs Evident on farther south ranges |
| | 15 | A-1-2 | 5 | P | M | W | |
| | - | Waves | 5 | Partial | - | DG | |
| | 13 | 10 | 5 | P | M | W | All matched to line 3 targets |
| | 16 | 7 | 5 | P | S | W | |
| | 16A | 8 | 5 | P | S | W | |
| | 27 | Polaris | 9 | P | S | W | Subdued Identified from other lines |
| | 28 | A-1-2 | 9 | P | S | W | |
| | - | Waves | 9 | P | - | DG | |
| | 29 | 26,23,17,13 | 9 | P | S | W | |
| Downwind | - | Polaris | 3 | X | - | - | |
| Downwave at 45° | 09 | A-1-2 | 3 | P | SE | W | |
| | - | Waves | 3 | A | - | - | |
| | 07 | - | 3 | P | S | G | Non-verified target |
| | 08 | - | 3 | P | S | G | Non-verified target |
| | 10 | - | 3 | P | S/M | W | Non-verified target |
| | 24 | Polaris | 7 | P | S | W | Left side mainly |
| | 22 | A-1-2 | 7 | P | M | W | |
| | - | Waves | 7 | Partial | - | - | |
| | 21 | 16 | 7 | P | M | W | |
| | 23 | 17,13 | 7 | P | S | W | |
| | 11 | Polaris | 4 | P | SE | W | Evidence of shape from spurs |
| | 12 | A-1-2 | 4 | P | M | W | |
| | - | Waves | 4 | A | - | - | |
| | - | Polaris | 8 | X | - | - | |
| | 25 | A-1-2 | 8 | P | M | W | Evidence of shape, shadow in signature. |
| | - | Waves | 8 | Partial | - | DG | Right side mainly |
| | 26 | 23,17,13 | 8 | P | S | W | |
| Crosswind | 06A | Polaris | 2 | P | S-M | W | |
| Crosswave at 45° | 06 | A-1-2 | 2 | P | S-M | W | |
| | - | Waves | 2 | P | - | DG | |
| | 20 | Polaris | 6 | P | S-M | W | |
| | 19 | A-1-2 | 6 | P | S-M | W | |
| | - | Waves | 6 | Partial | - | DG-B | |
| | 17 | 13 | 6 | P | SE | W | |

^aP - Present
A - Absent
X - Not in swath

^bM - Medium
S - Small
E - Elliptical

^cW - White
G - Grey
LG - Light Grey
DG - Dark Grey

Large Target Detection

The SLAR was able to detect the Polaris V and A-1-2 from all aspects, except for lines which ended before the target was imaged or when it was located underneath the aircraft in the blind zone. As with the other SLARs, the ship was distinguishable from the iceberg only when the shape of the latter could be perceived, usually in the nearer ranges where resolution was better.

Small Target Detection

The salt-and-pepper texture of the background gave rise to many returns which looked similar to point targets. Some of these may have been wave crests whereas others may have been small floes or growlers. Small, bright returns identified around A-1-2 have point-target signatures similar to other parts of the imagery in which there were no identified ice targets. Because the number of growlers and bergy bits was not known with any certainty, it is difficult to judge small target detection solely on the imagery of this day. It is suspected, however, that if similar texture was found on other days correct interpretation may be difficult.

III.3. ANALYSIS OF APRIL 3 IMAGERY

This day was the second research day for all aircraft except the CV 580. The target area was to the west of the one selected for April 2. There were more icebergs, bergy bits and growlers in the area, some of which had been photographed from the King Air on the previous day. The patterns of flight lines were similar to April 2, in that three to four different aspect angles were flown. The passes of this day were oriented more or less north-south and east-west to produce images orthogonal and parallel to the main wave and wind regime.

The STAR-1, AES, and IIP aircraft flew the target area at nearly the same time at staggered altitudes. MARS and the second flight of STAR-1 were conducted several hours later. The imaging times of the respective series of passes and the corresponding ground verification activity became important in following the movement of the icebergs, ice strings, bergy bits, and growlers which were present in the area. The times at which surface information, air photography, and image acquisitions relevant to the April 3 data set were collected are summarized in Table III-20. The King Air photographs noted in the table are those which could possibly have moved into the image swaths for this day.

The quantity of data collected on this day and time constraints did not allow for an exhaustive examination of all passes and all targets. Most of the targets were not aerially photographed or visited by the surface team and were of limited interest to this study. Since number of passes made by each aircraft was much larger than had been anticipated originally, a limited number were examined. The analysis concentrated on two small areas for which ground data and photographs were available of Polaris V, A-3, and B008.

III.3.1 AVAILABLE SURFACE INFORMATION

The specified target area given to the team aboard Polaris V was located near 47°00'N, 45°45'W, where some icebergs had been observed on overflights late in the previous day.

Several of the icebergs which had been photographed from the air on April 2 were visited on the April 3 by Polaris V. The positions of these icebergs, based on the air photograph logs of Polaris V positions together with other surface-verified icebergs, are illustrated in Figure III-16 (which covers the period from April 2 to 4). Two of the icebergs, A-3 and C-3, were revisited by Polaris V on the April 4 and their positions also are plotted. It was possible to track their general direction and rates of movement over the two-day period. This allowed reasonable projections of where

TABLE III-20

Data Acquisition Times for Iceberg Surface Data and Radar Imagery

| Date | Type | Time (GMT) | Targets |
|---------|----------------------------------|------------|---|
| April 2 | King-Air-RC10 Air photography | 1859-1920 | B005* (B-3) B006 B007 B008 B009 (C-3) |
| April 3 | <u>Polaris V</u> team | 0920-2345 | A-3 0920-1010 1300-2345 Standing off A-3 about 500 m B-3 1035-1110 (B005) C-3 1150-1226 (B009) D-3 1257-1301 (growler) |
| | AES SLAR oblique photography | 1414-1423 | B008 + adjacent ice string |
| | AES SLAR | 1402-1707 | <u>Polaris V</u> + A-3 B008+ice string |
| | IIP SLAR | 1429-1818 | <u>Polaris V</u> + A-3 B008+ice string |
| | STAR-1 SAR Flight 1 | 1511-1638 | <u>Polaris V</u> + A-3 (1 line) B008 + ice string |
| | Flight 2 | 2102-2322 | <u>Polaris V</u> + A-3 |
| | MARS SLAR | 2114-2335 | <u>Polaris V</u> + A-3 |
| April 4 | <u>Polaris V</u> Team | 0916 | A-3-4 (berg A-3 revisited on April 4) |
| | | 1159 | C-3-4 (berg C-3 revisited on April 4) |

* King Air nomenclature

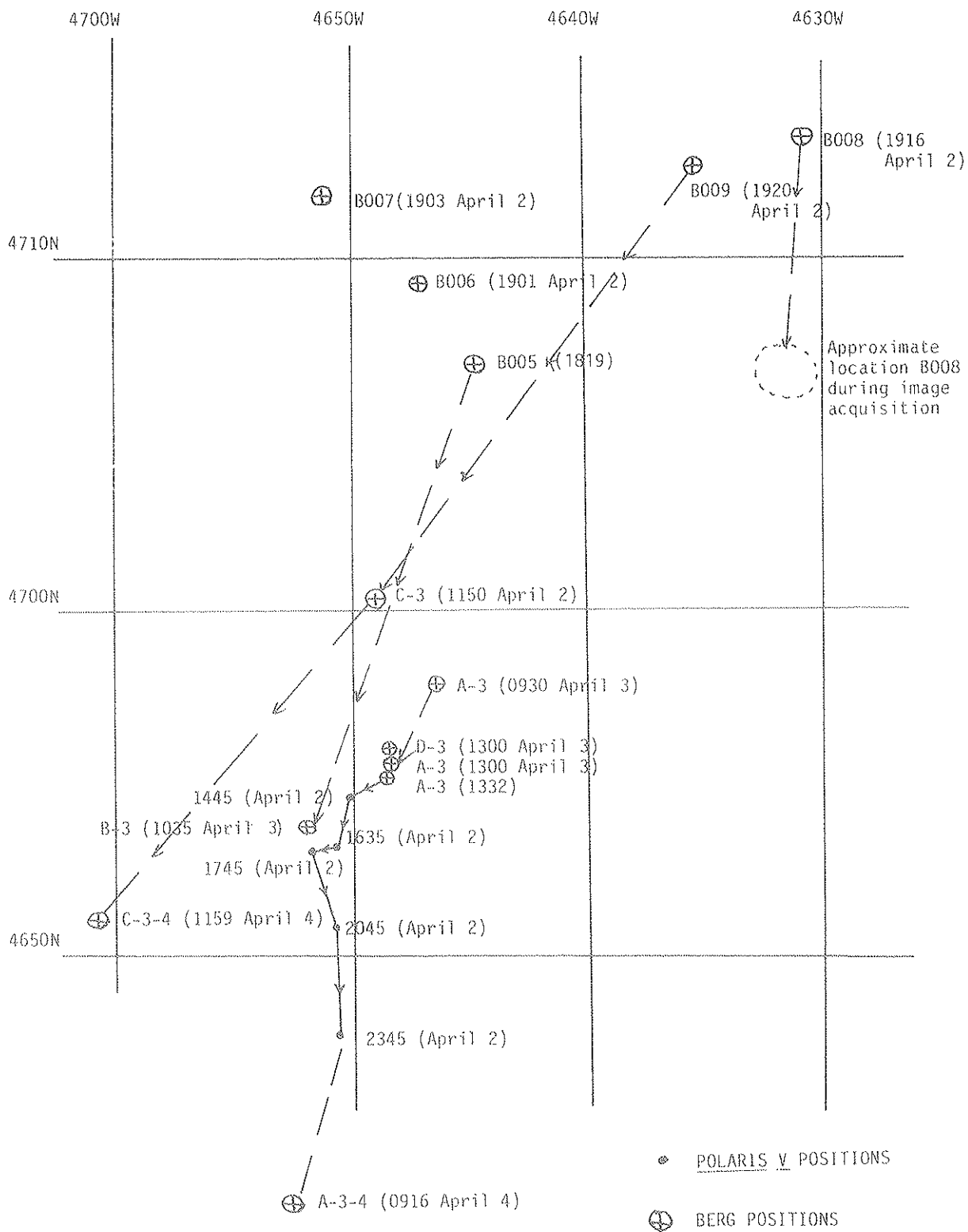


Figure 111-16. Polaris V and iceberg positions, 2-4 April 1984.

other iceberg targets, either verified by Polaris V or photographed from the air, might be located during the times of image acquisition. It is interesting to note that the drift rates for icebergs B-3 (B005 nomenclature on April 2) and C-3 (B009 nomenclature on April 2), between the times noted on April 2 and 3, closely match the estimates made by the surface team on the latter day.

In general the icebergs were moving in a south to south-westerly direction at a rate of 0.5 m/sec, or about 1.8 km/hour. Icebergs B005, B008, and B009 (April 2 nomenclature) had moved into the main imaging area overnight, whereas B006 and B007 appeared to have moved more westerly than southerly and were not within the target area (assuming a similar drift rate).

The characteristics of surface-verified icebergs and those photographed from the air are summarized in Table III-21. Iceberg A-3 was visited by Polaris V but was not photographed from the air on April 2, even though it should have been in the vicinity of the other icebergs. One growler from A-3 was documented in detail at about 1300 GMT (D-3, see Figure III-16) and other growlers were observed around A-3, although their distribution with time was not noted. Two views of A-3 are shown in Figures III-17 and III-18, and Figure III-19 shows a photograph of growler D-3.

Polaris V and Iceberg A-3

During the time of imagery acquisition Polaris V was located between 300 and 500 m to the north of A-3 and drifted along with it between 1300 and 2345 GMT. Notes on events relating to the Polaris V and the iceberg are summarized in Table III-22. Five significant events were recorded in the surface log during the period.

1. Iceberg A-3 underwent a number of rolls at various times during the day presenting different target cross-sections to the radars. There were also considerable bobbing and rotating motions.
2. The rolling action broke off growlers on more than one occasion; however, the resulting history of their movement in relation to the source iceberg was not documented, nor is it known whether all growler-creation events were recorded in terms of time and numbers.
3. The ship deployed a waverider buoy which was tethered up to 200 m away from the ship on its starboard side. This buoy was 73 cm in diameter and had a 2m high whip antenna. On April 3 it broadcast continually throughout its deployment at 27 MHz. Figure III-20 shows the waverider just after it was released from Polaris V.

TABLE III-21

Characteristics of Surface Verified and Air Photographed Icebergs
and Growlers 2-4 April, 1984

| Iceberg/growler identification | Description | Dimensions (m) | Size class |
|-----------------------------------|--|--|---------------|
| A-3 (Surface data only) | Drydock iceberg, smooth on lower slopes, serrated on higher slopes: Repeatedly rolled and rotated throughout day. | 80x43x22 | M |
| B-3 (B005 from King Air) | Wedge iceberg, angular upper surface with deep crevasses through its length. Iceberg was rotating. | 46x36x10 (surface data) 46x55 (air photo) | S-M |
| C-3 (B009 from King Air) | Spherical iceberg, smooth lower slopes with subangular serrated upper surface. | 33x26x7 (surface data) 45x58 (air photo) | S-M |
| D-3 (Surface data only) | Growler spawned from berg A-3. Additionally 3 growlers about same size and <20 small growlers also noted to NNE of A-3 at surface data time (1300GMT). | 2x1.5x0.2 | G |
| B008 (Air photography only) | Tabular iceberg, hourglass shape with small hole in centre. | 264x152 (air photo) | VL |
| B006 (Air photography only) | Drydock with smooth surface, L-shaped with broken edges on one side. | 36x128 | L |
| B007 (Air photography only) | Spherical berg with cracked surface. | 48x46 | M |



Figure III-17. Iceberg A-3, looking north at 0930 GMT, 3 April 1984.

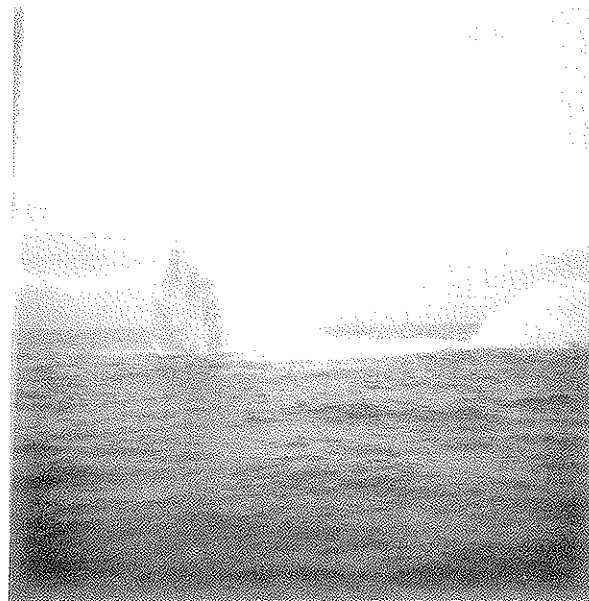


Figure III-18. Iceberg A-3, looking southwest at 0930 GMT, 3 April 1984.

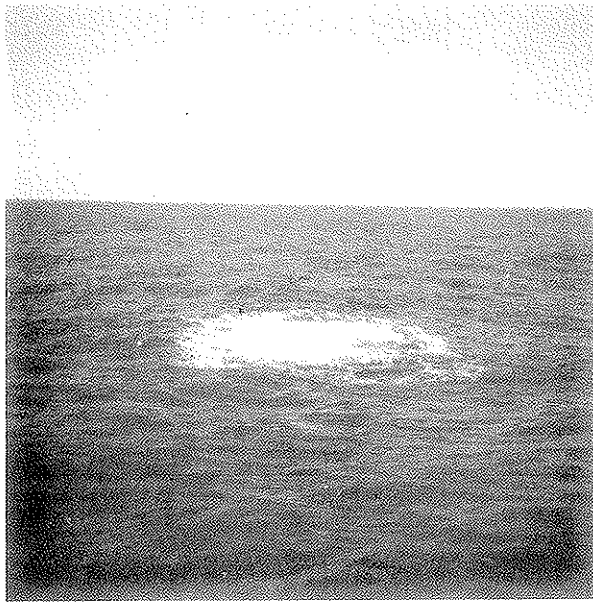


Figure III-19. Growler D-3, 1300 GMT, 3 April 1984.

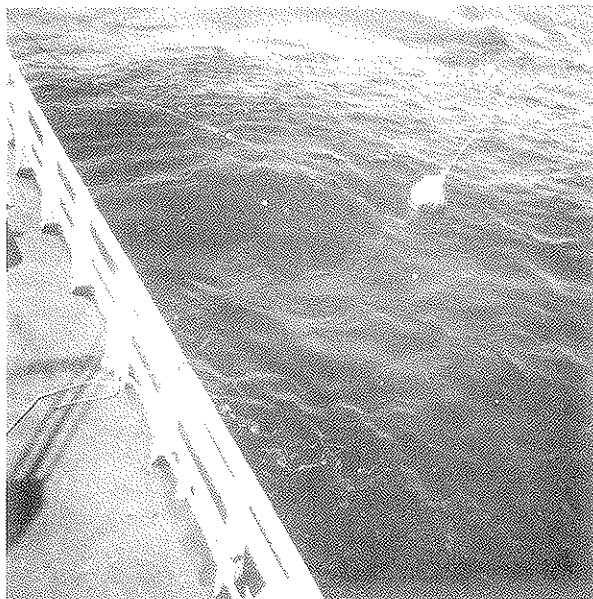


Figure III-20. Waverider deployment, 1320 GMT, 3 April 1984.

TABLE III-22

Synopsis of Events Relating to Iceberg A-3, 3 April 1984

| Time (GMT) | Observation |
|------------|--|
| 1300 | <u>Polaris V</u> off A-3. Creation of a growler D-3 and surface verification of it. Surface verification of iceberg A-3. Three growlers about the same size and >20 smaller growlers to the NNE of <u>Polaris V</u> . |
| 1320 | Waverider buoy is deployed. |
| 1336 | Growlers broke off iceberg during roll. |
| 1342 | Iceberg rolled. |
| 1354 | Ship's radar turned off. |
| 1401 | Transponder (X-band) turned on but was possibly not working. |
| 1436 | Iceberg rolled twice in rapid succession. It takes 10-15 minutes to change positions. |
| 1453 | Iceberg rolled 4 times in rapid succession. |
| 1600 | Iceberg drift reduced. |
| 1645 | Iceberg tipping again but during roll no ice break up. i.e., growler creation occurred. |
| 1704 | Sharp side pointing west. |
| 1730 | Waverider line caught in bow thruster. A small boat was deployed from <u>Polaris V</u> to assist in freeing the line. The boat was in the water between half and three-quarters of an hour before it was brought back on to the <u>Polaris V</u> . |
| 1915 | Waverider was recovered. |
| 2107 | Iceberg was actively rolling and turning. |

4. No attempt was made to keep either the Polaris V oriented with respect to north, or the iceberg, or the waverider buoy. The result was that the buoy line became caught in the bow thruster on more than one occasion.
5. On one occasion when the buoy line was caught, a small boat was deployed to assist in freeing it.¹ This boat was 5.5 m long and 2 m wide. If the time of deployment was correct then the boat was in the water only during the last few lines flown by IIP.

Iceberg B008 and Ice String

Although Polaris V and A-3 were the primary targets, there was considerable information on another iceberg which was not visited by Polaris V but which was photographed by the King Air aircraft on April 2. Figure III-21 shows the air photo of B008 (King Air nomenclature) which was a very large, tabular iceberg. Fortunately, during the AES flight this iceberg was photographed from the Electra on two successive lines (3 and 4), which are shown in Figures III-22 and III-23. The estimated positions of the aircraft at the time of the two photographs (1414 and 1423 GMT) place B008 in the position indicated in Figure III-16. The oblique photographs show that there was an ice string adjacent to B008 with a scattering of small floes, bergy bits, and growlers around the string.

Figure III-24 shows a sketch of the iceberg, ice string, and 17 individual targets distinguished on the oblique photographs, together with an accompanying nomenclature which was used for the purposes of analysis. The size category of the individual targets also is shown using the WMO nomenclature. These sizes were estimated from the oblique photographs, which compared the smaller targets to the larger B008 tabular iceberg. The smaller targets were classified into three size categories as follows:

- | | | |
|----------------------|---|-----------------------|
| . growler (G) | - | <10 m longest side |
| . bergy bit (BB) | - | 10-20 m longest side |
| . small iceberg (SB) | - | 20-50 m longest side. |

Exact dimensions could not be calculated; however, the comparison probably yielded the size class to which each target belonged.

These targets were traced over the next 1 1/2 hours on imagery of AES, IIP, and Star-1. The results are discussed under each respective subsection. Beyond this point in time the relative positions of the ice string, the identified smaller targets, and B008 had changed enough that confidence in the reidentification of the individual targets was drastically reduced.

¹J. Dempsey, Dobrocky Seatech, personal communication

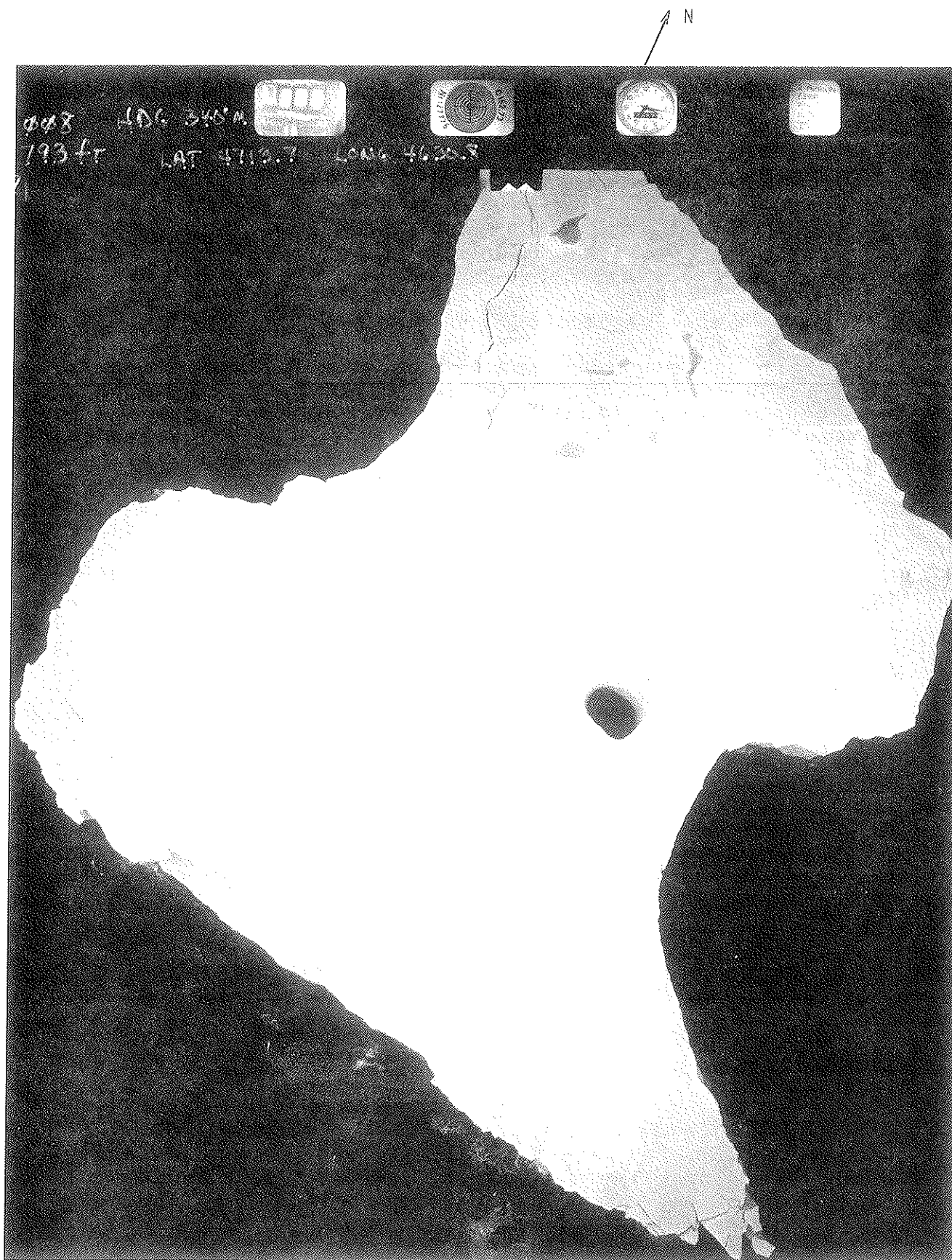


Figure III-21. Air photo of iceberg B008, 2 April 1984
(scale 1:250,000).

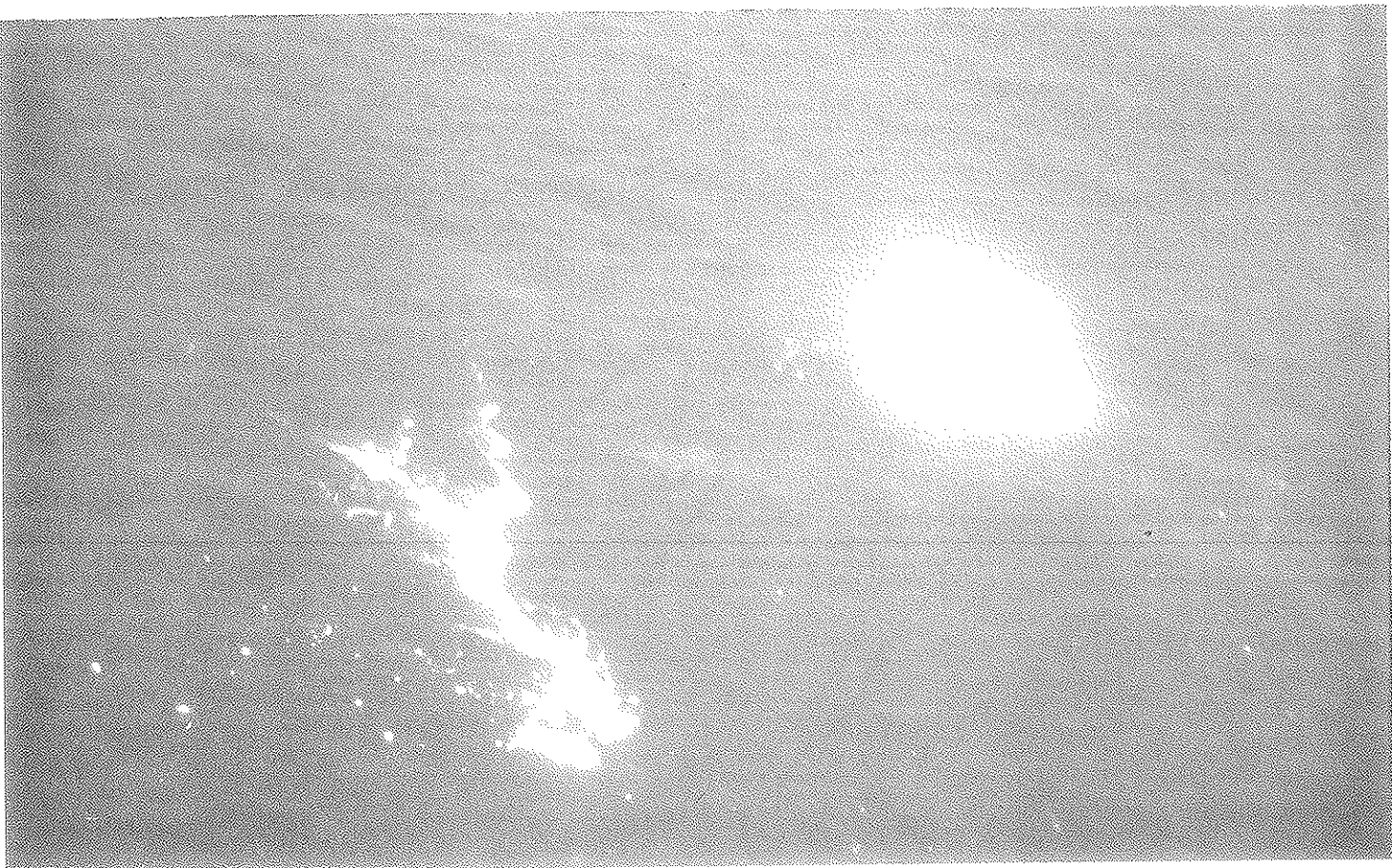


Figure III-22. B00I and ice string, looking south at 1414 GMT.

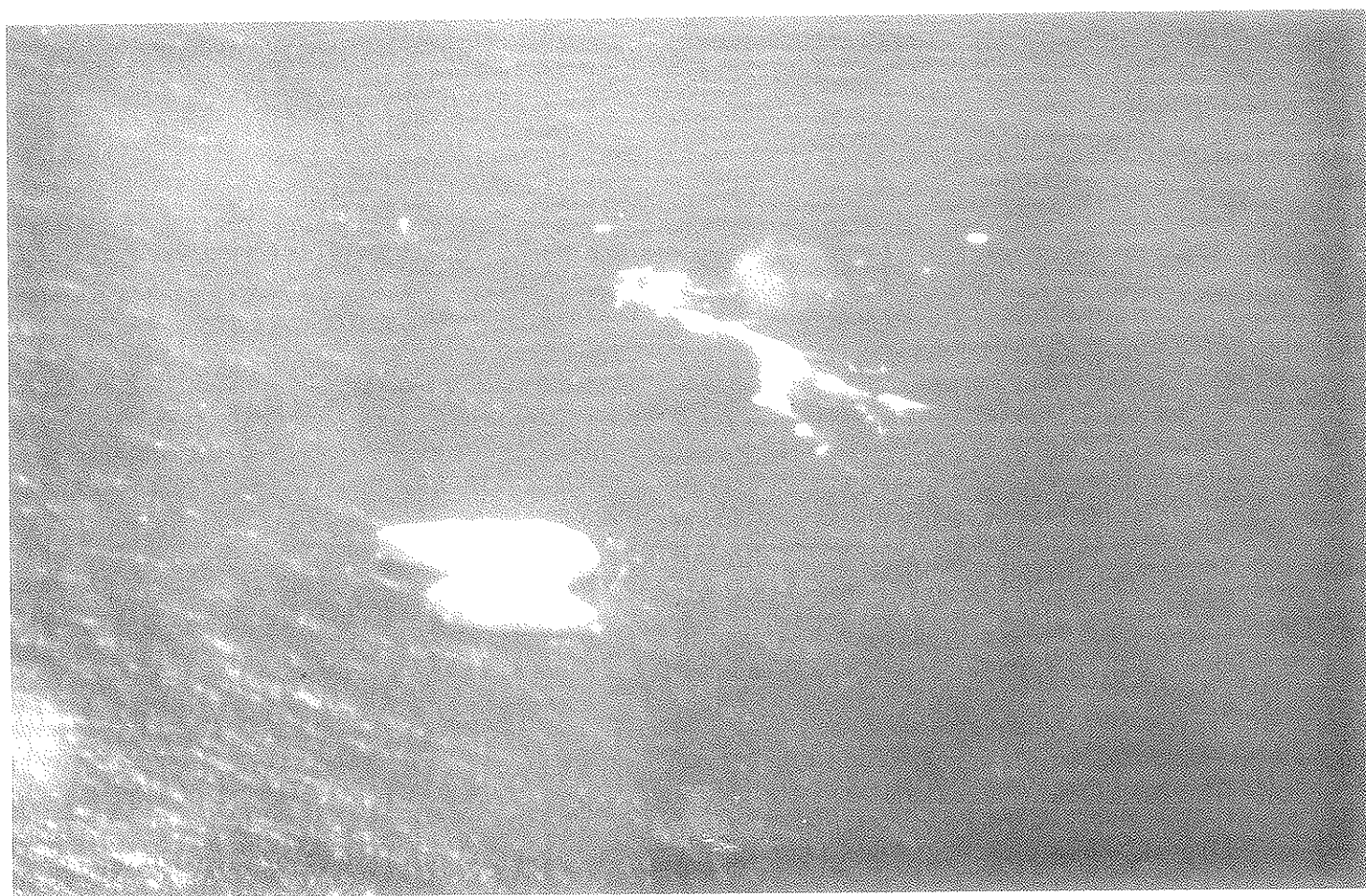


Figure III-23. B008 and ice string, looking northwest at 1423 GMT.

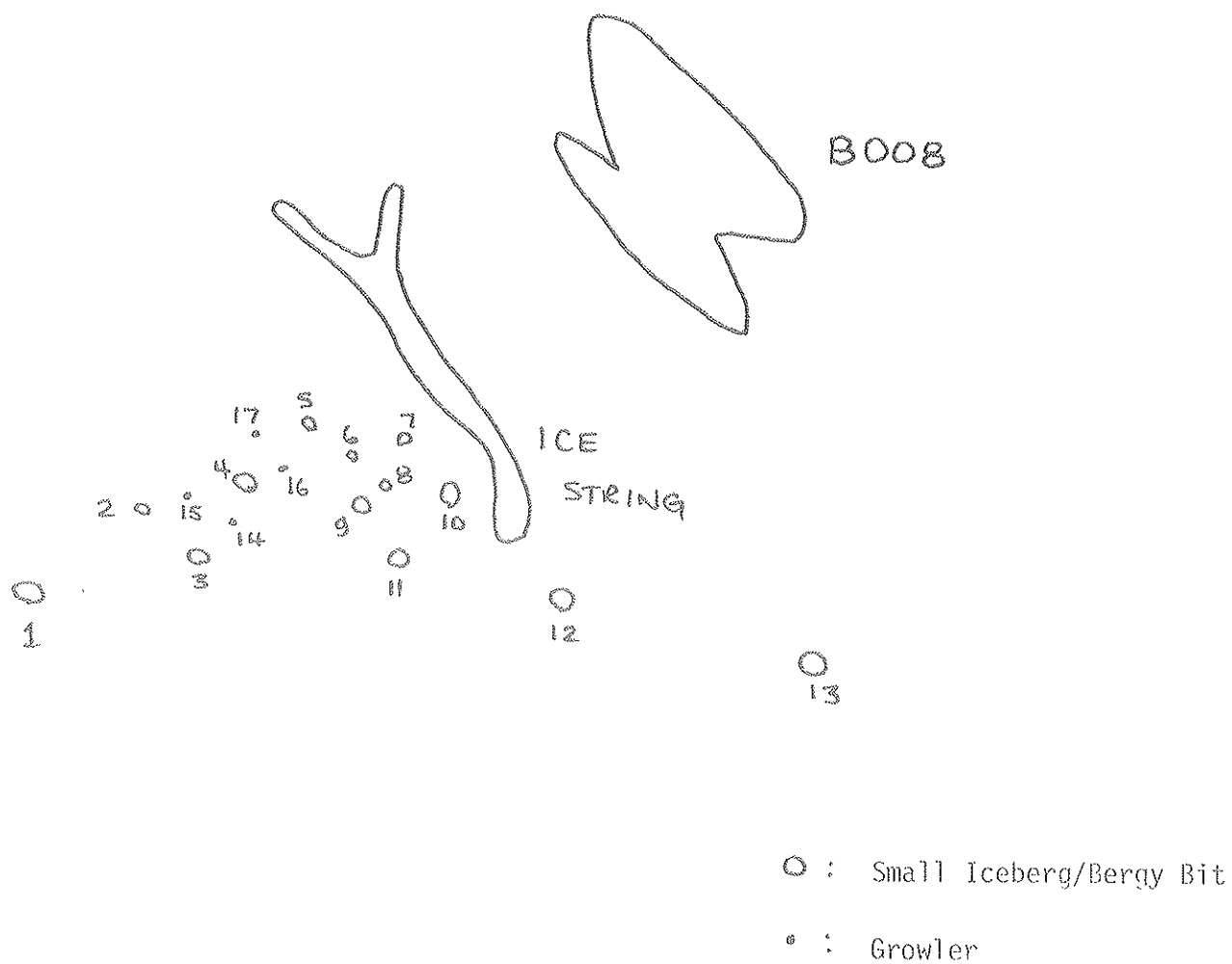


Figure III-24. Sketch and nomenclature for B008, ice string, and 17 targets (based on distribution at 1413 GMT).

Environmental Information

Table III-23 summarizes the hourly weather and wave data collected on Polaris V for April 3. In general, winds were very light starting from a mostly northwesterly direction, shifting to the west until 2100, when they swung back to the northwest. Waves were particularly light and were quite variable in direction during the day. These very light wind and wave conditions are an important factor to consider in reviewing the results.

III.3.2 STAR-1 SAR

Analysis of Star-1 imagery centred on the flight 1 lines for which more surface data were available. The first flight consisted of a number of repeatability lines which were flown in a north-south orientation imaging from west toward the target area. The relevant flight particulars for each pass are summarized in Table III-24. In general all the lines ended north of the position of Polaris V and A-3, with the exception of pass 5. No targets were found on either pass 4 or 6, suggesting the target area was missed, perhaps through an improper range delay setting or an error in the flight track. Useful imagery covering some of the surface truth areas was found for passes 5, 7, and 8. All lines were flown along the same longitude line at the same altitude, range delay and swath setting. Generally speaking, the radar was imaging downwind and downwave.

The dark background contrasted well with the point targets, which appeared as white specks streaked in azimuth. Larger targets had a central core either circular or elliptical in shape, with the accompanying azimuthal streaks. A comparison of targets between repeatability lines showed there was INS drift of a similar magnitude to other days. The plotting of targets on a base map clearly showed similar patterns between passes but in different locations. There is no "exactly" known reference point so the precise variations cannot be estimated.

The analysis of these targets shows that there were many smaller-sized targets which were not seen on particular lines. Table III-25 summarizes targets on each pass which were and were not identified as well as those which were not imaged. Lines 5, 7, and 8 had a larger common area and so the total number of comparable targets was higher. The targets were identified primarily on the basis of pattern, especially the smaller ones. Large targets, such as B008, were easily identified by their characteristic.

TABLE III-23

Hourly Weather and Environmental Data, 3 April 1984

| Time GMT | Primary Waves | | | Secondary Waves | | | Wind | | Temp. | | Cloud Height (m) | Vis (Naut mi.) | Ice Cond |
|-------------|---------------|------------|-----------------|-----------------|------------|-----------------|----------------|------------|------------|-------------|------------------------|----------------------|-------------|
| | Height (m) | Dir (°) | Period (sec) | Height (m) | Dir (°) | Period (sec) | Speed (kts) | Dir (°) | Air (°) | Sea (°C) | | | |
| 1300 | 0.2 | 10 | 1 | 1.4 | 260 | 6 | 2 | 333 | -0.2 | +1.5 | >600 | 10 | 25 0/w |
| 1400 | 0.2 | 10 | 1 | 1.2 | 280 | 7 | 3 | 320 | -0.1 | 1.5 | >600 | 10 | 15 0/w |
| 1500 | 0.1 | 280 | <1 | 1.2 | 330 | 3 | 4 | 320 | 0.0 | 1.5 | >600 | 10 | 15 0/w |
| 1600 | 0.2 | 310 | 1 | 1.1 | 350 | 8 | 4 | 258 | -0.5 | 1.5 | >600 | 10 | 15 0/w |
| 1700 | 0.1 | 120 | 1 | 1.0 | 320 | 8 | 3 | 230 | 0.0 | 1.5 | >600 | 10 | 15 0/w |
| 1800 | 0.1 | 240 | 1 | 1.0 | 330 | 11 | 4 | 250 | -0.2 | 1.5 | >600 | 10 | 15 0/w |
| 1900 | 0.2 | 300 | 1 | 0.8 | 320 | 9 | 3 | 240 | -0.3 | 1.5 | >600 | 10 | 10 0/w |
| 2000 | NO | DATA | | NO | | DATA | NO | DATA | | NO | DATA | NO | DATA |
| 2100 | 0.1 | 310 | 1 | 1.0 | 0 | 10 | 2 | 320 | -1.0 | 1.0 | >600 | 10 | 15 0/w |
| 2230 | DARK | | | 0.8 | 330 | 8 | 3 | 320 | -1.5 | 1.0 | >600 | 10 | 15 0/w |

TABLE III-24
STAR-1 Flight Line Particulars, Flight 1, 3 April 1984

| Pass No | Altitude (ft) | Heading (°T) | Start (GMT) | Finish (GMT) | Comments |
|---------|---------------|--------------|-------------|--------------|---|
| 2 | 29,000 | 180 | 1450 | 1455 | Mostly north of main target areas, <u>Polaris V and A-3 not imaged, B008 imaged</u> |
| 3 | 29,000 | 360 | 1511 | 1514 | 1:125,000 scale |
| 4 | 29,000 | 180 | 1527 | 1531 | 1:125,000 scale: target area completely missed; image dark with no point returns |
| 5 | 29,000 | 360 | 1547 | 1552 | Complete coverage of target area including <u>Polaris V and A-3</u> |
| 6 | 29,000 | 180 | 1603 | 1609 | No returns: imagery is black |
| 7 | 29,000 | 360 | 1619 | 1624 | Mostly north of main target area, <u>Polaris V and A-3 not imaged, B008 imaged</u> |
| 8 | 29,000 | 180 | 1632 | 1638 | Mostly north of main target area, <u>Polaris V and A-3 not imaged, B008 imaged</u> |

TABLE III-25

Target Identification STAR-1, 3 April 1984

| PASS 2 | PASS 3 | PASS 5 | PASS 7 | PASS 8 |
|----------------------------|--------|--------|--------|--------|
| 47 | - | 64 | 76 | 82 |
| 48 | - | 63 | 75 | 83 |
| 49 | 53 | 121 | 137 | 150 |
| 50 | 52 | 62 | 74 | 84 |
| 90 | 97 | 120 | 73 | 149 |
| 91 | 96 | NS | 136 | 148 |
| - | 51 | 56 | 68 | 89 |
| - | 92 | NS | NS | 139 |
| - | 93 | 110 | 126 | NS |
| - | 94 | 111 | 127 | NS |
| - | 95 | 112 | 128 | 147 |
| NS | 98 | NS | NS | NS |
| - | - | 57 | 69 | 88 |
| - | - | 58 | 133 | 142 |
| - | - | 59 | 70 | 87 |
| - | - | 60 | 71 | 86 |
| - | - | 61 | 72 | 85 |
| - | - | 65 | - | 80 |
| - | NS | 108 | NS | - |
| - | NS | 109 | - | NS |
| - | - | 113 | NS | NS |
| - | NS | 114 | 129 | 140 |
| - | - | 115 | NS | NS |
| - | - | 116 | 130 | NS |
| - | - | 117 | 131 | 143 |
| - | - | 118 | NS | 146 |
| - | - | 119 | NS | NS |
| NS | - | 122 | NS | NS |
| - | - | 123 | NS | 155 |
| - | - | 124 | NS | 157 |
| - | - | - | 77 | 81 |
| - | - | NS | 125 | NS |
| - | - | NS | 132 | NS |
| - | - | NS | 134 | 144 |
| - | - | NS | 135 | 145 |
| - | - | - | 138 | 153 |
| - | - | - | NS | 151 |
| - | - | NS | NS | 152 |
| - | - | NS | NS | 154 |
| - | - | NS | NS | 156 |
| - | - | NS | NS | 158 |
| - | - | NS | NS | 159 |
| NOT SEEN/ TOTAL TARGETS | 2/8 | 3/13 | 10/39 | 15/40 |

- = Not Imaged

NS = Not Seen

The stated number under each pass denotes target identification on imagery.

Polaris V and A-3

The one pass that did image Polaris V standing off the iceberg was pass 5, shown in Figure III-25. Polaris V and A-3 were imaged in the extreme near range (targets 55 and 54, respectively) which roughly corresponds to their noted position at that time (1548 GMT). Additional targets were detected 600-700 m north of the ship. Targets are also evident about 2 km to the east of Polaris V and A-3. No surface information was collected on these targets, but oblique photographs taken from AES NDZ show a total of five icebergs shaped in a "U" pattern extending eastwards from close to the location of Polaris V and A-3.

Iceberg B008 and Ice String

Three passes (5, 7, and 8) imaged the very large iceberg, B008, and adjacent ice string. In all three passes the iceberg and string were clearly identifiable on the basis of their shape. Both features saturated the imagery. However, for point targets in close proximity to either of these features, differentiation between them was a problem. The iceberg and string targets had some streaking in azimuth as did the smaller targets. In many cases the signatures blended together into one so that they could no longer be separated and individually resolved.

An analysis of the 17 targets identified from the oblique photography of the large iceberg and string is shown in Table III-26. The results show that 50% of the bergy bit targets (10-20 m) were detected and 33% of the growlers (<10 m) could be identified. These numbers are related to the azimuthal smearing and blending of the signatures of some of these targets. Clearly this smearing reduces the possibility of separating targets in close proximity to one another.

It appears that the smearing and blending of closely spaced iceberg signatures was the principle factor in reducing the detection ratios.

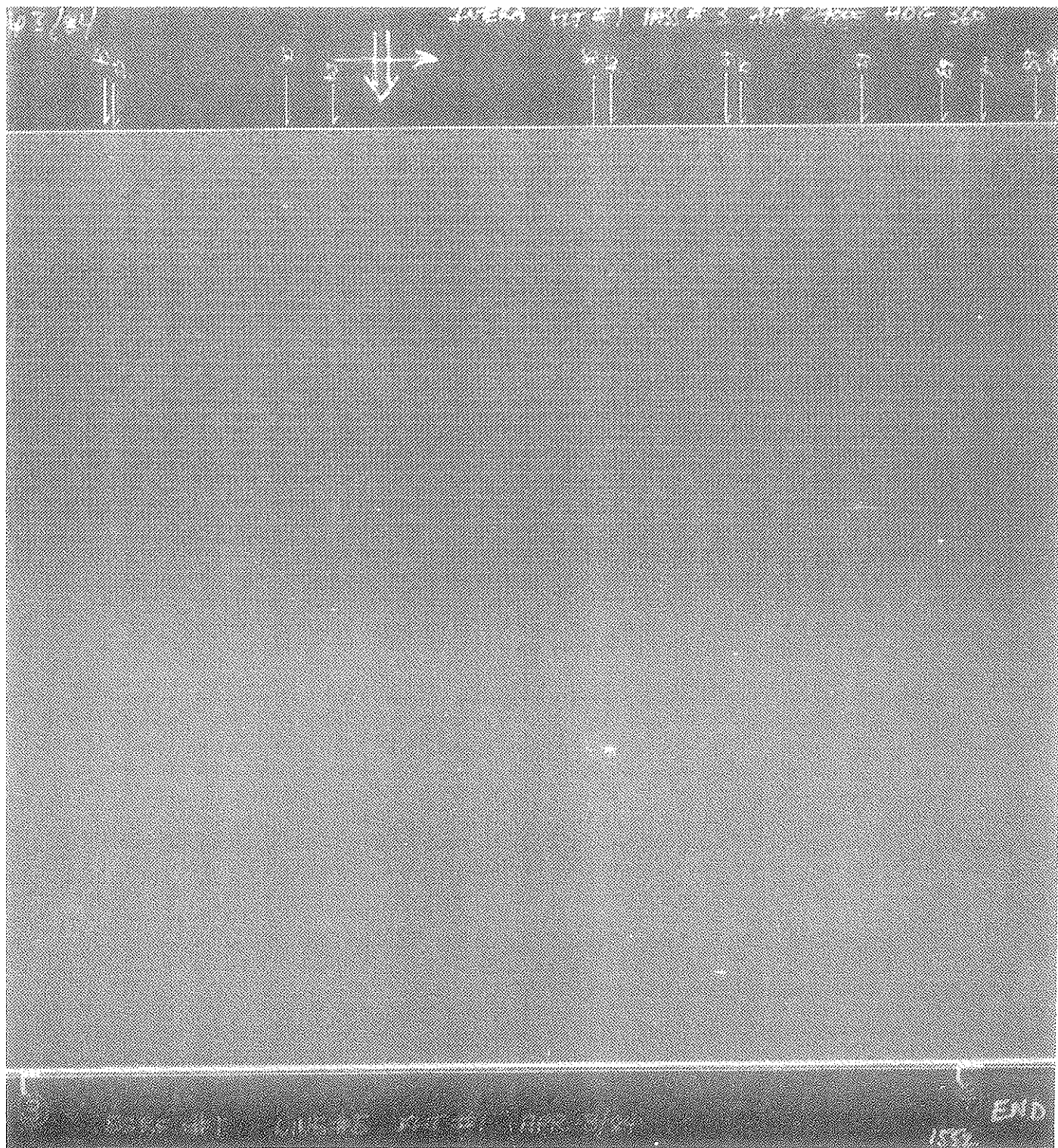


Figure III-25. STAR-1 SAR, flight 1 pass 3, 3 April 1984
(scale 1:250,000).

TABLE III-26

STAR-1 SAR Target Analysis, Flight 1

| Target Number | Size Category | Pass Number ^a | |
|------------------|--------------------|--------------------------|-----|
| | | 5 | 7 |
| 1 | SB | P | P |
| 2 | BB | P | P |
| 3 | BB | A | P |
| 4 | BB | P | P |
| 5 | BB | A | A |
| 6 | G | P | P |
| 7 | G | A | P |
| 8 | BB | A | A |
| 9 | BB | A | A |
| 10 | BB | P | P |
| 11 | BB | P | P |
| 12 | SB | P | P |
| 13 | BB | A | A |
| 14 | G | A | A |
| 15 | G | A | A |
| 16 | G | A | A |
| 17 | G | A | A |
| <hr/> | | | |
| <u>TOTALS</u> | Small Berg (SB) | P - 2 | 2 4 |
| | | A - 0 | 0 0 |
| | Bergy Bit (BB) | P - 4 | 5 9 |
| | | A - 5 | 4 9 |
| | Growler (G) | P - 1 | 2 3 |
| | | A - 5 | 4 9 |

^a P - Present

A - Absent

III.3.3 AES SLAR

Several passes that imaged the two sets of verified targets were obtained between 1402 and 1707 GMT. In general, the image background was grey to dark grey, and very uniform in tone regardless of aspect angle. This was the result of the light wind and wave regime throughout the flight. With the exception of lines 12 and 13, no ocean background clutter was observed. As a result, smaller, fainter targets were more evident. They had enough contrast with the background to warrant further investigation with an eyepiece to confirm their identification.

The flight line particulars and general comments on the imagery are summarized in Table III-27. The reproduced imagery had specks on it, and although most of these false targets were obvious, some had to be resolved with an eyepiece.

Polaris V and Iceberg A-3

Polaris V was positioned to the north of A-3 during the flight period which permitted identification of the two targets. However, the slight difference in the size and shape of their signatures would have been insufficient to differentiate them on that basis alone. It was apparent from its location relative to A-3 that Polaris V was located in a NE-to-NW orientation with respect to the iceberg, at a distance measured between 375 and 500 m, which agrees with surface information reports.

A very small, bright target (discussed later as the "mystery target" was detected near the Polaris V on passes 8 and 14, which were at 1519 and 1706 GMT respectively. Two additional small targets were detected east of Polaris V and A-3 on on passes 6 and 10. Line 8 recorded one of the targets, whereas neither appeared on line 14. These targets were too far away to be observed from the Polaris V, but they may have been growlers calved earlier from A-3. Table III-28 lists the depression angles and resolution cell sizes in which Polaris V and A-3 were detected. In general the angles were quite large and the resolution cell was larger than the targets, except for pass 14. In either case the lower depression angle had no effect on detectability of either target. The lack of shape in the signature resulted from the larger resolution cell size which the targets enlarged to fill. The improved resolution on pass 14 was insufficient to indicate any shape for either target.

B008 and Ice String

It was possible to track the relative movement of B008 and the ice string adjacent to it from 1413GMT through to 1656GMT. The oblique photographs taken at 1413GMT and 1423GMT were matched to the respective lines, and it was

TABLE III-27
AES SLAR Flight Line Particulars, 3 April 1984

| Pass No. | Altitude (ft) | Heading (°) | Start (GMT) | Finish (GMT) | Comments |
|----------|---------------|-------------|-------------|--------------|---|
| 1 | 10,000 | 270 | 1353 | 1356 | Polaris and A-3 in blind zone under aircraft. B008 not imaged. Imagery dirty with specks in reproduction. |
| 2 | 10,000 | 005 | 1402 | 1405 | Polaris and A-3 not imaged as line started north of their position. B008 outside of range. |
| 3 | 10,000 | 090 | 1410 | 1415 | Polaris and A-3 beyond range. B008 imaged. Oblique photography of B008 obtained at 1413Z. |
| 4 | 10,000 | 226 | 1420 | 1427 | Line completed before Polaris and A-3 imaged. B008 imaged + oblique photography (at 1423Z) obtained. |
| 5 | 10,000 | 270 | 1436 | 1439 | Polaris and A-3 imaged on right side. B008 beyond range. |
| 6 | 10,000 | 358 | 1444 | 1449 | Polaris and A-3 imaged on right side. B008 beyond range. |
| 7 | 10,000 | 090 | 1455 | 1503 | Polaris and A-3 beyond range. B008 imaged on right side. |
| 8 | 10,000 | 228 | 1509 | 1519 | Polaris, A-3 and B008 imaged on right side. |
| 9 | 10,000 | 226 | 1535 | 1541 | Line completed before Polaris and A-3 imaged. B008 imaged on right side. |
| 10 | 10,000 | 226 | 1555 | 1607 | Polaris, A-3 and B008 all imaged on right side. |
| 11 | 5,000 | 340 | 1627 | 1632 | Line started after Polaris and A-3 passed and B008 beyond range. |
| 12 | 5,000 | 090 | 1637 | 1647 | Polaris and A-3 beyond range. B008 imaged on right. More sea clutter evident in background. |
| 13 | 5,000 | 228 | 1651 | 1659 | Line completed before Polaris and A-3 imaged. B008 imaged on right. Higher sea clutter on right side of of imagery, virtually none on the left. |
| 14 | 5,000 | 270 | 1703 | 1707 | B008 not imaged. Polaris and A-3 on right side. Sea clutter now reduced to zero, background is dark grey. |

possible to track the 17 selected targets through to 1600GMT. After this time the string became more U-shaped and the individual targets adjacent to it could no longer be tracked. By 1600GMT, five new targets were observed to the NE of B008 which were quite possibly growlers or bergy bits. They were of the same size and intensity as the other smaller bergy bit and growler targets within and adjacent to, the string. A larger target was found to the NE of B008 by 1643GMT, which was probably a small iceberg which had calved and moved away. These targets were detected on subsequent passes during which B008 was imaged.

A comparison of the targets showed that small ice-floes could not be differentiated from the iceberg targets on the imagery. Oblique photographs show the targets to the west of the string to be of the growler and bergy bit size range, but these may have been small floes.

B008 was clearly identifiable on the imagery by its hourglass shape and some shadows within the target. The ice string had a fainter, more diffused signature which did not show any individual targets within it. Table III-29 summarizes the depression angle and azimuthal resolution cell of the iceberg and the string. B008 was 8 to 30 times larger than the resolution cell.

The results of the analysis of the presence or absence of the 17 targets is shown in Table III-30. Small iceberg targets were detected 100% of the time, bergy bits 50%, and growlers under 10 m could not be seen at all. The growlers are an order of magnitude smaller than the azimuth resolution.

III.3.4 IIP SLAR

A total of 13 passes out of the 25 flown on this day were analysed in conjunction with surface targets. The image background was uniformly grey to dark grey in the near range, and there was a noticeable dropoff to almost black in the far range of both sides. On three of the passes (2, 5, and 8), the background on the right side had a cloud-like texture and contained some fuzzy specular returns. These did not extend over the entire pass, and it was thus concluded that the returns were from local rain cells. Their effect on small target detectability could not be established quantitatively, but smaller targets did not contrast as well as in other passes.

Flight line particulars for the analysed lines are contained in Table III-31. The reproduced imagery required an eyepiece to resolve dust from real targets.

TABLE III-28

Depression Angle and Azimuth Cell Size for Detected Polaris V
and A-3 on AES SLAR, 3 April 1984

| Pass | <u>Polaris V</u> (1200 m ²) | | A-3 (3440 m ²) | |
|------|---|-----------------------------|----------------------------|-----------------------------|
| | Depression Angle (°) | Cell Size (m ²) | Depression Angle (°) | Cell Size (m ²) |
| 5 | 22.5 | 1992 | 23.9 | 1965 |
| 6 | 14.2 | 3261 | 14.1 | 3288 |
| 8 | 12.5 | 3726 | 12.0 | 3861 |
| 10 | 13.2 | 3510 | 13.7 | 3375 |
| 14 | 22.1 | 1014 | 22.1 | 1014 |

TABLE III-29

Depression Angle and Azimuth Cell Size for Detected B008
and Ice String, AES SLAR, 3 April 1984

| Pass | B008 (42786 m ²) | | Ice String | |
|------|------------------------------|-----------------------------|----------------------|-----------------------------|
| | Depression Angle (°) | Cell Size (m ²) | Depression Angle (°) | Cell Size (m ²) |
| 3 | 20.6 | 2193 | 21.8 | 2058 |
| 4 | 29.6 | 1452 | 30.1 | 1419 |
| 7 | 12.7 | 3645 | 11.9 | 3915 |
| 8 | 14.3 | 3240 | 14.8 | 3105 |
| 9 | 15.3 | 3000 | 15.8 | 2904 |
| 10 | 15.8 | 2904 | 16.4 | 2802 |
| 12 | 5.5 | 4254 | 5.5 | 4254 |
| 13 | 8.7 | 5379 | 8.7 | 5379 |

TABLE III-30
AES SLAR Target Analysis, 3 April 1984

| Target Number | Size Category | Pass Number ^a | | | | | | |
|-----------------------|------------------|--------------------------|---|---|---|---|----|--------------|
| | | 3 | 4 | 7 | 8 | 9 | 10 | |
| 1 | SB | P | P | P | P | P | P | |
| 2 | BB | A | A | A | P | P | P | |
| 3 | BB | A | A | P | A | P | P | |
| 4 | BB | P | A | P | A | A | A | |
| 5 | BB | A | A | A | A | A | A | |
| 6 | G | A | A | A | A | A | A | |
| 7 | G | A | A | A | A | A | A | |
| 8 | BB | A | A | A | P | P | A | |
| 9 | BB | P | P | P | P | P | P | |
| 10 | BB | A | A | A | P | P | A | |
| 11 | BB | P | A | P | P | P | P | |
| 12 | SB | P | P | P | P | P | P | |
| 13 | BB | P | P | A | P | P | A | |
| 14 | G | A | A | A | A | A | A | |
| 15 | G | A | A | A | A | A | A | |
| 16 | G | A | A | A | A | A | A | |
| 17 | G | A | A | A | A | A | A | |
| <u>Totals</u> | | | | | | | | <u>Total</u> |
| Small Iceberg (SB) | P- | 2 | 2 | 2 | 2 | 2 | 2 | 12 |
| | A- | 0 | 0 | 0 | 0 | 0 | 0 | 0 |
| Bergy Bits (BB) | P- | 4 | 2 | 4 | 6 | 7 | 4 | 27 |
| | A- | 5 | 7 | 5 | 3 | 2 | 5 | 27 |
| Growlers (G) | P- | 0 | 0 | 0 | 0 | 0 | 0 | 0 |
| | A- | 6 | 6 | 6 | 6 | 6 | 6 | 6 |

^a P - Present
A - Absent

TABLE III-31
IPP Flight Line Particulars, 3 April 1984

| Pass No. | Altitude (ft) | Heading (°) | Start (GMT) | Finish (GMT) | Comments |
|----------|------------------|----------------|----------------|-----------------|--|
| 2 | 4,000 | 090 | 1438 | 1443 | <u>Polaris</u> and A-3 imaged on right. Background on right looks like clouds. Drop-off in background to black on outer half of imagery on both sides. |
| 3 | 4,000 | 320 | 1446 | 1451 | <u>Polaris</u> and A-3 beyond range. B008 imaged on right. Drop-off in background on right side outer half to black. Imagery very dirty. |
| 4 | 4,000 | 175 | 1455 | 1459 | <u>Polaris</u> and A-3 imaged on right. B008 beyond range. Imagery very dirty. |
| 5 | 4,000 | 355 | 1504 | 1512 | <u>Polaris</u> and A-3 imaged on left. B008 on right side. Cloud-like background on right side. Fall-off to black background on outer half of both sides. |
| 7 | 4,000 | 180 | 1516 | 1521 | <u>Polaris</u> and A-3 imaged on left side. Left side dark. Right side has some wave patterns, but these are blurred and fuzzy. |
| 8 | 4,000 | 360 | 1523 | 1530 | <u>Polaris</u> and A-3 on left. Best on right side. Cloud-like background on right side especially in near range line. |
| 10 | 4,000 | 360 | 1543 | 1549 | <u>Polaris</u> and A-3 on left, B008 on right. Cloud-like background on right side imagery. Both sides have background becoming black for outer half of imagery. |
| 11 | 4,000 | 165 | 1554 | 1559 | <u>Polaris</u> and A-3 on left. B008 beyond range. Similar drop-off in background as with other passes. |
| 13 | 8,000 | 260 | 1621 | 1626 | <u>Polaris</u> and A-3 on left. B008 not imaged. Background has become dark. |
| 15 | 8,000 | 310 | 1636 | 1641 | <u>Polaris</u> and A-3 on left. B008 on right. Some specular returns from waves especially on left imagery. |
| 16 | 8,000 | 185 | 1643 | 1647 | <u>Polaris</u> and A-3 on left. B008 beyond range. Background is dark grey. |
| 17 | 8,000 | 045 | 1653 | 1658 | <u>Polaris</u> and A-3 on left. B008 not imaged. Background is dark grey with no ocean background. |
| 19 | 8,000 | 090 | 1718 | 1722 | <u>Polaris</u> and A-3 on left. B008 beyond range. Dark grey background with no detail. |

Polaris V and Iceberg A-3

Both targets were visible as bright white targets against the subdued background. The range of depression angles and resolution cell sizes for relevant passes are summarized in Table III-32. In general, they were imaged in near-to mid-range at depression angles between 7.2 and 23.0 degrees. No noticeable effect of increasing depression angle was found for either target. The resolution cell did appear to affect the signature of A-3 in terms of shape information. Passes 2, 4, 7, 11, 13, 16, and 17 showed some shape to the A-3 signature, enough to identify it as being an iceberg. If the cell size was about 75% or less than the size of the iceberg the signature had shape, with one exception (pass 5).

The signature of Polaris V remained almost the same for all the passes regardless of depression angle or resolution cell. No identifying shape characteristic could be found on any of the passes.

A small target was detected on many of the IIP passes at both altitudes. The target appeared as a distinct but faint white signature located between Polaris V and A-3 at a measured distance of about 50 m. The target was seen on passes 7, 8, 11, 13, 15, 17, and 19 but was not seen on passes 4, 5, 10, and 16. Aspect angle may have some effect here as 4, 5, and 10 imaged the targets from flight lines on the east, looking west. This target was investigated in more detail and is reported later under the heading "mystery" target.

Some additional small targets were observed to the east of Polaris V and A-3, but no surface information was available. It is believed these are the same two targets appearing in some of the AES passes. Two targets were observed about 75 m west of A-3 on line 13. The next two passes (lines 15 and 16) did not show the targets while passes 17 and 19 showed a small target about 75 m to the east of A-3. There is no record of these possible growlers coming off A-3 nor their subsequent history. These passes occurred between 1623 and 1719GMT.

B008 and Ice String

The large iceberg and ice string were imaged on six passes between 1440 and 1640 GMT. These matched closely to the AES imaging times, so it was possible to analyse four of the lines to 1547GMT for the detection of the 17 targets identified around the ice string. The results are summarized in Table III-23 for presence and absence of targets. There was a 100% detection of small iceberg targets and a 66% detection for bergy bits. The detection of growlers was not

TABLE III-32

Depression Angle and Cell Size
for Polaris V, A-3 and B008 on IIP SLAR, 3 April 1984

| PASS | Polaris V (1200 m ²) | | A-3 (3440 m ²) | | B008 (42,768 m ²) | |
|------|----------------------------------|--------------------------------|----------------------------|--------------------------------|-------------------------------|--------------------------------|
| | DEPRESSION ANGLE (°) | CELL SIZE (m ²) | DEPRESSION ANGLE (°) | CELL SIZE (m ²) | DEPRESSION ANGLE (°) | CELL SIZE (m ²) |
| 2 | 15.2 | 1260 | 18.0 | 1065 | 3.7 | 5073 |
| 3 | - | - | - | - | 7.7 | 2451 |
| 4 | 18.0 | 1065 | 18.0 | 1065 | - | - |
| 5 | 7.9 | 2385 | 8.0 | 2352 | 3.7 | 5073 |
| 7 | 11.0 | 1719 | 10.8 | 1752 | - | - |
| 8 | 7.2 | 2619 | 7.4 | 2553 | 3.8 | 5007 |
| 10 | 7.2 | 2619 | 7.5 | 5037 | 3.6 | 5208 |
| 11 | 7.4 | 2553 | 8.4 | 2253 | - | - |
| 13 | 16.0 | 2388 | 15.2 | 2517 | - | - |
| 15 | 9.5 | 3969 | 9.5 | 3969 | 6.4 | 5910 |
| 16 | 23.0 | 1686 | 22.1 | 1749 | - | - |
| 17 | 11.5 | 3306 | 12.0 | 3174 | - | - |
| 19 | 13.4 | 2844 | 13.7 | 2778 | - | - |

TABLE III-33

IIP SLAR Target Analysis, 3 April 1984

| Target Number | Size Category | | Pass | | Number ^a | | |
|------------------|------------------|------------|------|---|---------------------|----|--------|
| | | | 3 | 5 | 8 | 10 | |
| 1 | | SB | P | P | P | P | |
| 2 | | BB | P | P | P | P | |
| 3 | | BB | P | P | A | P | |
| 4 | | BB | P | P | P | P | |
| 5 | | BB | A | P | A | P | |
| 6 | | G | A | A | A | A | |
| 7 | | G | A | A | A | A | |
| 8 | | BB | P | A | A | A | |
| 9 | | BB | A | P | P | A | |
| 10 | | BB | P | P | P | A | |
| 11 | | BB | P | P | P | A | |
| 12 | | SB | P | P | P | P | |
| 13 | | BB | A | A | P | P | |
| 14 | | G | A | A | A | A | |
| 15 | | G | A | A | P | A | |
| 16 | | G | A | A | A | A | |
| 17 | | G | A | A | A | A | |
| Totals | Small Iceberg | P- | 2 | 2 | 2 | 2 | Total |
| | | (SB) A- | 0 | 0 | 0 | 0 | 8 0 |
| | Bergy Bit | P- | 6 | 7 | 6 | 5 | 24 |
| | | (BB) A- | 3 | 2 | 3 | 4 | 12 |
| | Growler | P- | 0 | 0 | 1 | 0 | 1 |
| | | (G) A- | 6 | 6 | 5 | 6 | 23 |

^a P - Present
A - Absent

much better than AES. With the exception of line 3, all the targets were imaged from the same aspect angle and had nearly the same depression angle and cell size relationships. Line 3, which had similar statistics, imaged the targets at a greater depression angle (7.7° versus $3.6-3.8^{\circ}$) but with about one-half the resolution cell size. These limited data suggest that within the ranges of these variables there was not much effect on the detection of bergy bit targets.

B008 was nearly an order of magnitude larger than the resolution cell so its shape and signature allowed its identification.

III.3.5 MARS SLAR

MARS flew the area about 3 1/2 hours after the completion of the AES mission. The flight particulars for interpreted lines are shown in Table III-34. As with the other aircraft, two altitudes and four aspect angles were flown in a regular box pattern. The imaged background was dark grey with no texture or detail within it. The imagery looked more similar to AES and IIP than that of April 2. Presumably this is because of the near absence of waves or winds, which continued to diminish after the earlier flights.

The pattern of flight lines was such that Polaris V and A-3 were imaged on every pass, whereas B008 was seen on only one of the lines. It was impossible to determine the distribution of targets around the latter iceberg as there were no photographs or surface data available.

Polaris V and A-3

The ship was still to the north of A-3 about 500 m away during the mission. The only observation of note from the surface data log was that the iceberg was actively rolling and turning at 2107GMT, just before the mission started. There is no record of any growlers calving off the iceberg at that time.

Both Polaris V and A-3 appeared as medium-white targets on all passes. Table III-35 shows the depression angles and cell sizes for each target. The relatively large depression angle and range of cell sizes do not appear to have affected iceberg detectability.

No signature differences between Polaris V and A-3 were found on any of the passes and their relative sizes were almost always the same. These targets filled only one or two cell sizes which was insufficient to show shape.

TABLE III-34

MARS Flight Line Particulars, 3 April 1984

| Pass No. | Altitude (ft) | Heading (-) | Start (GMT) | Finish (GMT) | Comments |
|----------|------------------|----------------|----------------|-----------------|---|
| 2 | 12,000 | 180 | 2114 | 2117 | <u>Polaris and A-3 on right.</u> Background is dark grey with no detail. Numerous specular reflections appearing as dashes oriented in range. |
| 3 | 12,000 | 270 | 2123 | 2127 | <u>Polaris and A-3 on right.</u> Background similar to line 2. |
| 4 | 12,000 | 360 | 2137 | 2141 | <u>Polaris and A-3 on right.</u> B008 beyond range. Similar background to line 2. |
| 5 | 12,000 | 135 | 2146 | 2150 | <u>Polaris and A-3 on right.</u> B008 on left at extreme range. Similar background to line 2. |
| 6 | 12,000 | 180 | 2154 | 2156 | <u>Polaris and A-3 on right.</u> B008 not imaged. Similar background to line 2. |
| 7 | 12,000 | 270 | 2200 | 2205 | <u>Polaris and A-3 on right.</u> Right side has dash-like returns as for line 2 but the left now does not. |
| 8 | 12,000 | 360 | 2210 | 2215 | <u>Polaris and A-3 on right.</u> B008 beyond range. |
| 9 | 12,000 | 135 | 2218 | 2223 | As for line 8. |
| 10 | 6,000 | 180 | 2230 | 2233 | <u>Polaris and A-3 on right.</u> Appears to be many more targets in the area. Background virtually black. |
| 11 | 6000 | 270 | 2237 | 2240 | <u>Polaris and A-3 on right.</u> Some sea clutter evident. |

TABLE III-35

Depression Angle and Cell Size for Polaris V and A-3
on MARS SLAR, 3 April 1984

| Pass | <u>Polaris V (1200 m²)</u> | | <u>A-3 (3440 m²)</u> | |
|------|---------------------------------------|--------------------------------|---------------------------------|--------------------------------|
| | Depression Angle (°) | Cell Size (M ²) | Depression Angle (°) | Cell Size (m ²) |
| 2 | 18.3 | 2682 | 19.0 | 2568 |
| 3 | 27.1 | 1740 | 28.6 | 1632 |
| 4 | 21.0 | 2304 | 22.0 | 2196 |
| 5 | 17.4 | 2826 | 18.8 | 2604 |
| 6 | 10.2 | 4878 | 10.5 | 4752 |
| 7 | 12.0 | 4140 | 12.8 | 3888 |
| 8 | 9.8 | 5100 | 10.2 | 4920 |
| 9 | 8.6 | 5802 | 8.9 | 4752 |
| 10 | 11.5 | 2625 | 12.2 | 2484 |
| 11 | 31.8 | 1170 | 34.6 | 1098 |

Over the course of the mission A-3 may well have been calving bergy bits and even growlers. The first pass 2 shows two small targets located between 750 and 1000 m from Polaris V and A-3. The progression of these targets and others from line to line are listed below:

- 2115 GMT Line 2: Two small targets 750-1000 m east of Polaris V and A-3.
- 2123 GMT Line 3: Same two targets as pass 2 plus a third to the ENE of Polaris V about 2 km away.
- 2138 GMT Line 4: Same two targets as in pass 2 but there are now two targets at position noted in pass 3.
- 2147 GMT Line 5: Same as 4 with slightly different pattern.
- 2155 GMT Line 6: Same as 4 with a new target between Polaris V and A-3.
- 2203 GMT Line 7: Same as 5, new target not seen.
- 2212 GMT Line 8: Same as 7 except now there are four discrete targets in place of two ENE of Polaris V. More point targets to the south and north of area.
- 2222 GMT Line 9: Targets to the east not seen. More point targets to the west and east.
- 2231 GMT Line 10: (Lower altitude) Many more small point targets in between, and around, Polaris V and A-3. They are smaller on the imagery than previous passes probably because of the smaller cell sizes.
- 2239 GMT Line 11: No targets between Polaris V and A-3. Similar target distributions to that seen on line 10.

A considerable difference was noticed in the imagery collected at the lower altitude. There were many more point targets around the ship and iceberg which were not seen on the higher altitude passes. It is not clear whether these targets had always been there or whether significant calving had occurred between passes 9 and 10, which were 9 minutes apart. Another cause may have been an increase in sea clutter. Without ground data at this time on the specifics of possible calving and movement it is difficult to draw definite conclusions. However, the significantly increased number of small point targets for all the lower altitude passes suggests that more small targets were detected at the lower altitudes than at the higher altitudes.

III.4 ANALYSIS OF APRIL 5 IMAGERY

The four aircraft flew an operational type of mission over a given test area bounded by 46°40'N, 47°30'W, 47°30'N, and 49°00'W (Figure III-26). Each team chose their flight pattern, swath width, and altitude from experience gained in the previous research missions. A far greater number of icebergs had entered the test area compared to the flights on 02 and 03 April, but they were not uniformly distributed; the south and southwest areas were ice free whereas the north and northeast had numerous icebergs (of all sizes up to more than 200 m length) and plumes of sea-ice floes. The imagery collected is summarized in Table III-36.

For this preliminary study two to four passes by each aircraft were examined carefully, usually at 1:250,000 scale, for direct comparison of target detectability. Much effort was required to be satisfied that the targets documented by low-level photography and surface vessel visits were identified in the imagery. The difficulty arose as a result of the time differences and relative motion of the icebergs. AES, IIP, and STAR-1 flew 2-5 hours before the air photography, whereas MARS flew 2-4 hours after. The Polaris V crew worked long hours but its best documentation of small targets was carried out between the flights; these targets were in close proximity and differential movement of the pieces is evident, making reidentification difficult from pass to pass as well as from aircraft to aircraft.

III.4.1 AVAILABLE SURFACE INFORMATION

The King Air aircraft photographed 22 icebergs, two sea-ice plumes, three oil rigs, and three vessels between 1737 and 1812 GMT (see Figure III-26).

The Polaris V visited and documented 36 targets, none of which were photographed by the air-photo aircraft, from 1005 to 2114 GMT. These locations are shown in Figure III-26 by alphabetical identification, abbreviated from the Polaris V identifier which included the date, e.g., A-5 or J-5.

The targets from both sources are listed in Table III-37 with a brief description and dimensions (by measuring length and width from the air photographs or taken from the Polaris V data sheets).

The hourly wind and wave data collected by the ship show a changeable wind regime and a lagging trend in the wave direction during the overflight period. Table III-38 is reproduced from the surface log sheets. Often the wind and wave directions were 40-50° different, and occasionally 80° different. Because the aircraft flew their lines in cardinal directions, the relationship of radar look direction to wave

TABLE III-36
Imagery for 5 April 1984

| Pass no | Altitude (FT) | Heading (o) | Swath width a (KM) | Start (GMT) | Finish (GMT) | General Comments |
|---------------|------------------|----------------|-----------------------|----------------|-----------------|------------------------------|
| <u>STAR-1</u> | | | | | | |
| 1 | 29,000 | 180 | 50 | 1410 | 1422 | Used for study. |
| 2 | 29,000 | 360 | 50 | 1429 | 1444 | Used for study. |
| 3 | 29,000 | 180 | 50 | 1453 | 1503 | Equipment problems. |
| 4 | 29,000 | 360 | ~12 | 1522 | 1538 | |
| 5 | 29,000 | 180 | ~12 | 1522 | 1601 | |
| 6 | 29,000 | 360 | ~12 | 1615 | 1632 | |
| <u>IIP</u> | | | | | | |
| 1 | 8,000 | 082 | 25 | 1318 | 1333 | Used for study. |
| 2 | 8,000 | 274 | 25 | 1337 | 1353 | Used for study. |
| 3 | 8,000 | 080 | 25 | 1358 | 1409 | Used for study. |
| 4 | 8,000 | 275 | 25 | 1418 | 1432 | |
| 5 | 8,000 | 080 | 25 | 1436 | 1450 | |
| 6 | 8,000 | 275 | 25 | 1453 | 1510 | |
| 7 | 8,000 | 080 | 50 | 1516 | 1530 | |
| 8 | 8,000 | 354 | 50 | 1531 | 1533 | |
| 9 | 8,000 | 277 | 50 | 1536 | 1627 | |
| <u>AES</u> | | | | | | |
| 1 | 9,000 | 082 | 25 | 1407 | 1421 | Used for study. |
| 2 | 9,000 | 277 | 25 | 1429 | 1447 | Used for study. |
| 3 | 9,000 | 080 | 25 | 1456 | 1510 | Used for study. |
| 4 | 9,000 | 278 | 50 | 1518 | 1535 | |
| 5 | 9,000 | 080 | 100 | 1551 | 1605 | Target area very small. |
| 6 | 9,000 | 354 | 100 | 1614 | 1629 | Target area very small. |
| <u>MARS</u> | | | | | | |
| 1 | 12,000 | 083 | 25* | 2028 | 2047 | Used for study. |
| 2 | 12,000 | 281 | 25* | 2052 | 2111 | Ocean bright in left swath. |
| 3 | 12,000 | 085 | 25* | 2116 | 2135 | Used for study. |
| 4 | 12,000 | 280 | 25* | 2140 | 2159 | Ocean bright in left swath. |
| 5 | 6,000 | 086 | 25* | 2208 | 2225 | |
| 6 | 6,000 | 276 | 25* | 2231 | 2245 | |
| 7 | 16,000 | 081 | 25+ | 2257 | 2316 | Ocean bright in right swath. |
| 8 | 16,000 | 280 | 25+ | 2320 | 2339 | |

a:

* Plus delay of 5 km

+ Plus delay of 10 km

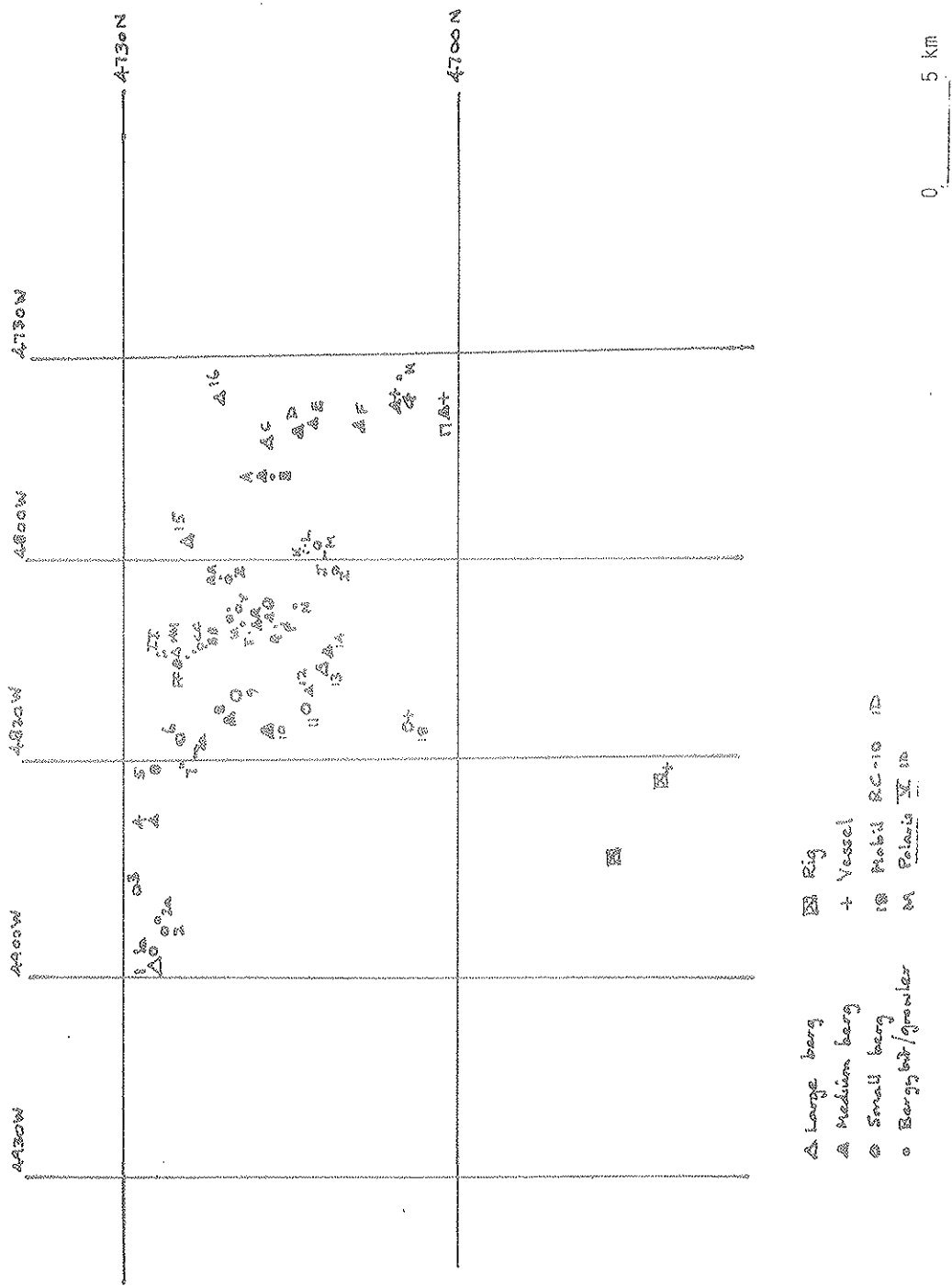


Figure III-26. Location of surface targets on 5 April 1984.

TABLE III-37
Targets Photographed and Visited on 5 April 1984

| Target ID | Type | Size(m) | Size Class a |
|-----------|--|-----------|-----------------|
| 1 | Tabular, blocky, steep sides, smooth | 205x93 | VL |
| 1a | Eroding dry-dock, irregular | 32x25 | S |
| 2 | Eroding breached dry-dock | 20x19 | S |
| 2a | Bergy bit | 10x7 | VS |
| 3 | Three pinnacles, irregular | 34x18 | S |
| 4 | Pinnacled block, triangular | 90x55 | M/L |
| 5 | Eroded block, pinnacles | 46x45 | S |
| 6 | Eroding dry-dock, rough surface | 37x24 | S |
| 7 | Growler, rounded | 7x4 | VS |
| 7a | Growler, two parts above water | 6x3 | VS |
| 7b | Growler | 6x4 | VS |
| 8 | Drydock, serrated, eroding | 96x78 | M/L |
| 9 | Drydock, blocky | 50x35 | M/S |
| 10 | Block, part smooth, gullies | 54x30 | M |
| 11 | Pinnacled, 2 parts | 49x48 | S/M |
| 12 | Tabular, serrated surface | 52x42 | M |
| 13 | Elongated dry-dock, pinnacled | 120x61 | L |
| 14 | Block, pinnacled | 56x41 | M |
| 15 | Pinnacled, 2 parts, smaller is blocky | 191x175 | VL |
| 16 | 2 parts, large smooth long dome, small pinnacle, in sea ice | 120x73 | L |
| 17 | 2 parts, under tow. Large, long serrated dome, small pinnacle. See H. | 77x38 | M |
| 18 | Under tow. Irregular breached block. | 37x17 | S |
| A | Tabular/spherical, serrated edges, smooth top | 42x21x7 | S |
| B | Bergy bit | | VS |
| C | Drydock, 3 parts, pinnacled | 108x60x35 | L |
| D | Pinnacled and dome section | 66x37x20 | M |
| E | Wedge, smooth, triangular | 54x42x16 | M |
| F | Drydock, wedge/dome | 70x70x25 | M |
| G | Pinnacle with slight dry-dock | 74x74x24 | M |
| H | Bergy bit, tabular. May be 17 later | x2.5 | VS |
| I | Drydock. 3 growlers to NE | 23x17x8 | S |

TABLE III-37: continued

| Target ID | Type | Size(m) | Size Class a |
|-----------|---|-----------|-----------------|
| J | 2 growlers | 4x 2x.5 | VS |
| | | 1.5x 1x.5 | VS |
| K | Group of 3 growlers; dimensions of one not given. | 4x 3x.8 | VS |
| | | 1.5x 1x.5 | VS |
| L | Bergy bit, serrated, between sea ice | 15x10x2 | VS |
| M | Textured, serrated | 30x20x3 | S |
| N | Growler, bobbing | 4x 3x.5 | VS |
| O | Pinnacled, large | | |
| P | Bergy bit | 5x 4x2.5 | VS |
| Q | Growler, bobbing | 3x 3x1 | VS |
| R | Tabular | 65x ?x12 | M |
| S | Growler, rough | 2x1.5x.75 | VS |
| T | Pinnacled, rough, 2 peaks | 15x 7x2 | VS |
| U | 2 bergy bits close together | 11x10x2 | VS |
| | | 8x 6x2 | |
| V | Wedge, eroded, sharp surfaces | 30x20x10 | S |
| W | Bergy bit, flat | 10x10x1 | VS |
| X | Bergy bit, weathered, 2 parts | 25x ?x3 | S |
| Y | Bergy bit, spherical, weathered, bobbing | 18x10x5 | S |
| Z | Drydock, wedge, rough surface | 25x 9x5 | S |
| AA | Growler | 6x 4x1 | VS |
| BB | 2 growlers in sea ice | 1x 1x.5 | VS |
| | | 1x.5x.5 | VS |
| CC | Drydock, smooth top, incised sides | 33x29x10 | S |
| DD | Growler, weathered | 1x 1x.3 | VS |
| EE | 2 growlers | 1x 2x.5 | VS |
| | | 1x 3x.5 | VS |
| FF | 20 growlers | | VS |
| GG | Multiple dry-dock, serrated | 25x20x4 | S |
| HH | Drydock, smooth surface | 40x30x20 | S |
| II | Many growlers in sea ice | 2x 2x.7 | VS |

a - Approximate classification: VS - growler and bergy bit
S - small iceberg
M - small-medium iceberg
L - medium-large iceberg
VL - large-very large iceberg

TABLE III-38

Hourly Weather and Environmental Data, 5 April 1984

| Time GMT | Primary Waves | | Secondary Waves | | Wind | | Temp. | | Cloud Height (m) | % Height | Vis (Naut mi.) | Ice Cond | |
|-------------|---------------|------------|-----------------|---------------|------------|----------------|------------|------------|------------------------|-------------|----------------------|-------------|-------------|
| | Height (m) | Dir (°) | Period (sec) | Height (m) | Dir (°) | Speed (kts) | Dir (°) | Air (°) | | | | | Sea (°C) |
| 1000 | 0.6 | 33 | 1 | 2.0 | 0 | 22 | 310 | -4.5 | -1.0 | 200 | 90 | >15 | 0/w |
| 1100 | 0.3 | 27 | 1 | 1.5 | 310 | 18 | 330 | -4.8 | -1.0 | 200 | 90 | >15 | 0/w |
| 1200 | 0.7 | 330 | 1 | 2.0 | 320 | 25 | 340 | -4.0 | -1.0 | 200 | 75 | >15 | 0/w |
| 1300 | 0.8 | 330 | 1 | 2.0 | 310 | 13 | 253 | -3.8 | -1.0 | 200 | 60 | >15 | 0/w |
| 1400 | 0.6 | 300 | 2 | 1.7 | 320 | 13 | 253 | -4.0 | -0.2 | 200 | 70 | >15 | 0/w |
| 1500 | 0.8 | 270 | 3 | 2.0 | 270 | 24 | 316 | -4.0 | -0.2 | 200 | 80 | >15 | 0/w |
| 1600 | 0.8 | 280 | 3 | 1.5 | 280 | 25 | 301 | -3.5 | -0.2 | 200 | 60 | >15 | 0/w |
| 1700 | 0.8 | 270 | 3 | 1.5 | 270 | 21 | 312 | -4.0 | -0.2 | 200 | 60 | >15 | 0/w |
| 1800 | 1.2 | 300 | 3 | 1.7 | 270 | 22 | 308 | -4.5 | -0.2 | 200 | 40 | >15 | 0/w |
| 1900 | 0.9 | 350 | 2 | 1.5 | 340 | 20 | 310 | -4.2 | -0.2 | 200 | 60 | >15 | 0/w |
| 2100 | 1.5 | - | 4 | 2.0 | 340 | 15 | 300 | -3.5 | -0.1 | dark | - | - | - |
| 0000 | 1.0 | - | 3 | 2.0 | 340 | 13 | 300 | -4.5 | -0.5 | dark | - | - | - |

direction was not usually perpendicular or parallel, and could vary during the mission.

III.4.2 STAR-1 SAR

All the STAR-1 lines were flown at 29,000 ft. on longitudes from $49^{\circ}20'W$ to $48^{\circ}20'W$ between 1410 and 1632 GMT. Passes 1 to 3 were planned to image all of the test area, but equipment problems during pass 3 resulted in no data for the northeast quadrant. These passes were on a 50-km swath width at 1:250,000 scale, passes 4 to 6 repeat pass 1 and part of pass 2 with a 12-km swath at 1:62,500 scale.

A tabulation of targets detected is given in Table III-39. The depression angle effect seems to be minor as the targets looked almost identical at the far range of pass 1 and near range of pass 2.

At 1:250,000 the SAR detected all the iceberg targets larger than bergy bits (such as iceberg 2). For the medium and larger icebergs the size of the target was roughly proportional to the target size, although the return did not often reflect the iceberg shape; few returns were L- or T-shaped or double. Typically the returns approached real scale in range but were elongated on both sides in azimuth, sometimes with a central brighter "core" indicating iceberg dimension. The contrast between ice, icebergs, vessels, and the ocean background was very good. None of the bright returns appeared to be wave spikes.

For targets smaller than 20 m across the detectability varied. Target N-5 ($4 \times 3 \text{ m}^2$) was imaged in pass 2 (target 58) whereas target 2a ($10 \times 7 \text{ m}^2$) was not apparent; of the bergy bits ($>10 \text{ m}$ length) five out of six were detected whereas the growlers ($<10 \text{ m}$ length) were detectable in 5 out of 12 cases. It is clear from the Polaris V notes that several of the growlers were bobbing and could, in effect, almost be submerged some of the time. In addition, relative to the radar viewpoint growlers and bergy bits may be hidden "behind" waves.

These small targets have a brightness and "crispness" so that they are, on the whole, distinguishable from the floes. However, the vessels in the scene do not have a recognizably different signature from the icebergs. The drilling rigs have a large bright return which is sufficiently different from icebergs and ships; sometimes the anchoring buoys are detectable in a recognisable pattern around them.

At a scale of 1:62,500 scale the SAR imagery shows returns from individual waves in a subdued, elongated pattern, but the contrast between target and ocean is reduced enough that it is not possible always to differentiate waves from growlers. For instance, the ice fragment 2a could be

TABLE III-39

STAR-1 Target Analysis for 5 April 1984

| Look Direction | Target ID | Other ID a | Pass | Pres- ence b | Size c | Tone d | Comments |
|-----------------------------|--------------|------------------|------|--------------------|-----------|-----------|--|
| Downwave cross-wind e | 40 | | 1 | P | VS | G | Comment for all passes: waves not imaged; smallest ice return brighter than brightest wave. Incidence angle effect, berg at far range in pass 1, near range in pass 2. |
| | 42 | 8 MB | 1 | P | M/E | W | |
| | 43 | | 1 | P | S | LG | |
| | 44 | 9 MB | 1 | P | S | W | |
| | 45 | 10 SB | 1 | P | S/E | W | |
| | 46 | 11 SB | 1 | P | S/E | W | |
| | 62 | 12 MB | 1 | X | | | |
| Downwave cross-wind | 76 | | 2 | P | VS | W | |
| | 75 | 8 MB | 2 | P | S | W | |
| | 74 | 9 BB | 2 | P | S/E | W | |
| | 70 | 10 MB | 2 | P | S/E | W | |
| | 69 | | 2 | P | S | W | |
| | 63 | 11 SB | 2 | P | S/E | W | |
| | 62 | 12 MB | 2 | P | S | W | |
| Downwave cross-wind | 1 | 1 VGB | 1 | P | L | W | Resolution effect with bergs of known dimension, pass 1 using wide swath, pass 4 at high resolution. |
| | 2 | 1a SB | 1 | P | VS | W | |
| | 4 | 2 SB | 1 | P | S | W | |
| | 11 | 3 SB | 1 | P | S | LG | |
| Downwave cross-wind | 93 | 1 | 4 | P | VL | W | |
| | 92 | 1a | 4 | P | VS/E | W | |
| | 94 | 2 | 4 | P | VS/E | W | |
| | 95 | 3 | 4 | P | S | W | |
| Downwave cross-wind | 3 | | 1 | P | M | W | Resolution effect with unknown bergs, passes as above. |
| | 5 | | 1 | P | S | LG | |
| | 6 | | 1 | P | M | W | |
| | 7 | | 1 | P | S | W | |
| | 8 | | 1 | P | M | W | |
| | 9 | | 1 | P | VS | W | |
| | 10 | | 1 | P | M | W | |
| | 12 | | 1 | P | M | W | |
| | 13 | | 1 | P | S | W | |
| | (103) | | 1 | A | | | |
| Downwave cross-wind | 96 | | 4 | P | E | W | |
| | 100 | | 4 | P | M/E | W | |
| | 101 | | 4 | P | SE | W | |
| | 102 | | 4 | P | S | W | |
| | 105 | | 4 | P | S/E | W | |

continued...

TABLE III-39: continued

| Look Direction | Target ID | Other ID a | Pass | Pres- ence b | Size c | Tone d | Comments |
|------------------------|--------------|------------------|-------|--------------------|-----------|-----------|--|
| | (9) | | 4 | A | | | |
| | 99 | | 4 | P | M/E | W | |
| | 97 | | 4 | P | M | W | |
| | 98 | | 4 | P | S/E | W | |
| | 103 | | 4 | P | VS/E | LG | |
| Downwave cross-wind | 59 | M SB | 2 | P | M | W | Large/Small targets verified by Polaris V. 206 could be L. |
| | 58 | N G | 2 | P | VS | LG | |
| | 206 | L BBB | 2 | P | VS | LG | |
| | 67 | O LB | 2 | P | L | W | |
| | 73 | R BB | 2 | P | L | W | |
| | 86 | T BB | 2 | P | S | W | |
| | 88 | X BB | 2 | P | VS | W | |
| | 191 | Y BB | 2 | P | VS | W | |
| | 193 | V SB | 2 | P | M/S | W | |
| | 195 | Z BB | 2 | P | M | W | |
| | 90 | W BB | 2 | P | VS | W | |
| | 192 | U BO(2) | 2 | P | VS | W | |
| | 197 | CCSB | 2 | P | M | W | |
| | 194 | - | 2 | P | VS/E | LG | |
| Downwind cross-wave | 60 | 14 | 2 MB | P | M | W | Other Mobil bergs. |
| | 61 | 13 | 2 LB | P | L | W | |
| | 98 | 15 | 2 VLB | P | VL | W | |

a - identifier on Mobil photography
(numbers) or Polaris V data
(letters)

b - P - present
A - absent
X - not in pass

c - VS - very small
S - small
M - medium
L - large
VL - very large
E - elongated

d - G - grey
LG - light grey
W - white

e - Looking 090, waves 270,
wind 316

southwest of target 94 (small iceberg 2) on pass 4, but there are three brighter returns there. None may be 2a if the growler was bobbing beneath the waves at that time.

This scale of imagery appears to be imaging more of the small targets (but these were not surface-verified), and the larger targets also are differentiated better. Target 93 (iceberg 1) shows a return with double indentation, for example, and the target size estimate can be made more readily, as given in Table III-40.

TABLE III-40

Target Size Estimate from STAR-1 Pass 4

| Iceberg no. | Size (m ²) | Target no. | Radar image size azim. | Range (m) |
|----------------|------------------------|---------------|---------------------------|--------------|
| 1 | 205x93 | 93 | 240 | 120 |
| 1a | 32x25 | 92 | 44 | 19 |
| 2 | 30x19 | 94 | 50 | 25 |
| 3 | 34x18 | 95 | 35 | 31 |

Resolution

An area of pass 1 wide-swath imagery with numerous targets (mostly icebergs with two small sea-ice plumes) was flown less than two hours later on pass 5 with high-resolution configuration. None of the icebergs were visited by the Polaris V or by the air-photo aircraft, so target size is unknown, but by comparison with other known targets there were about six icebergs of small and medium size, and about 25 bergy bits and growlers.

In the 12 x 9 km² area there were 29 targets detected on pass 1, with a resolution cell of 6 x 12 m², and 34 targets detected on pass 5 with a resolution cell of 6 x 6 m². Twenty-five of the targets are detected in both pass 1 and pass 5.

III.4.3 AES SLAR

AES flew five lines in the longitudinal direction at 9,000 ft altitude; passes 1 to 3 were at 1:250,000 with 25-km swath width, pass 4 at 1:500,000 with 50-km swath width, and pass 5 at 1:1,000,000 with 100-km swath width. The last pass, 6, was flown south to north at 1:1,000,000 (100-km swath) and covers much of the test area with the left swath. The mission lasted from 1407 to 1629 GMT.

Passes 1 to 3 with a 25-km swath width were the best quality of imagery whereas the later AES passes at 50-km and 100-km swath widths do not show the small targets, or even some of the medium-sized icebergs (see also the comments on IIP 100-km swath imagery on 06 April). Table III-41 documents the targets identified in passes 2 and 3.

Pass 1 covered the southern part of the test area only and its background tone is subdued. The right-looking swath covers the drilling rigs and other vessels, with the former identifiable as the larger returns. There are several small, crescent-shaped artifacts in the left swath, and only a few other faint targets, such as iceberg 18 and the M.V. Nordentor, which look similar. Some targets are not detectable, such as icebergs 17 and G-5, and the vessel Wimpey Sea Hunter. Pass 2 covered the central area of surface-verified icebergs, most of which were detected, although the elongation of scale along-track is such that care must be taken in cross-referencing the icebergs, especially those moving differentially. This was less of a problem in pass 3, although its imagery also was stretched; this pass covered the central and northern areas. The grey-tone range is better on pass 3 also, so that more targets are visible without magnification, and with the use of a magnifier many of the small and very small targets were detected (e.g. eight returns in the northern cluster of targets verified from Polaris V).

III.4.4 IIP SLAR

The mission was flown between 1317 and 1623 GMT (starting somewhat earlier than STAR-1), with all passes at 8,000 ft altitude. Passes 1 to 6 display a 25-km swath at a scale of 1:250,000 whereas pass 8 was flown at this scale from south to north.

The most useful imagery for the study was flown in passes 1 to 3, 7, and 9, which show the pertinent areas of known icebergs. The later 50-km swath images show only the medium and larger icebergs, so just the first three passes were documented, shown in Table III-42. The IIP identification for the targets is cross-referenced to both the STAR-1 and surface-verified iceberg identifiers.

Passes 1 to 3 show most of the identifiable targets larger than 30 m, although detection is difficult close to nadir where the imagery is affected by along-track banding, possibly caused by the antenna beam pattern. There is reasonable contrast between ocean background and ice targets. Targets in the 20-30 m class are not as reliably detected, as the returns are very small, and many would be missed or would be assumed to be pieces of sea ice. A magnifying glass and long scrutiny is required, even when a target location is known from other sources. For example, with a very careful

TABLE III-41
AES Target Analysis for 5 April 1984

| Look Direction | Target ID | Other ID a b | Pass | Pres- ence | Size | Tone | Swath | Comments |
|----------------------------|--------------|--------------------|------|---------------|------|------|-------|---|
| Cross- wave upwind | - | 40 | 2 | X | | | R | Ground-verified bergs seen also on STAR-1 |
| | - | 42 8 | 2 | X | | | R | |
| | - | 43 9 | 2 | X | | | R | |
| | - | 44 10 | 2 | X | | | R | |
| | 1 | 45 | 2 | P | VS/E | LG | R | Fuzzy |
| | 2 | 46 11 | 2 | P | S | LG | R | |
| | 3 | 62 12 | 2 | P | S | LG | R | Fuzzy |
| | 4 | 61 13 | 2 | P | M | W | R | Double return |
| | 6 | 60 14 | 2 | P | S | LG | R | |
| | 17 | 59 M | 2 | P | M | W | R | Double return-Polaris V |
| | 16 | 202 L | 2 | P | S | W | R | at berg. |
| | 7 | 67 0 | 2 | P | LE | LG | R | |
| | - | 58 N | 2 | A | | | R | |
| waves | | | | P | | | | Most apparent on R. swath from 5 km range to far range. |
| Cross- wave downwind | 33 | 12 | 3 | P | S | LG | R | Some of above opposite wind/wave. |
| | 34 | 13 | 3 | P | M | W | R | |
| | 36 | 14 | 3 | P | S | W | R | |
| | 47 | 59 M | 3 | P | L | W | R | Double return |
| | 44 | 58 N | 3 | P | VS | LG | R | |
| | 48 | 206 L | 3 | P | VS | LG | R | Double return, may be 2 growlers, L and K |
| | 45 | 98 15 | 3 | P | L | W | L | On edge of sea ice. |
| | 39 | 73 R | 3 | P | M | G | L | |
| | 37 | 86 T | 3 | P | S | G | L | |
| | 38 | 90 W | 3 | P | VS | G | L | |
| | 40 | 191 Y | 3 | P | VS | G | L | |
| | 41 | 192 U | 3 | P | VS | G | L | |
| | 42 | 193 V | 3 | P | S | LG | L | |
| | - | 195 Z | 3 | A | | | L | In sea-ice plume |
| | 45 | 197 CC | 3 | P | S | | L | |
| waves | | | | | | | | Much less apparent than pass 2. Overall image tone less dynamic, small bergs hard to see without magnifier. |
| | - | 1 1 | 3 | X | | | | Other Icebergs |
| | - | 95 3 | 3 | A | | | | |
| | 25 | 25 4 | 3 | P | M/E | LG | | |
| | 26 | 26 5 | 3 | P | S | W | | Near sea-ice |
| | 27 | 28 7 | 3 | P | VS | G | | |
| | 28 | 42 8 | 3 | P | M | LG | | |
| | 29 | 44 9 | 3 | P | S | W | | |

a - Identifier on Star-1 imagery.

b - Identifier is surface-truthed data.

Note: Other footnotes as in
Table III-37.

TABLE III-42
IIP Target Analysis for 5 April 1984

| Look Direction | Target ID | Other ID a b | Pass | Pres- ence | Size | Tone | Swath | Comments |
|-------------------|--------------|--------------------|------|---------------|------|------|-------|---------------------------------|
| | | | | | | | | Surface/Star-1 Truthed Bergs |
| Cross- wave | 1 | 1 | 1 | P | L | W/G | R | Triangular with shadow |
| Downwind | - | | 2 | A | | | R | |
| | - | | 3 | P | | | R | |
| | 3 | 25 | 4 | P | S | W | R | Shadow |
| | 5 | 26 | 5 | P | S | LG | R | |
| | 207 | 40 | | P | VS | G | R | |
| | 7 | 42 | 8 | P | L | W | R | Shadow |
| | 9 | 43 | 9 | P | M | W | R | |
| | 8 | 44 | 10 | P | E/M | W | R | |
| | - | 46 | 11 | X | | | R | |
| | 28 | 73 | R | P | L/E | W | R | Shadow |
| | 19 | 88 | X | P | M | W | R | |
| | 20 | 191 | Y | P | VS | G | R | |
| | 21 | 192 | U | P | VS | G | R | |
| | 22 | | | P | S | W | R | |
| | 23 | | | P | VS | G | R | Faint |
| | 24 | 86 | T | P | S/E | G | R | |
| | 26 | 193 | V | P | M | W | R | |
| | 2 | 194 | | P | VS | G | R | Very faint |
| | 35 | 195 | Z | P | M | W | R | Shadow |
| | 27 | 197 | CC | P | S | LG | R | |
| | 60 | 98 | 15 | P | VL | W | R | Double, shadow |
| Cross- wave | 137 | 45 | | P | VS | W | L | |
| Downwind | 136 | 46 | 11 | P | VS | W | L | |
| | 135 | 62 | 12 | P | S | W | L | |
| | 133 | 61 | 13 | P | M | W | L | L-shape return |
| | 132 | 60 | 14 | P | VS | LG | L | |
| | 129 | 57 | | P | S | LG | L | |
| | - | 58 | N | A | | | L | |
| | 126 | 59 | M | P | S | W | L | |
| | 128 | 206 | L | P | S | LG | L | |
| | 130 | 67 | O | P | S | LG | L | |
| | 131 | 73 | R | P | M | LG | L | |
| Cross- wave | 185 | 88 | X | P | S | G | R | Pale, near nadir |
| Downwind | - | 90 | W | X | | | | At nadir, not imaged |
| | - | 192 | U | X | | | | In altitude gap |
| | - | 193 | V | X | | | | " " |
| | - | 194 | | X | | | | " " |
| | - | 191 | Y | X | | | | " " |
| | - | 86 | T | X | | | | " " |
| | - | 195 | Z | X | | | | " " |
| | - | 197 | CC | X | | | | " " |

TABLE III-42: continued

| Look Direction | Target ID | Other ID | Pass | Presence | Size | Tone | Swath | Comments |
|-------------------------------|-----------|----------|------|----------|------|------|-------|----------|
| Cross-wave upwind | 161 | 45 | 3 | - | P | VS | G | L |
| | 162 | 42 | 8 | 3 | P | M | G | L |
| | 163 | 44 | 10 | 3 | P | S | G | L |
| | 164 | 46 | 11 | 3 | P | S | LG | L |
| | 167 | 62 | 12 | 3 | P | VS | LG | L |
| | 174 | 61 | 13 | 3 | P | M | W | L |
| | 175 | 60 | 14 | 3 | P | S | W | L |
| | 185 | 57 | | 3 | P | VS | G | L |
| | - | 58 | N | 3 | A | | | L |
| | 185 | 59 | M | 3 | P | S | W | L |
| | 165 | 43 | 9 | 3 | P | S | W | L |
| | - | 206 | L | 3 | A | | | L |
| | 177 | 67 | O | 3 | P | S | W | L |
| | 176 | 73 | R | 3 | P | L | W | L |
| | 179 | 86 | T | 3 | P | S | LG | L |
| | 178 | 88 | X | 3 | P | M | G | L |
| | 181 | 90 | W | 3 | P | VS | G | L |
| | - | 191 | Y | 3 | A | | | L |
| | 182 | 192 | U | 3 | P | VS | G | L |
| | 183 | 193 | V | 3 | P | S | W | L |
| | 180 | 197 | CC | 3 | P | M | G | L |
| | 184 | 195 | Z | 3 | P | M | LG | L |
| <u>Mobil/Polaris Visited</u> | | | | | | | | |
| <u>Bergs to East of Above</u> | | | | | | | | |
| Cross-wave downwind | 200 | 98 | 15 | 2 | P | VL | W | R |
| | 201 | | 16 | 2 | P | VL | W | R |
| Cross-wave upwind | - | | A | 2 | A | | | L |
| | 124 | | C | 2 | P | L | W | L |
| | 122 | | D | 2 | P | M | G | L |
| | 121 | | E | 2 | P | S | LG | L |
| | 118 | | F | 2 | P | VL/E | W | L |
| | - | 98 | 15 | 3 | A | | | L |
| | 205 | | 16 | 3 | | VL/E | W | L |
| | - | | A | 3 | | | | L |
| | 202 | | C | 3 | | M | W | L |
| | 203 | | D | 3 | | S | G | L |
| | 204 | | E | 3 | | S | LG | L |
| | 207 | | F | 3 | | M | LG | R |
| Cross-waves downwind | 208 | | G | 3 | | M | W | R |
| | 206 | | Pol | 3 | | S | W | R |
| NB: none on pass 1,4,5,6 | | | | | | | | |

a - identifier on STAR-1 imagery.

b - identifier in surface-truthed data.

Note: Other footnotes as for Table III-37.

search on passes 1 and 3, eight and six smaller targets, respectively, can be determined in the northern cluster.

III.4.5 MARS SLAR

All the MARS flight lines ran along latitude lines, with four passes at 12,000 ft, two passes at 6,000 ft, and two passes at 16,000 ft altitude, all with 25-km swath width at 1:250,000 scale. The later mission time (2013 to 2340 GMT) makes it more difficult to confirm small targets viewed by the other aircraft, because many bergy bits and growlers, and even larger icebergs, had moved differentially, to the extent that patterns were not recognizable in some areas. The data on target detection on passes 1 to 3 are given in Table III-43.

The MARS SLAR imagery has a quite different appearance to that of the AES and IIP radars; it is black and white rather than varied grey tone. The ocean/ice grey-tone contrast is greater at all altitudes, with resulting better detection of targets. The exceptions occur when the ocean surface is brighter: such as the far range (20-25 km) in most of the 12,000 ft imagery, or the left swaths of passes 1 and 3 and right swath of pass 6. These were flown at two different altitudes, but all three had upwave (and crosswind) radar look-direction. The more marked wave returns which result tend to be confused with small target returns.

Although many of the iceberg targets are bright and "crisp," the sea ice is correspondingly more well defined, so that even medium to large icebergs near or within sea-ice plumes become lost, probably to a similar extent as on the other SLAR and SAR imagery. The very small targets may not be separated from isolated floes and patches of sea ice.

III.4.6 EVALUATION OF POST-FLIGHT MAPS

The post-flight operational maps prepared by each aircraft were evaluated. The objective was not to compare the ability of each radar and crew, but to assess the range of variability in interpretation in a typical setting. However, different crews had differing resources available for preparation of their maps. For example, the AES crew had other operational commitments unrelated to this project and the STAR-1 team did not have as many personnel.

Table III-44 gives a short comparison of the targets located on the maps drawn after the operational flight. The estimated "real" number of targets used in this analysis is a best guess from Mobil photographs, Polaris V surface visits, and estimates of iceberg motion. It shows that problems arise when an area includes many small targets, when targets relocate differentially with time, when the scale of imagery

TABLE III-43
MARS Target Analysis for 5 April, 1984

| Look Direction | Target ID | Other ID a b | | Pass | Pres- ence | Size | Tone | Swath | Comments | |
|----------------------------|--------------|--------------------|----|------|---------------|------|------|-------|----------------------------------|--|
| | | | | | | | | | Verified Bergs also on Star-1 | |
| Upwave cross- wind | 600 | 1 | 1 | 1 | P | L | | W L | | |
| | 601 | 25 | 4 | 1 | P | M | | W L | | |
| Downwave cross- wind | 01 | 42 | 8 | 1 | P | S | | W R | | |
| | 02 | 45 | 10 | 1 | P | S | | W R | | |
| | 03 | 46 | 11 | 1 | P | M | | W R | | |
| | 04 | 43 | | 1 | P | S | | W R | | |
| | 05 | 44 | 9 | 1 | P | S | | W R | | |
| | 06 | 62 | 12 | 1 | P | M | | W R | | |
| | 07 | 61 | 13 | 1 | P | L | | W R | | |
| | 10 | 60 | 14 | 1 | P | M | | W R | | |
| | - | 58 | N | 1 | A | | | | R | |
| | 15 | 57 | | 1 | P | S | LG/E | | R | |
| | 19 | 206 | L | 1 | P | M | | LG | R | |
| | 20 | 59 | M | 1 | P | L | | W | L | |
| | waves | | | | | P | | | L | Most visible in left swath, all range |
| | waves | | | | | A | | | R | Less visible in right swath far range, none in near |
| Upwave cross- wind | 229 | 1 | 1 | 2 | P | VL | | W/G R | Double, half fuzzy | |
| | 228 | 1a | 1a | 2 | P | S/E | | G R | | |
| | 219 | 25 | 4 | 2 | P | L/E | | W R | | |
| | 218 | 26 | 5 | 2 | P | M/E | | LG R | | |
| | 216 | 42 | 8 | 2 | P | M | | W R | | |
| | 217a | 29 | 7 | 2 | P | VS | | G R | | |
| | 214 | 43 | 9 | 2 | P | S | | W R | | |
| | 217 | 27 | 6 | 2 | P | S | | LG R | | |
| | 213 | 44 | | 2 | P | S | | W R | | |
| | 215 | 45 | 10 | 2 | P | S | | LG R | | |
| | - | 46 | 11 | 2 | X | | | | | In altitude gap |
| | - | 62 | 12 | 2 | X | | | | | " " |
| | - | 61 | 13 | 2 | X | | | | | " " |
| | - | 63 | 14 | 2 | X | | | | | " " |
| | - | 57 | N | 2 | X | | | | | " " |
| | - | 59 | M | 2 | X | | | | | " " |
| | - | 206 | L | 2 | X | | | | | " " |
| | 177 | 58 | | 2 | P | S | | W L | | |
| | waves | | | | | P | | | | Visible in far half of range, both sides (Small bergs north of M verified by <u>Polaris V</u> not positively identified) |

TABLE III-43: continued

| Look Direction | Target ID | Other ID a b | Pass | Pres- ence | Size | Tone | Swath | Comments |
|---|--------------|--------------------|------|---------------|------|------|-------|--|
| Large Bergs to East Visited by Mobil/ <u>Polaris V</u> | | | | | | | | |
| Upwave | 170 | 98 15 | 2 | P | VL | W | R | Bright, crisp |
| Cross- | - | A | 2 | X | | | | In altitude gap |
| wind | - | C | 2 | X | | | | " " |
| | - | D | 2 | X | | | | " " |
| | - | E | 2 | X | | | | " " |
| | 112 | F | 2 | P | L | W | L | |
| | 92 | G | 2 | P | L | W | L | |
| Downwave | - | 98 15 | 1 | X | | | R | In altitude gap |
| Cross- | 22 | A | 1 | P | VL | W | R | May not be A |
| wind | 24 | C | 1 | P | L | W | R | |
| | 25 | D | 1 | P | M | W | R | |
| | 26 | E | 1 | P | S | G | R | Near sea ice, less crisp |
| | - | F | 1 | X | | | R | Beyond range |
| | - | G | 1 | X | | | R | " " |
| Upwave | 233 | 45 10 | 3 | P | M/E | W | L | |
| Cross- | 234 | 46 11 | 3 | P | S | W | L | |
| wind | 235 | 44 9 | 3 | P | M/E | W | L | |
| | 236 | 62 | 3 | P | M | W | L | |
| | 237 | 61 13 | 3 | P | M | W | L | |
| | 240 | 60 14 | 3 | P | S | W | L | |
| | 250 | 58 | 3 | P | VS | LG | L | |
| | - | 57 N | 3 | A | | | L | Shape information |
| | 264 | 59 M | 3 | P | M | W | L | |
| | 263 | 206 L | 3 | P | M | W | L | |
| | - | 98 15 | 3 | X | | | L | |
| | 270 | A | 3 | P | L | W | L | |
| | 272 | C | 3 | P | L | W | L | |
| | 273 | D | 3 | P | M | W | L | Next to sea ice which is fuzzier |
| | 274 | E | 3 | P | S | W | L | |
| | 276 | F | 3 | P | M | W | L | Almost a double feature. |
| waves | | | | P | | | L | Most visible in left swath, far half of range |
| waves | | | | A | | | R | Almost absent, minor flecks in far half of range |

a - identifier on STAR-1 imagery.

b - identifier in surface-truthed data

Note: Other footnotes as in Table III-39

is not true, and that vessels cannot be distinguished reliably from icebergs.

STAR-1

The STAR-1 map of targets drawn after the mission on 5 April is an interesting mixture. Good accuracy was obtained in locating most icebergs, ships, and rigs, and in estimating the size of the medium and larger icebergs. A few exceptions included underestimating the size of iceberg 1 (100 m instead of 200 m); questioning iceberg 4; missing iceberg M. One ship next to iceberg 18 was identified as another iceberg. Many small and very small targets were identified in the north-western area. The northern clusters of targets verified from Polaris V are not well mapped. Only two of the three larger returns are called icebergs, whereas all the very small returns must have been assumed to be sea ice.

AES SLAR

Because AES performed fewer passes in total, and fewer using a 25-km swath, the total target count on their post-flight map is lower in number than the other aircraft. Some very small targets (growlers and bergy bits) were missed, a few spurious targets appear, two icebergs were mis-identified as vessels, a few targets (both icebergs and vessels) were absent. In addition, the along-track stretch yielded imprecise locations for the targets.

IIP SLAR

In the IIP map some of the small and medium icebergs, and some sea-ice patches, are shown as growlers, probably because of the small return size. In addition, several single targets are shown as a cluster of two or three icebergs as a result of drift with time, so an overestimate would be made in total targets present. In the northern cluster of targets verified from Polaris V, only two returns are shown on the map, these are evident in passes 1, 3, and 9 but with a very careful search on passes 1 and 3, eight and six smaller targets, respectively, can be determined in the northern cluster.

MARS SLAR

The MARS post-flight target map shows confirmed targets as icebergs or ships and unconfirmed as radar targets, the latter in the majority. The number and location is quite good, although there are small and very small targets missing in those areas where surface data existed. Since the targets were drawn for each line, the total target number is too high, and interpretation is needed to conclude which targets are duplicated and which targets were real but seen on only one pass.

TABLE III-44

Comparison of Number of Targets Given on Post-Operation Flight Maps
For 5 April 1984

| Area | Estimated No. of Targets | STAR-1 | IIP | AES | MARS |
|--|-----------------------------|--------|-------|-----|--------|
| Northwestern group (many small targets) | 34 | 37 | 21 | 10 | 14 |
| Central Icebergs | 10 | 7 | 11 | 5 | 21/13+ |
| Northern cluster (Polaris V S to Y) | ~12 | 3 | 2 | x | 7 |
| Far north cluster (Polaris V BB to II) | >30 | NI | 3 | x | 6 |
| Early Polaris targets | 4 | NI | 7 | 4 | * |
| No. of vessels | 7 | 4 | 13/6+ | 10 | 8/6+ |

NI - not on imagery.

x - within area with comment "numerous very small tabular icebergs or multi-year floes."

* - location not positively identified due to time/drift change.

+ - first number is total targets shown including repeats on several passes, second number is probable target number without repeats.

TABLE III-45

Detectability of Small Targets in the Northern Cluster
on 5 April 1984

| Source | Pass | Swath Width (km) | Total Targets | Small Targets | Very Small Targets |
|--------|------|------------------------|------------------|------------------|-----------------------|
| STAR-1 | 2 | 25 | 11 | 2 | 9 |
| IIP | 1 | 25 | 8 | 2 | 6 |
| | 3 | 25 | 6 | 2 | 4 |
| | 7 | 50 | 0 | 0 | 0 |
| | 9 | 50 | 2 | 2 | 0 |
| AES | 3 | 25 | 8 | 2 | 6 |
| | 4 | 50 | 1 | 1 | 0 |
| | 5 | 50 | 0 | 0 | 0 |
| | 6 | 50 | 1 | 1 | 0 |
| MARS | 1 | 25 | 11 | 2 | 9 |
| | 2 | 25 | 12 | 2 | 10 |
| | 7 | 25 | 4 | 2 | 2 |
| | 8 | 25 | 1 | 1 | 0 |

III.4.7 TARGET MOVEMENT

An attempt was made to document the target movement over a number of hours on 5 April data. It was apparent early in the study that large drift rates were involved over a few hours and differential movement of targets was observed between quite close targets, which added to the problems of positively identifying the surface verified targets and of relocating these targets on the following days.

Figure III-27 was derived over a 6-hour time period using STAR-1 SAR and MARS SLAR imagery. Many icebergs were moving at 0.75 to 1.0 km/hour on 5 April, with the fastest target (probably a bergy bit) travelling at 1.46 km/hour. There is as much as 122° difference in the directions of movement of targets within the area, and the directions even for icebergs close together differ by 30 to 50°.

III.4.8 SUMMARY

Detectability of Targets

Optimal mapping of iceberg targets and discrimination from sea ice and vessels appeared to be achieved at 1:250,000 scale (25 km swath). This discrimination was particularly apparent for the detection of small (20-50 m) and very small (<20 m) targets.

For AES and IIP the imagery is clearest at a range of 5 - 20 km on this imagery; MARS SLAR was less range dependent, but small targets were somewhat less certain to be identified at close range, where they had a less distinct appearance and look more like sea-ice floes. AES and IIP flew at the same altitude throughout, but the MARS mission indicated that 12,000 ft altitude is to be preferred to 16,000 ft. for that radar system. Insufficient surface-verified targets were present to determine if 6,000 ft was better than 12,000 ft altitude.

For an area of small targets verified by the Polaris V near 47°20'N and 48°10'W, the number of returns detected by the various radars on various passes is summarized in Table III-45. The surface group may not have documented all the ice pieces in the area, and these may have drifted differentially over the mission time period, but from 1740 to 1900 GMT the Polaris V visited two small icebergs, four bergy bits, and three growlers in this area. It should be noted that some IIP and AES passes occurred at different swath widths, and the MARS passes were at two altitudes.

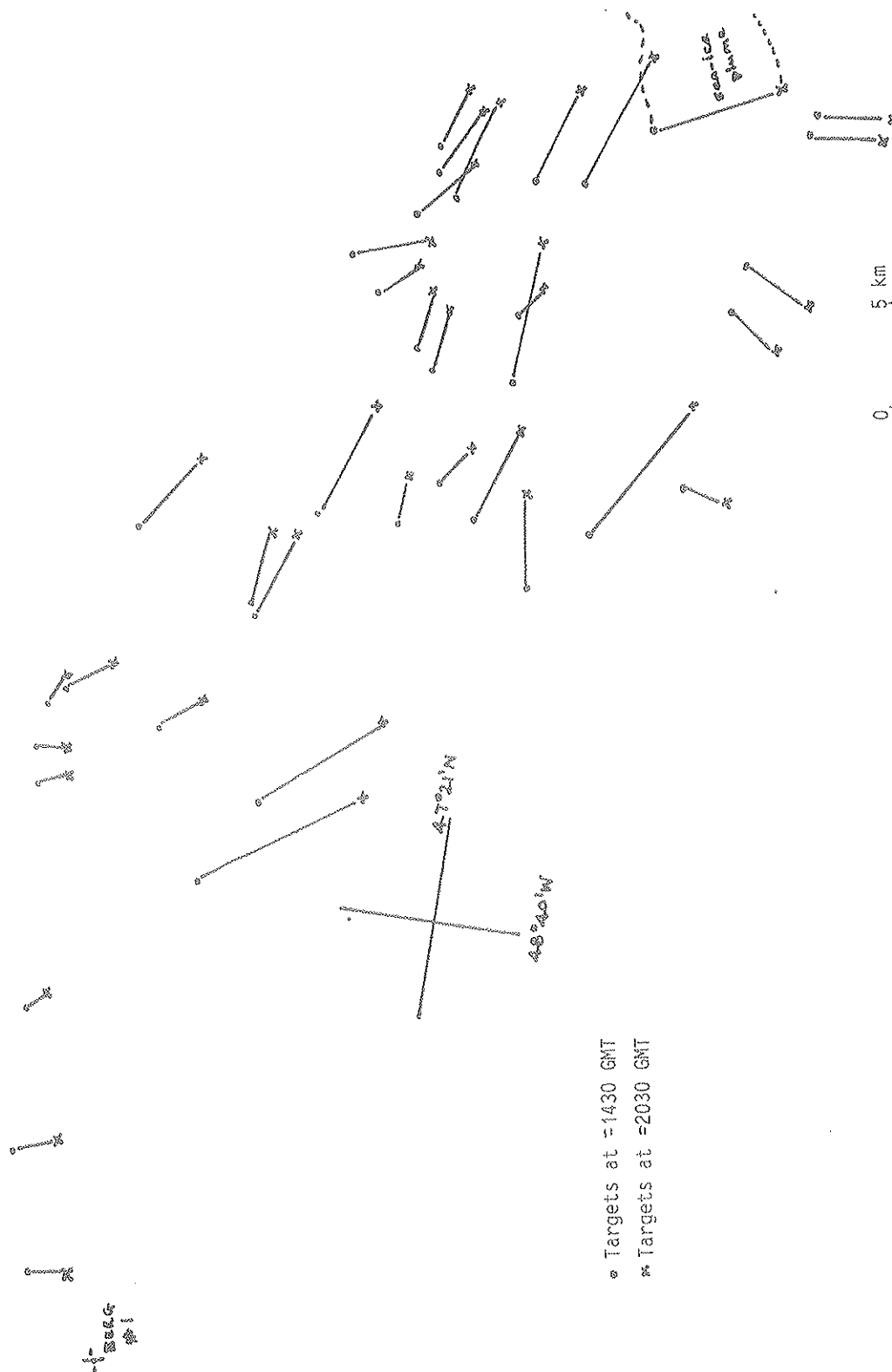


Figure III-27. Target movement on 5 April 1984.

III.5 ANALYSIS OF APRIL 6 IMAGERY

Only data from STAR-1 and IIP are available for this day because no formal experimental missions were planned. However, as good surface and airborne photo data were available, the imagery collected were analysed for iceberg detectability. As on April 3, winds and waves were calm.

III.5.1 AVAILABLE SURFACE INFORMATION

Data were collected by the Polaris V and King Air aircraft on 20 and 50 targets, respectively, with a number of targets (about 12) observed by both (Figure III-28). In addition, a few icebergs had been photographed also on 5 April so that movement information is available; the icebergs had moved southeast from 5 April, and moved eastwards during 6 April. Environmental data are summarized in Table III-46.

III.5.2 STAR-1 SAR

Most of the STAR-1 imagery covers an area to the north of the research area with surface information, or to the south east, where there were no ice targets. The exception is pass 4, flown from south to north with a 25 km swath width at 1900 GMT. The eastern-central part of the pass covers the western area visited by the Polaris V and photographed by the Mobil aircraft. The targets are listed in Table III-47.

TABLE III-47
Icebergs Detected on Pass 4 of STAR-1 Imagery

| STAR-1 ID | KING AIR no. | Air photo Size (m) | POLARIS no. | POLARIS V dimension estimates (m) | SAR size estimate |
|--------------|-----------------|--------------------------|----------------|---|-------------------------|
| 59 | B010 | 125x63 | - | - | L |
| 60 | B003 | 47x35 | C-6 | 46x42x7 | S |
| 61 | B002 | 49x25 | - | - | M |
| 62 | B001 | 91x87 | B-6 | 70x?x20 | L |
| - | - | - | A-6 | 14x7x2 | VS |
| 63 | - | - | - | - | M |

All the confirmed targets are visible in the imagery, with target size related to actual target size. Shape information is present for the larger targets (59 and 62), while bergy bit (A-6) is visible as a point target. Target 63 was not confirmed by surface or photographic data.

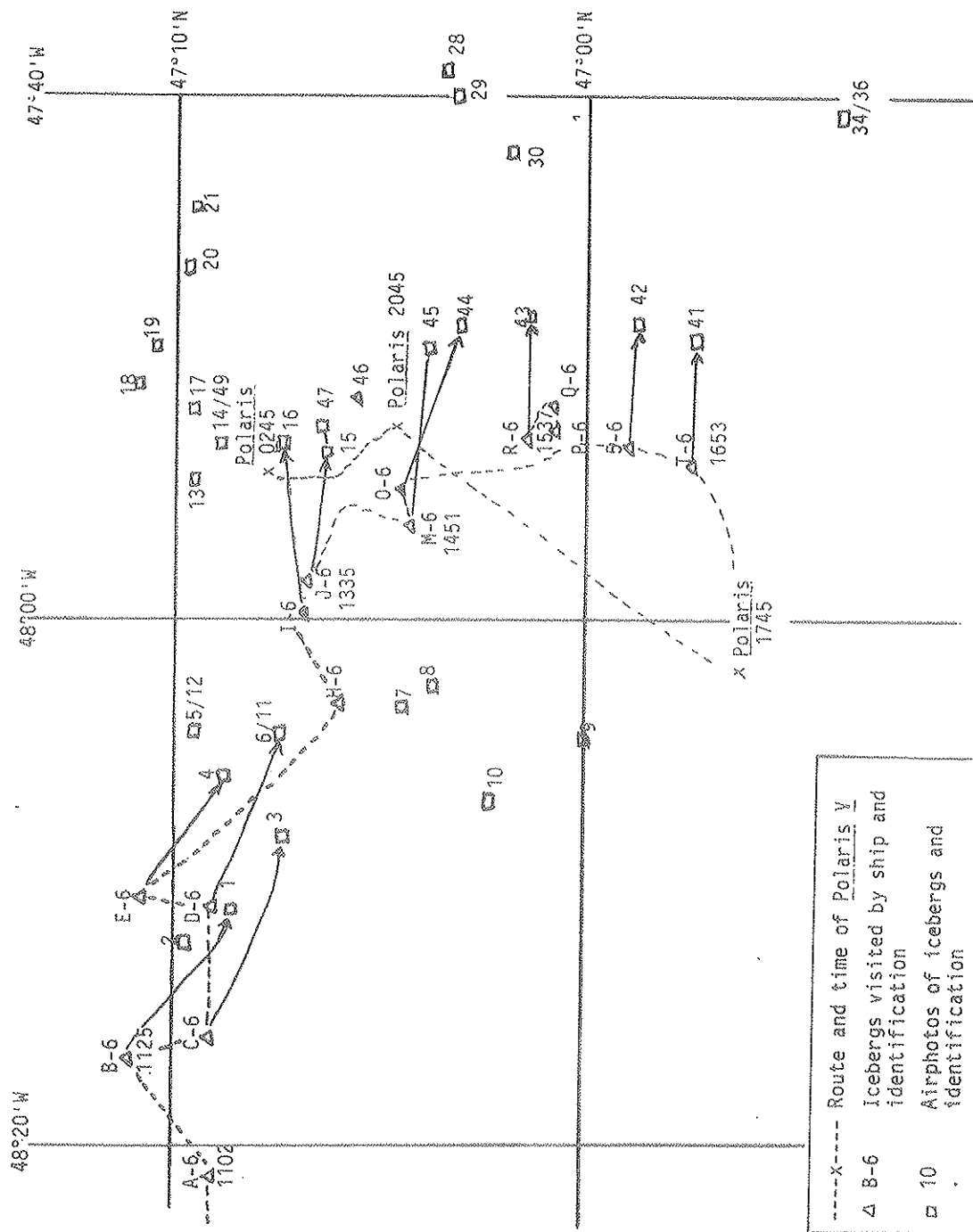


Figure III-28. Confirmed targets on 6 April 1984.

TABLE III-46
Hourly Weather and Environmental Data, 6 April 1984

| Time GMT | Primary Waves | | | Secondary Waves | | | Wind | | Temp. | | Cloud Height (m) | Vis (Naut mi.) | Ice Cond |
|-------------|---------------|------------|-----------------|-----------------|------------|-----------------|----------------|------------|------------|-------------|------------------------|----------------------|-------------|
| | Height (m) | Dir (°) | Period (sec) | Height (m) | Dir (°) | Period (sec) | Speed (kts) | Dir (°) | Air (°) | Sea (°C) | | | |
| 0900 | 0.5 | 280 | 3 | 1.5 | 310 | 8 | 13 | 127 | -1.0 | 0.5 | 200 | >15 | 0/w |
| 1000 | 0.6 | 270 | 1 | 1.0 | 290 | 8 | 14 | 260 | -0.6 | -0.1 | 200 | >15 | 0/w |
| 1100 | 0.5 | 270 | 2 | 1.2 | 290 | 10 | 14 | 260 | -0.6 | -0.1 | 200 | >15 | 0/w |
| 1200 | 0.5 | 270 | 3 | 1.2 | 290 | 10 | 15 | 272 | -0.5 | 0.0 | 200 | >15 | 0/w |
| 1300 | 0.5 | 240 | 3 | 1.0 | 290 | 10 | 12 | 258 | -0.2 | 0.0 | 200 | >15 | 0/w |
| 1400 | - | - | - | - | - | - | - | - | - | - | - | - | - |
| 1500 | 0.4 | 290 | 3 | 1.0 | 270 | 10 | 13 | 266 | +0.5 | 0.0 | 200 | >15 | 0/w |
| 1700 | 0.4 | 310 | 3 | 1.0 | 270 | 10 | 10 | 262 | +0.2 | 0.0 | 600 | >15 | 0/w |
| 1800 | - | - | - | 1.0 | 270 | 3 | 10 | 230 | +0.5 | 0.0 | 600 | >15 | 0/w |
| 2100 | - | - | - | 1.0 | 230 | 3 | 06 | 230 | 0.0 | 0.0 | 600 | >15 | 0/w |
| 0000 | - | - | - | 1.5 | 230 | 3 | 08 | 200 | 0.0 | 0.0 | 600 | >15 | 0/w |

III.5.3 IIP SLAR

IIP was flying an operational mission and imaged the area with one 100-km swath at about 1800 GMT. On this display the targets are very small and, in this case, have very little contrast to the ocean background. Three attempts were made with a strong magnifier to find the targets identified by the IIP crew in their post-flight analysis, and to locate the surface-characterized icebergs. Table III-48 shows the targets identified, and Table III-49 summarizes these by size category.

It can be seen that only one target less than 45 m (length) was detected, whereas targets with length greater than 50 m were all detected. Small icebergs of 45-50 m length were detected on about half the occasions.

TABLE III-48

IIP Imagery, 6 April 1984

| Mobil ID | POLARIS V ID | Size | | Presence on IIP imagery a |
|-------------|-----------------|---------------|--------------|---------------------------------|
| | | Length (m) | Width (m) | |
| 1 | B-6 | 91 | 87 | P |
| 3 | C-6 | 47 | 35 | P |
| 4 | E-6 | 133 | 63 | P |
| 5/12 | | 48 | 32 | A |
| 6/11 | D-6 | 46 | 27 | A |
| 7 | | 45 | 30 | A |
| 8 | | 53 | 44 | P |
| 9 | | 61 | 40 | P? |
| 10 | | 125 | 63 | P |
| 13 | | 80 | 72 | P |
| 14/49 | | 82 | 71 | P |
| 15/47 | J-6 | 50 | 40 | P |
| 16/50 | I-6 | 82 | 62 | P |
| 17 | | 46 | 44 | P |
| 20 | | 89 | 61 | P |
| 21 | | 129 | 135 | P |
| 23 | | 279 | 93 | P |
| 24 | | 36 | 34 | A |
| 25 | | 85 | 53 | P |
| 26 | | 116 | 110 | P |
| 27 | | 172 | 95 | P |
| 28 | | 57 | 34 | P |
| 29 | | 87 | 44 | P |
| 30 | | 105 | 61 | P |
| 41 | T-6 | 64 | 45 | P |
| 42 | S-6 | 54 | 33 | P |
| - | Pol. | 62 | 10 | P |
| - | P-6 | 30 | 13 | A |
| - | Q-6 | 35 | 30 | A |
| 43 | R-6 | 25 | 22 | A |
| 44 | O-6 | 31 | 18 | P |
| 45 | M-6 | 24 | 18 | A |
| 46 | H-6? | 69 | 33 | P |

a - 12,000 ft. alt.

100 km swath

Left swath only, displayed at 2 gain settings.

TABLE III-49

IIP 100-km Swath Imagery on 6 April 1984

| TARGET TYPE | LENGTH (m) | NO. DETECTED | NO. NOT DETECTED | NO. IN CLASS | % DETECTED |
|------------------------|---------------|-----------------|---------------------|-----------------|---------------|
| SMALL ICEBERGS | | | | | |
| 1. | 21 - 30 | 0 | 3 | 3 | 0 |
| 2. | 31 - 40 | 1 | 3 | 4 | 25 |
| 3. | 41 - 45 | 0 | 1 | 1 | 0 |
| 4. | 45 - 50 | 3 | 2 | 5 | 60 |
| MEDIUM ICEBERGS | | | | | |
| 1. | 51 - 60 | 3 | 0 | 3 | 100 |
| 2. | 60 - 100 | 10 | 0 | 10 | 100 |
| LARGE ICEBERGS | | | | | |
| 1. | 101 - 150 | 5 | 0 | 5 | 100 |
| 2. | 151 - 200 | 1 | 0 | 1 | 100 |
| VERY LARGE ICEBERGS | | | | | |
| | 200 | 1 | 0 | 1 | 100 |

III.6 ANALYSIS OF APRIL 7 IMAGERY

The aircraft flew research-oriented missions on 7 April, typically flying a crossed-box pattern at different altitudes, repeating lines for a repeatability test and, in the case of STAR-1, changing the resolution cell size. The flight parameters are given in Table III-50.

III.6.1 AVAILABLE SURFACE INFORMATION

Surface data were limited to one location adjacent to the Polaris V hence detailed target detectability tests were carried out only on these few documented growlers and bergy bits.

The King Air photo reconnaissance plane did not fly a mission on 7 April, and it was not possible to re-identify any of the icebergs photographed on 6 April as targets on the imagery of 7 April.

The Polaris V was positioned next to a growler by 1100 GMT, and maintained station at 300-500 m from it, drifting near the target, with a waverider buoy deployed. This drift began at 47°07.2'N and 47°45.7'W at 1145 GMT and continued until 2345 GMT at 47°10.8'N and 47°44.2'W. A typical configuration of ship and targets is shown in Figure III-29.

The wind and waves during this period are summarized in Table III-51, taken from the surface data report. The wind and primary wave directions agree within 10-30°, but the drift of the iceberg and Polaris V were generally at right angles to this the wind and waves were from south-east and the drift was to north-east. Drift on the previous day had been roughly to the east.

The Polaris V did not measure many targets in detail on 7 April. The closest growler, designated A-7, was documented and a series of diagrams show its position relative to the vessel and the waverider buoy about every 30 minutes. Other nearby targets also occur in the diagrams from time to time, and occasionally in the surface photography. These are summarized in Table III-52. The Polaris V personnel described their operation:

"Diagrams drawn during the period of overflights were intended to provide a record of the position of the ship, the target and the waverider. Other icebergs and growlers noted were incidental. During this period the ship moved so as to keep the waverider on a slack rope but extended sufficiently that the rope should not become entangled in the

TABLE III-50
Imagery for 7 April 1984

| Pass No. | Altitude (Ft.) | Heading (Deg.) | Swath Width (km) | Start (GMT) | End (GMT) | General Comments |
|----------|----------------|----------------|------------------|-------------|-----------|---|
| STAR-1 | | | | | | |
| 1 | | | | | | |
| 2 | | | | | | |
| 3 | 27000 | 070 | 25 | 1922 | 1924 | Passes 3-5, aspect angle test, 3 views |
| 4 | 27000 | 329 | 25 | 1931 | 1935 | |
| 5 | 27000 | 241 | 25 | 1943 | 1947 | |
| 6 | 27000 | 150 | 25 | 1958 | 2000 | Passes 6-12, repeatability test, equivalent to pass 4 |
| 7 | 27000 | 329 | 25 | 2009 | 2012 | |
| 8 | 27000 | 148 | 25 | 2018 | 2021 | |
| 9 | 27000 | 330 | 25 | 2028 | 2031 | |
| 10 | 27000 | 149 | 25 | 2038 | 2041 | |
| 11 | 27000 | 329 | 25 | 2048 | 2051 | |
| 12 | 27000 | 149 | 25 | 2057 | 2101 | |
| 13 | 27000 | 329 | 25 | 2108 | 2110 | Resolution test; wide swath near half, compare with pass 12 |
| 14 | 27000 | 149 | 25 | 2119 | 2123 | Look-angle test; wide swath far half, compare with pass 13 |
| 15 | 27000 | 243 | 25 | 2132 | 2139 | |
| 16 | 27000 | 062 | 25 | 2145 | 2148 | |
| AES | | | | | | |
| 1 | 10000 | 058 | 25 | 1902 | 1907 | |
| 2 | 10000 | 160 | 25 | 1912 | 1916 | |
| 3 | 10000 | 237 | 25 | 1922 | 1929 | |
| 4 | 10000 | 010 | 25 | 1932 | 1937 | |
| 5 | 10000 | 067 | 25 | 1942 | 1945 | |
| 6 | 10000 | 161 | 25 | 1949 | 1954 | |
| 7 | 10000 | 239 | 25 | 1959 | 2009 | |
| 8 | 10000 | 014 | 25 | 2013 | 2019 | |
| 9 | 10000 | 012 | 25 | 2040 | 2048 | |
| 10 | 10000 | 011 | 25 | 2106 | 2114 | |
| 11 | 10000 | 012 | 25 | 2131 | 2139 | |
| 12 | 5000 | 070 | 25 | 2147 | 2150 | |
| 13 | 5000 | 160 | 25 | 2155 | 2201 | |
| 14 | 5000 | 236 | 25 | 2207 | 2215 | |
| 15 | 5000 | 015 | 25 | 2222 | 2228 | |

continued...

TABLE III-50 continued

| Pass No. | Altitude (Ft.) | Heading (Deg.) | Swath Width (km) | Start (GMT) | End (GMT) | General Comments |
|----------|----------------|----------------|------------------|-------------|-----------|------------------|
| MARS | | | | | | |
| 3 | 12000 | 050 | 25* | 0228+ | 0231 | |
| 4 | 12000 | 137 | 25 | 0241 | 0244 | |
| 5 | 12000 | 224 | 25 | 0250 | 0257 | |
| 6 | 12000 | 355 | 25 | 0302 | 0305 | |
| 7 | 12000 | 052 | 25 | 0310 | 0313 | |
| 8 | 12000 | 137 | 25 | 0316 | 0321 | |
| 9 | 12000 | 226 | 25 | 0325 | 0333 | |
| 10 | 12000 | 351 | 25 | 0337 | 0341 | |
| IIP | | | | | | |
| 1 | 8000 | 068 | 25 | 1740 | 1745 | |
| 2 | 8000 | 235 | 25 | 1748 | 1755 | |
| 3 | 8000 | 319 | 25 | 1806 | 1811 | |
| 4 | 8000 | 185 | 25 | 1813 | 1820 | |
| 5 | 8000 | 068 | 25 | 1823 | 1829 | |
| 6 | 8000 | 237 | 25 | 1835 | 1845 | |
| 7 | 8000 | 315 | 25 | 1857 | 1904 | |
| 8 | 8000 | 195 | 25 | 1906 | 1915 | |
| 9 | 8000 | 317 | 25 | 1924 | 1930 | |
| 10 | 8000 | 160 | 25 | 1935 | 1942 | |
| 11 | 8000 | 317 | 25 | 1947 | 1953 | |
| 12 | 8000 | 159 | 25 | 1957 | 2004 | |
| 13 | 8000 | 317 | 25 | 2008 | 2015 | |
| 14 | 8000 | 160 | 25 | 2019 | 2031 | |
| 15 | 4000 | 070 | 25 | 2042 | 2048 | |
| 16 | 4000 | 239 | 25 | 2051 | 2058 | |
| 16a | 4000 | 112 | 25 | 2101 | 2107 | |
| 17 | 4000 | 193 | 25 | 2118 | 2126 | |

* - All with 5 km delay

+ - 8 April GMT, 7 April local time.

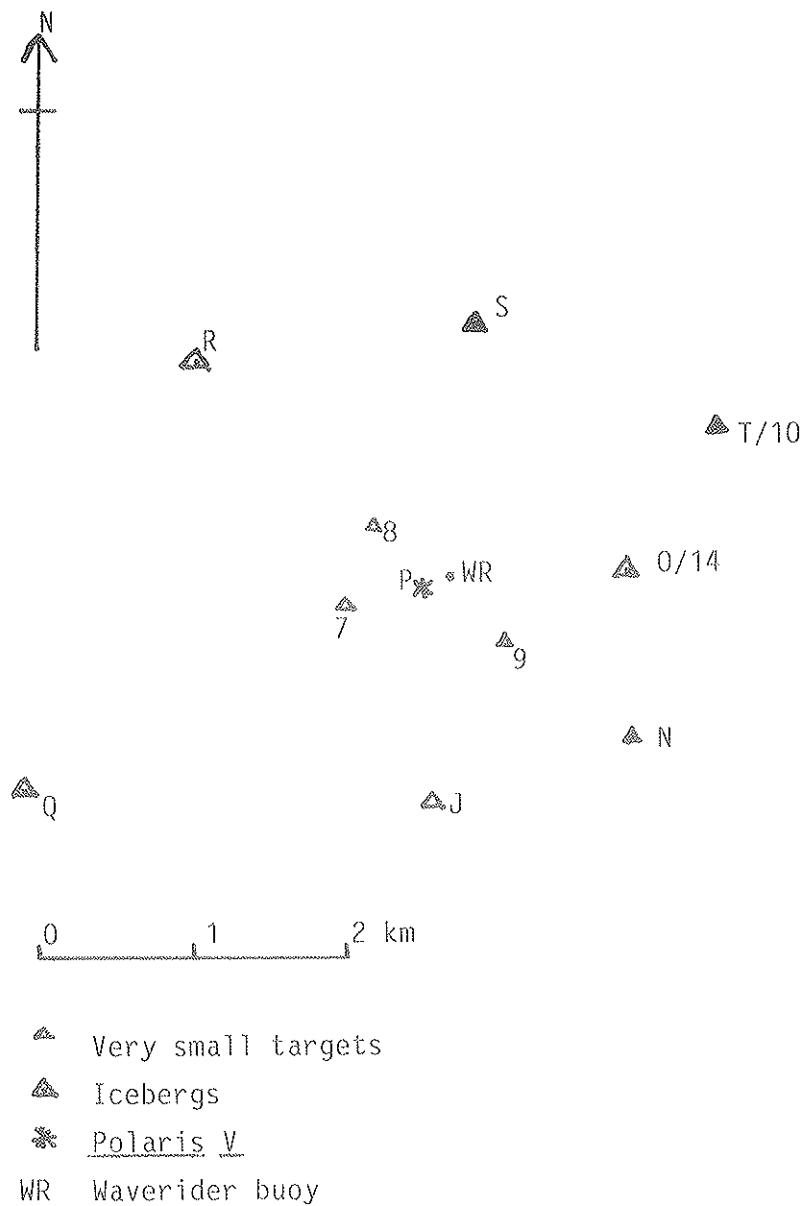


Figure III-29. Typical configuration of targets during missions of STAR-1, IIP, and AES near 47° 10'N and 47° 40'W, 7 April 1984.

TABLE III-51

Hourly Weather and Environmental Data from Polaris V, 7 April 1984

| Time GMT | Primary Waves | | Secondary Waves | | Wind | | Temp. | | Cloud % | Vis (Naut mi.) | Position |
|-------------|---------------|------------|-----------------|---------------|------------|----------------|------------|------------|-------------|----------------------|-------------|
| | Height (m) | Dir (°) | Period (sec) | Height (m) | Dir (°) | Speed (kts) | Dir (°) | Air (°) | Sea (°C) | | |
| 1230 | 0.3 | 160 | 1 | 1.2 | 160 | 20 | 135 | 0.5 | -0.5 | 90 | 15 |
| 1300 | 0.4 | 180 | 1 | 1.5 | 180 | 20 | 150 | 0.75 | -0.5 | 100 | 15 |
| 1418 | 0.6 | 130 | 2 | 2.0 | 190 | 20 | 135 | 0.7 | +0.5 | 90 | 15 |
| 1501 | 1.5 | 150 | 3 | 2.0 | 180 | 22 | 146 | 1.0 | +0.5 | 90 | 15 |
| 1600 | 2.0 | 150 | 4 | 2.0 | 160 | 24 | 150 | 1.25 | +0.5 | 90 | 15 |
| 1700 | 1.5 | 160 | 0.3 | 2.0 | 160 | 22 | 130 | 0.9 | +0.5 | 90 | 15 |
| 1800 | 1.0 | 140 | 2 | 2.0 | 140 | 21 | 150 | 1.2 | 0.5 | 90 | 15 |
| 1900 | 1.0 | 100 | 4 | 2.5 | 140 | 24 | 155 | 1.1 | 0.5 | 100 | 15 |
| 2000 | 1.0 | 140 | 4 | 2.5 | 140 | 25 | 155 | 1.5 | 0.5 | 100 | 10 |
| 2100 | 1.0 | 140 | 3 | 2.7 | 140 | 25 (30) | 150 | 1.7 | 0.5 | 100 | 7 |
| 2200 | - | - | - | - | - | 25 (30) | 150 | 1.5 | 0.5 | 100 | 4 |
| | | | | | | (30) | | | | | 47° 44.25'N |

*Possibly incorrect as this is duplicated in radar data.

°. Inaccuracy due to navigation instrument failure.

TABLE III-52

Targets Seen From Polaris V On 7 April 1984

| Target ID | <u>Polaris V</u> Description | Size (m) | Time First Seen | Photo |
|-----------|---|---------------------|--------------------|--|
| 7 | Target A-7, berg bit | 8x4x3 | 1600 | Polaroid 1-5 print 12-19,20, 31,32,13-15 |
| 8 | Small iceberg | 8 | 1600 | |
| 9 | Low, small iceberg | 7 | 1600 | |
| T/10 | Dome iceberg | est. 50 L, 15 H | 1632 | 13-11 |
| 11 | 2 growlers past ship | est. <3L,1 H | 1630 | |
| 12 | Growler between ship and wave rider | est. <1 H | 1641 | |
| 13 | Bergy bit | est. 1-2 H | 1645 | |
| 0/14 | Tabular, very large iceberg | est. 100 L, 20 H | 1710 | 13-11 |
| 15 | | | 1733 | |
| 16 | Growler | est. <3 H | 1805 | |
| S/17 | Very large iceberg | est. 120 L, 25 H | 2000 | 13-18 |
| 18 | Berg, 2 peaks, may be dry-dock | est. large | 2130 | |
| Y | large | | 2036 | 13-18 |

bow thrusters, consequently the ship's heading and position was constantly changing."

III.6.2 TARGET DETECTABILITY

Each pass of STAR-1, AES, and IIP that covered the area around the Polaris V was examined to determine which targets were detected. In addition to the verified targets (see Table III-52) seven other targets were found consistently, plus the Polaris V itself. Five small targets were seen on some passes, but not on others, and of these only three (7,8, and 9) have known size. Examining Table III-53 gives the following estimates of the detectability of the three verified targets 7, 8, and 9.

For all radars:

| | | |
|-----------------------|--------------|-----|
| Total, all directions | - 61 present | 46% |
| | - 72 absent | 54% |
| Upwind | - 6 present | 31% |
| | - 13 absent | 69% |
| Cross-wind | - 31 present | 52% |
| | - 29 absent | 48% |
| Oblique-wind | - 6 present | 25% |
| | - 18 absent | 75% |
| Downwind | - 19 present | 58% |
| | - 14 absent | 42% |

Target 7 was classed as a growler here even though its estimated height would classify it as a bergy bit. J and N were unverified targets but were seen consistently. They were probably a bergy bit and a small iceberg, respectively, judging from target size comparison with other known features.

The MARS data were not included in this analysis because the flight occurred much later and the targets had moved differentially; it was not even possible to identify Polaris V with certainty.

III.6.3 TARGET MOVEMENT

Drift rates were examined using STAR-1 imagery over a 2-hour period, as shown in Figure III-30. The fastest iceberg was moving at 2.87 km/hour, and many were travelling at 2.0 to 2.5 km/hour. The directional variations were greater than on April 5; there seem to be some eddies involved. Close icebergs diverged by about 60°, whereas distant icebergs across the area showed up to 180° differences in movement direction.

TABLE III-53

Detection Of Very Small Targets on 7 April 1984

| Look Direction | Radar | Pass No. | Presence of Target ^a | | | | |
|----------------------|--------|----------|---------------------------------|------|-----|-----|-----|
| | | | 7 | 8 | 9 | J | N |
| Downwind | STAR-1 | 3 | P | P? | P | P/E | P/E |
| | | 15 | P/E | P? | P | A | P |
| | | 16 | P | P/E? | P | P | P/E |
| | IIP | 1 | P | A | A | A | P? |
| | | 5 | A | A | A | ? | ? |
| | | 15 | P | A | P | P/E | P |
| | | 16a | P | A | A | P/E | P |
| | AES | 3 | P | A | P? | P | P |
| | | 7 | P/E | A | P? | P | P |
| | | 12 | P | A | A | P | P |
| | | 14 | P | A | A | ? | P |
| Upwind | STAR-1 | 5 | P | A | A | P | P |
| | | 6 | P | A | A | A | P? |
| | AES | 16 | A | A | A | P? | P |
| | | 1 | A | A | P | P/S | P |
| | | 5 | P | A | P? | A | A |
| | | 12 | A | A | A | P | P |
| | | 14 | P | ? | ? | A | P |
| Oblique upwind | IIP | 4 | P? | A | P? | ? | P |
| | | 8 | A | A | A | P | P |
| | | 17 | P | A | A | P | P |
| | AES | 4 | P | A | A | A | A |
| | | 8 | P? | A | A | P | P |
| | | 9 | P/S | A | A | A | A |
| | | 10 | A | A | A | A | P |
| | | 11 | A | A | A | A | P |
| Cross-wind from East | STAR-1 | 4 | P | P | P | P | P |
| | | 6 | P | A | P | P/E | P/E |
| | | 7 | P | P | A | P/E | P |
| | | 8 | P | A | P | P | P/E |
| | | 9 | P | A | P | P/E | P/E |
| | | 10 | P | A | P | P | P/E |
| | | 11 | P/E | A | P/E | P/E | P/E |
| | | 12 | P | A | P | P/E | P/E |
| | | 13 | P | A | P/F | P/F | P |
| | | 14 | P/S | A | P/E | P | P |
| | IIP | 7 | P | A | P | P | P |
| | | 9 | P | A | P? | P | P |
| | | 11 | P | A | A | P | P |
| Cross-wind from East | IIP | 13 | A | A | A | P | P |
| | AES | 2 | P | A | P | P | P |
| | | 6 | P | A | A | P | P |
| | | 13 | P | A | A | P | P |
| Cross-wind from West | IIP | 10 | P | A | A | P | P |
| | | 12 | P | A | A | P | P |
| | | 14 | A | A | A | P/S | P |

^a - present A - absent E - elongated in azimuth direction
 ? - identification/location of target uncertain
 F - fuzzy edge to target S - very small or faint target

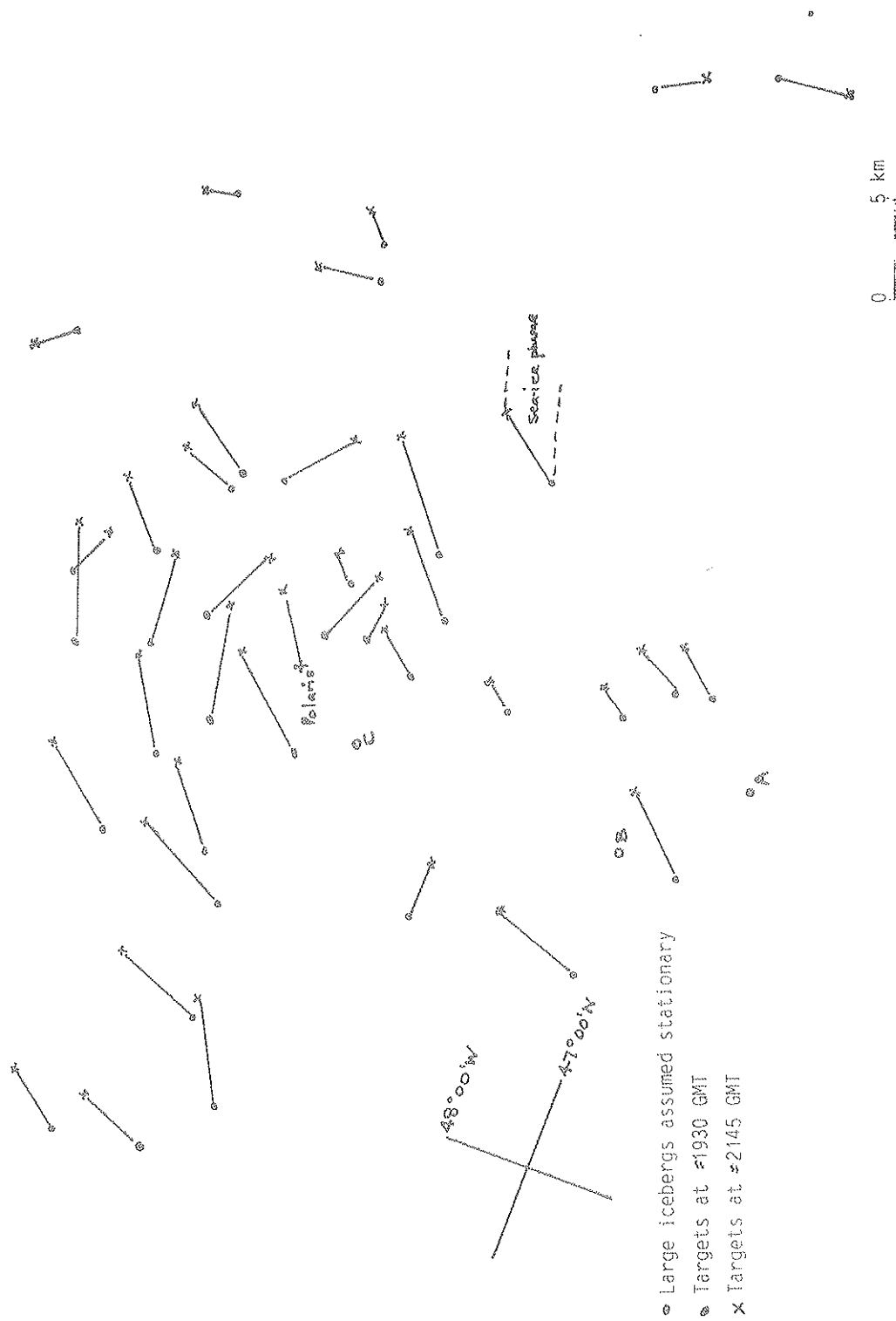


Figure III-30. Target movement from STAR-1 imagery, 7 April 1984.

III.6.4 TARGET REPEATABILITY

The objective of this investigation was to examine the repeatability of radar targets from pass to pass. The investigation was similar to that of an interpreter working in an operational situation, i.e., without aid of surface information.

Two approaches were taken. First, a box region was selected and a frequency count was performed for target occurrence within this region on each pass for a given radar. For each radar, fluctuations in frequency were described according to the category of look, i.e., upwind, downwind, or cross-wind. Each box selected for each radar was unique in geographical location and was chosen so as to make use of the maximum number of passes for that radar. Secondly, a region was chosen which all radars had covered on one pass each; for this single pass a comparison was made between radars on the basis of number of targets imaged. Examples of imagery from each of the four radars covering a similar area and as close in time as possible are shown in Figures III-31 to III-34.

A complicating factor in performing a gross frequency count from pass to pass is the presence of sea clutter which, on any given pass, might produce false targets which do not repeat on other passes. To investigate this phenomenon, 20 targets were chosen for each radar. Each target was then checked for its recurrence from pass to pass on the radar in question.

Pass-to-Pass Target Fluctuation

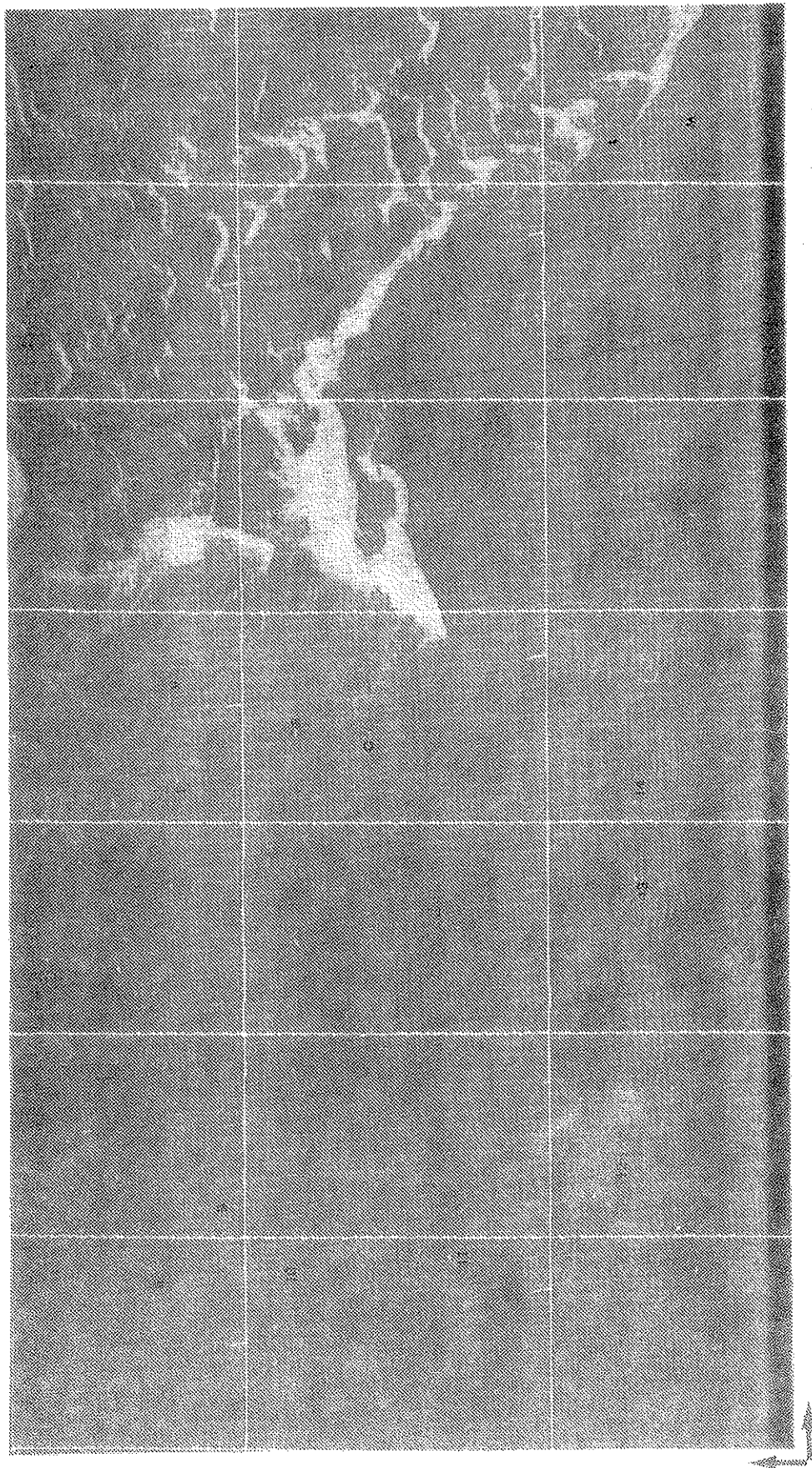
Because of the large number of icebergs encountered on April 7, identification of a single small target from pass to pass was difficult; aggravating factors included the presence of sea clutter as well as differential drift between icebergs. Considering also the temporal lag between aircraft passes, the net effect from pass to pass was a redistribution of about 40-60 targets within an area of imagery which could be as small as 6.5 cm square. Aircraft position errors further complicated matters. Therefore, for each radar pass examined on April 7, control was established by denoting specific icebergs as "control" targets; these icebergs gave strong returns and recurred on all passes with about the same relative spatial position. A polygon was drawn around these icebergs; these control targets were selected in a pattern such that their layout resembled this geometry. On subsequent passes the icebergs were reidentified and the box drawn around them; a count was then made of the number of targets occurring within the box for each pass. The results are given by radar and look direction with respect to the wind in Table III-54.

For most radars, the number of targets decreases when the system is looking upwind. Hence, look direction relative



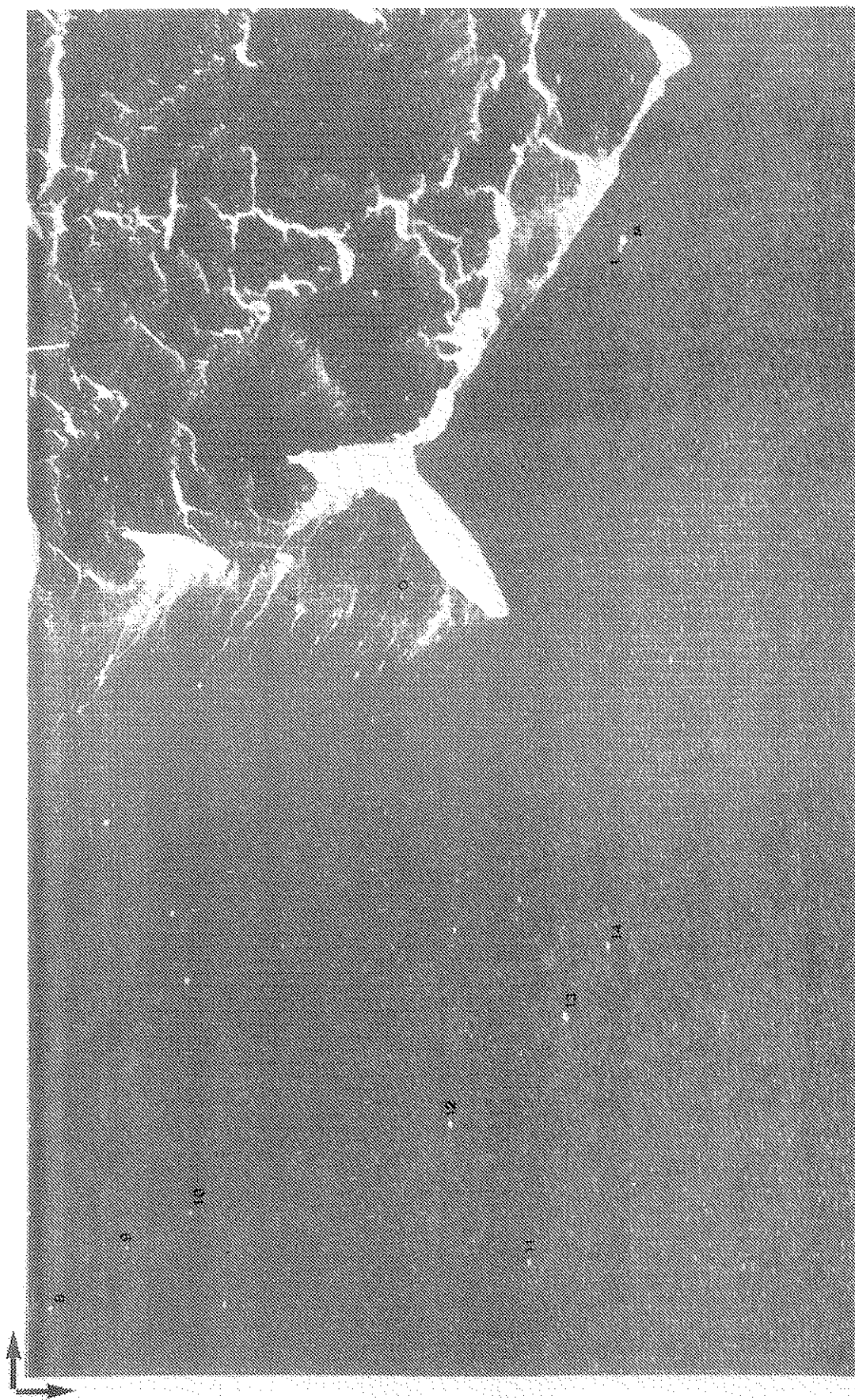
STAR-1 Pass 2 350° HDG. 29000 ft. Alt. 1429 GMT.

Figure III-31. STAR-1, pass 2, 7 April 1984.



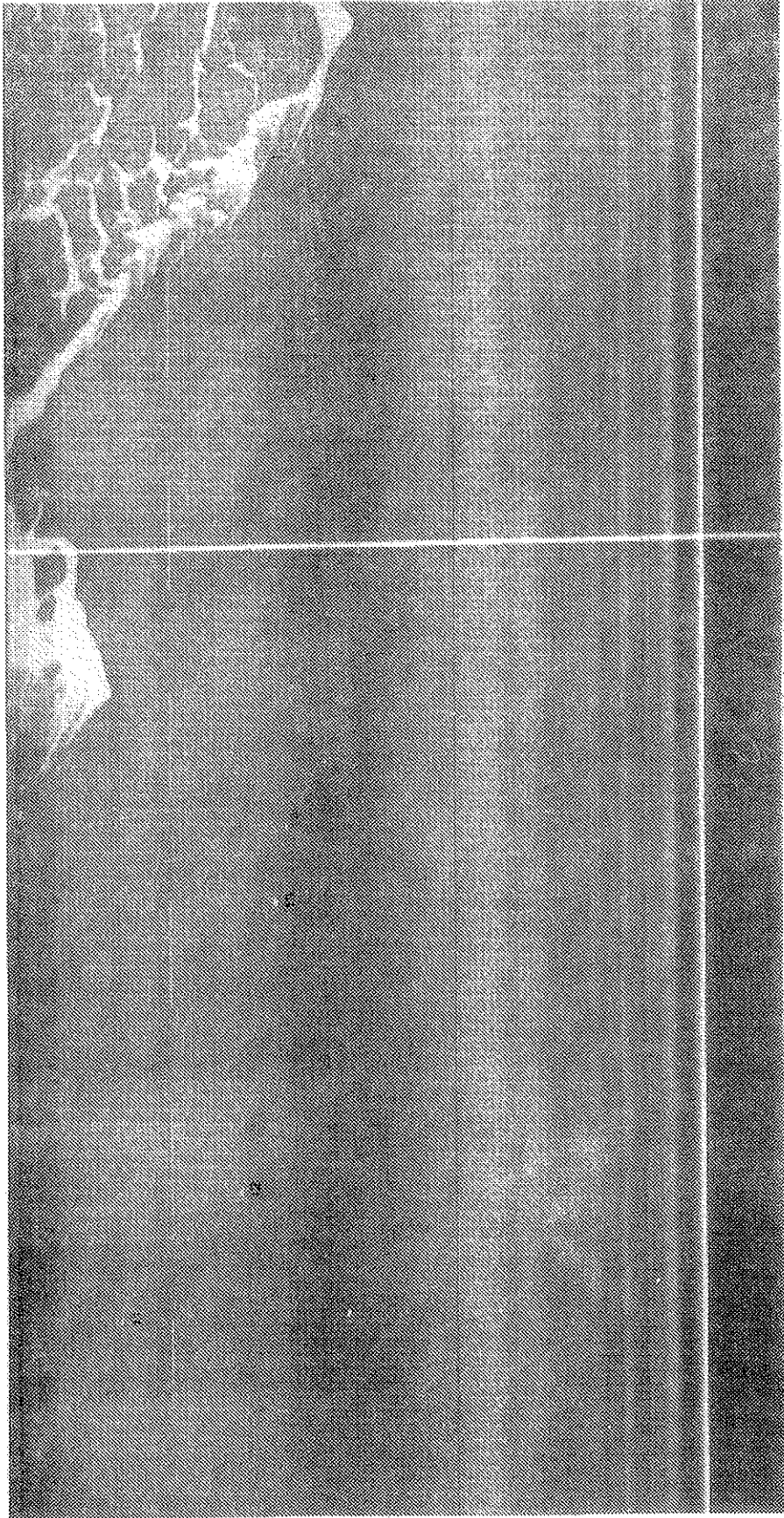
IIP Pass 3 - 080° HDG. 8000 FT. ALT. 1401 GMT.

Figure III-32. IIP, pass 3, 7 April 1984.



MARS Pass 1 082° HDG. 12000 FT. ALT. 2028 GMT.

Figure III-33. MARS, pass 1, 7 April 1984.



AES Pass 2 275° HDG 9000 FT. ALT. 1438 GMT.

Figure III-34. AES, pass 2, 7 April 1984.

TABLE III-54

Repeatability of Targets by Look Direction

| Aircraft | IIP | STAR-1 | AES | MARS |
|------------------------------|-------------------|-------------------|-------------------|-------------------|
| Time (GMT) | 1748-2051 | 1922-2145 | 1907-2222 | 0222-0351 |
| Approximate Box Size (km) | 350 | 270 | 140 | 260 |
| Wave Ht. (m) | 0.5-1 | 0.5-1 | 0.5-1m | 1.0 |
| Predominant Swell Ht. (m) | 2-2.5 | 2-2.5 | 2-2.5 | 2.5 |
| Wind Speed & Dir. (°True) | 28 knots @ 150 | 28 knots @ 150 | 28 knots @ 150 | 30 knots @ 130 |
| Upwind No. of Passes | 2 | 41 | 3 | 2 |
| No. of Targets | 37-52 | 56 | 28-31 | 72-80 |
| Cross-Wind No. of Passes | 3 | 7 | 2 | 2 |
| No. of Targets | 55-62 | 68-90 | 33 | 68-69 |
| Downwind No. of Passes | 1 | 1 | - | 1 |
| No. of Targets | 47 | 86 | - | 86 |

Note: Region imaged is unique to each radar.

to wind probable will be one of the factors in determining the number of targets detected. This effect could result from greater obscuration of small icebergs by waves when looking upwind. However, the effect of sea clutter must also be considered. Table III-54 dicates that typical fluctuation from pass to pass (cross-wind) is about 5-10%.

For comparison between aircraft on this date, a common area of about 140 km² was located on one pass from each radar. For STAR-1 and MARS this common area was located within the same box used to analyse target fluctuation between passes; on the AES and IIP imagery it constituted a zone lying outside this box.

Comparison of the number of targets found is given in Table III-55. All radars were looking at an angle of 1-10° deviation from the wind direction (i.e., looking downwind). Number of targets detected on the imagery ranged from 32 to 59; however, the flight times were not identical.

Reidentification of Targets From Pass to Pass

Targets were selected from the same box regions used for each radar; targets less than 0.4 mm in size (range direction) were usually chosen. For each pass, the selected target was measured in the range direction; its position with respect to neighbouring targets was reidentified for all subsequent passes. The only target confirmed on the surface was a growler near Polaris V measuring 8 x 4 m² which was detected on several passes of each radar. The target was detected on all passes of STAR-1 (6), MARS (5), and on AES (4). On IIP imagery, the target could not be found on three passes of five.

III.6.5 "MYSTERY" TARGET

An attempt was made to locate a "mystery" target which was seen on some radar imagery near Polaris V, but not observed by the surface team. This target was not seen on STAR-1 or MARS imagery for 2-3 April; neither was it seen IIP imagery for 2 April. For 2 April it was seen on one pass of AES imagery. On April 3 it was seen on imagery from 1 pass of AES, and 17 passes of IIP, and 4 passes by CCRS. Occurrences of this target by pass are summarized in Table III-56.

As the target appeared during cross-wind, upwind, and downwind passes, wind direction does not appear to be a factor. A point to note is that the time of occurrence on IIP imagery coincides with the time during which the waverider buoy was deployed from Polaris V. Although STAR-1 also was flying at this time, the target was not seen on its imagery.

TABLE III-55

Gross Target Counts For Common 140 Km² Area

| Aircraft | STAR-1 | MARS | IIP | AES |
|---|----------|----------|--------|-------|
| Time (GMT) | 2145 | 0325 | 2045 | 2212 |
| Sea Clutter On Imagery | Moderate | Moderate | Slight | Heavy |
| Pass No. | 16 | 9 | 15 | 14 |
| Altitude (ft) | 27,000 | 12,000 | 4,000 | 5,000 |
| No. of Targets | 59 | 38 | 32 | 53 |
| Dir. (°) | 153 | 130 | 150 | 150 |
| Look From Azimuth/Dir. | L/332 | R/316 | L/340 | R/327 |
| Look Relative To Wind Dir. ^a (i.e. Downwind) | 10°L | 60°R | 100°L | 30°L |
| Swath Width (km) | 25 | 25 | 25 | 25 |
| Location In Swath | Near | Far | Near | Far |

^aL - left
R - right

TABLE III-56
Occurrences of "Mystery" Target

| Radar | Pass | Date | Time (Z) | Aircraft HDG (°) | Wind Dir (°) | Look Dir. Heading To Wind (°) Dist(m) | HDG | Target HDG & Dist From Polaris |
|-------|-------------------|-------|-------------|---------------------|-----------------|--|-----|--------------------------------------|
| AES | TURN | APR 3 | 1400 | - | - | - | - | - |
| AES | 15 | APR 2 | 1839 | - | - | - | - | - |
| IIP | TURN | APR 3 | 1758 | - | - | - | - | 81 |
| IIP | 22 | APR 3 | 1757 | 179 | 250 | 109R | 177 | 108 |
| IIP | 19a | APR 3 | 1718 | 87 | 230 | 37R | 87 | 81 |
| IIP | 11 | APR 3 | 1557 | 180 | 258 | 102R | 180 | 54 |
| IIP | 25 | APR 3 | 1816 | 355 | 250 | 75L | 355 | 81 |
| IIP | TURN ^a | APR 3 | - | - | - | - | - | - |
| IIP | 20 | APR 3 | 1727 | 308 | 230 | 102L | 308 | 134 |
| IIP | TURN ^a | APR 3 | 1745 | - | - | - | - | 134 |
| IIP | 17a | APR 3 | 1653 | 38 | 230 | 12L | 038 | 81 |
| IIP | 18 | APR 3 | 1706 | 267 | 230 | 143L | 267 | 161 |
| IIP | 12 | APR 3 | 1614 | 40 | 258 | 38L | 40 | 27 |
| IIP | 13a | APR 3 | 1624 | 267 | 258 | 171L | 267 | 108 |
| IIP | 14 | APR 3 | 1632 | 87 | 230 | 37R | 87 | 81 |
| IIP | 15 | APR 3 | 1637 | 307 | 230 | 103L | 307 | 161 |
| IIP | 9b | APR 3 | 1533 | 179 | 320 | 39R | 179 | - |
| IIP | 8c | APR 3 | 1524 | 5 | 320 | 135L | - | - |
| IIP | 7d | APR 3 | 1519 | 175 | 320 | 35R | 175 | 27 |
| CCRS | 5 | APR 3 | | N TO S | | | | |
| CCRS | 8 | APR 3 | | W TO E | | | | |
| CCRS | 11 | APR 3 | | W TO E | | | | |
| CCRS | 12 | APR 3 | | N TO S | | | | |

^aNearby iceberg also has similar target with same relative distance and range as has mystery target from Polaris V.

^bTarget merged with ship target in near range; a single target emerges with a fine dark line demarking the separation between target and ship.

^cTarget behind berg next to ship, but not behind ship.

^dA second target at 700T, range 27 m from Polaris V.

Investigation of IIP imagery also indicated that the target always appeared "up azimuth" from the ship and always at an azimuth angle relative to the ship which was equivalent to the aircraft heading. Unfortunately, the ship was always imaged in the left swath on IIP, so no comparison could be made between left and right images. Because the target appeared on most of the passes by IIP, and always later in time relative to the return from Polaris V, it is thought that for the IIP imaging, this return might be an artifact of the radar. The average distance of the target from Polaris V as a function of range position is as follows:

| Range position | Passes | Average distance of target from <u>Polaris V</u> (m) |
|----------------|--------|--|
| FAR | 1 | 161 |
| MID | 10 | 104 |
| NEAR | 4 | 54 |

suggesting that the target is possibly an artifact of the antenna beam pattern. This would not explain the occurrence for other radars, especially CCRS. For the AES imagery a target was seen next to Polaris V on two passes as detailed for 3 April. It is still possible that this target might have been the waverider buoy because it only appeared on two passes and did not exhibit a regularity in its position relative to Polaris V as in the case for IIP. Also, two passes, one each by AES and IIP, coincided over the ship at the same time (1519GMT). When the two passes were superimposed so that iceberg A-1-2 and the ship were properly oriented with respect to true North, the mystery target seen by AES did not coincide with the position of the mystery target seen by IIP, nor did it exhibit a relationship to azimuth as on IIP. When it was seen on another pass, the target had changed its position relative to Polaris V; the azimuthal heading was the same for both passes.

III.7 ANALYSIS OF STAR-1 DIGITAL DATA, 7 APRIL

This study examined STAR-1 digital radar imagery to assist in determining the detectability of discrete targets (suspected icebergs) in an open ocean environment. Examination involved describing target and ocean (background) pixel grey-level statistics and spatial properties, illustrating various enhancements for target-background discrimination, and evaluating options for image display on target detectability. Analysis was performed using an ARIES II digital image-analysis system. Only a single data set from a single flight was available for analysis.

III.7.1 DATA

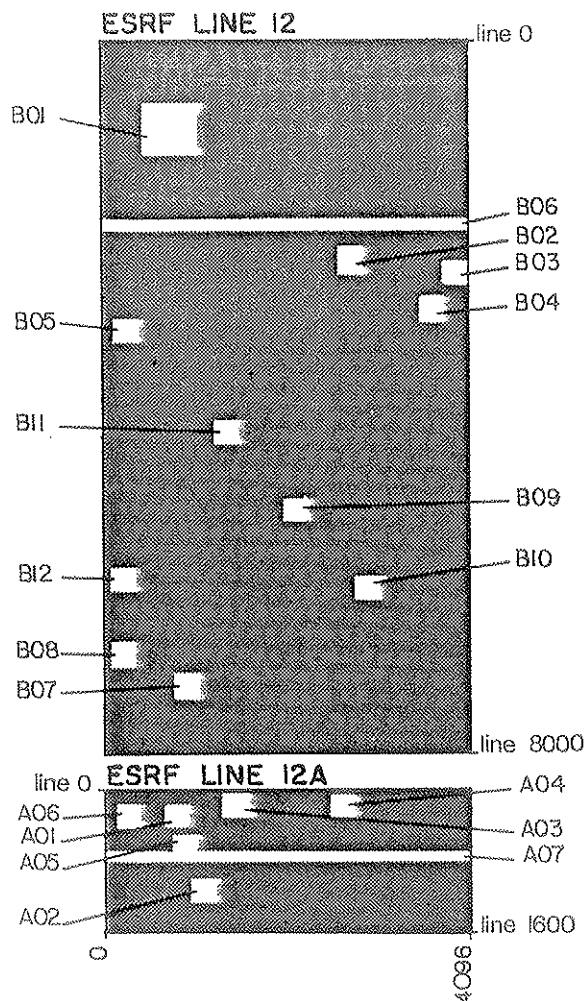
Three STAR-1 SAR 8-bit Computer Compatible tapes were provided by Intera Technologies Ltd. including data for passes 12 and 12a from 7 April 1984 (Bergsearch Line 9). Two of the CCTs covered the study area. "Windows" were extracted for detailed study (Figure III-35). The quality of STAR-1 SAR digital data appears excellent. Less than 0.5% dropped scan lines occur in the data which span and fully use the available 8-bit, 256 grey-level range. A gain change occurs once, at the start of the CCT, on ESRF Line 12.

III.7.2 TECHNIQUES AND PROCEDURES

ARIES II tasks were used; in particular, spectral and spatial enhancements were applied for discrimination between target and ocean. Image display options were used for tests on the effects on target detectability. Pixel dump and training area tasks were used to extract grey-level information over both ocean and targets (suspected icebergs).

Surface data have not been verified, because they were not compiled at the time of analysis. The work and results pertain to visually observable targets on the high-resolution video monitor, labelled for this study as suspected icebergs. Digital data provided were previously resampled such that pixel surface dimensions are on the order of about 4-5 m.¹ This information was not essential to conduct the study since results are presented on a pixel basis, without units. This information was not essential to conduct the study as results are presented on a pixel basis, without units.

¹ B. Mercer, 1984 personal communication



SUBSCENE LOCATIONS ON CCTs

| | Line | 694-1294 | Pixel | 424-1026 |
|-----|------|-----------|-------|-----------|
| B01 | | 2300-2600 | | 2600-2900 |
| B02 | | 2450-2750 | | 3650-3950 |
| B03 | | 2850-3150 | | 3550-3850 |
| B04 | | 3300-3600 | | 150- 450 |
| B05 | | 2000-2100 | | 1-3988 |
| B06 | | 7100-7400 | | 800-1100 |
| B07 | | 6750-7050 | | 100- 400 |
| B08 | | 5700-6000 | | 2000-2300 |
| B09 | | 6000-6300 | | 2800-3100 |
| B10 | | 4250-4550 | | 1250-1550 |
| B11 | | 5900-6200 | | 150- 450 |
| B12 | | | | |
| A01 | | 150- 450 | | 675- 975 |
| A02 | | 1000-1300 | | 975-1275 |
| A03 | | 65- 365 | | 1275-1575 |
| A04 | | 25- 325 | | 2500-2800 |
| A05 | | 450- 750 | | 775-1075 |
| A06 | | 175- 475 | | 175- 475 |
| A07 | | 700- 800 | | 1-3989 |

Figure III-35. Digital "windows" extracted from CCT ESRF 12 and CCT ESRF 12A, for detailed study.

III.7.3 RADAR IMAGE AND TARGET CHARACTERISTICS

Reliable detection of targets requires that they differ from their background in a consistent, predictable fashion. To explore fully enhancement techniques, an understanding of target and background image properties is needed.

Ocean Background

A first task was to look at changes in grey level over open water areas along ESRF Flight Line no. 9, both in the along-track (different recording time) direction and in the range direction. Figure III-36 illustrates these changes. Each point on the curve of this figure represents the average grey level for 100 X 100 pixel windows, that is averages for about 10,000 data values per window.

Significant changes in grey-level intensity occur between ESRF Lines 12 and 12a (see Figure III-36). This change may result from drift in the radar system or from changing surface conditions along the flight line. Furthermore, significant changes in grey-level intensity occur across the image swath for ESRF Line 12a. Similarly, this may indicate instrument drift, but is more likely to represent changing surface conditions. In any case, along-track and across-track grey-level changes are real and must be considered in image enhancement for target discrimination, especially if ocean and target grey levels become more alike. Closer examination of Figure III-36 shows increased grey level variation in mid-swath for both along-track positions, possibly revealing antenna beam pattern effects.

These results suggest a need to develop enhancements sensitive to geometric position within a flight line, once these along-track and across-track grey-level changes are understood and quantified. ARIES II tasks that were available did not allow for application of position-sensitive enhancements. Furthermore, the imagery was not stratified to eliminate range or along-track changes in this study. Another difficulty foreseen in these grey-level changes is in the absolute comparison of multiple data sets. Corrections to the data are likely prerequisites.

A next step toward understanding ocean background information was the extraction of subscenes throughout the flight line, and the calculation of the mean grey level and grey level variation for each subscene. Figure III-37 shows a plot relating mean and standard deviation of subscene grey levels. Further examination of the subscenes allowed grouping of the points in the plot into broad classes; namely, subscenes containing only discrete targets such as icebergs, subscenes containing extended and discrete targets such as icestrips, strings and pieces, subscenes over land areas covered by snow, and one subscene with a gain change.

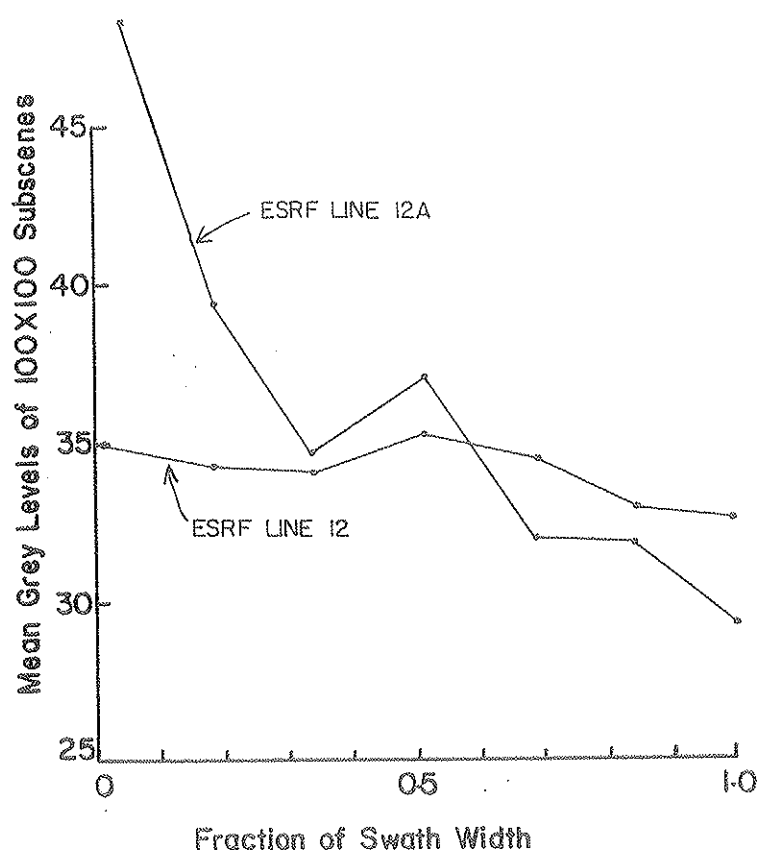


Figure III-36. Grey-tone change in both along-track and azimuthal directions.

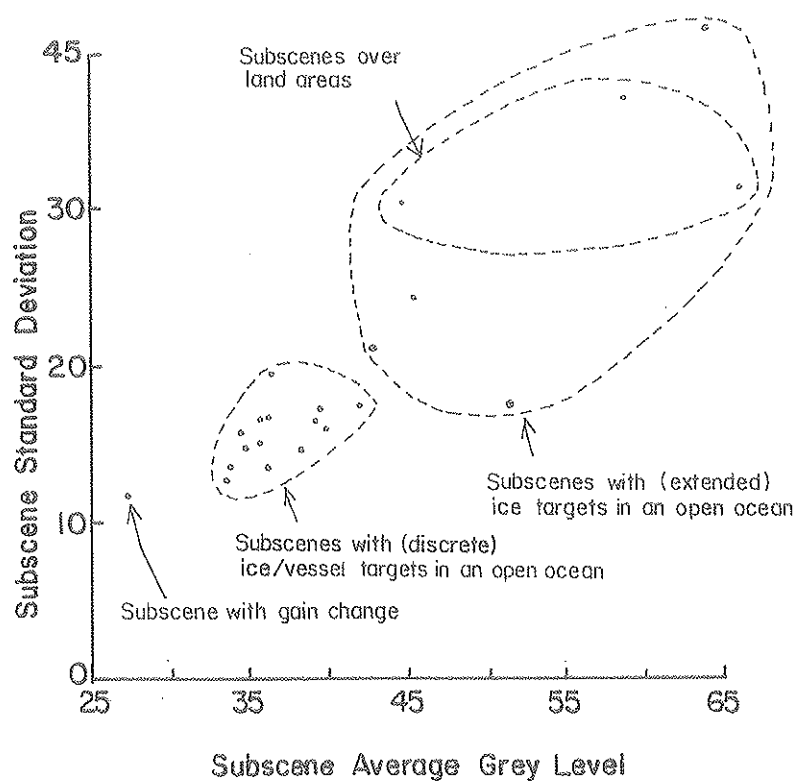


Figure III-37. Distribution of subscene grey levels.

The result was unexpected but useful in that it raised the question whether this grouping was possibly applicable to other flights.

Discrete Targets

Grey-level profiles, or cross-sections, were measured at the mid-azimuth point of 11 discrete targets, (Figure III-38). Grey levels were recorded over the adjacent open ocean, across the target, and over the adjacent ocean on the opposite side of the target. Profiles were taken at a representative mid-azimuth section in the across-track, or range, direction. Normalized grey level on Figure III-38 indicates that all grey levels measured were divided by 255, the maximum available grey level. Normalized target range dimension indicates that the pixel dimension in the range direction was taken as unity. In this way all targets could be better compared visually on the one figure.

Data for the targets selected indicate a marked difference between adjacent ocean profiles and target profiles, for average grey level and for root mean square (RMS) grey-level variation. Statistically, adjacent ocean and targets are distinct based on these measures. The data indicate that target cross-sections average about 80 grey levels more than adjacent open ocean, have a grey-level RMS about 100 more than adjacent open ocean, and have a grey-level standard deviation about 40 more than adjacent open ocean. Figure III-38 also shows that profiles change rapidly at the target's near range and far range edges. A further discriminator for targets, then, can be grey level separation from the ocean background or grey level variation and the rapid tonal change across the boundary between ocean and target. A spatial filter using these properties could help enhance and detect discrete targets.

Probability Distributions

Pixel dumps of grey-level values over areas of open ocean and over selected targets were collected to examine more closely the sample population characteristics between ocean and target grey levels, (Figure III-39).

It is seen that open ocean and target pixels appear distinct though with some overlap in grey levels below 100. Figure III-39 provided a measure of target probability of detection and probability of false alarm, (Figure III-40) was based on sampling 739 open-ocean pixels and 984 target pixels.

Using a selected grey level threshold value both probability of target detection and false alarm can be determined. However, this result is based on data from one flight only. Further work is required to compare results under different flight and surface conditions.

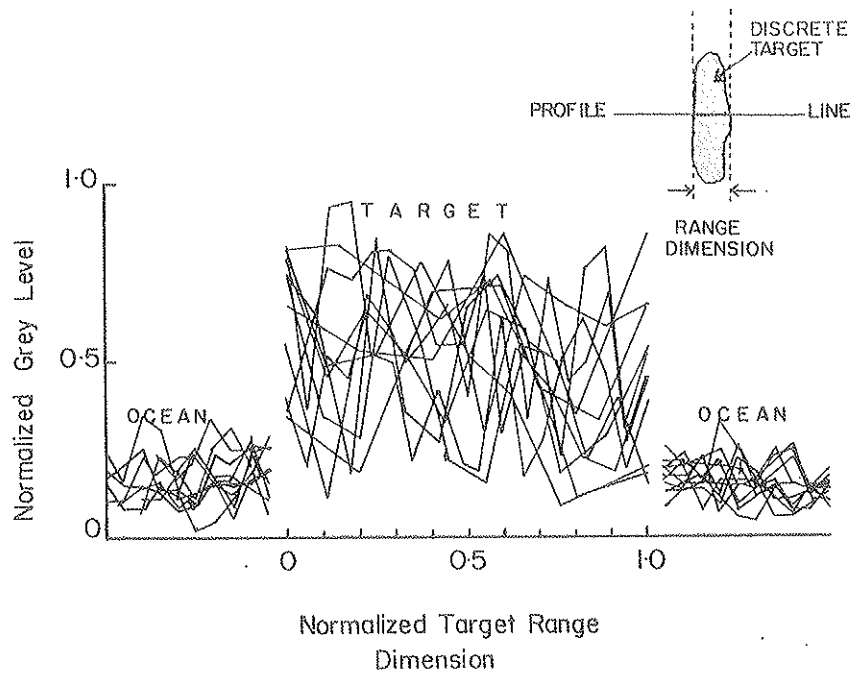


Figure III-38. Cross-section profiles for discrete targets.

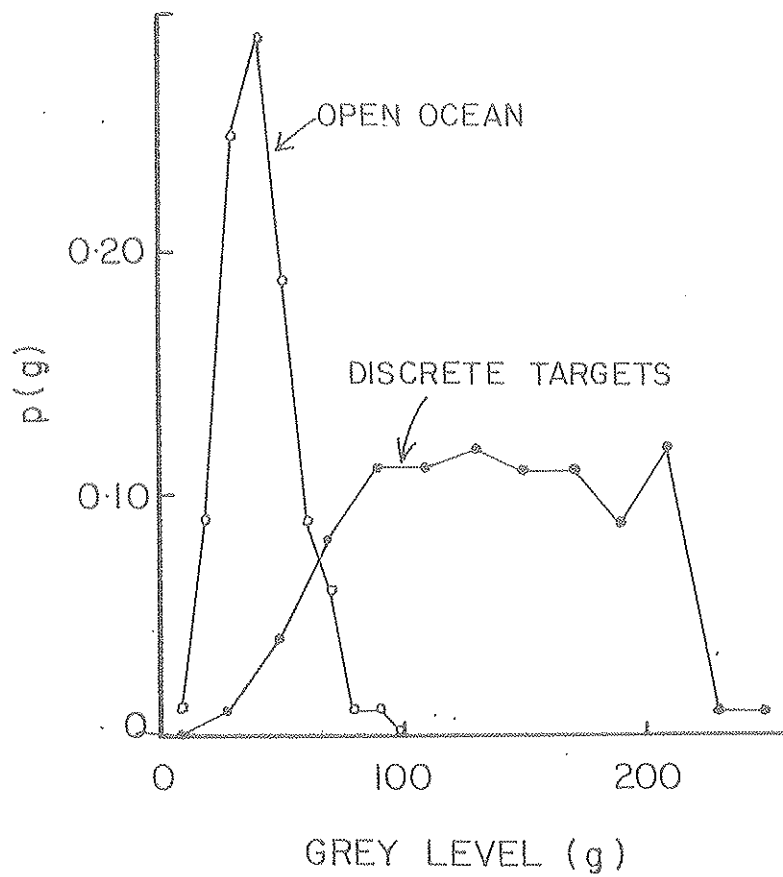


Figure III-39. Sample probability distribution for grey levels over open ocean and discrete targets.

III.8 CCRS PRELIMINARY ANALYSIS, APRIL 1

Data were collected by CCRS on 29 March and on 1, 2 and 3 April using the CV-580 multi-channel SAR. Because the optical recorder was not available, all data were collected on digital tape, which severely restricted the amount of data that could be collected. These data were not digitally processed until late in the BERGSEARCH program, and therefore only a preliminary analysis of April 1 data is available. The Convair was the only aircraft which flew on that date.

III.8.1 AVAILABLE SURFACE INFORMATION

Polaris V was stationed at approximately 46°49'N, 46°49'W, during the overflight. A small iceberg, D-1, and a very large iceberg, B003, as well as two growlers were observed by the surface team. Characteristics of the two larger icebergs are as follows:

| Iceberg | Dimensions (m) | Type | Comments |
|---------|----------------|---------|--------------------------------|
| B003 | 248 x 140 x 35 | Tabular | -- |
| D-1 | 35 x 30 x 10 | Drydock | Unstable; bobbing and rotating |

Significant wave height varied between 3.5 and 4.0 m during the time of the overpass, and a waverider buoy was deployed which gave characteristic wave height of 4.0 to 4.5 m. Wind speed varied between 5 and 25 knots from the southwest.

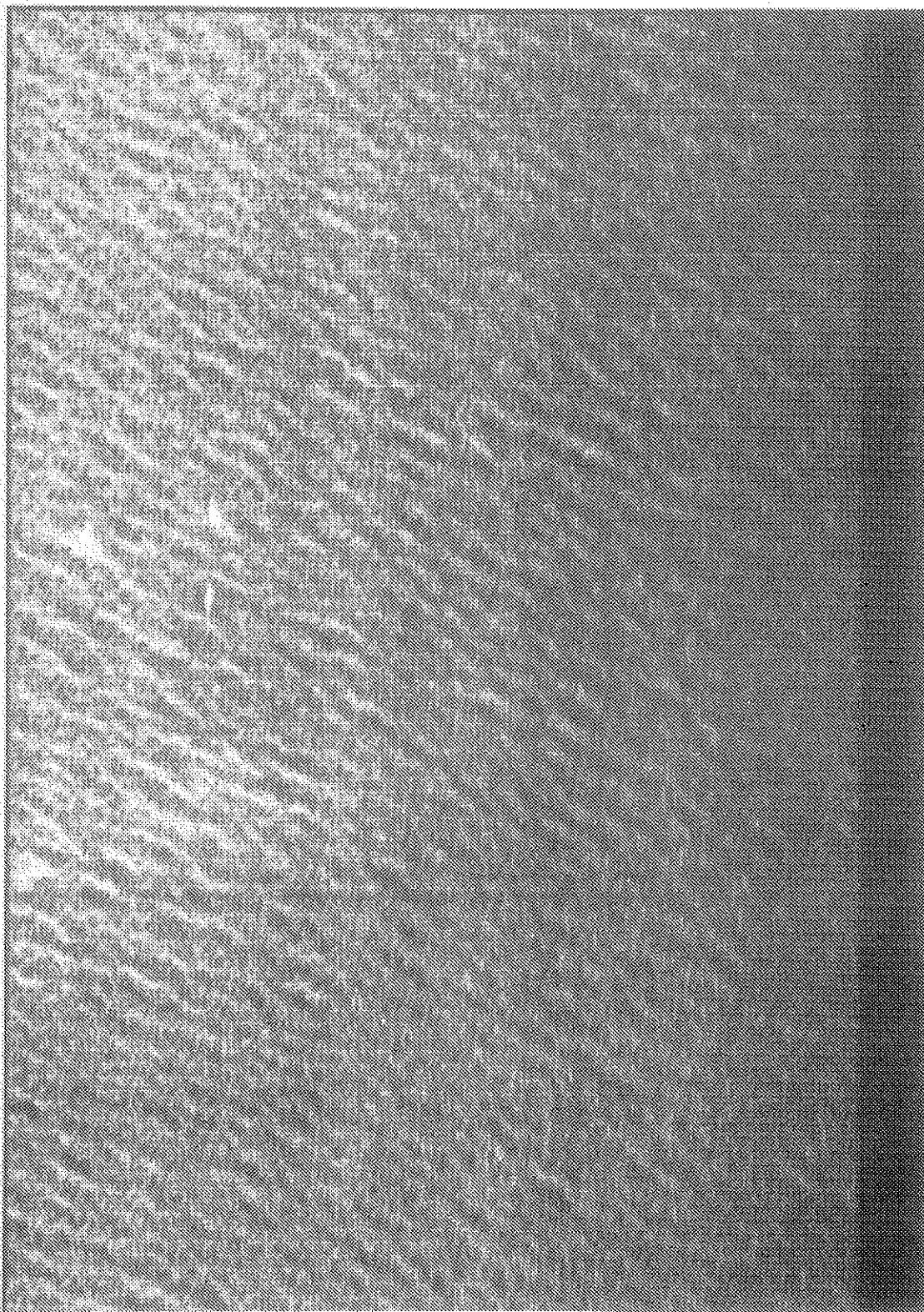
III.8.2 CV-580 SAR DATA

X and C-band, HH data were recorded on this day on three passes at different look angles with respect to wind. The incidence angles were relatively steep, about 45° to 60°.

Data from the three passes are given in Figures III-40 through III-43. From this data set, five preliminary conclusions were reached by Dr. L. Gray of CCRS.

CANADA CENTRE FOR REMOTE SENSING

SIO#308 HIBERNIA PR#5580-83-75 RADARSAT-SDA00419
 SAR580 HRNS-X HH FLIGHT 001002 19840401192040000 PRM.CNTR.46:48: 0 N 46:48: 0 U
 PROCESS CANADA CCRS CSHARP 19840716 IMAGED 07:40 29-JUL-84
 RESOLUTION: 1.4M RA X 1.4M AZ. LOOKS: 1 X 1 SCALE 0 2.0KM
 AZIMUTH

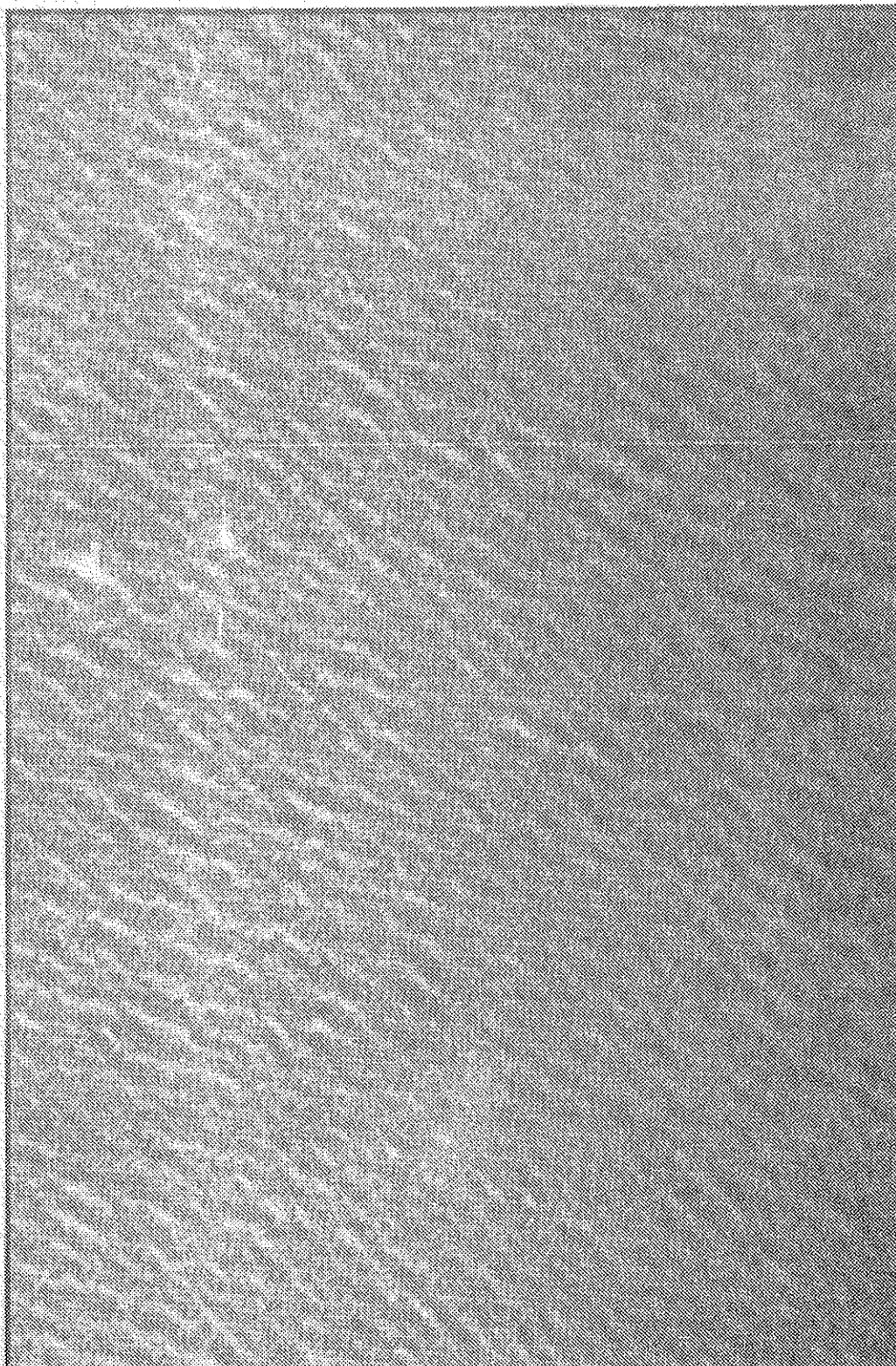


BRUNDAGE RANGE

Figure III-40. CV-580 imagery, pass 2, X-band, 1 April 1984.

CANADA CENTRE FOR REMOTE SENSING

S10#309 HIBERNIA PR#S580-83-75 RADARSAT-SDA0418
 SARSB0 HRNS-C HH FLIGHT 001002 19840401 092040000 PRM.DNTR.46:48: 0 N 46:48: 0 W
 PROCESS CANADA CCRS CSHARP 19840717 IMAGED 08:42 29-JUL-84
 RESOLUTION: 1.4M RA X 1.4M AZ LOOKS: 1 X 1 SCALE 0 2.0KM
 AZIMUTH



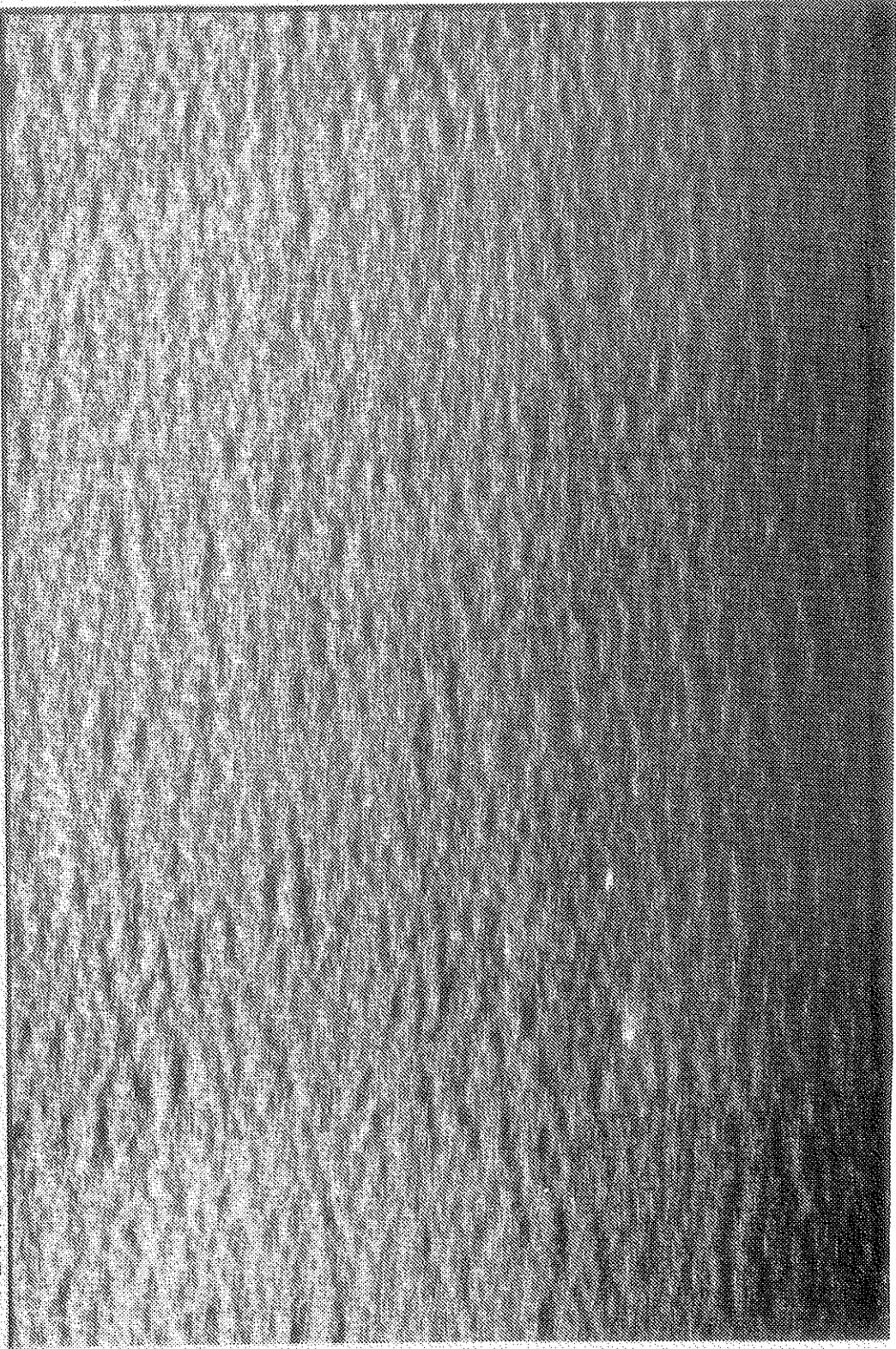
GROUND RANGE

Figure III-41. CV-580 imagery, pass 2, C-band, 1 April 1984.

CANADA CENTRE FOR REMOTE SENSING

SIO#305.HIBERNIA.PR#SS80-83-7S RADARSAT-SDA00424
SAR580 HRN5-X HH FLIGHT 004003 19840401183450000 FRM.CNTR.46:48: 0 N 46:48: 0 W
PROCESS CANADA CCRS CSHARP 19840718 IMAGED 10:40 29-JUL-84
RESOLUTION: 1.4M RA X 1.4M AZ LOOKS: 1 X 1 SCALE 0 2.0KM

AZIMUTH



GROUND RANGE

Figure III-42. CV-580 imagery, pass 3, X-band, 1 April 1984.

CANADA CENTRE FOR REMOTE SENSING

SIO#307.HIBERNIA.PR#5580-83-75 RADARSAT-SDA0423
 SAR580 HRNS-C HH FLIGHT 004003 19840401193450000 FRM.CNTR,45:48: 0 N 46:48: 0 W
 PROCESS CANADA CCRS CSHARP 19840718 IMAGED 11:42 29-JUL-84
 RESOLUTION: 1.4M RA X 1.4M AZ. LOOKS: 1 X 1 SCALE 0 2.0KM
 AZIMUTH

GROUND RANGE

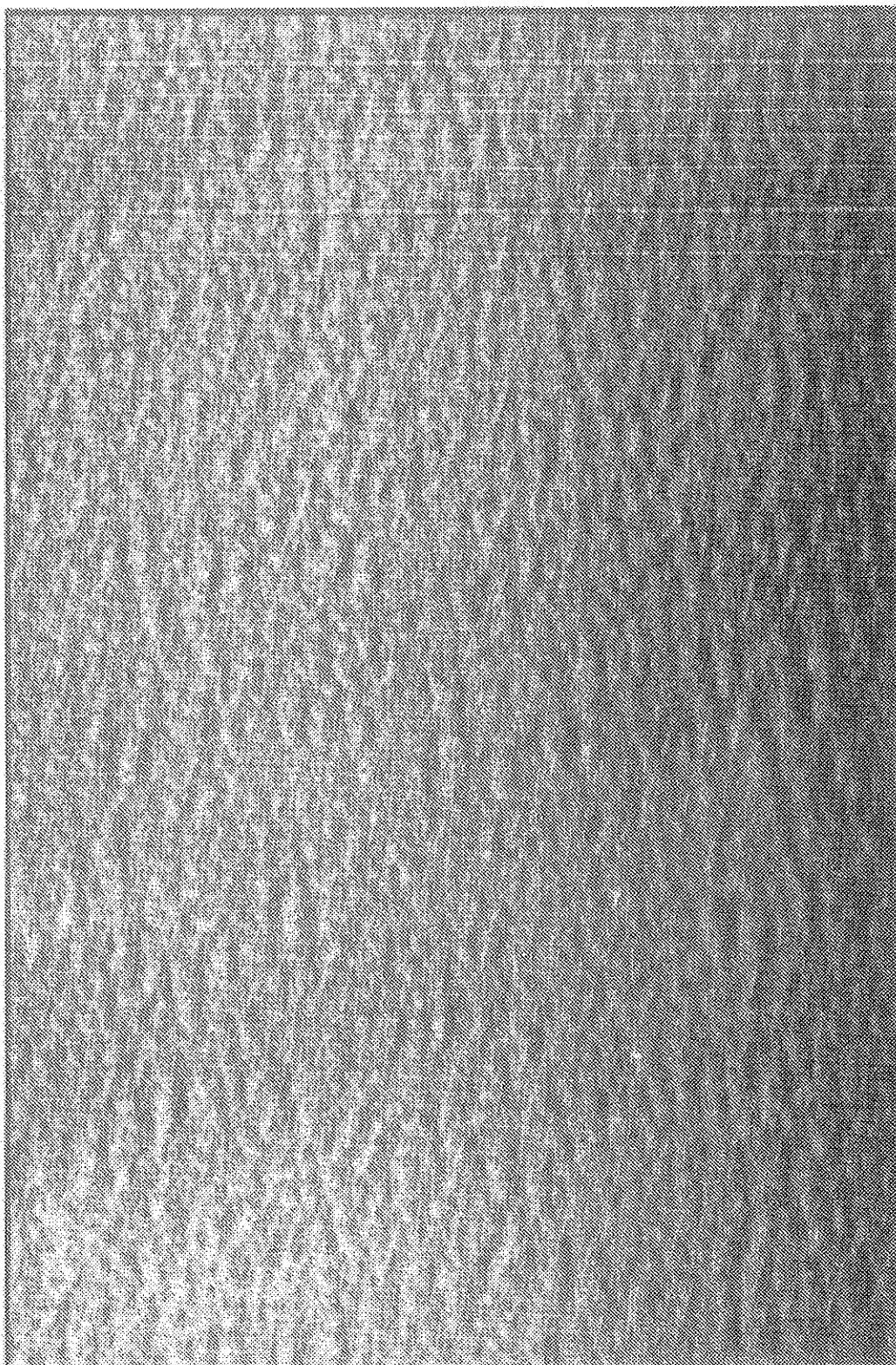


Figure III-43. CV-580 imagery, pass 3, C-band, 1 April 1984.

- a) Growlers or bergy bits would not be detected reliably with the SAR-580 at these steep incidence angles and these conditions of wind and sea state, with either the X or C- band channels.
- b) High sea state clearly broadens the distribution of ocean back-scatter. Consequently, detectability models based on an average back-scatter due to wind speed must also include the variation in modulation of the backscatter due to waves.
- c) For moderate winds but high sea state the swell direction appears to be more important than wind direction.
- d) The azimuthal smear, which is common to SAR imagery of icebergs appears greater with higher sea state.
- e) In this data set, X-band SAR imagery appears to detect icebergs more clearly than does C-band imagery. This conclusion may differ from those of other investigators, such as the European Space Agency.

It is expected that further work on these and other data collected during the project will be undertaken. In particular, the effects of azimuthal smear is of great interest to the problem of using SAR for detecting icebergs.

III.9 CONSIDERATIONS OF DEPRESSION ANGLE

The product of two independent factors determines the average received clutter from a rough ocean for a given radar: the radar cross-section of the ocean at a particular viewing geometry, and the illuminated area. For SLARs, both the geometry (depression angle) and the resolution cell size change across a radar swath.

Several models have been developed for estimating the ocean clutter; e.g., by Sittrop (1977) for near grazing angles, and by Chan and Fung (1977) for intermediate angles. Examples of the radar cross-section for horizontal (HH) polarization are shown in Figure III-44 for these two empirical models. At high wind speeds the models do not merge well, possibly because of the lack of data in the original data sets.

To estimate the effect of SLAR viewing geometry on ocean clutter, the Chan and Fung model was used for various slant ranges and altitudes. The results are shown in Figures III-45 to III-48 for wind speeds from 5-40 knots, viewed cross-wind. The detrimental effect of increasing altitude and far range can be seen. Use of Sittrop's model (applicable at far ranges) would accentuate the trend shown.

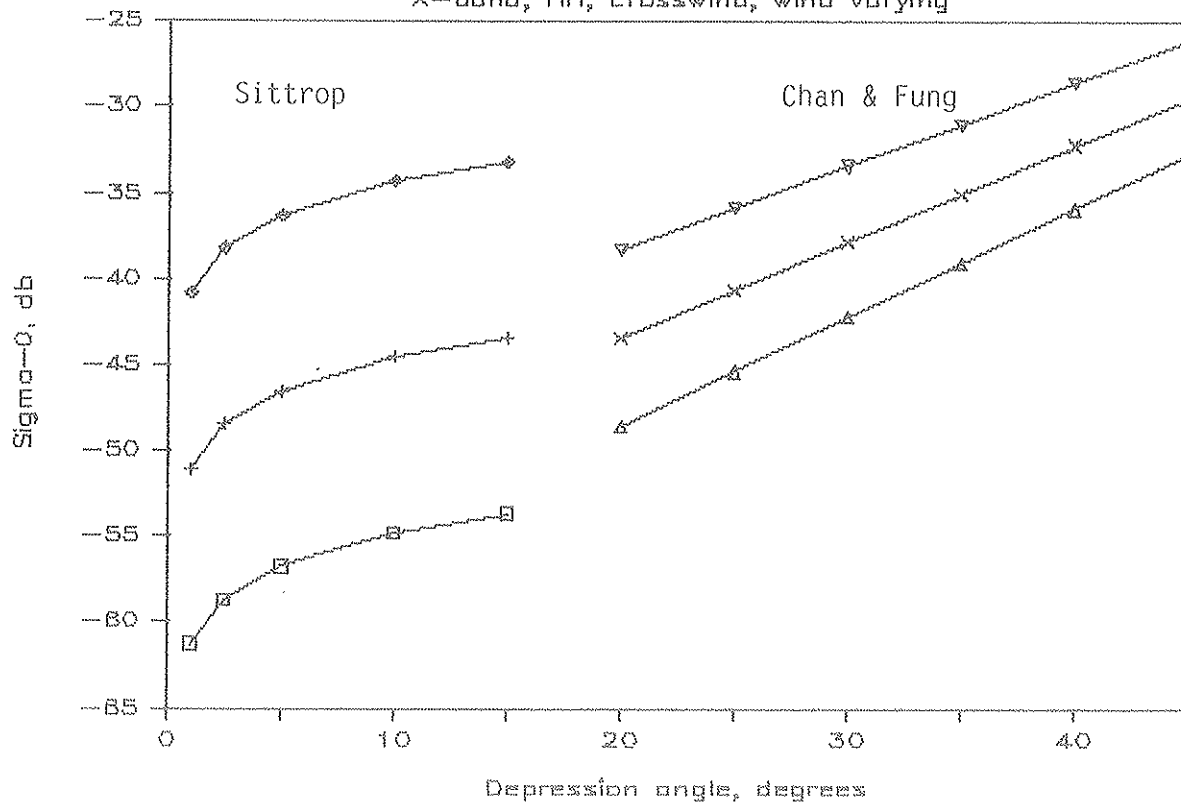
In addition to the clutter estimates, the target strength of ice also decreases with decreasing depression angle (Onstott et al. 1979). Although icebergs do not necessarily show a flat horizontal surface to the radar, the trend will be to lower radar signatures for far ranges.

Therefore, to detect icebergs best, SLARs should be flown at generally lower altitudes. At a given altitude, there is an optimum range for detection; typically 10-30 km. Of course, the altitude will be constrained by operational factors, such as turbulence and air traffic control.

For SARs, only the ocean and ice radar cross-sections are relevant. Therefore SARs can fly at higher altitudes and look with a viewing angle well offset from nadir to reduce the depression angle. This offset could have another advantage in increasing the integration time of the SAR looks and hence increasing the probability of detecting a bobbing iceberg.

OCEAN BACKSCATTER

X-band, HH, crosswind, wind varying



Wind Speed:

- \square 5 knots
- \times 10 knots
- \diamond 20 knots

FIGURE III-44. TWO MODELS FOR OCEAN RADAR CROSS-SECTION, σ_0 , AS A FUNCTION OF WINDSPEED AND DEPRESSION ANGLE

FIGURE III-45.

SLAR Clutter

x-band, HH, for 40 knot wind

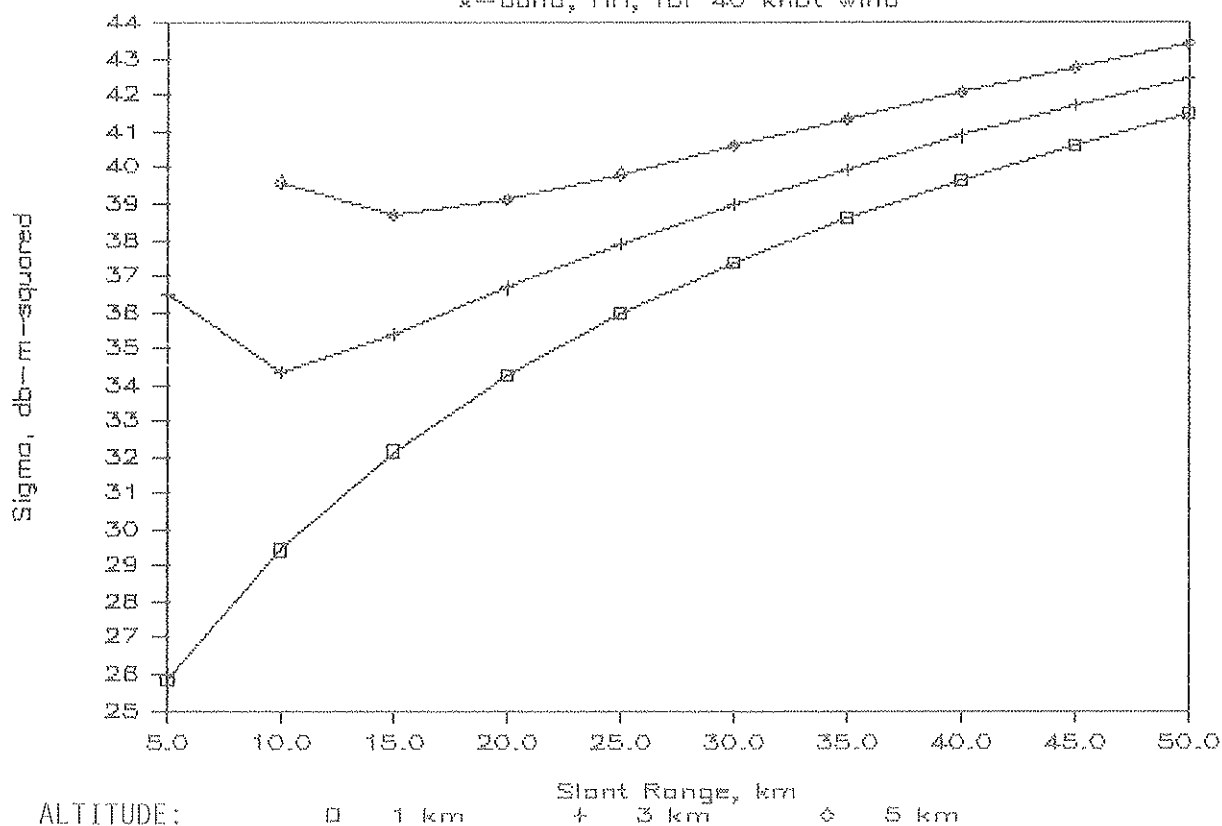


FIGURE III-46.

SLAR Clutter

x-band, HH, for 20 knot wind

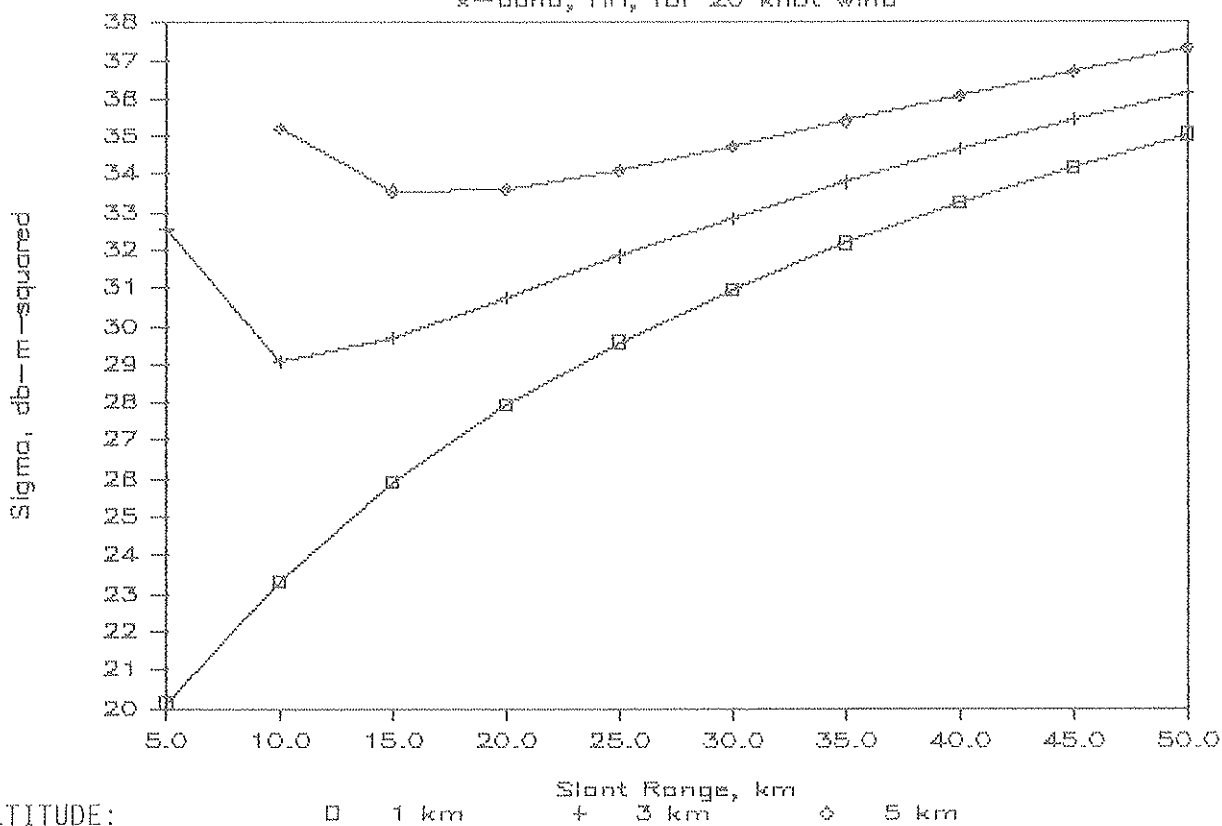


FIGURE III-47.

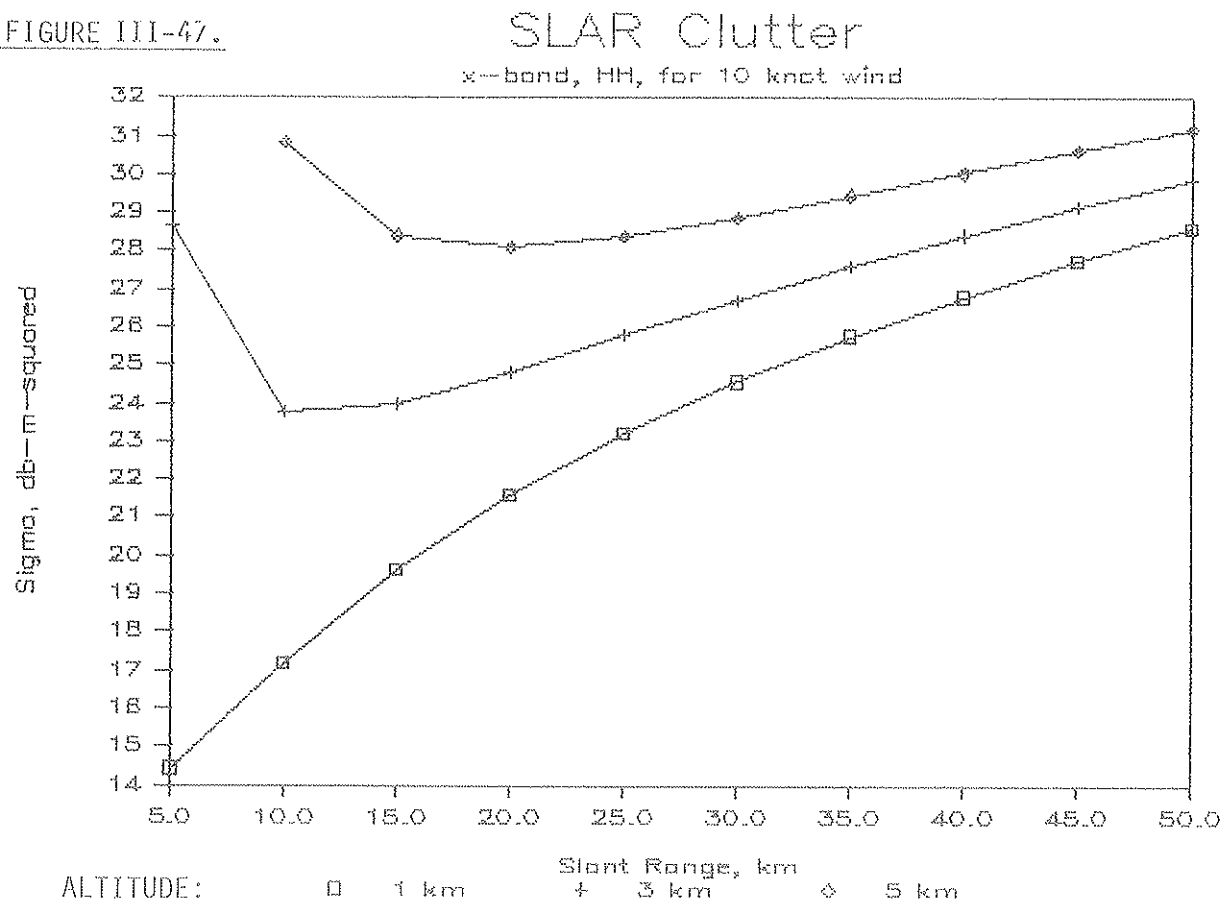
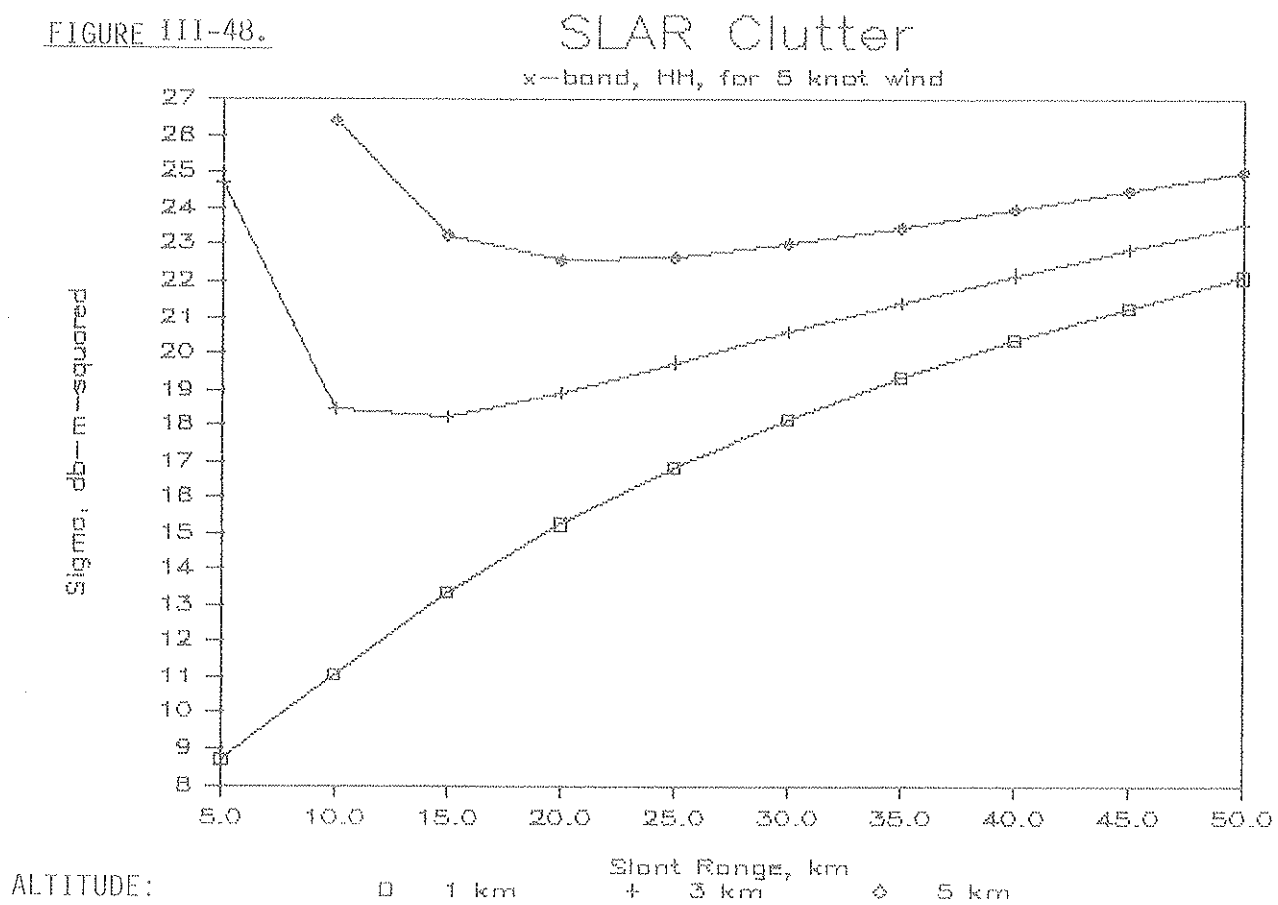


FIGURE III-48.



REFERENCES

- Chan, H. L., and A. K. Fung (1977), "A Theory of Sea Scatter at Large Incidence Angles", J. Geophys. Res., v. 82, pp. 3429-3444.
- Onstott, R.G., et al., (1979) "Surface-Based Scatterometer Results of Arctic Sea Ice," IEEE Transactions on Geoscience Electronics, Vol, GE-17, No.3, July 1979, pg. 78-85.
- Sittrop, H. (1977), "On the Sea-Clutter Dependency on Windspeed", Proc. RADAR '77, pp. 110-114.

III.10 RESULTS

The main results from each analysis are brought together here, particularly to estimate iceberg detectability as a function of the parameters described earlier. These results were presented at a small technical workshop held in Toronto on 28 November 1984, and the results of that discussion have also been incorporated here.

Icebergs that were observed during the **BERGSEARCH '84** experiment were categorized according to WMO iceberg size classification (see Table III-1). All data presented in diagrams and tables of this section conform to that standard.

III.10.1 TARGET DETECTABILITY BY ICEBERG SIZE

The number of targets detected by iceberg class, for each radar except MARS, during flights on April 3, 5, and 7 is shown in Figure III-49. Figure III-49 shows that all radars (AES, IIP, and STAR-1) were 96-100% effective in detection of surface-truthed targets of the medium size class. For the small size class, STAR-1 had a 100% success rate, whereas IIP and AES detected 96% and 85%, respectively. In the bergy bit class, STAR-1 detected 81% of the verified targets, whereas IIP and AES detected 71% and 59%, respectively. For the growler class, IIP detected 9%, AES 17%, and STAR-1 49%.

Data presented in Figure III-49 are also tabulated in Table III-57; percentages are calculated as a ratio of the number of targets known to be in the area from surface measurements compared to the number of targets appearing on the imagery. Table III-58 also shows the percentage of targets detected by the MARS aircraft for April 5. Because the data from the MARS aircraft cover only one day the results are not directly comparable to results obtained by the other aircraft during three days of data collection.

III.10.2 TARGET DETECTABILITY BY SEA STATE

Figure III-50 shows target detectability for bergy bits as a function of sea state, for each radar except MARS for bergy bits. Figure III-51 shows detectability for growlers; there were insufficient data for some days. Table III-58 gives the number of targets detected compared with the number of surface-checked icebergs for each radar and sea state. Although the results are sparse for some sets of parameters, in general detectability decreased measurably as sea state increased.

FIGURE III-49. TARGETS DETECTED BY CLASS

For Each Radar (Apr3,5,7); Legend Below

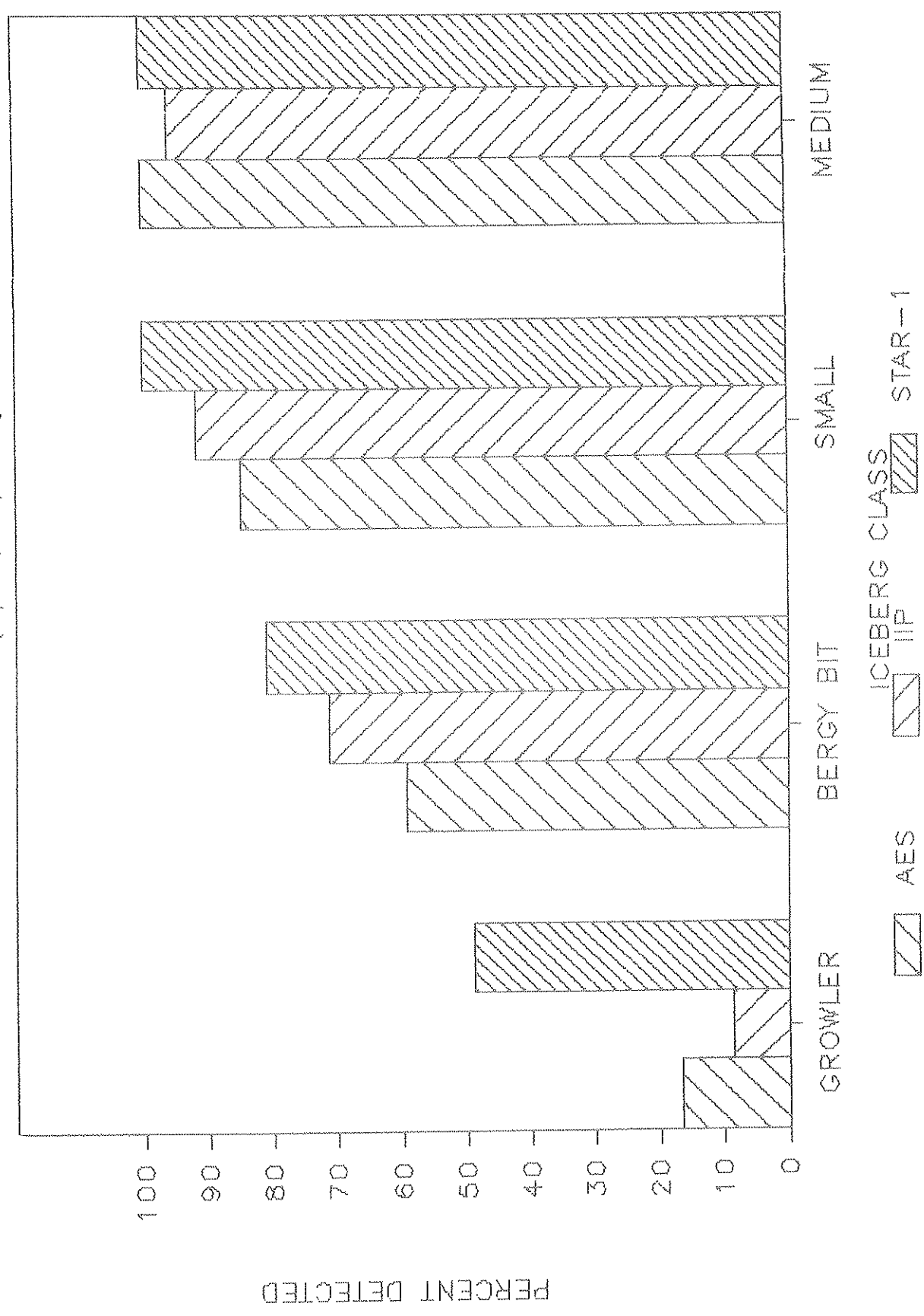


TABLE III-57

Ratio of Targets Present to Total Targets
by Radar and Size Class, April 3, 5, and 7 Data Combined

| RADAR | SIZE CLASS | TARGETS PRESENT/TOTAL TARGETS | PERCENTAGE |
|-------------------|----------------|-------------------------------|------------|
| AES | Medium Iceberg | 9/ 9 | 100 |
| | Small Iceberg | 28/33 | 85 |
| | Bergy Bit | 52/88 | 59 |
| | Growler | 6/36 | 17 |
| IIP | Medium Iceberg | 23/24 | 96 |
| | Small Iceberg | 33/36 | 92 |
| | Bergy Bit | 57/80 | 71 |
| | Growler | 5/58 | 9 |
| MARS ^a | Medium Iceberg | 24/24 | 100 |
| | Small Iceberg | 4/ 4 | 100 |
| | Bergy Bit | 2/ 2 | 100 |
| | Growler | 1/ 3 | 33 |
| STAR-1 | Medium Iceberg | 6/ 6 | 100 |
| | Small Iceberg | 31/31 | 100 |
| | Bergy Bit | 43/53 | 81 |
| | Growler | 20/41 | 49 |

^a Based on April 5 imagery only

TABLE III-58

Summary of Targets Present vs Total Target Population
by Radar Type, Size Class, and Day of Observation

| RADAR | SIZE CLASS | APRIL 3 | APRIL 5 | APRIL 7 |
|--------|----------------|---------------------------------------|--------------------------------|---------------------------------------|
| | | (ALL ASPECTS) (S.W.H.=2.45-2.89 m) | (ALL ASPECTS) (S.W.H.=≤1 m) | (ALL ASPECTS) (S.W.H.=1.61-2.06 m) |
| AES | MEDIUM ICEBERG | - | 9/ 9 | - |
| | SMALL ICEBERG | 12/12 100% | 5/ 7 71% | 11/14 79% |
| | BERGY BIT | 27/54 50% | 6/ 6 100% | 19/28 68% |
| | GROWLER | 0/ 6 0% | 1/ 2 50% | 5/28 18% |
| IIP | MEDIUM ICEBERG | - | 23/24 | - |
| | SMALL ICEBERG | 8/ 8 100% | 10/12 83% | 15/16 94% |
| | BERGY BIT | 24/36 67% | 10/12 83% | 23/32 72% |
| | GROWLER | 1/24 4% | 0/ 2 0% | 4/32 13% |
| MARS | MEDIUM ICEBERG | - | 24/24 | - |
| | SMALL ICEBERG | - | 4/ 4 | - |
| | BERGY BIT | - | 2/ 2 | - |
| | GROWLER | - | 1/ 3 | - |
| STAR-1 | MEDIUM ICEBERG | - | 6/ 6 | - |
| | SMALL ICEBERG | 4/ 4 100% | 13/13 100% | 14/14 100% |
| | BERGY BIT | 9/18 50% | 7/ 7 100% | 27/28 96% |
| | GROWLER | 3/12 25% | 1/ 1 100% | 16/28 57% |

FIGURE III-50. DETECTABILITY VS SEA STATE
(Bergy Bit Size Class)

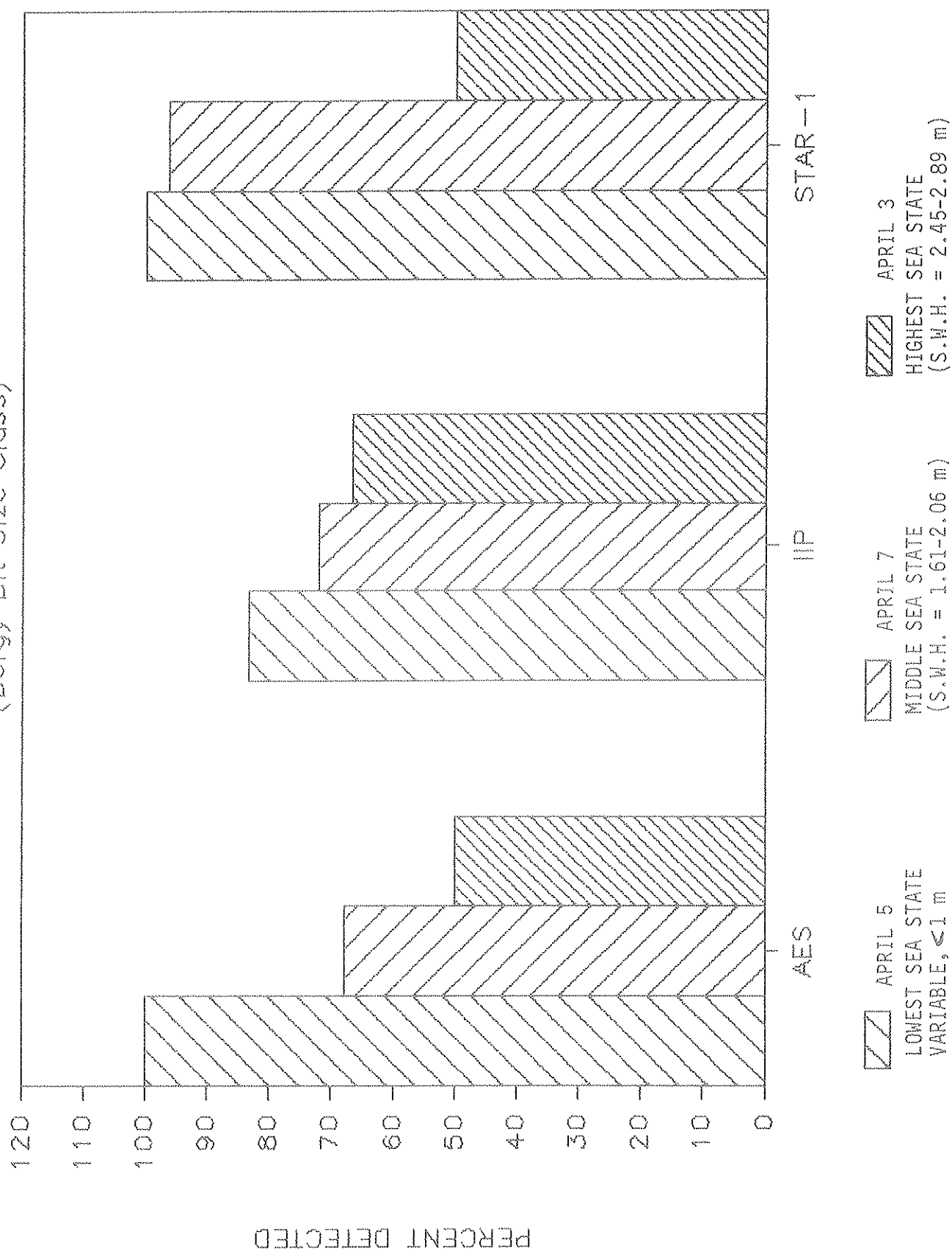
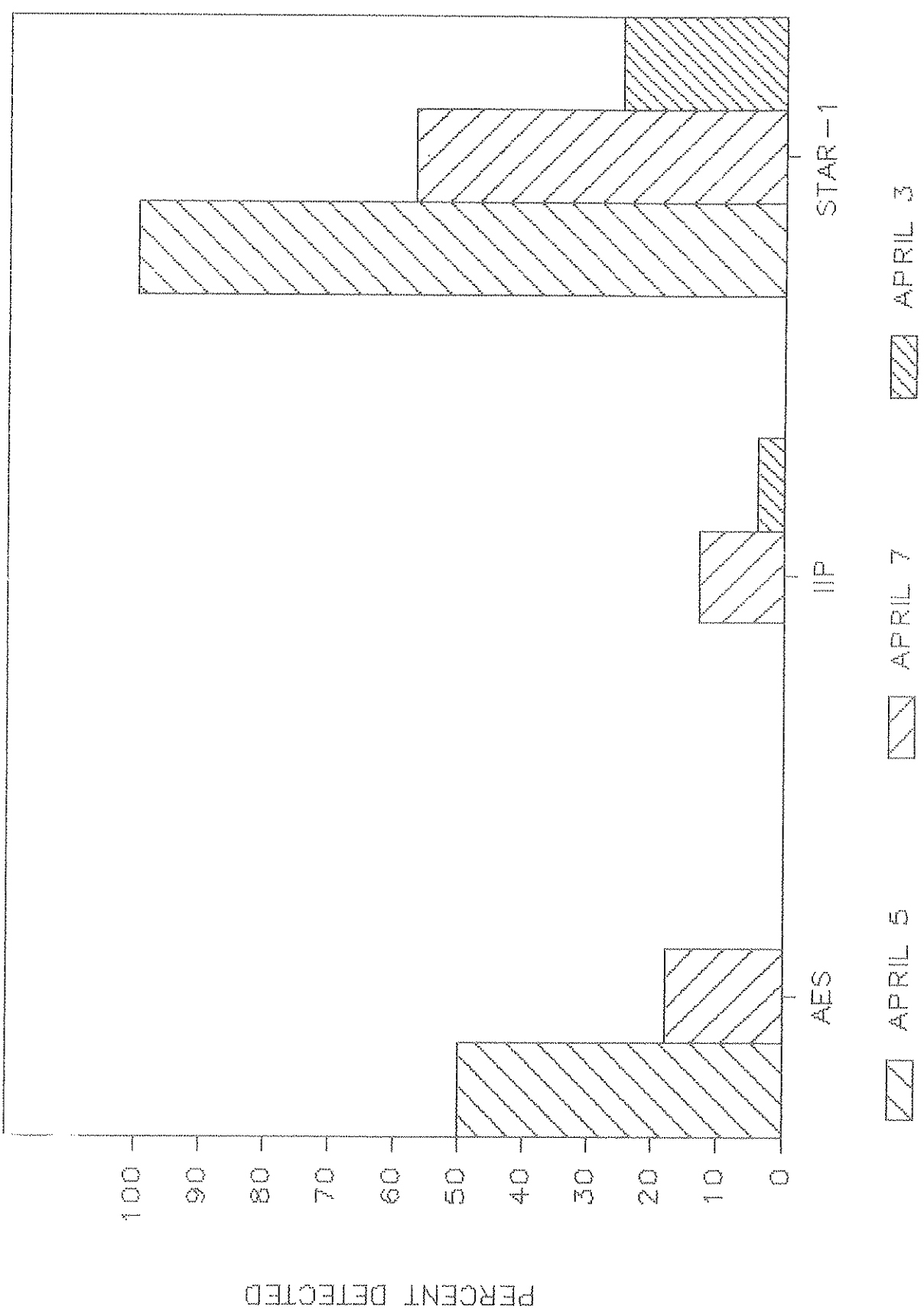


FIGURE III-51. DETECTABILITY VS SEA STATE
(Growler Size Class)



III.10.3 TARGET DETECTABILITY BY ASPECT ANGLE

Figure III-52 shows the target detectability for bergy bits as a function of radar aspect angle on April 7. Although there are variations from radar to radar, the general trend is that detectability is best when the radar is looking cross-wind, is moderately good when looking downwind, and is worst when looking upwind. Table III-59 summarizes detectability data by aspect angle for the various iceberg size classes.

III.10.4 TARGET DETECTABILITY BY RADAR

Figure III-53 shows the detectability of targets by size class for SAR (STAR-1) and SLAR systems (AES, IIP, and MARS). For the medium icebergs and larger, the performance of both types of radar is about 100%, under the conditions encountered. However, as iceberg size decreased, the relative performance of the higher-resolution SAR improved over that of SLAR. Table III-60 shows the ratio of targets detected to the number actually known to be present for each size class and radar type.

III.10.5 TARGET DETECTABILITY BY ALTITUDE

Figure III-54 shows target detectability by size class as a function of radar altitude for IIP and AES SLARs. In general, detectability of targets in the bergy bit and small-iceberg classes increased as altitude decreased. However, the detectability of growlers does not appear to be greatly affected by altitude. Perhaps detection of growlers is more dependent upon other factors. Table III-61 compares the number of targets imaged with the number known to be present.

III.10.6 TARGET DETECTABILITY VS. RADAR RESOLUTION

Figure III-55 shows the percentage of icebergs detected as a function of the ratio of iceberg area to radar resolution cell size for SLAR and SAR. If resolution cell size were the only factor in determining detectability, then the percentage of targets detected should increase monotonically as a function of the X-axis variable. Clearly other factors, such as sea clutter, are affecting detectability. Hence radar resolution is not the sole factor controlling the detectability of small targets.

FIGURE III-52. DETECTABILITY BY ASPECT ANGLE; APRIL 7
FOR BERG BIT CLASS

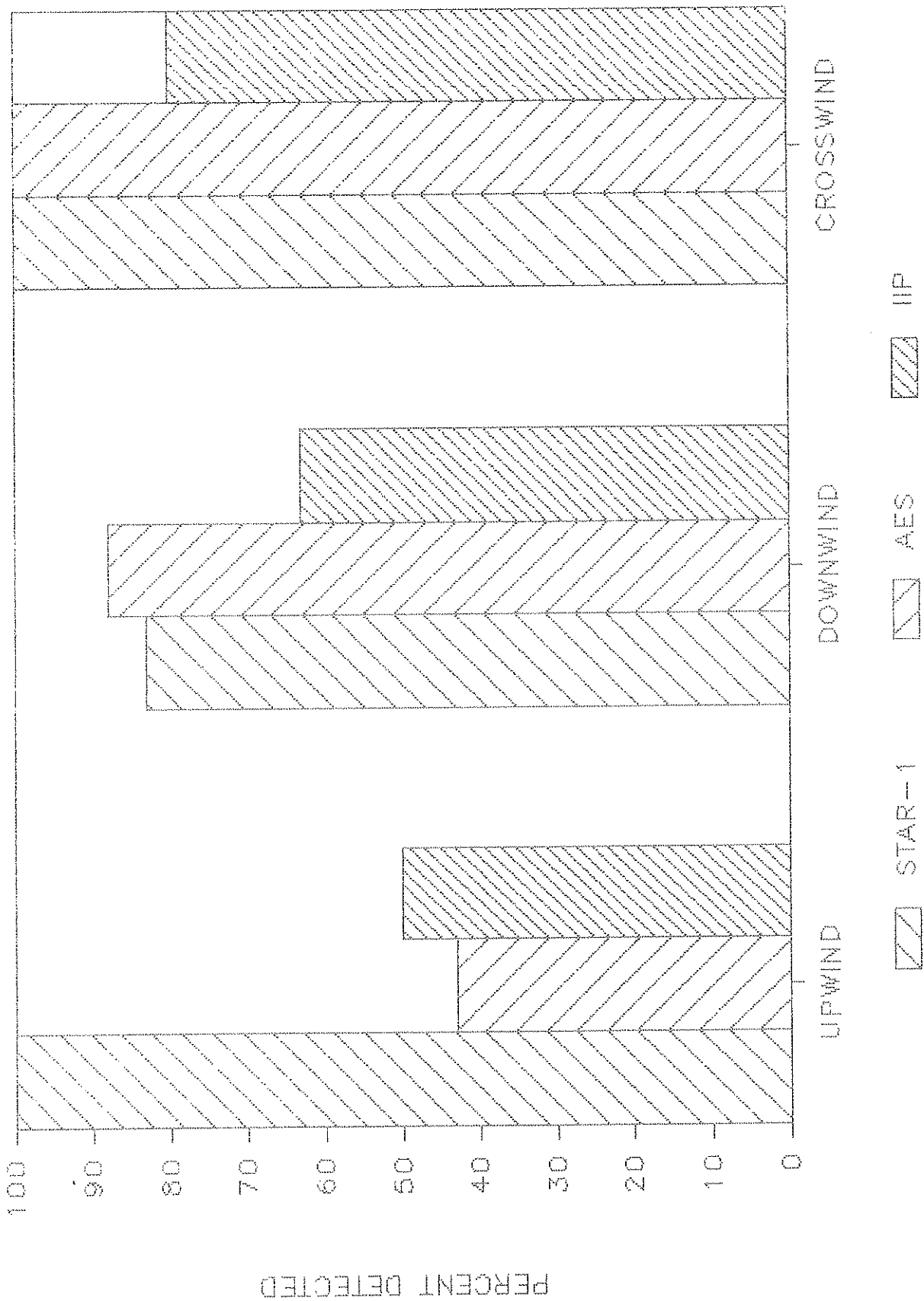


TABLE III-59

Aspect Angle Comparison for Detectability
 April 7 Results
 Targets Present/Total Number of Targets

| Radar | Aspect Angle | Small Iceberg (SB) | | Bergy Bits (BB) | | Growlers (G) | |
|--------|--------------|-----------------------|-----|--------------------|-----|-----------------|-----|
| | | No. | % | No. | % | No. | % |
| STAR-1 | Total | 14/14 | 100 | 27/28 | 96 | 16/28 | 57 |
| | Upwind | 1/ 1 | 100 | 2/ 2 | 100 | 0/ 2 | 0 |
| | Downwind | 3/ 3 | 100 | 5/ 6 | 83 | 6/ 6 | 100 |
| | Crosswind | 10/10 | 100 | 20/20 | 100 | 10/20 | 50 |
| AES | Total | 11/14 | 79 | 19/28 | 68 | 5/28 | 18 |
| | Upwind | 4/ 7 | 57 | 6/14 | 43 | 2/14 | 14 |
| | Downwind | 4/ 4 | 100 | 7/ 8 | 88 | 2/ 8 | 25 |
| | Crosswind | 3/ 3 | 100 | 6/ 6 | 100 | 1/ 6 | 17 |
| IIP | Total | 15/16 | 94 | 23/32 | 72 | 4/32 | 13 |
| | Upwind | 2/ 2 | 100 | 2/ 4 | 50 | 0/ 4 | 0 |
| | Downwind | 3/ 4 | 75 | 5/ 8 | 63 | 1/ 8 | 13 |
| | Crosswind | 10/10 | 100 | 16/20 | 80 | 3/20 | 15 |

FIGURE III-53.

DETECTABILITY: All Days

For SLAR and SAR; See Legend at Bottom

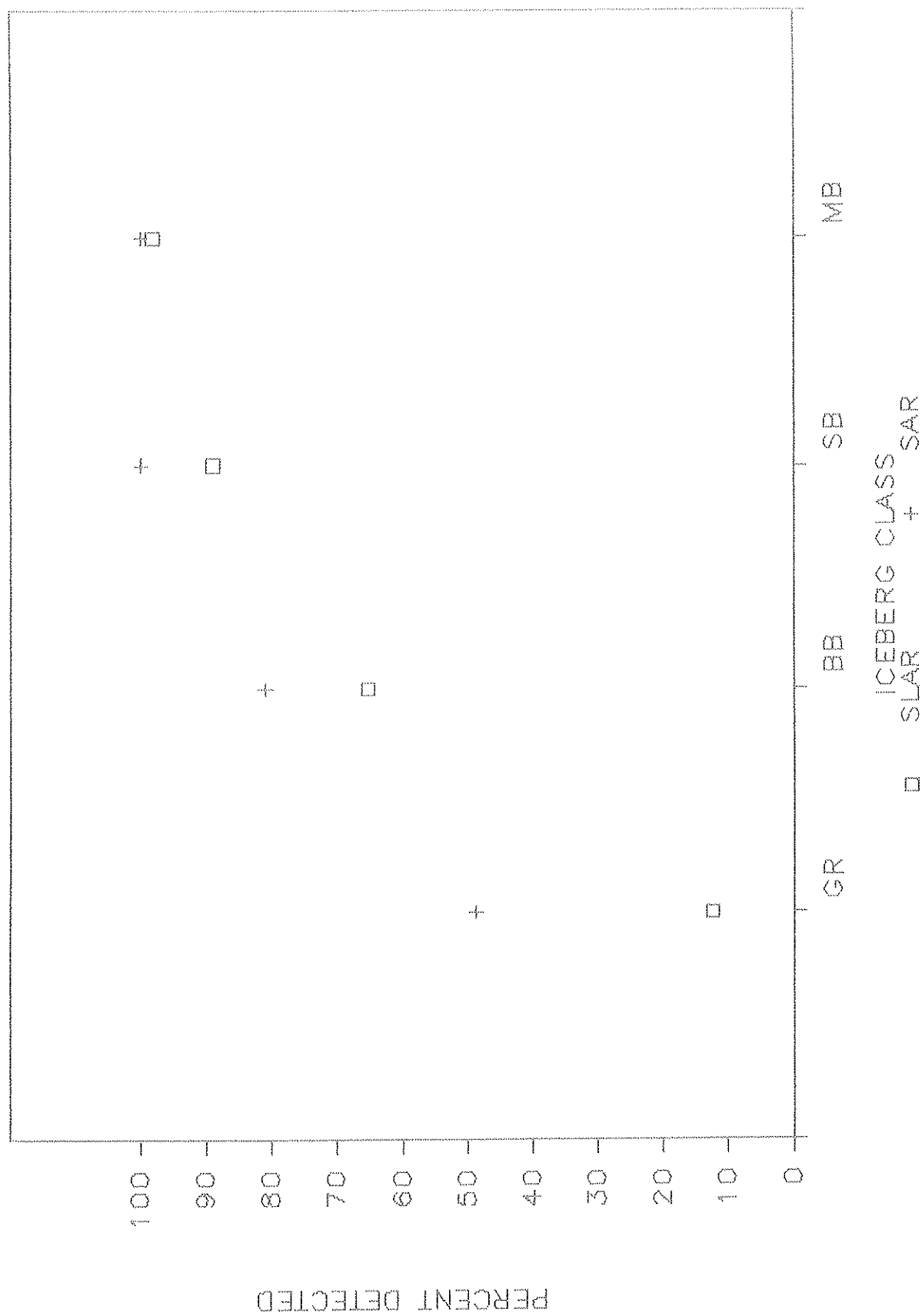


TABLE III-60

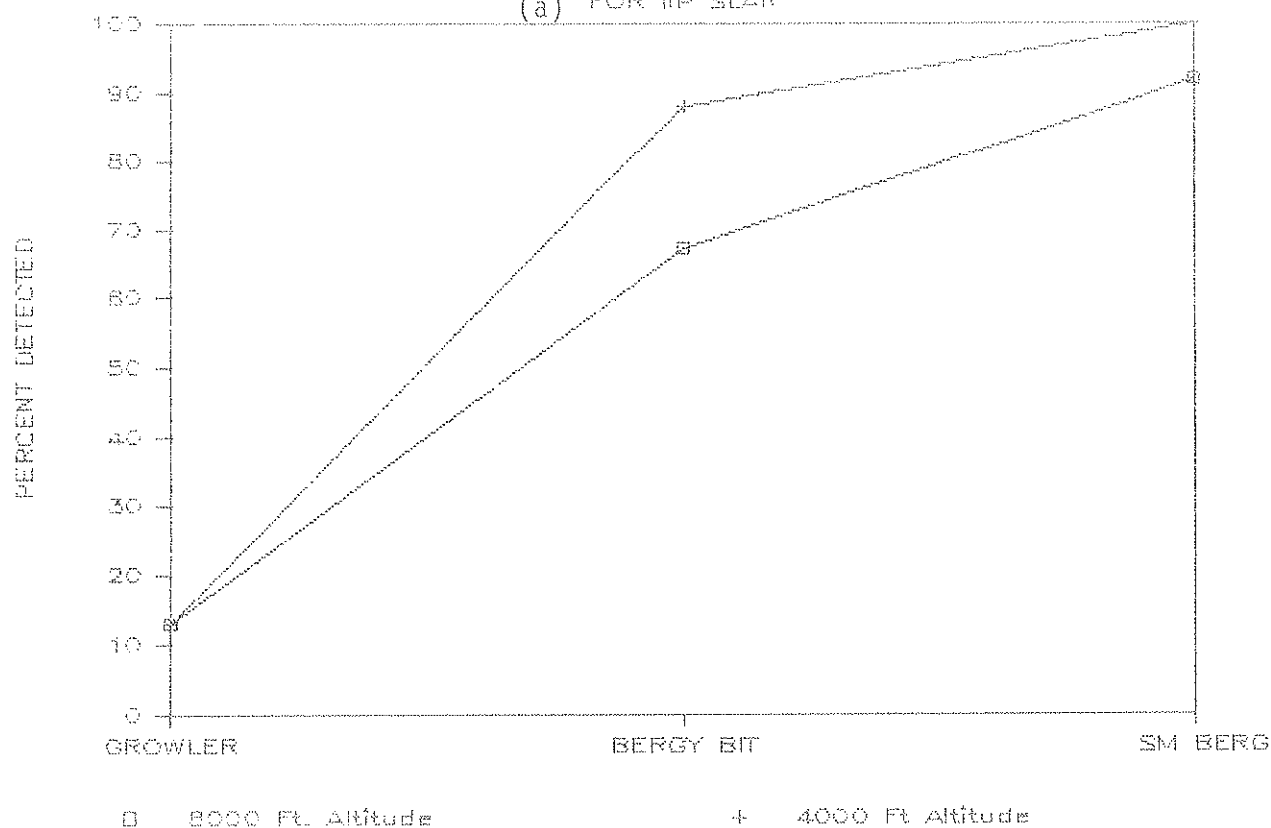
Ratio of Targets present to Total Targets
by Radar and Size Class; April 3, 5, and 7 Data combined

| Radar | Size Class | Targets Present/Total Targets | Percentage |
|-------|----------------|-------------------------------|------------|
| SLAR | Medium iceberg | 56/ 57 | 98.2 |
| | Small iceberg | 65/ 73 | 89.0 |
| | Bergy bit | 111/170 | 65.3 |
| | Growler | 12/ 97 | 12.4 |
| SAR | Medium iceberg | 6/ 6 | 100.0 |
| | Small iceberg | 31/ 31 | 100.0 |
| | Bergy bit | 43/ 53 | 81.1 |
| | Growler | 20/ 41 | 48.8 |

FIGURE III-54.

DETECTABILITY AS A FUNCTION OF ALTITUDE

(a) FOR IIP SLAR



DETECTABILITY AS A FUNCTION OF ALTITUDE

(b) FOR AES SLAR

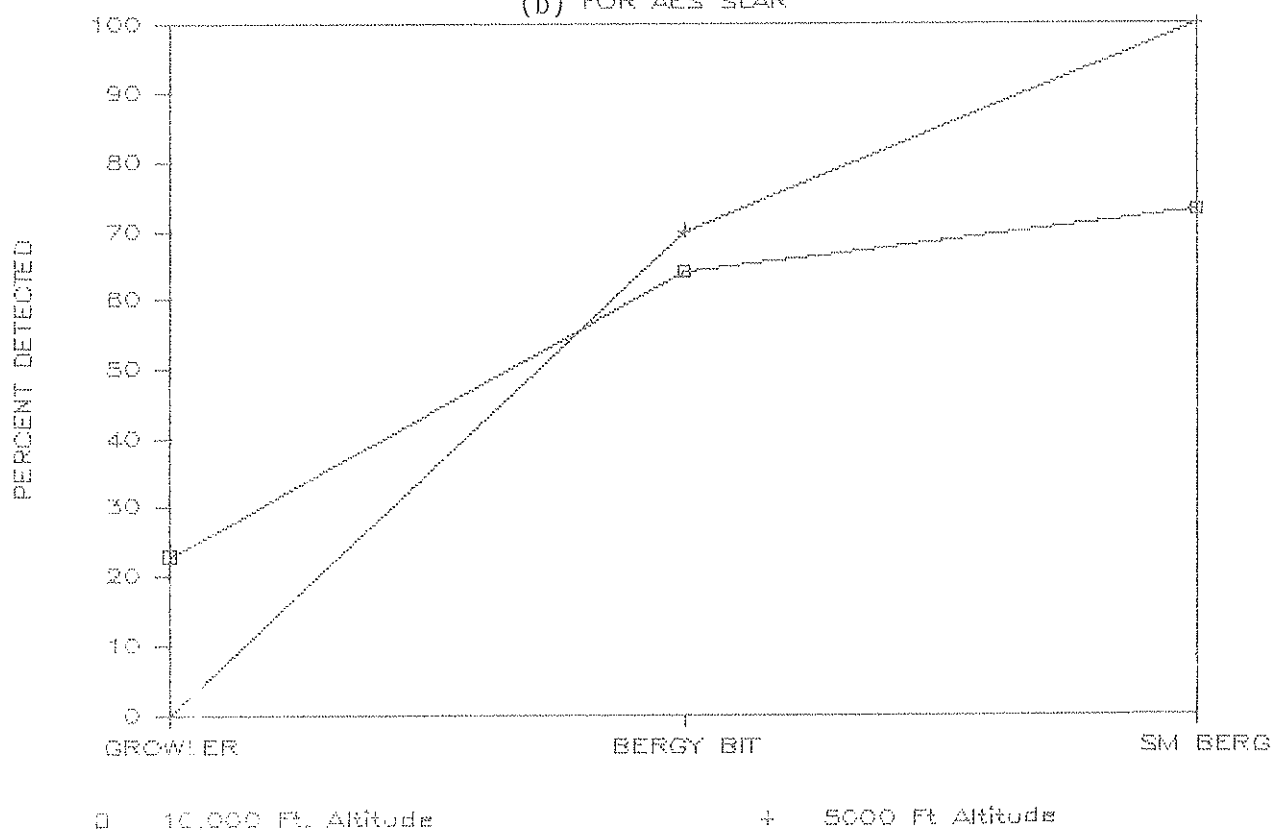
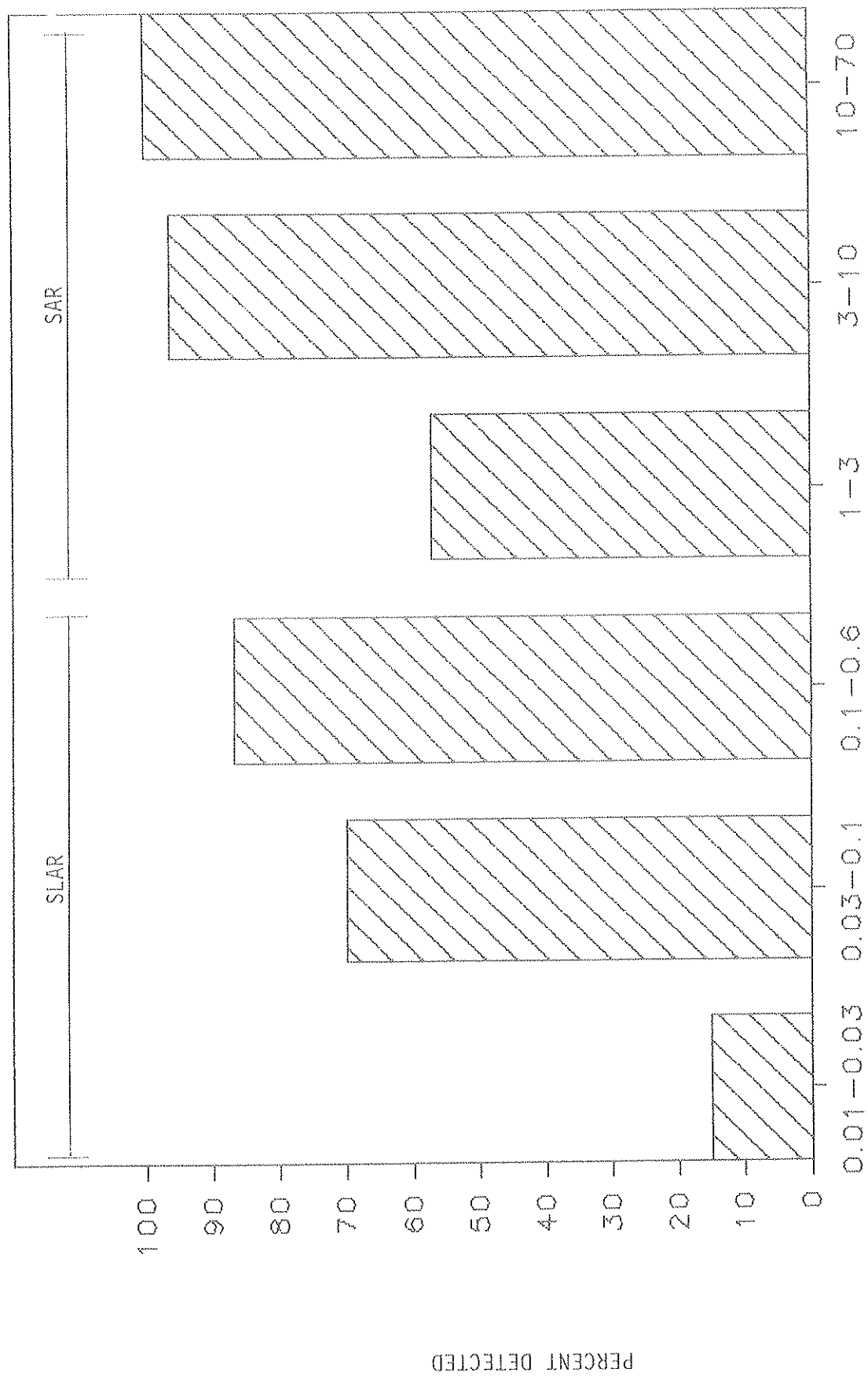


TABLE III-61

Detectability as a Function of Altitude and
Target Size Class

| Radar | Altitude | Growler | | Bergy Bit | | Small Iceberg | |
|-------|----------|---------|----|-----------|----|---------------|-----|
| | | No. | % | No. | % | No. | % |
| HIF | 8,000 | 3/24 | 13 | 16/24 | 67 | 11/12 | 92 |
| | 4,000 | 1/ 8 | 13 | 7/ 8 | 88 | 4/ 4 | 100 |
| AES | 10,000 | 5/22 | 23 | 14/22 | 64 | 8/11 | 73 |
| | 5,000 | 0/10 | 0 | 7/10 | 70 | 5/ 5 | 100 |

FIGURE III-55. DETECTABILITY VS RESOLUTION



ICEBERG AREA/RADAR RESOLUTION

III.10.7 TARGET REPEATABILITY

Table III-62 summarizes repeatability of detection of 17 verified targets (two small icebergs, nine bergy bits, six growlers) on April 3.

As can be seen, each radar detected more targets by flying repeated passes. Not suprisingly, the growlers were seen less often on all passes. The limited results shown in Table III-62 suggest that two or three passes provide significantly greater detectability than a single pass, although flying more than three passes probably does not add significantly.

III.10.8 PRECIPITATION EFFECTS

Table III-63 lists the number of passes that contained clutter attributed to precipitation echoes. Imagery from the SLAR systems showed that 10-20% of passes contained some clutter attributed to precipitation. Because the aircraft were flying at different times, it is not possible directly to compare individual radars. For the SAR system however, rain clutter was present on only 2% of the passes. It appears that the doppler shift of rain enables the SAR processor to filter out rain echoes.

Operational results using SLARs in this region suggest that the high percentage of precipitation clutter given here is anomalous, perhaps because local storms co-incided with the experiment flight times.

III.10.9 PLOTTER RESOLUTION

Table III-64 shows a comparison of the radar resolutions at various scales to the standard plotter resolution. For a 25-km swath, the plotters are reasonably well matched to the radar resolution, although the smallest target is less than 0.1 mm in size. However, for 50- and 100-km swaths, the radar resolution is finer than the plotter resolution, so that information is lost during plotting.

In general, the small-format (10-cm) display is not ideal for detection of small targets. Significant operational improvement could be achieved by using larger plotters, especially for the wider radar swaths.

TABLE III-62

Number Of Targets Out Of 17 Which Were Seen On Repeated Passes
On 3 April 1984

| Radar | Number of Passes | | | | | | |
|--------|------------------|------|------|-------|-----|-----|------|
| | Six | Five | Four | Three | Two | One | None |
| STAR-1 | - | - | - | - | 7 | 9 | 8 |
| IIP | - | - | 4 | 7 | 10 | 12 | 5 |
| AES | 3 | 4 | 5 | 7 | 10 | 10 | 7 |

TABLE III-63

Precipitation detected

| Aircraft | Number of passes examined | Number of passes with clutter | Percent precipitation |
|----------|------------------------------|----------------------------------|--------------------------|
| MARS | 38 | 8 | 21 |
| AES | 60 | 14 | 23 |
| IIP | 70 | 7 | 10 |
| STAR-1 | 58 | 1? | 2 |

TABLE III-64

Plotter and Radar Resolution

(a) Motorola SLAR; 10-cm image display

| Swath (km) | 25 | 50 | 100 |
|--|-----------|-----------|-----------|
| Radar range resolution (m) | 30 | 30 | 30 |
| Range pixel size (mm) | 0.12 | 0.06 | 0.03 |
| Approximate radar azimuth resolution (m) | 20-225 | 45-450 | 90-900 |
| Azimuth pixel size (mm) | 0.08-0.90 | 0.09-0.90 | 0.09-0.90 |

Note: plotter resolution approximately 0.07 mm (?)

(b) STAR-1 SAR; 20-cm image display

| Swath (km) | 25 | 50 |
|------------------------------|------|------|
| Radar range resolution (m) | 6 | 12 |
| Range pixel size (mm) | 0.06 | 0.06 |
| Radar azimuth resolution (m) | 6 | 6 |
| Azimuth pixel size (mm) | 0.06 | 0.03 |

Note: plotter resolution approximately 0.07 mm

III.11 CONCLUSIONS

A technical review of the results presented here was presented at Atmospheric Environment Service in Downsview, Ontario, on 28 November 1984, during which meeting the following general conclusions were reached.

It is possible that the detectability of growlers and bergy bits given here are somewhat pessimistic, because they are averages over the entire week. It was felt that results collected on the final days were enhanced by the experience gained during the initial days of the experiment. Hence, in an operational situation the results might be better on average. Also, the limited number of verified targets (less than 50 total) needs to be considered.

The major limitation of the experiment was the low sea states encountered. Further work should be carried out to evaluate airborne radar systems during higher sea states than those encountered during **BERGSEARCH '84**.

Air photography should be used as often as possible in conjunction with airborne radar operations. The use of air photos is very effective in verifying the existence of targets detected by the radars and, therefore, acts as standard against which to evaluate the performance of radars under given environmental conditions.

As Global Positioning System (GPS) will not be available until the late 1980s or early 1990s, an interim measure is needed to ensure accurate positioning offshore. A possible solution might be to moor a set of reflecting buoys at a known position on the Grand Banks. The buoys should be arranged in a distinct pattern which would be recognized unambiguously on radar imagery. When imaged, the difference between the known position of the buoys and the computed position of the aircraft would give an indication of aircraft INS drift.

It is important that efforts be made to determine the number of repeat passes needed to be made over a given area to ensure detectability. This is crucial for missions far from land when it becomes necessary to minimize the number of repeat passes to maximize the areal coverage.

III.11.1 DETECTABILITY

1. Estimates of average detectability for icebergs of various sizes in significant wave heights below 2.9 m, based on comparison to available surface and air-photo information for April 3, 5, and 7, are listed according to size category:

| | |
|---|---------|
| Growlers (<100 m ² area) | 10- 50% |
| Bergy bits (100-300 m ² area) | 60- 80% |
| Small icebergs (300-2500 m ² area) | 85-100% |
| Medium and large icebergs | 100% |

These results are from all radars and at all aspect angles combined. Optimum results are expected to be better than these averages.

2. The repeatability of detecting confirmed targets from pass to pass showed that target detectability (especially for growlers) increased with repeated passes. Two factors can affect single-pass detectability.
 - a) Small icebergs were observed by surface observers to have significant vertical bobbing motion. It is possible to have a bergy bit or growler substantially submerged or obscured by waves at any particular point in time. Radars that average over a period of more than a few seconds are expected to overcome this problem.
 - b) Targets in close proximity to one another have signatures that blend together.
3. Iceberg detectability decreased with increasing sea state, particularly for smaller targets. However, this experiment did not encounter conditions above 4-m wave height, and thus it is not possible to confirm how detectability will change for higher sea states. Higher resolution systems appeared to be more successful for detection of small targets as sea state increased, which is in agreement with theory.
4. Ships, icebergs, and small floes of sea ice generally do not display different radar target signatures on either SAR or SLAR analog imagery. Occasionally larger icebergs exhibited distinctive shape information on SLAR which was sufficient to make a positive and correct identification. On SAR all targets were smeared in azimuth. No attempt was made in this study to distinguish targets on the basis of radiometric information.
5. Smaller targets appeared to be more visible and more easily interpreted for lower-altitude SLAR passes.

III.11.2 ASPECT ANGLE

1. Detectability of medium size and larger icebergs was not affected by aspect angle for the wave regimes encountered during the experiment.
2. Smaller icebergs, bergy bits, and growlers are slightly more likely to be detected looking in the cross-wave direction. This is due to decreased sea surface return and a lower likelihood of targets being obscured by waves.

For SAR, wave signatures in the upwave or downwave direction closely matched the azimuthal smearing of iceberg targets so that the latter could not be distinguished readily. The azimuthal smearing of targets looking cross-wave gave a signature which was perpendicular to the wave patterns seen on the imagery, thus making them more visible.

III.11.3 RESOLUTION

1. In low wave regimes, detectability of smaller targets does not appear to improve greatly with higher resolution. However, in moderate sea states a higher resolution detected more smaller targets (especially viewed cross-wave). It is postulated that the differences would be even more apparent for higher wave regimes.
2. The better resolution of SAR has limits in detecting individual targets in close proximity to one another because the azimuthal smear signatures blend together.

III.11.4 IMAGERY INTERPRETATION

1. Typical aircraft positioning errors of up to 5 km were found, which is probably inadequate for many offshore applications and for reidentification of targets. Updating to known position references is important so that imagery can be used for target verification, reidentification, and iceberg motion. The availability of the satellite Global Positioning System by the late 1980s should alleviate this problem and will make possible registration of multiple passes of data.
2. Automatic latitude and longitude gridlines on imagery was very useful and speeded up data analysis.
3. The smallest iceberg targets are less than a single resolution cell in size for all the radars used. Hence,

carefully to the radar resolution. For example, a 25-km swath displayed over 10 cm of film gives only 0.12 mm per 30 m range increment, a size which can be missed easily without magnification or which can be confused with dust particles. Interpretation of smaller, more subtle targets required the aid of an eyepiece for all SLAR passes and for SAR passes in higher wave regimes.

4. Precipitation echoes were noted in 10-20% of the SLAR passes, but in few of the SAR passes. The doppler shift of rain itself appears to allow a SAR processor to filter out rain echoes.
5. The dynamic range of scenes imaged is relatively high. Therefore benefits are to be expected through operational use of digital data to overcome deficiencies of the limited grey level available on film. Limited digital analysis carried out in this project showed that iceberg targets could be separated from ocean clutter on the basis of signal intensity 88% of the time with a 5% false alarm in 2- to 4-m sea states.

III.12 RECOMMENDATIONS

III.12.1 OPERATING PROCEDURES

1. Flight lines using SAR or SLAR should be flown to a given wave direction so that targets are imaged cross-wave.
2. Repeated coverage is required to increase the probability of detection of growlers and bergy bits, especially if they are bobbing.
3. SLARs should be flown at the lowest altitudes consistent with operational constraints, including turbulence and swath width, to reduce sea clutter and to maximize resolution.
4. The most accurate navigation system available should be employed and navigation updates should be made to known references offshore. Conversion to the Global Positioning System is recommended when available. Moored reference radar targets might be useful.
5. It is important to match the output plotter resolution carefully to the radar resolution and to present the film in a format large enough for interpretation. A larger scale of imagery would facilitate easier, less time-consuming analysis.
6. The addition of latitude and longitude grid lines on imagery would be very desirable.
7. Imagery should be handled with the greatest of care to minimize dust specks and dirt particles which can be confused with real targets.
8. For an iceberg survey, post-flight analysis would involve using additional information sources not likely to be available on board the aircraft, such as:
 - previous ice and iceberg charts;
 - comparison to known ice and iceberg regime;
 - comparison to reported iceberg sightings by ships and shore stations;
 - comparison to reported ship positions to eliminate these as iceberg targets; and
 - comparison to accurate charts of shoals and land references to eliminate the former as targets.

During a survey it is probable that all or some of these additional sources will not be available. Such a post-flight analysis should be performed by different

personnel who are very familiar with the iceberg regime, who are monitoring, collecting, and plotting ship and iceberg sighting information, and who are experts in the appropriate analysis of radar imagery for icebergs. The situation would be somewhat analogous to an ice technician and an ice forecaster, except in this case the equivalent would be imagery analysis technician and regional iceberg analyst.

III.12.2 FURTHER ANALYSIS OF DATA SET

1. More digital scenes need to be analysed to generate more statistical data on target identification in an ocean background. A similar analysis should be performed on passes with known targets established from ground data. In particular, the differentiation of ships from icebergs using digital techniques should be done to determine whether such differentiations are possible on the basis of the imagery alone. Calibration should be made using the radar reflector data.
2. Additional CCRS CV-580 data should be incorporated into this data set, particularly to examine the effects of SAR azimuthal smear, C-band imagery, and cross-polarized echoes.

III.12.3 FURTHER EXPERIMENTAL WORK

1. Data need to be collected in higher sea states and wind conditions than were encountered in this experiment. Surface and air-photo information is essential, particularly at the exact time of radar passes and documenting smaller targets carefully.
2. Trials should be undertaken with SAR using single and multi-look passes over a known set of targets to investigate means of reducing azimuthal smear for targets in close proximity to one another.
3. The experiment used SLARs at their optimum settings and swath width. However, if these sensors are to be used in regional surveys a 25-km swath width requires twice the number of flight lines of a 50-km swath. Additional experiments should be performed with SLAR using 25- and 50-km swath settings over a known set of targets to determine exactly what is lost in going to the larger swath width.
4. A theoretical and observational study should be undertaken on the distribution and duration of growlers and bergy bits calving off larger icebergs in the Hibernia area. Such a study might determine how far away growlers travel from a source iceberg and their survival time under various environmental conditions. The

motivation here is to determine a radius from the iceberg of possible growler targets, recognizing that larger icebergs are more readily detectable using airborne radar.

III.13 REFERENCES

- Chan, H.L., and A.K. Fung. (1977), A theory of sea scatter at large incidence angles. Journal Geophysical Research, 82:3429-3444.
- Onstott, R.G., et al. (1979), Surface-based scatterometer results of Arctic sea ice, IEEE Transactions on Geoscience Electronics, GE-17:78-85.
- Sittrop, H. (1977), On the sea-clutter dependency on windspeed. Proceedings RADAR '77, pp.110-114.

